CONSTRUCTION OF A *Pseudomonas aeruginosa* DIHYDROOROTASE MUTANT AND THE DISCOVERY OF A NOVEL LINK BETWEEN PYRIMIDINE BIOSYNTHETIC INTERMEDIATES AND THE ABILITY TO PRODUCE VIRULENCE FACTORS

Dayna Michelle Brichta, B.S., M.S.

Dissertation Prepared for the Degree of

DOCTOR OF PHILOSOPHY

UNIVERSITY OF NORTH TEXAS

August 2003

APPROVED:

Gerard A. O'Donovan, Major Professor
Mark Shanley, Minor Professor
Dan Kunz, Committee Member
Robert Benjamin, Committee Member
Rollie Schafer, Committee Member
C. Neal Tate, Dean of the Robert B. Toulouse School of Graduate Studies

Brichta, Dayna Michelle. Construction of a *Pseudomonas aeruginosa* Dihydroorotase Mutant and the Discovery of a Novel Link between Pyrimidine Biosynthetic Intermediates and the Ability to Produce Virulence Factors. Doctor of Philosophy (Molecular Biology), August 2003, 236 pp., 13 tables, 68 figures, references, 72 titles.

The ability to synthesize pyrimidine nucleotides is essential for most organisms. Pyrimidines are required for RNA and DNA synthesis, as well as cell wall synthesis and the metabolism of certain carbohydrates. Recent findings, however, indicate that the pyrimidine biosynthetic pathway and its intermediates maybe more important for bacterial metabolism than originally thought. Maksimova *et al*., 1994, reported that a *P. putida* M, pyrimidine auxotroph in the third step of the pathway, dihydroorotase (DHOase), failed to produce the siderophore pyoverdin. We created a PAO1 DHOase pyrimidine auxotroph to determine if this was also true for *P. aeruginosa*. Creation of this mutant was a two-step process, as *P. aeruginosa* has two *pyrC* genes (*pyrC* and *pyrC2*), both of which encode active DHOase enzymes. The *pyrC* gene was inactivated by gene replacement with a truncated form of the gene. Next, the *pyrC2* gene was insertionally inactivated with the *aacC1* gentamicin resistance gene, isolated from pCGMΩ. The resulting pyrimidine auxotroph produced significantly less pyoverdin than did the wild type. In addition, the mutant produced 40% less of the phenazine antibiotic, pyocyanin, than did the wild type. As both of these compounds have been reported to be vital to the virulence response of *P. aeruginosa*, we decided to test the ability of the DHOase mutant strain to produce other virulence factors as well. Here we report that a block in the conversion of carbamoyl aspartate (CAA) to dihydroorotate significantly impairs the ability of *P. aeruginosa* to affect virulence. We believe that the accumulation of CAA in the cell is the root cause of this observed defect. This research demonstrates a potential role for pyrimidine intermediates in the virulence response of *P. aeruginosa* and may lead to novel targets for chemotherapy against *P. aeruginosa* infections.

ACKNOWLEDGEMENTS

This dissertation and the research reported herein, could not have been completed without the assistance and support of several individuals. The guidance and friendship provided by my mentor, Dr. Gerard O'Donovan, have been boundless and invaluable. I may have been born with a predisposition for the sciences, but I am a Microbiologist who loves and appreciates science so much more, because of you (Thank you GO'D!). My mother, Dr. Harriet E. Brichta, has been my inspiration and pillar of strength. Thank you mom, for always being the light that shone the way. To my friends and lab mates throughout the years, I owe special thanks, for all of the wonderful discussions and scientific bantering – I wish you guys all the best in your future endeavors. And finally, I would like to thank my better half, Brian Pritchett. Your encouragement and understanding made this trial so much easier than it would have been without you. Thank you for standing by me and always being there.

TABLE OF CONTENTS

Page

LIST OF TABLES

LIST OF FIGURES

Page

CHAPTER I

INTRODUCTION

"…one of life's strangest qualities – (is) its eternal dissatisfaction with what is, its persistent habit of reaching out into new environments and, by degrees, adapting itself to the most fantastic of circumstances."

Loren Eiseley

The Immense Journey

It is unlikely that Loren Eiseley had *Pseudomonas aeruginosa* specifically in mind when he wrote that in 1957, but as I read it, it appealed to me as a fitting summary of the notoriously versatile organisms "approach" to life. This Gram-negative bacillus, while readily isolated from environmental sources such as soil, marshes and water, is also a noted opportunistic pathogen, able to proliferate in hosts as varied as plants (Rahme *et al*., 1995; 1997), insects (D'Argenio *et al.*, 2001), nematodes (Mahajan-Miklos *et al.*, 1999) and mammals (Lomholt *et al.*, 2001). And while *P. aeruginosa* thrives in these relatively copiotrophic environments, it is equally adept at surviving in oligotrophic environments such as sterile water, for more than 200 days (Byrd *et al*., 1991). Finally, though it is characterized as an aerobic organism, even certain anaerobic environments can host *P. aeruginosa*, as it is capable of anaerobic respiration using nitrate, instead of

oxygen, as a final electron acceptor. And so, perhaps more so than any other bacterial organism, *P. aeruginosa* deserves the classification “ubiquitous.”

The research presented in this dissertation focuses primarily on pyrimidine biosynthesis in *P. aeruginosa*, and specifically on the third step of the pyrimidine *de novo* pathway catalyzed by the enzyme dihydroorotase. Rather unexpectedly, a link was discovered between pyrimidine biosynthesis and the ability of *P. aeruginosa* to produce virulence factors. Given the persistent nature of *P. aeruginosa* infection and its inherent resistance to current antibiotic therapy, many research laboratories around the world are studying the virulence factors produced and the mechanisms governing their synthesis, in a quest for new targets for chemotherapy. Thus, the research reported herein is significant, as it is the first report to date of the connection between pyrimidine metabolism and *P. aeruginosa* virulence. But before delving into the depths of pyrimidine biosynthesis, it seems fitting to give a brief history of the organism and the many ways it can inflict damage on the host it infects.

P. aeruginosa probably first drew the attention of scientists and physicians of the 19th century because the frequency with which it was associated with wound infections and because of the characteristic pigments that it produced. The organism was originally named *Bacterium aeruginosum* by the German scientist J. Schroeter in 1872, in what is likely the first publication describing it. The species name, *aeruginosum*, translates from Latin as “full of copper rust or verdigris, hence green” (Bergey’s). In fact, it was initially described as the causative agent of “blue pus”-- thus another early descriptive name was *Bacillus pyocyaneus*. In an 1882 article entitled “On the Coloration of Green and Blue Bandages,” the French scientist Gessard showed that the bacterium produced two

pigments, a bluish green pigment now called pyocyanin and a fluorescent yellow-green pigment, originally called fluorescine, but now commonly called pyoverdin (Fig. 1).

It did not take long for the first scientists working with *P. aeruginosa* to notice its ability to produce toxic substances that were equally harmful to both other microorganisms and the human or animal host (Fig.s 2 and 3). As early as 1877, Louis Pasteur published an observation, which became known as the Pasteur paradoxon: when he inoculated animals with both *Bacillus anthracis* and other pathogenic bacilli (now known to have been *P. aeruginosa*), the animals failed to develop anthrax. And in a further study in 1889, Bouchard mentioned specifically *Bacillus pyocyaneus* as a potent antagonist. Today, an extensive body of research exists on the numerous virulence factors produced by *P. aeruginosa*.

One of the first virulence factors studied was probably also the most physically evident, the previously mentioned blue phenazine pigment, pyocyanin (Fig. 4a). Pyocyanin is a redox-active compound capable of reducing oxygen to form super-oxide radicals and hydrogen peroxide. As a defense mechanism and competitive tool, the structure of pyocyanin allows it to readily cross the membranes of rival microorganisms, resulting in toxic oxygen intermediates that kill the competitor. *P. aeruginosa* avoids harming itself with this compound by increasing the production of the detoxifying enzymes, catalase and superoxide dismutase.

In the lungs, pyocyanin has been shown to inhibit ciliary beat frequency in airway epithelial cells. This inhibition correlates with decreased cellular levels of ATP and cAMP (Denning *et al*., 1998). Pyocyanin has also been shown to induce rapid and

overwhelming apoptosis in neutrophil populations *in vitro*, which is associated with reactive oxygen

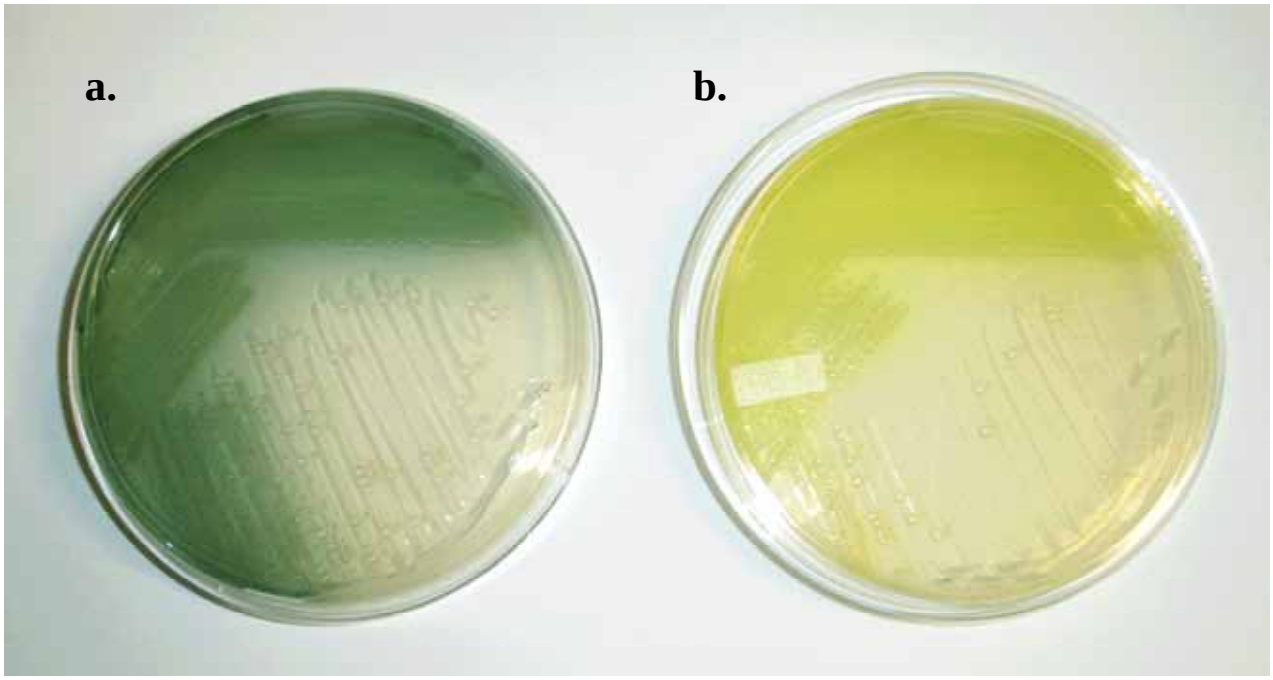

Fig. 1. Demonstration of the pigments pyocyanin and pyoverdin produced by *P. aeruginosa*. Plate (a) shows *P. aeruginosa* growing on *Pseudomonas* P agar which enhances the production of the blue-green pigment pyocyanin. Plate (b) shows the organism growing on *Pseudomonas* F agar which enhances the production of the fluorescent siderophore pigment, pyoverdin. The plates were incubated at 37°C for 24 h.

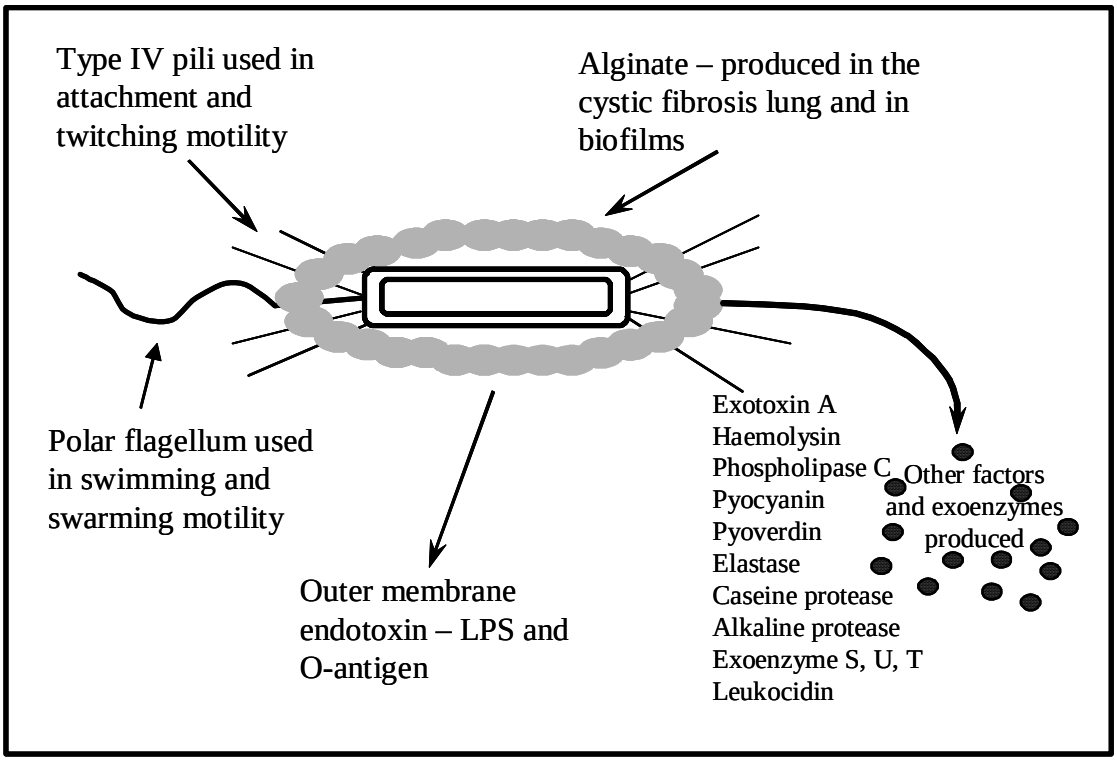

Fig. 2. Virulence factors produced by *P. aeruginosa*. Adapted from Iglewski et al., www.iglewski.com.

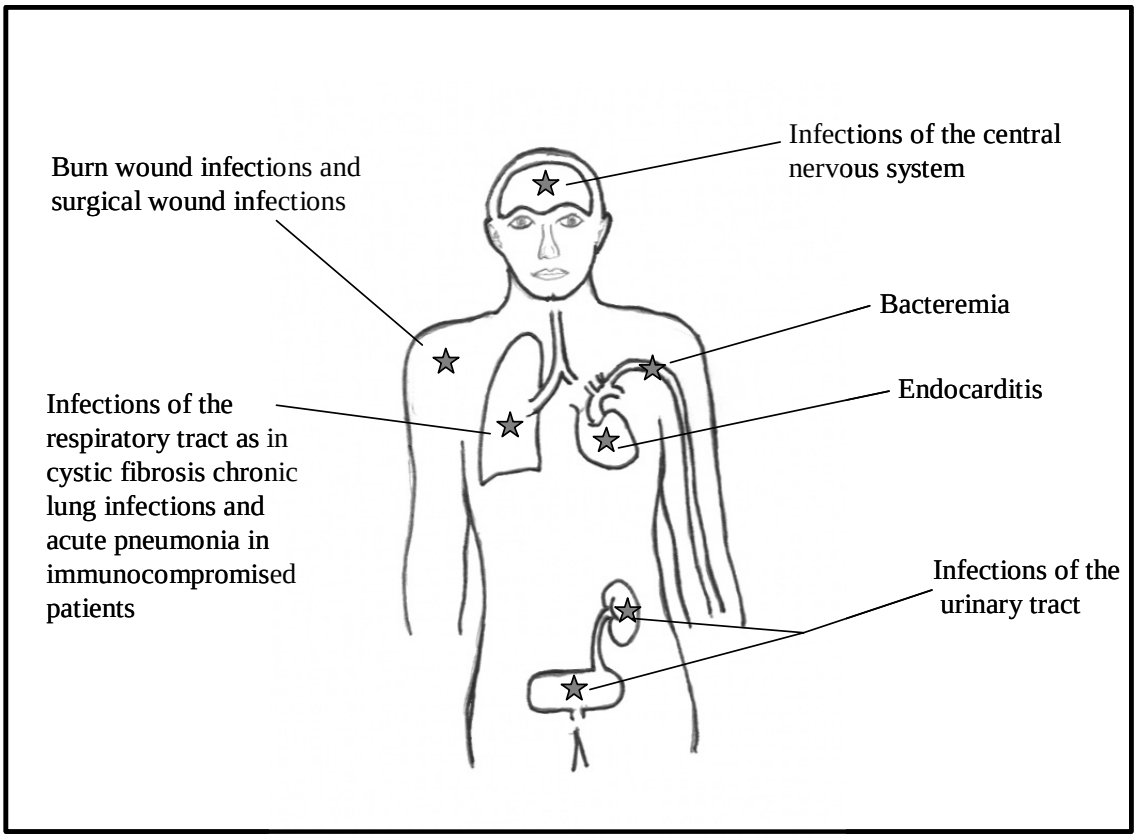

Fig, 3. Common sites of *P. aeruginosa* infection in the human host. Adapted from Iglewski et al., at www.iglewski.com.

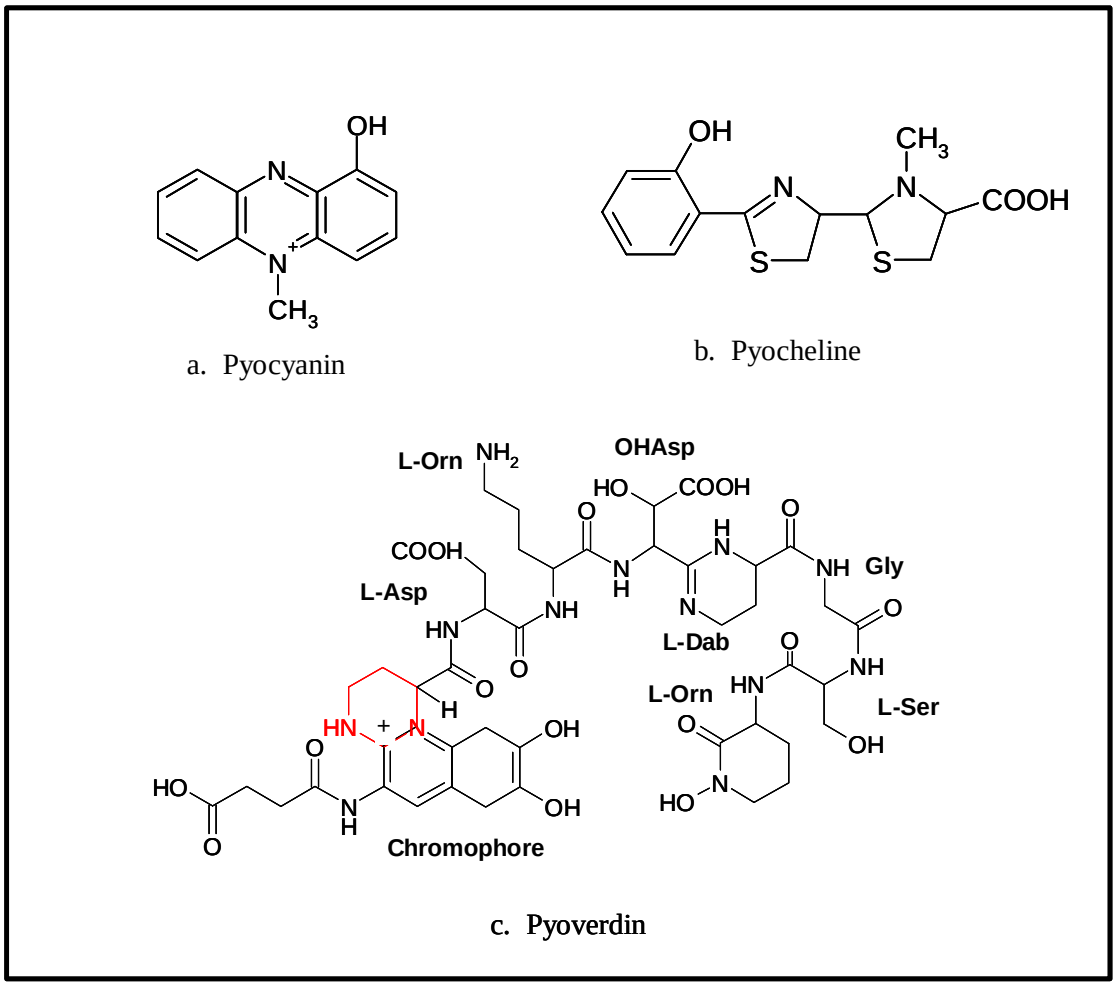

Fig. 4. Secondary metabolites produced by *P. aeruginosa*. The red ring structure represents the site where DHO could participate in pyoverdin biosynthesis as proposed by Maksimova et al., 1994.

intermediate generation and lowering of intracellular cAMP (Usher *et al.*, 2002). Thus a common indication of *P. aeruginosa* bacteremia is neutropenia (a low neutrophil count).

Proteases comprise another branch of the *P. aeruginosa* virulence arsenal. These proteases, which are secreted into the environment, include elastase, alkaline protease, casein protease and staphylolysin. Elastase, also referred to as LasB or pseudolysin (Lomholt *et al*., 2001), is noted for its broad substrate specificity. Host proteins sensitive to elastase include elastin, transferrin, collagens types III and IV, laminin, immunoglobulins A and G, complement components, and α1-antiproteinase inhibitor (Kessler *et al*., 1993). Alkaline protease (also designated as AprA or aeruginolysin) and elastase have been shown to be responsible for the degradation of a large variety of tissue components, such as proteinaceous elements of connective tissue. They also cleave cell surface receptors on neutrophils resulting in the inhibition of chemotaxis, phagocytosis and oxidative burst.

The staphylolysin protease (also known as LasA) has been shown to play a role in the pathogenesis of corneal and lung infections (Preston *et al.*, 1997). LasA renders elastin more susceptible to degradation by elastase through a nicking activity and it aids in the lysis of *Staphylococcus aureus* by cleaving the peptide bonds within the pentaglycine cross-linking peptides of its cell wall peptidoglycan (Lache *et al*., 1969, Kessler *et al*., 1993). Thus the activity of these enzymes provides a basis for the virulence and persistence of *P. aeruginosa* infections.

Exotoxin A is a protein toxin produced by *P. aeruginosa*. This protein is another major virulence factor that kills susceptible cells by ADP ribosylation of cytoplasmic elongation factor 2, thus inhibiting the translocation step of protein synthesis (Lowry

1986). This mechanism of action is identical to that of the diphtheria toxin produced by *Corynebacterium diphtheriae*. The production of exotoxin A is controlled at the transcriptional level by the alternative sigma factor PvdS (Vasil & Ochsner 1999). When the iron concentration in the medium or environment is low, PvdS activates the transcription of the *toxA* gene along with many other genes encoding proteins necessary for survival during iron limitation. In fact, iron concentration is a "signal" of sorts used by *P. aeruginosa*, and many other pathogens, to indicate their presence in a host. The acquisition of iron poses a unique problem to microorganisms and the solution that they "devised" to circumvent it is worthy of further discussion.

Iron is an essential oligoelement for almost all organisms. It is particularly important for aerobic bacteria such as *Pseudomonas*. The biological significance of iron results from its chemistry, which involves a reversible one-electron oxidation-reduction reaction that exchanges ferrous (Fe^{3+}) and ferric (Fe^{2+}) iron between its two common oxidation states. Because of its redox potential, this element is involved in many primary biological functions, such as electron transport, nitrogen fixation and nucleic acid biosynthesis. Iron is a constituent of all heme enzymes, which include cytochromes of the respiratory chain. Additionally, the common type of ribonucleotide reductase that converts NDPs to dNDPs contains iron, as do diverse "forms" of iron-sulfur proteins. Furthermore, the detoxifying enzymes, superoxide dismutase (SOD), catalase and peroxidase, require iron as a cofactor. Thus, iron is an essential component for proper growth and yet, organisms need to monitor iron uptake, as surplus iron can react with oxygen resulting in toxic oxidizing radicals. The danger of having too much iron lies in

Fenton-Harber-Weiss chemistry (Flitter *et al*., 1983). Iron can react with oxygen radicals in the following ways:

$$Fe(III) + O_2^{\cdot -} \rightarrow Fe(II) + O_2 \quad \text{(Fenton reaction)}$$

$$Fe(II) + H_2O_2 \rightarrow Fe(III) + {}^{\cdot}OH + OH^- \quad \text{(Harber-Weiss reaction)}$$

In combination these reactions generate the toxic oxidizing hydroxyl radical ($^{\cdot}OH$). Thus it was necessary for organisms to develop ways of taking up iron, but then maintaining it in a nontoxic and bioavailable form.

There was yet another hurdle for microorganisms to overcome with respect to iron, how to get it. Although iron is the fourth most abundant element on earth, its accessibility is remarkably limited as a consequence of its tendency to be hydrolyzed, forming the highly insoluble compound $Fe(OH)_3$ (Stintzi *et al*., 2000). At physiological pH, free Fe^{3+} is limited to 10^{-18} M, while virtually all living microorganisms require a minimal concentration of 10^{-8} M for growth (Braun & Hantke, 1997). Within humans and animals, most iron is found intracellularly in ferritin or heme (Griffiths, 1987). Extracellular iron is tightly bound to the high-affinity iron-binding glycoproteins, transferrin (in serum) and lactotransferrin (in secretions) (Heinrichs & Poole, 1993). In order to gain access to iron, either in the environment or during infection, many bacteria synthesize and release siderophores.

Siderophores are low molecular mass, high affinity, iron chelators capable of delivering iron to bacterial cells *via* specific receptor proteins on the cell surface (Neilands, 1982). *P. aeruginosa* produces two known siderophores, pyochelin and the previously mentioned yellow-green, fluorescent pigment, pyoverdin. Pyochelin is a derivative of salicylic acid (Fig. 4b) and binds iron in a 2:1 stoichiometric ratio with a

binding constant (K_f) of 2 x 10^5 (Cox & Graham, 1979; Visca *et al*., 1992). Pyoverdin is perhaps the more medically relevant siderophore, as its binding constant for iron is 10^{32} at neutral pH, and it has been reported to be able to steal iron from serum transferrin (Ankenbauer *et al*., 1985; Sriyosachati & Cox, 1986).

Pyoverdin is composed of a dihydroxyquinoline-containing fluorescent chromophore, joined to a partly cyclic octapeptide (Fig. 4c) (Briskot *et al*., 1989). Among the pseudomonads, the chromophore structure is highly conserved while the amino peptide is variable and thought to be responsible for specificity in ferric-siderophore uptake (Meyer, 2000). Translocation of iron through the bacterial outer membrane as the ferric-siderophore requires the formation of an energy-transducing complex with the proteins TonB, ExbB and ExbD. These proteins couple the electrochemical gradient across the cytoplasmic membrane to a highly specific receptor and so promote transport of the iron complex across the outer membrane (Stintzi *et al*., 2000).

The biological significance of siderophores has been demonstrated for a number of species, for example, siderophore deficient mutants of pathogenic bacteria are invariably less virulent in disease models (Ratledge & Dover, 2000; Meyer *et al*., 1996.). Thus, while pyoverdin itself is not a virulence factor, it is a secreted product that enables *P. aeruginosa* to survive as a pathogen.

Perhaps the most well-known aspect of *P. aeruginosa* pathogenicity is its colonization of the lungs of cystic fibrosis (CF) patients. The resulting lung disease is currently the leading cause of morbidity and mortality in CF (Wilson & Dowling, 1998). Individuals with CF have abnormal air way epithelial cells that are incapable of efficiently exporting chloride ions. The build up of chloride ions within the epithelial

cells results in an increase in the absorption of sodium ions and water. This leads to a decrease in the airway surface liquid volume and thickened mucus. The cilia that would normally clear away mucus and debris become matted down and ineffective. The result is a veritable breeding ground for opportunistic pathogens such as *P. aeruginosa*, *S. aureus*, *Haemophilus influenzae* and *Burkholderia cepacia* (Hassett *et al*., 2002). Unfortunately for the host, *P. aeruginosa* is remarkably adept at surviving in the CF lung, thus as the airway disease progresses, it outcompetes many other microorganisms and becomes the predominant colonizer. Here, the organism changes its mode of growth. Instead of living and propagating in a free-floating, planktonic manner, *P. aeruginosa* attaches and aggregates, growing in a "social" form of existence known as a *biofilm*.

By definition a biofilm describes bacterial growth on any substratum such as teeth, bones, organs, catheters or prostheses (Hassett *et al*., 2002). Biofilm formation in CF airway disease begins when *P. aeruginosa* cells are seeded onto the thick mucus surface by inhalation. The bacteria then penetrate the mucus and become embedded. It has been shown that CF airway mucus has a tendency to become anaerobic, especially during chronic infection. Thus, *P. aeruginosa* residing in CF airway mucus undergoes anaerobic metabolism using nitrate or nitrite as final electron acceptors (Hassett *et al*., 2002). Both compounds are plentiful, as the concentration of nitrate (NO_3^-) in CF mucus is 383 ± 42 μM and that of nitrite (NO_2^-) is 125 ± 55 μM (Jones *et al*., 2000; Hassett, 1996).

As the infection progresses, *P. aeruginosa,* growing within CF mucus, senses an oxygen gradient (low oxygen deep within the mucus layer and higher oxygen near the surface) and this signals the cells to convert to a mucoid phenotype (Hassett *et al*., 2002).

This phenotype is characterized by the production of the hyper-viscous substance alginate, which has been referred to as the most significant virulence determinant in the context of CF airway disease (Hassett *et al*., 2002). Alginate is a linear polymer of acetylated β-D-mannuronate and its C-5 epimer, α-L-guluronate and its production contributes to the impairment of airway mucus clearance. Thus, the clinical course of infection in CF patients is significantly worsened by the formation of *P. aeruginosa* biofilms, and the concomitant production of alginate in airway mucus.

P. aeruginosa biofilms also occur in nature. Here they grow as an organized community of cells embedded in an extracellular polysaccharide matrix that is attached to surfaces such as rocks or wood (Deziel *et al*., 2001). One of the advantages of biofilms is that they provide an environment where nutrients are continuously trapped by the exoplysaccharide matrix and are available to the bacteria (Costerton *et al*., 1995). As such, the biofilm way of life selects for a particular phenotype, one that is highly adherent but with decreased motility.

Motility is arguably one of the most impressive features in microbial physiology and a necessary aspect of virulence. Mirroring its diversity in so many other areas, *P. aeruginosa* has been shown to employ three modes of translocation. The first two modes, swimming and swarming, are dependent on flagella. *P. aeruginosa* has a single polar flagellum that enables it to swim in aqueous environments and in low agar (less than 0.4 %) medium. Swarming, on the other hand, takes place on semisolid surfaces, such as medium containing 0.5 to 0.7 % agar, and is induced by growth in the presence of certain amino acids, such as glutamate and histidine, and the carbon and energy source glucose. Swarmer cells are elongated and hyperflagellated, as they have two polar flagella, and

produce the biosurfactant, rhamnolipid, which is believed to aid in swarming motility (Köhler *et al*., 2000).

The third mode of motility, twitching, depends on polar fimbriae also known as type IV pili. Twitching enables the organism to move on solid surfaces and interfaces, for example between a layer of medium and the petri dish. Twitching motility is believed to result from the extension and retraction of the pilus filament, which propels the cell across the surface. Type IV pili have also been shown to be important for bacterial attachment to epithelial cells (Costerton *et al*., 1999; Gupta *et al*., 1994). Thus, they contribute to the virulence of *P. aeruginosa* in animal models (Hahn, 1997; Tang *et al*., 1995; Tang *et al*., 1996).

Furthermore, twitching motility and, therefore type IV pili, is required for the formation of the previously mentioned biofilms on biotic and abiotic surfaces (O'Toole & Kolter, 1998), and mutants in pili or flagellar synthesis show reduced infectivity (Comolli *et al*., 1999; Hazlett *et al*., 1999). Thus, whether it is the ability to move away from toxic compounds or towards food sources or to attach to host epithelial cells, motility is necessary for the survival and pathogenicity of *P. aeruginosa*.

Given the various proteases and toxic substances produced, *P. aeruginosa* virulence is clearly multi-factorial. This, in addition to its ability to survive in diverse ecological niches, is likely a reflection of its extraordinary genetic complexity. The sequencing of the *P. aeruginosa* PAO1 genome was completed in 2000 (Stover *et al*., 2000) and to date, it remains the largest bacterial genome sequenced at 6,264,403 bp. Computer analysis has predicted 5570 open reading frames (orfs). Thus, the complexity of the *P. aeruginosa* genome approaches that of the simple eukaryote *Saccharomyces*

cerevisiae whose genome encodes about 6200 proteins (Ball *et al*., 2000). Consistent with its genetic complexity, *P. aeruginosa* has the greatest percentage of genes devoted to command and control systems observed in a bacterial genome. Analysis predicts that 9.4 % (521 genes) of the *P. aeruginosa* genome encode either transcriptional regulators or two-component regulatory proteins (Stover *et al*., 2000). It is likely that this inherent ability to fine-tune gene expression patterns is what allows *P. aeruginosa* to be so versatile. To date, the best studied of these "fine tuning" control mechanisms is that used to express genes in a cell-density dependent manner, and it is generally referred to as quorum-sensing (QS).

The basic principle behind the concept of QS is this; bacteria do not want to express the genes encoding certain virulence factors until the bacterial population is large enough to launch an overwhelming assault on the host. Thus, *P. aeruginosa*, and other pathogenic bacteria, evolved a way to sense the number of bacteria in a population *via* the production of QS molecules known as N-acyl-homoserine lactones (AHLs) (Fig. 5). *P. aeruginosa* contains two known QS systems, termed *las* and *rhl* (Latifi *et al*., 1996; Pesci *et al*., 1997).

The *las* system is composed of the transcriptional activator protein LasR, the AHL synthase LasI, which produces N-(3-oxododecanoyl)-L-homoserine lactone also known as 3-oxo-C_{12}-HSL, OdDHL, or autoinducer-1 (AI-1) (Fig. 6a.) and a repressor of virulence gene expression called RsaL (De Kievet *et al*., 1999). RsaL represses *lasI* transcription by binding to and blocking its promoter region. This occurs when the concentration of AI-1 is low, thus preventing early induction of the QS system. As the

cell density increases and the level of AI-1 in the cell reaches a threshold concentration, it

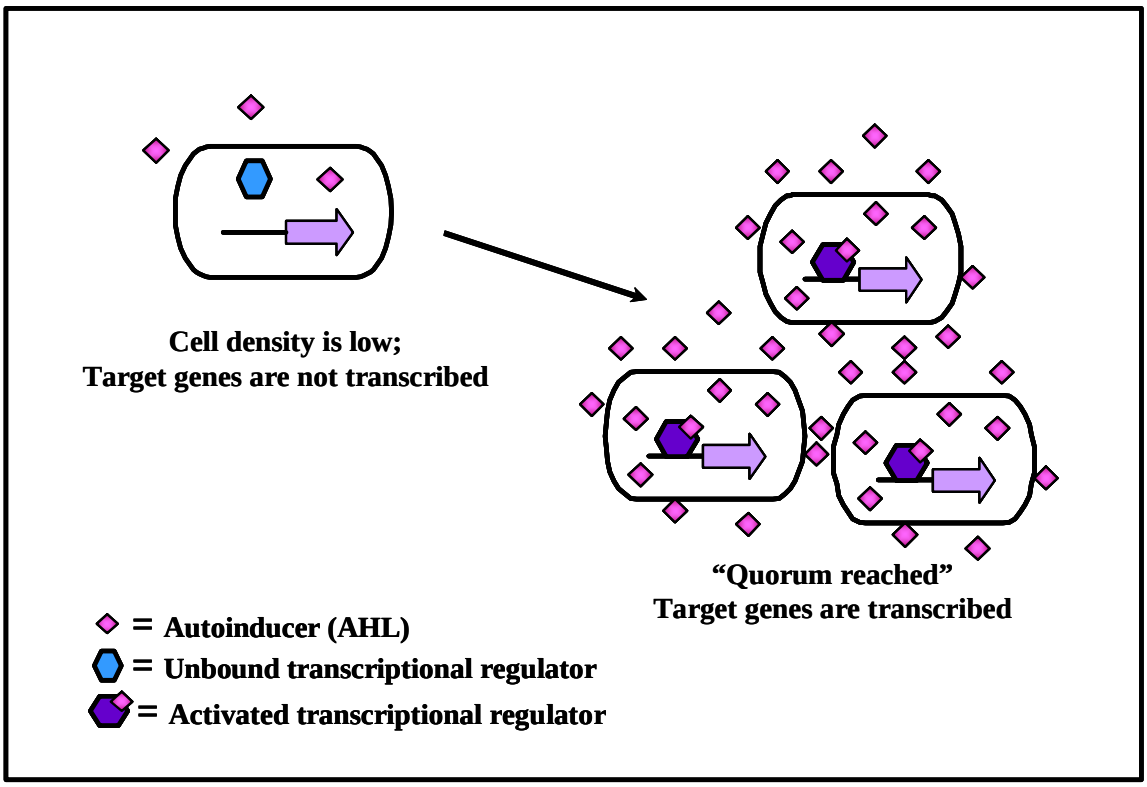

Fig. 5. Overview of quorum sensing.

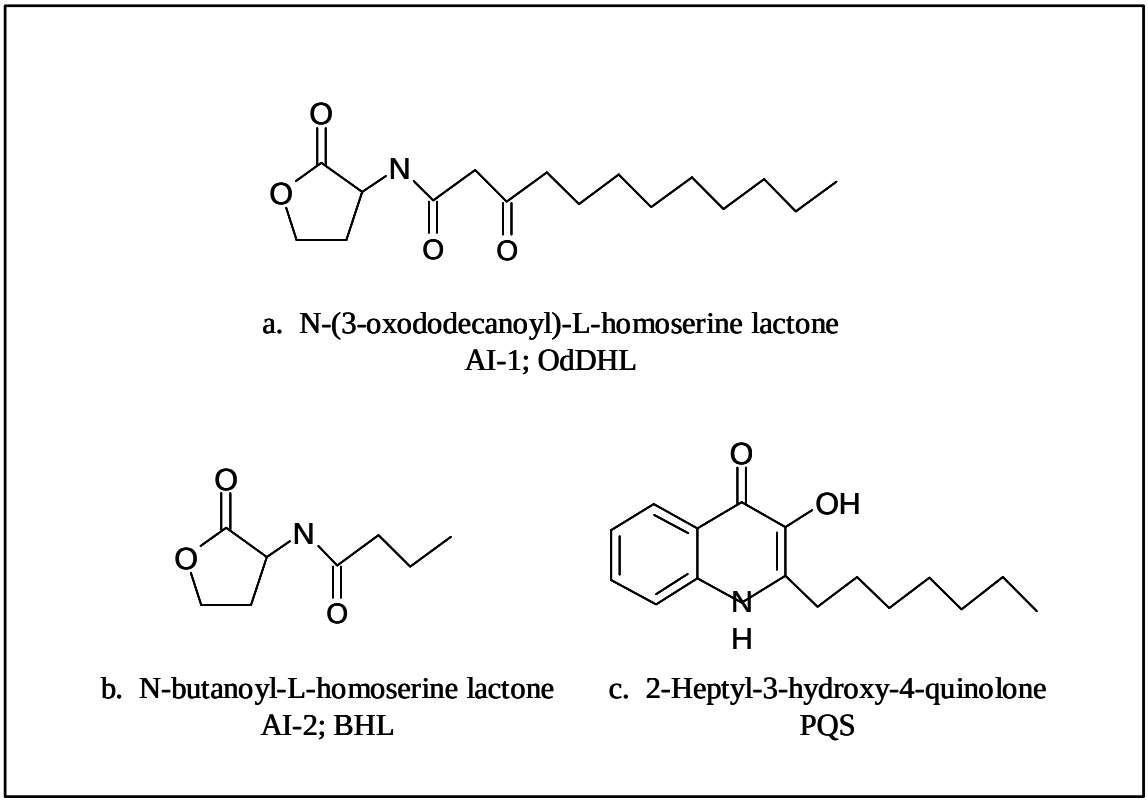

a. N-(3-oxododecanoyl)-L-homoserine lactone
AI-1; OdDHL

b. N-butanoyl-L-homoserine lactone
AI-2; BHL

c. 2-Heptyl-3-hydroxy-4-quinolone
PQS

Fig. 6. Quorum sensing molecules produced by *Pseudomonas aeruginosa*.

binds to LasR. The LasR-AI-1 complex then out-competes RsaL for binding at the *lasI* promoter, resulting in the induction of LasI synthesis. The synthesis of AI-1 is greatly enhanced, and the LasR-AI-1 complex activates the transcription of genes encoding numerous virulence factors including *lasA, lasB, apr,* and *toxA* as well as *rhlR* of the *rhl* QS system.

The transcriptional regulator, RhlR, is affected by the concentration of the AHL produced by RhlI which is called N-butanoyl homoserine lactone (C_4-HSL, BHL or AI-2) (Fig. 6b.). RhlR bound to AI-2 activates the transcription of its own AI synthase, *rhlI,* and several more virulence factor genes, namely *rhlA*, *rhlB*, *lasB* and *phzA*. Thus, the *las* and *rhl* QS systems operate in a hierarchical cascade responsible for regulating the expression of multiple virulence determinants and secondary metabolites (Whitehead *et al*., 2001).

P. aeruginosa has been found to produce a third intracellular signal in addition to the two homoserine lactone-type autoinducers. The signal was identified as 2-heptyl-3-hydroxy-4-quinolone and was called the *Pseudomonas* quinolone signal (PQS) (Fig. 6c) (Pesci *et al*., 1999). PQS was reported to activate the transcription of the *lasB* gene, encoding elastase, and to affect the production of pyocyanin (Calfee *et al*., 2001; Gallagher *et al*., 2002). It was determined, however, that maximal production of PQS occurred in late stationary phase, suggesting that this signal was not involved in sensing cell density, but may instead be associated with signaling at a time of increased cell stress (McKnight *et al*., 2000).

Explained in this fashion, the control of virulence factor synthesis by the QS system seems quite straight forward. However, in truth, it is a tangled web of

interconnecting regulators and signals and, as yet, the entire mechanism is not clearly understood. Several additional regulatory proteins have been shown to either exert control over or at least in some way affect the *las* or *rhl* systems. These include the proteins Vfr, GacA/S, RsmA, PPK, and RpoS (Fig. 7).

Vfr, which stands for virulence factor regulator, has been described as a global regulator of virulence factors because of its control over the transcription of *lasR* and *regA*, a positive regulator of exotoxin A synthesis (Albus *et al*., 1997; West *et al*., 1994). Vfr has also been identified as a regulator of normal twitching motility (Beatson *et al*., 2002). As a homolog of the catabolite repressor protein (CRP) from *E. coli*, amino acid sequence alignments of Vfr and CRP show that they have 67 % identical and 91 % similar residues (Beatson *et al*., 2002). In *E. coli*, CRP is activated to control the expression of catabolite repressed carbon utilization genes when it binds cAMP. Vfr also binds cAMP, however, in *P. aeruginosa* cAMP does not appear to correlate with carbon source availability (Phillips & Mulfinger 1981) thus, Vfr does not appear to be required for catabolite repression (Suh *et al*., 2002).

It has recently been suggested that Vfr may be capable of differential regulation of virulence factor expression. Beatson and coworkers have suggested that Vfr could regulate elastase and pyocyanin production by activating *lasR* in response to cAMP. Alternatively, Vfr could be activated to control twitching motility in response to another regulator which is likely to be cGMP (Beatson *et al*., 2002). This is significant because *P. aeruginosa* appears to use guanine nucleotides, including (p)ppGpp and cGMP as physiological signals indicating the onset of stationary phase (Kim *et al*., 1998), precisely when virulence factor production is initiated.

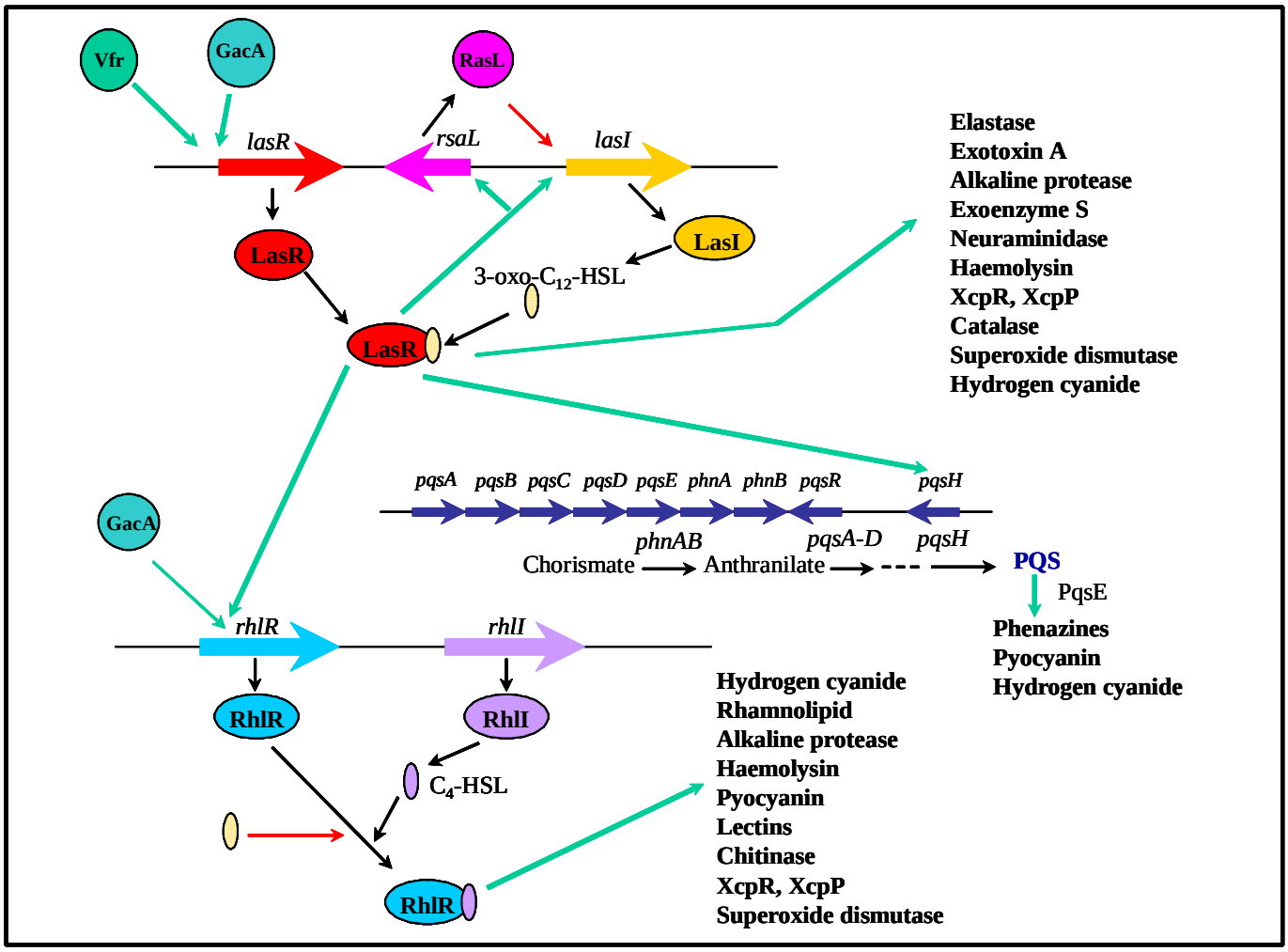

Fig. 7. Summary of the current model for the quorum sensing cascade control of virulence factor synthesis in *P. aeruginosa*.

The two component global activator GacS/A system, a member of the FixJ family of response regulators (Laville *et al*., 1992), has been shown to regulate the expression *lasR* and *rhlR* and the production of AI-2 (Reimmann *et al*., 1997). Here, the sensor kinase GacS activates the GacA response regulator by phosphorylation. GacA has been found to positively regulate *rhlI* synthase at the posttranscriptional level (Blumer *et al*., 1999). Thus, GacA mutants, deficient in the RhlRI QS system, demonstrate a significantly reduced ability to affect pathogenicity in burned mice as well as in infiltrated *Arabidopsis* plants (Rahme *et al*., 1995).

Another global regulator that acts at the posttranscriptional level is RsmA, which stands for regulator of secondary metabolites. It has been shown to negatively affect production of virulence determinants, as over-expression of *rsmA* results in a severe decrease in protease, elastase and stapholytic activities as well as reduced hydrogen cyanide (HCN) and pyocyanin levels (Pessi *et al*., 2001). Conversely, an *rsmA* mutant is hyper-virulent and produces virulence factors prior to stationary phase. It is speculated that the interplay between the positive regulator GacA, and the negative regulator RsmA, at ribosomal binding sites of target genes, represents a post-transcriptional control system that aids *P. aeruginosa* in the timing of virulence factor production (Pessi *et al*., 2001).

Phosphate concentration has also been found to influence *P. aeruginosa* virulence through a number of regulatory mechanisms. Previous studies have shown that media low in phosphate enhance virulence factor production while media high in phosphate show the opposite effect (Liu, 1964; Cox, 1986). This phenomenon is mediated in part by the transcriptional activator PhoB, through the recognition of promoters sensitive to phosphate starvation. The transcriptional activator AlgR2 is expressed under phosphate

limitation and it, in turn activates the expression of nucleoside diphosphate kinase (Ndk) (Kim *et al*., 1998). The *ndk* gene encodes a 16 kDa polypeptide that forms a tetramer in the cytoplasm and is responsible for the nonspecific conversion of (d)NDPs to (d)NTPs. As *P. aeruginosa* approaches stationary phase or encounters nutrient deprivation, Ndk is cleaved by intracellular elastase (LasB), yielding a 12 kDa polypeptide that associates with the cell membrane (Kamath *et al*., 1998). The truncated Ndk polypeptide forms a complex with pyruvate kinase and in so doing, becomes specific for the conversion of GDP to GTP. This shift in metabolism is important, as there is an increased demand in *P. aeruginosa* for GTP in both the stationary phase and the stress response (Kim *et al*., 1998).

The stringent response regulator (p)ppGpp, is the principal signal produced when *P. aeruginosa* encounters deficiencies in phosphate, nitrogen, amino acids, and other nutrients which are common during starvation or entry into the stationary phase. RelA produces (p)ppGpp, and recent evidence suggests that there is a link between RelA and the QS system. Van Delden and co-workers discovered that the over-expression of RelA in *P. aeruginosa* resulted in the activation of the QS regulators LasR and RhlR. Thus, the stringent response is capable of activating the QS system independently of cell density (Van Delden *et al*., 2001). This "by-pass" would be advantageous to *P. aeruginosa* in the event that it encountered nutritional stress before a critical cell density had been reached. As pointed out by Van Delden *et al*, the expressed virulence factors would provide the bacteria with new nutrients through their enzymatic activity or allow them to disseminate to more favorable niches.

Another way in which (p)ppGpp has been found to be important for the *P. aeruginosa* virulence response is its necessity for the formation of polyphosphate (poly(P)) (Shiba *et al*., 1997). Poly(P) is a linear polymer of tens to hundreds of orthophosphate (P_i) residues connected by ATP-like, high-energy phosphoanhydride bonds and it is synthesized by the ubiquitous enzyme polyphosphate kinase (PPK). Potential functions of poly(P) in the cell have been suggested to include the following: 1) a substitute for ATP for sugar and adenylate kinases (Hsieh *et al*., 1993; Phillips *et al*., 1993; Bonting *et al*., 1991), 2) a phosphate reservoir (Kulaev, 1979), 3) a chelator of divalent cations (van Veen *et al*., 1993; Archibald & Fridovich, 1982), 4) a buffer for alkaline stress (Pick & Weiss, 1991), 5) a component in competence for DNA entry and transformation (Reusch & Sadoff, 1988; Castuma *et al*., 1995), and 6) a factor in regulatory responses to stresses and nutritional deficiencies (Rao & Kornberg, 1996).

The formation of poly(P) is dependent on the concentration of (p)ppGpp as a consequence of the fact that (p)ppGpp strongly inhibits the enzyme exopolyphosphatase (poly(P)ase) which is responsible for the beakdown of poly(P). Thus as the (p)ppGpp concentration in the cell increases, so does the formation of poly(P). Conversely, in a *relA* mutant, which does not make the stringent response regulator, little or no poly(P) accumulates (Van Delden *et al*., 2001). *P. aeruginosa* PPK mutants have been shown to be deficient in all three forms of motility, attachment, biofilm formation and virulence factor production (Rashid *et al*., 2000a; Rashid *et al*., 2000b). The exact mechanism of how PPK affects motility and virulence in *P. aeruginosa* is not known. However, it has been shown that (p)ppGpp and poly(P) induce the expression of the alternative sigma factor RpoS (Gentry *et al*., 1993; Shiba *et al*., 1997). RpoS is responsible for the

transcription of a variety of genes expressed after cells enter stationary phase or during starvation and stress conditions (Loewen & Hengge-Aronis, 1994). In addition, RpoS has been reported to play a role in the *P. aeruginosa* QS response (Latifi *et al*., 1996; Whitely *et al*., 2000) but controversy exists as to its exact function here and further studies are needed to determine the precise interaction.

With approximately 521 genes encoding either transcriptional regulators or two-component regulator proteins, it is evident that scientists have just begun to scratch the surface of virulence factor regulation in *P. aeruginosa*. Recent advances however, such as the completion of the *P. aeruginosa* genome sequence and production of gene chips for microarray analysis of mRNA expression patterns, from mutant strains in comparison with wild type PAO1, should speed the progress with which this massive puzzle will be pieced together. But, as with any good story worthy of pursuit, this is likely to become more complicated before it is resolved. The data presented in this dissertation represent another piece of this puzzle, specifically, the effect of pyrimidine biosynthetic intermediates on *P. aeruginosa* virulence factor production. It undoubtedly adds to the confusion—perhaps, one day, it will aid in solving the mystery of *P. aeruginosa* virulence regulation.

In our laboratory, we have endeavored to understand pyrimidine metabolism in *P. aeruginosa*. This is an important undertaking for at least two reasons: 1) pyrimidine metabolism is central to so many cellular processes and thus provides a good starting point for learning about potential targets for drug therapy and 2) few labs in the world are studying this aspect of metabolism in *P. aeruginosa*. A brief summary of what is

currently known about pyrimidine metabolism in general and specifically in *P. aeruginosa* follows.

Purines and pyrimidines, the molecules that make up RNA and DNA, are essential for cellular growth and for passing genetic information from one generation to the next. The enzymes for the synthesis of these molecules appear to be universal and follow the same sequence in all organisms thus far studied (O'Donovan & Neuhard, 1970; Grogan & Gunsalus, 1993). There are six enzymatic steps in the biosynthesis of uridine-5'-monophosphate (UMP; Fig. 8), which serves as a precursor for all pyrimidine nucleotides. This pathway has been studied extensively in bacteria (Neuhard & Kelln, 1996), fungi (Denis-Duphil, 1989), plants (Doremus, 1986) and animals (Jones, 1980). Although the sequence of enzymatic reactions is virtually the same, the architecture of the enzymes in the pathway can vary from one organism to the next.

General features of the pathway. The pathway responsible for UTP and CTP biosynthesis is shown in Fig. 8. The nine enzymes in this pathway have been studied most extensively in *Escherichia coli*. The pathway is initiated by the formation of carbamoylphosphate from glutamine (or ammonia), bicarbonate and ATP. The reaction is catalyzed by carbamoylphosphate synthetase (CPSase) encoded by the *carAB* operon (Anderson & Meister, 1965). Aspartate transcarbamoylase (ATCase), a multimeric enzyme encoded by the *pyrBI* genes, catalyzes the first unique reaction of pyrimidine biosynthesis (Yates & Pardee, 1956; Gerhart & Pardee, 1962), namely, the condensation of carbamoylphosphate and the amino group of aspartate to form carbamoylaspartate (ureidosuccinate) and inorganic phosphate. The reaction is driven by the hydrolysis of the high-energy acid anhydride bond of carbamoylphosphate. In the next two steps, the

pyrimidine ring is formed through cyclization and oxidation. Cyclization of carbamoylaspartate is catalyzed by dihydroorotase (DHOase; *pyrC*) and yields

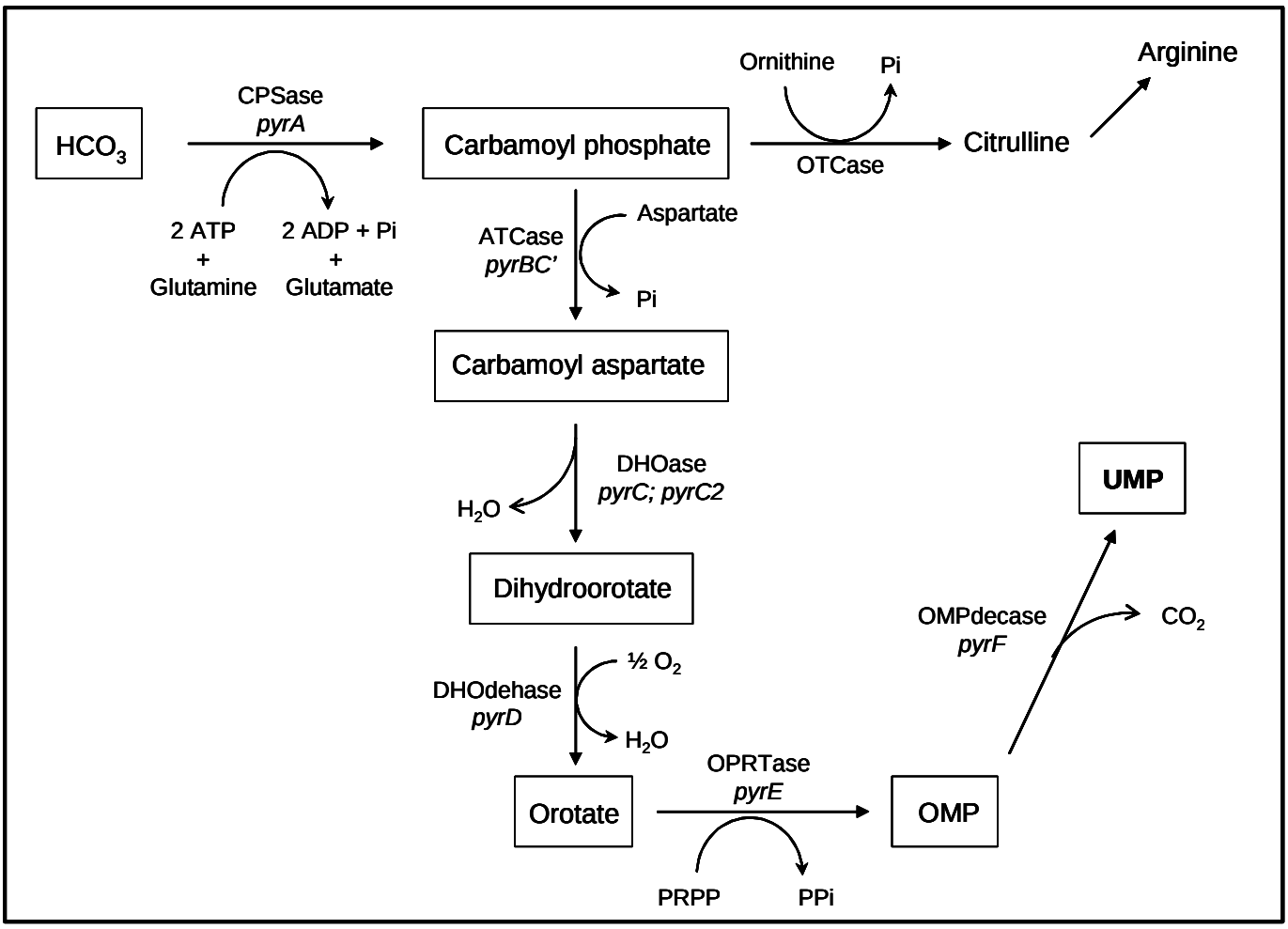

Fig. 8. The pyrimidine biosynthetic pathway in *P. aeruginosa*. The enzyme names are abbreviated as in the text. The gene designations for each of the pyrimidine enzymes is listed beneath in italics.

dihydroorotate (Washabaugh & Collins, 1986). Dihydroorotate dehydrogenase (DHOdehase; *pyrD*), a membrane bound enzyme that is linked to the electron transport system, carries out the oxidation of dihydroorotate to orotate (Larsen & Jensen, 1985; Karabian & Couchoud, 1974). The first pyrimidine nucleotide is formed by the transfer of ribose-5'-phosphate from γ-D-5'-phosphoribosyl-1'-pyrophosphate (PRPP) to orotate, to produce orotidine 5'-monophosphate (OMP) and PP_i (Lieberman & Kornberg, 1954), a reaction that is catalyzed by orotate phosphoribosyltransferase (OPRTase; *pyrE*). Next OMP is decarboxylated to UMP by OMP decarboxylase (OMPdecase; *pyrF*) (Scapin *et al.*, 1993).

The generation of UTP involves phosphorylation of UMP to UDP and then to UTP by the sequential action of UMP kinase (*pyrH*) (O'Donovan & Gerhart, 1972; Serina *et al.*, 1995), a highly specific enzyme, and nucleoside diphosphate kinase (*ndk*) which is non specific (Ginther & Ingraham, 1974). Finally, UTP is aminated to CTP by the enzyme CTP synthetase (*pyrG*) which uses glutamine as the preferred amino group donor and ATP to energize the reaction (Long & Koshland, 1968; Anderson, 1983).

Properties of the enzymes. Carbamoylphosphate synthetase - CPSase (*pyrA; carAB)* (EC 6.3.5.5) is an allosteric enzyme that catalyzes the synthesis of carbamoylphosphate (CP) from bicarbonate and glutamine or ammonia at the expense of two molecules of ATP. One ATP is required for the formation of the reaction intermediate, carboxyphosphate, and the other is required for a kinase reaction in which enzyme-bound carbamate becomes phosphorylated (Anderson & Meister, 1965). Several different types of CPSase have been identified on the basis of their specificity for either

ammonia or glutamine as the physiological nitrogen donor, and their requirement for N-acetyl-L-glutamate as cofactor (Legrain *et al.*, 1995).

Aspartate transcarbamoylase - ATCase (*pyrB)* (EC 2.1.3.2) encoded by *pyrBI* in *E. coli*, catalyzes the first step unique to pyrimidine synthesis and exists in a number of forms (Fig. 9). The basic catalytic component of all bacterial ATCases, however, is a homotrimer of approximately 34 kDa polypeptides. This arrangement has been shown in *E. coli* (Ke *et al.*, 1984) and *Bacillus subtilis* (Brabson & Switzer, 1975), and is a consequence of the active sites being shared between adjacent polypeptides (Robey & Schachman, 1985). The classification of bacterial ATCases is based on molecular size, which varies depending on whether or not the catalytic subunit is associated with other non-catalytic subunits, and the nature of these subunits. In the earliest classification, Bethell & Jones (1969) proposed three classes of bacterial ATCases on the basis of size (Fig. 9).

Class A ATCases are the largest and the most prevalent class in nature. A number of these enzymes have been purified to date from *Pseudomonas fluorescens* (Bergh & Evans, 1993), *P. syringae* (Shepherdson & McPhail, 1993), *P. putida* (Schurr *et al.*, 1995) *P. aeruginosa* (Vickrey, 1993), *Thermus* sp. Z015 (Van de Casteele *et al.*, 1997), *Acinetobacter calcoaceticus, Azotobacter vinelandii, Azomonas agilis, Deinococcus radiophilus, Paracoccus denitrificans* and *Leucothrix mucor* (Kenny *et al.*, 1996). These enzymes were shown to have molecular masses ranging from 450 to 500 kDa. In addition to the six 34 kDa PyrB polypeptide chains, the holoenzyme contains six polypeptide chains of around 45 kDa, forming a dodecameric structure composed of two

catalytic trimers (34 kDa X 3) associated with three (frequently non-catalytic) dimers (45 kDa X 2)

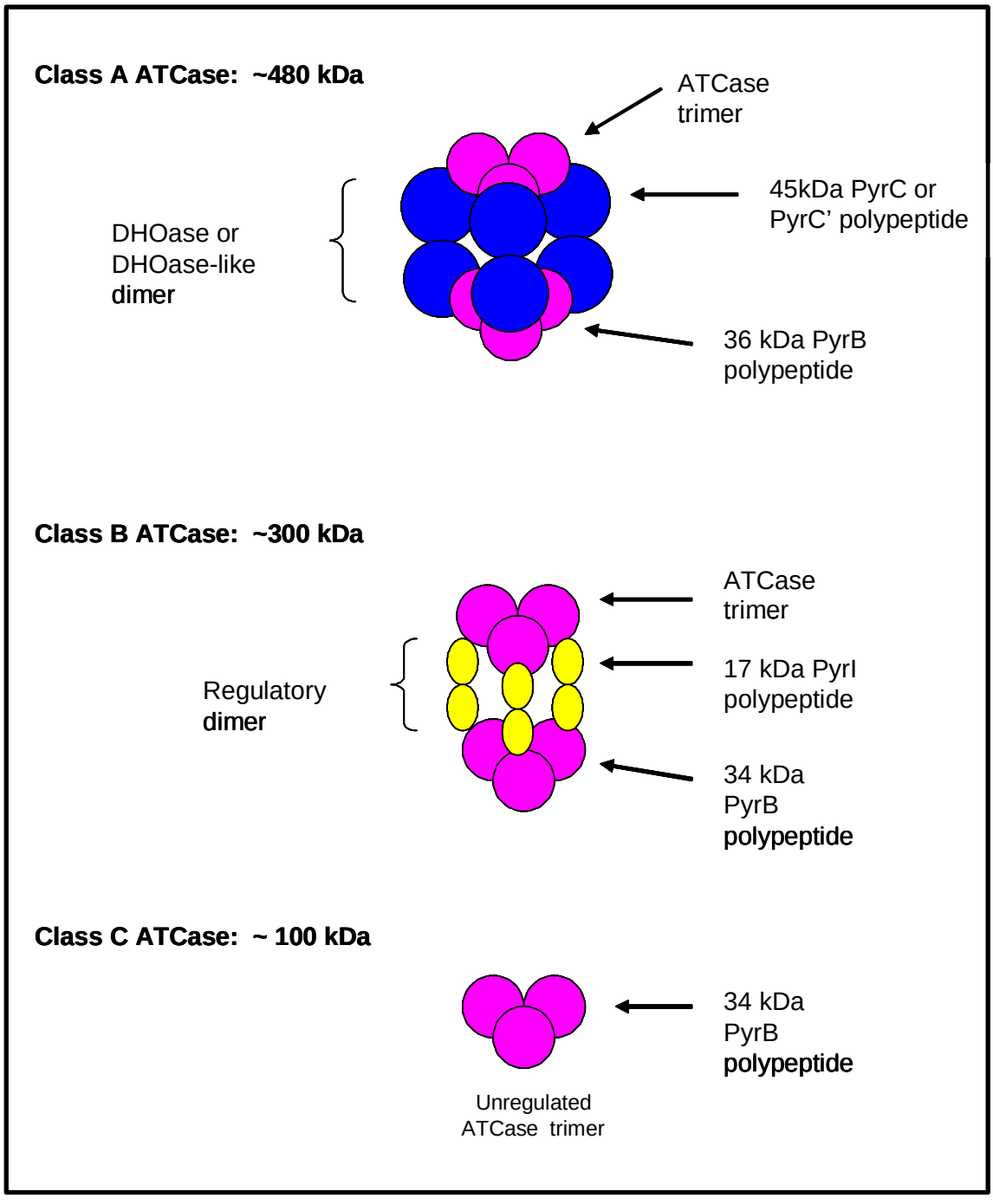

Fig. 9. The three classes of bacterial ATCases. Adapted from Bergh & Evans, 1993; Schurr et al., 1995.

(Fig. 9). The enzyme kinetics of class A ATCases have been shown to follow the Michaelis –Menten model typical of non-cooperativity. Also, the ATCase from *P. aeruginosa* was found to be inhibited by the effectors ATP, CTP and UTP, with ATP showing the greatest inhibitory effect (Linscott, 1996).

Dissociation of the class A enzymes into separate subunits under conditions which retain activity has not been achieved (Bergh & Evans, 1993; Shepherdson & McPhail, 1993; Schurr *et al.*, 1995; Kenny *et al.*, 1996). The function of the 45 kDa chains is not yet fully known, but a BLAST search of the protein data base with the derived amino acid sequence suggests that this polypeptide is, in some cases, a non-functional homolog of the next enzyme in the pathway, namely DHOase. The DHOase-like polypeptide is encoded by a gene designated *pyrC'* in the pseudomonads (Schurr *et al.*, 1995). The PyrC' polypeptide has considerable amino acid sequence identity with active DHOases, and currently it is the most similar to the *pyrC* encoded DHOase from *Ralstonia solanocarum* with 41 % amino acid identity and 61 % homology. PyrC' chains lack DHOase activity most likely because of the absence of essential histidine residues in conserved regions of the DHOase-like sequence (Zimmerman *et al.*, 1995). It appears that the PyrC' polypeptides are required to maintain the structure and thus, the function of the catalytic ATCase (Schurr *et al.*, 1995). The *pyrB* and *pyrC'* genes of *P. aeruginosa* and *P. putida* have been cloned into individual plasmid vectors. When the *pyrB* plasmids (pAKB10 and pDBAB) were transformed into the *E. coli pyrB* auxotroph, TB2, prototrophy was not achieved. The same was true for the *pyrC'* plasmids (pDBAC' and pDBPC'), such that when they were transformed into the *E. coli pyrC* auxotroph, X7014a, prototrophy was not obtained. However, co-transformation of both *pyrB* and

pyrC' plasmids (from the same species or one each from *P. putida* and *P. aeruginosa*) into TB2 does result in prototrophy and the production of a 480 kDa ATCase. These data show that neither the *pyrB* nor *pyrC'* gene products are active alone (Brichta *et al*,. 1997).

Class B ATCase holoenzymes have a molecular mass of 310 kDa, are composed of two catalytic homotrimers and three regulatory homodimers, and are allosterically regulated (Kantrowitz & Lipscomb, 1988; Fig. 9). This class of enzyme cooperatively binds substrates and thus the saturation kinetics are sigmoidal. Extensive studies have been conducted on the ATCases from several enteric bacteria including *E. coli, Salmonella typhimurium, Yersinia enterocolitica, Proteus vulgaris* and *Serratia marcescens* (Shanley *et al.*, 1984; Wild *et al.*, 1976; Beck *et al.*, 1989). The ATCase of *E. coli* is activated by ATP and inhibited by CTP and UTP (Wild *et al.*, 1989). These effectors bind to the N-terminal region of the regulatory chains and cause a conformational change in the dodecameric enzyme. When an activator is bound, the enzyme assumes the R-state where substrate binding sites are more accessible. When the negative effector CTP is bound, the enzyme assumes the T-state where substrate binding is more difficult. The regulatory chains bind one zinc atom per regulatory subunit at the C-terminus, six zinc atoms per holoenzyme. The zinc atoms are necessary to maintain the dodecameric structure. Mercury has been used to displace the zinc resulting in the dissociation of the catalytic trimers from the regulatory dimers. The trimers are active but unregulated (Gerhart & Holoubek, 1967). Dialysis in ATCase buffer, containing zinc, to remove the mercury and replace zinc allows the dodecameric enzyme to be reconstituted.

Class C ATCases are 100 kDa catalytic trimers which are not associated with any other polypeptides. This form is also widely represented in nature having been found in

all Gram-positive bacterial ATCases thus far examined including *Bacillus subtilis* (Brabson & Switzer, 1975), *Lactobacillus leichmanii* (Becker & Brendel, 1996) and three Gram negative organisms, *Lysobacter enzymogenes (*Switzer & Quinn, 1993*),* *Stenotrophomonas maltophilia* (Linscott, 1997) and *Xanthomonas campestris (*Kenny *et al.*, 1996). This form of ATCase is not regulated by nucleotide effectors and displays Michaelis-Menten saturation kinetics.

In higher eukaryotic organisms, the first three enzymes of the pyrimidine biosynthetic pathway are found in the multifunctional enzyme CAD (CPSase, ATCase and DHOase). This enzyme has a subunit molecular mass of 240 kDa and has been isolated in trimeric and hexameric form (Hemmens & Carrey, 1994). Limited trypsin digests of the multifunctional enzyme results in three protein domains, each possessing a different catalytic activity. The deduced amino acid sequence of the ATCase domain shows 44 % identity with the catalytic subunit of the *E. coli* enzyme. CAD has no domain homologous to the regulatory chain of the bacterial ATCase, which accounts for the absence of allosteric effects by ATP or pyrimidine nucleotides as in enteric bacteria (Hemmens & Carrey, 1994).

Dihydroorotase - DHOase (*pyrC*) (EC 3.5.2.3) in *E. coli* is a homodimer with a subunit molecular mass of 38 kDa (Sander & Heeb, 1971). It catalyzes the cyclization of N-carbamoyl-L-aspartate (CAA), the product of the ATCase reaction, to dihydroorotate (DHO). The DHOase from *E. coli* was found to bind preferentially to L-CAA with a K_m of 0.47 mM, while the K_m for the D-form was 41 mM. Assays with a mixture of D,L-CAA resulted in a K_m value of 0.85 mM (Daniel *et al*., 1996). The conversion of CAA to DHO is readily reversible, however, the cyclization reaction has a pH optimum range of

5.8 to 6.2, while the hydrolysis reaction occurs preferentially from pH 7.5 to 9.0 (Taylor *et al*., 1976; Christopherson & Jones, 1979). The enzyme has been purified to homogeneity from *Clostridium oroticum* and was found to be a homodimer with subunit molecular mass of 55 kDa (Taylor *et al.*, 1976). DHOase has also been purified from *E. coli* (Sander & Heeb, 1971; Washabaugh & Collins, 1984) and *P. putida* (Ogawa & Shimizu, 1995) where it was found to be a homodimer with a subunit molecular mass of 38 kDa. DHOase is a metallo-enzyme and has been reported to contain one tightly bound essential zinc ion per subunit (Washabaugh & Collins, 1984) in addition to two weakly bound structural zinc ions per subunit which are not essential for activity (Washabaugh & Collins, 1986). This enzyme is discussed in more detail below.

Dihydroorotate dehydrogenase - DHOdehase (*pyrD*) (EC 1.3.3.1), also called dihydroorotate oxidase (Karibian, 1978) catalyzes the only redox reaction in the synthesis *de novo* of UMP. DHOdehase, which is membrane bound, catalyzes the oxidation of dihydroorotate to orotate. In *E. coli*, there is evidence that the physiological electron acceptor in the presence of oxygen is ubiquinone (Kerr & Miller, 1968); in anaerobically grown cells, menaquinone appears to be an obligatory electron carrier between dihydroorotate and fumarate (Andrews *et al.*, 1977). The homodimeric enzyme (subunit mass, 37 kDa) was purified to near homogeneity from *E. coli* (Karibian & Couchoud, 1974; Larsen & Jensen, 1985). The absorption spectrum of the oxidized enzyme indicates one flavin nucleotide (FMN) per subunit**.**

Lactococcus lactis contains two *pyrD* gene sequences (*pyrDa* and *pyrDb*) both of which code for DHOdehases (Andersen *et al.*, 1994). The A form of DHOdehase, encoded by *pyrDa*, is a homodimer and has significant amino acid identity with the

DHOdehase of yeast (Andersen *et al.*, 1994). The B form of DHOdehase has amino acid identity with the enzyme from *B. subtilis* and consists of two different subunits, encoded by *pyrDb* and *pyrK* (Nielsen *et al.*, 1996). The *L. lactis* DHOdehase complex appears to be a hetero-tetramer of two PyrDb and two PyrK subunits. It has been suggested that this tetrameric form of the enzyme is representative of the DHOdehases from Gram-positive bacteria (Nielsen *et al.*, 1996).

Orotate phosphoribosyltransferase - OPRTase (*pyrE*) (EC 2.2.4.10) formerly known as OMP pyrophosphorylase, catalyzes the nucleotide-forming step in the pathway. Products OMP and PP_i are produced from the substrates orotate and PRPP in a Mg^{2+}-dependent reaction. The active form of OPRTase is a homodimer formed of 23 kDa subunits. The enzyme from both *E. coli* and *S. typhimurium* has been crystallized (Aghajari *et al.*, 1994; Scapin *et al.*, 1993).

Orotidine monophosphate decarboxylase - OMPdecase (*pyrF*) (EC 4.1.1.23) catalyzes the sixth step of the *de novo* pathway whereby OMP is irreversibly decarboxylated to UMP, the precursor compound for all other pyrimidine nucleotides. While essentially all of the reactions in the *de novo* pathway up to this one are reversible, this irreverisble step “pulls” the pathway forward to the product UMP. The decarboxylation reaction does not require a coenzyme. The subunit molecular mass is 26 kDa in *E. coli* as well as in other bacteria, with the enzyme being catalytically active as a dimer (Donovan & Kushner 1983; Jensen *et al.*, 1984). Whereas in bacteria, the OPRTase (*pyrE*) and OMPdecase (*pyrF*) activities are catalyzed by two monofunctional enzymes, in higher eukaryotes, these last two reactions are catalyzed by the bifunctional enzyme known as UMP synthase (Jones, 1980). Limited proteolysis of UMP synthase

with elastase or trypsin produces two separate domains: the amino terminal domain containing the OPRTase polypeptide and the carboxy-terminal domain containing the catalytic OMPdecase (Lin & Suttle, 1993). The *pyrE* and *pyrF* encoded functions are fused into a bifunctional protein in mammalian cells most likely because the covalent union in UMP synthase stabilizes the domains containing the respective catalytic centers. This stability is necessary in eukaryotic organisms where the molar concentration of UMP synthase is found to be far lower than are the *pyrE* and *pyrF* products in microorganisms (Yablonski *et al.*, 1996).

Uridine monophosphate kinase - UMP kinase (EC 2.7.4.4)(*pyrH*) catalyzes the next step in pyrimidine synthesis which is the phosphorylation of UMP to UDP. The deduced subunit molecular mass is 26 kDa. Purified UMP kinase is active as a homohexamer and is specific for UMP. The nucleotide phosphates dUMP, CMP, and dCMP are not substrates for this reaction. UMP kinase is one of the control points in the pyrimidine pathway and thus is allosterically regulated by the nucleotides GTP, a positive effector, and UTP, a negative effector (Serina *et al.*, 1995).

Nucleoside diphosphate kinase - NDK (*ndk*) (EC 2.7.4.6) catalyzes the synthesis of all NDPs to their corresponding NTPs. As mentioned previously, this enzyme, in its cytoplasmic form, has little substrate specificity, as all rNTPs and dNTPs can function as donors of the γ-phosphate group, and any rNDP or dNDP may serve as the phosphate acceptor (Ohtsuki *et al.*, 1984; Ginther & Ingraham, 1974). Mg^{2+} is required for activity, and the reaction occurs in two steps, with the intermediate formation of a phosphoenzyme (Ginther & Ingraham, 1974; Hama *et al.*, 1991). The *E. coli* K-12 enzyme has a subunit molecular mass of 16 kDa and the active form of the enzyme

appears to be a tetramer of molecular mass 64 kDa (Ohtsuki *et al.*, 1984). However, as previously stated, in *P. aeruginosa* Ndk is cleaved by elastase as the cells enter stationary phase. The new 12 kDa form of the enzyme associates with pyruvate kinase in the membrane and becomes specific for the conversion of GDP to GTP. This shift in metabolism is necessary, as there is an increased demand for GTP which is necessary for the synthesis of alginate and signaling molecules (Kim *et al*., 1998).

Cytidine triphosphate synthetase – CTP synthetase (EC 6.3.4.2) (*pyrG*) catalyzes the ninth step in pyrimidine ribonucleotide biosynthesis, the formation of CTP from UTP, ATP, and glutamine. The activity of this enzyme is stimulated by GTP (Koshland & Levitzki, 1974). Like other glutamine amidotransferases, CTP synthetase can utilize ammonia instead of glutamine, although with much lower efficiency. The molecular mass of the *E. coli* CTP synthetase polypeptide is 60 kDa. The enzyme was purified to homogeneity, and its physical and kinetic properties have been described (Anderson, 1983; Koshland & Levitzki, 1974). Under assay conditions, the enzyme exists as a homotetramer, but in the absence of ATP and UTP, it dissociates to active dimers. The reaction mechanism involves the initial glutamylation of a specific cysteine residue on the enzyme, with the liberation of ammonia. The nascent ammonia immediately reacts with UTP, and in a series of steps that probably involves a phosphorylated amido-derivative of UTP (von der Saal *et al.*, 1985), CTP is formed at the expense of one ATP. The glutamine reaction is markedly accelerated by GTP which increases the V_{max} and decreases the K_m for glutamine, but has no effect on the reaction with ammonia as the amide donor.

The importance of studying dihydroorotase. DHOase was first identified in extracts from *Zymobacterium oroticum* (now *Clostridium oroticum*) by Lieberman & Kornberg in 1954 where they found the enzyme to be involved in both the biosynthesis and the degradation of pyrimidines. Purification studies indicated that the enzyme was a homodimer with a molecular mass of 110 kDa and it required two atoms of zinc or cobalt per monomer (Sander *et al*., 1965; Taylor *et al*., 1976). DHOase activity was first detected in extracts from *E. coli* by Yates & Pardee in 1956 where partial purification indicated that the enzyme in this organism was also a homodimer but with a molecular mass of 82 kDa. DHOase is one of the few biosynthetic enzymes to synthesize an amide bond without a directly coulpled energy source such as ATP hydrolysis to drive the reaction (Brown & Collins, 1991). As previously stated, the reaction is influenced by the ambient pH as the cyclization reaction is favored when the pH is below 7.1, while hydrolysis is favored at pH 7.1 or greater (Christopherson & Jones, 1979). The substrate N-carbamyl-L-aspartate is also cabable of some interesting transformations. In the absence of DHOase, the amide cyclization reaction product is a 5-membered hydantoin, while in the presence of the enzyme the amide cyclization product is the 6-membered pyrimidine ring, DHO (Fig. 10) (Daniel *et al*., 1996).

The catalytic mechanism of action for DHOase has been probed by several research groups using techniques such as site-directed mutagenesis (Williams *et al*., 1995; Zimmermann *et al*., 1995), the preparation of metal-substituted variants (Brown & Collins, 1991), and amino acid sequence alignments indicating conserved residues that likely interact with metals or substrates (Williams *et al*., 1995). These studies allowed a general model of the DHOase active site to be generated, where one zinc atom is tightly

bound per active site and three conserved histidine residues (His 16, His 18, and His 177) are direct metal ligands. Other amino acids (Arg 20, Asp 250 and His 139) were proposed

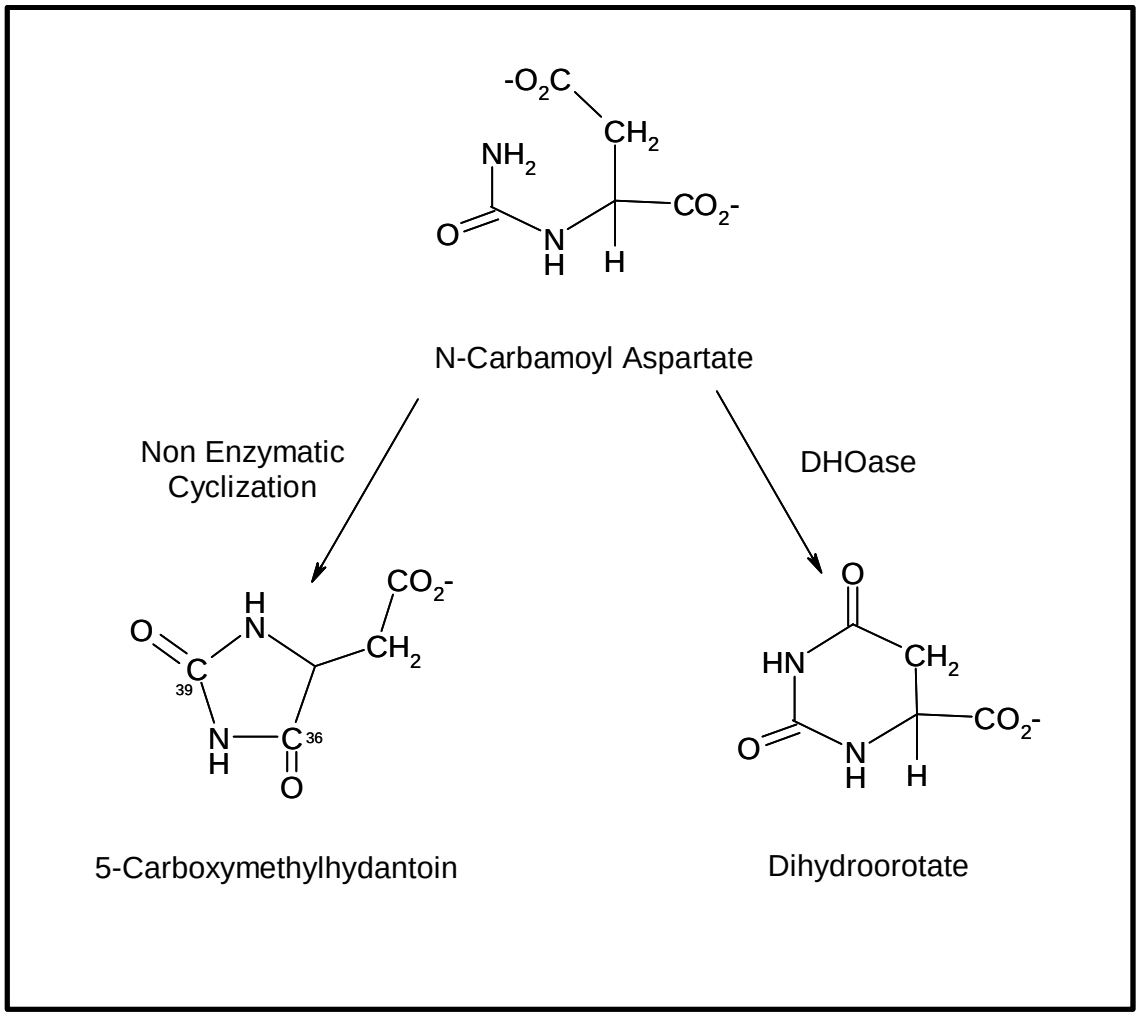

Fig. 10. Enzymatic and nonenzymatic cyclization reactions for N-carbamoyl aspartate.

to function as general acid-base catalysts and/or in the binding of substrates to the active site (numbering refers to that of the *E. coli* enzyme) (Fig. 11).

Analysis of the three-dimensional structure of DHOase revealed that it was a member of a broad set of amidohydrolases related to urease, known as the amidohydrolase superfamily (Holm & Sander, 1997). Members of this family also include allantoinases and hydantoinases (involved in the catabolism of purines and pyrimidines), and adenosine and cytosine deaminases, to name a few. These enzymes share a common structural core consisting of an ellipsoidal $(\beta\alpha)_8$ barrel with a conserved metal binding site at the C-terminal end of strands β_1, β_5, β_6 and β_8. The common reaction mechanism involves the activation of water, making it a good nucleophile, by decreasing its pK_a from that of free water, 15.7, to 7 when bound to a four-coordinated cation, such as zinc in the case of DHOase (Holm & Sander, 1997; Syldatk *et al*., 1999).

Recently, however, the crystaline structure for the *E. coli* DHOase has been elucidated (Thoden *et al*., 2001). This new evidence indicates that the active site contains a binuclear center, with the ε-amino group of Lys 102 carboxylated and serving as one of the two bridging ligands to the pair of zinc atoms. This report contradicts the original conclusion that DHOase contained a single zinc atom per active site (Washabaugh & Collins, 1984). The new model of the DHOase active site predicts that four histidine residues (His 16, His 18, His 139 and His 177) in conjunction with Lys 102, with a posttranslationally carboxylated ε-amino group, and Asp 250, coordinate two zinc ions with the help of a hydroxide ion (Fig. 12). These components bind DHO or CAA and promote the hydrolysis or cyclization of the substrates respectively. CAA preferentially binds to the protonated form of the binuclear metal center, where the bridging hydroxide

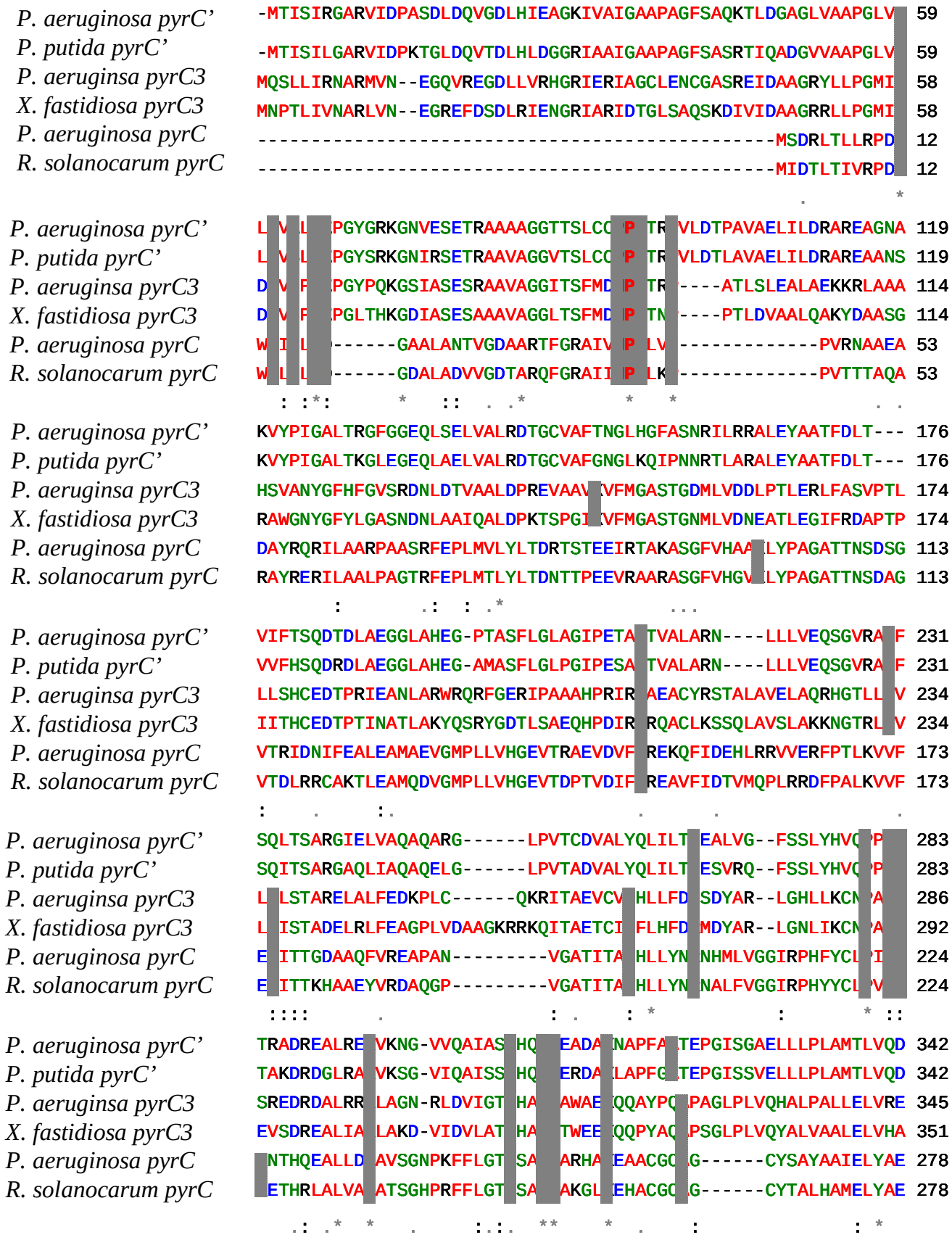
P. aeruginosa pyrC'
P. putida pyrC'
P. aeruginsa pyrC3
X. fastidiosa pyrC3
P. aeruginosa pyrC
R. solanocarum pyrC

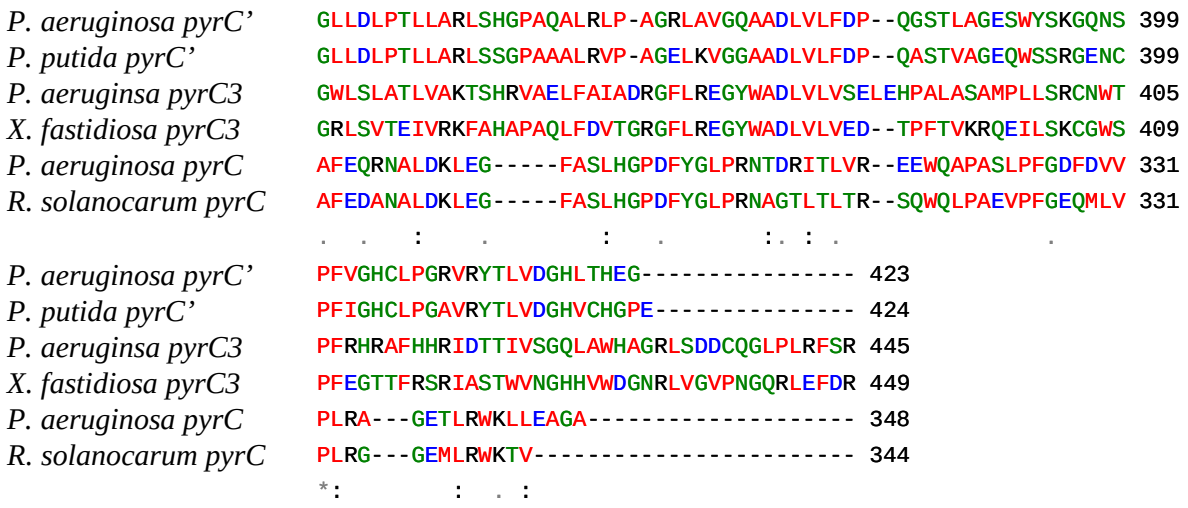

Figure 11. Amino acid alignment of the three *P. aeruginosa* PyrC sequences with their three closest homologues. Each of the PyrC sequences was aligned using the CLUSTAL W alignment tool. The amino acids are colored according to class. Red are nonpolar, aliphatic residues (A, V, L, I, P) and the aromatic residues F and W. Blue are negatively charged residues (D, E). Green are the polar, uncharged residues (S, T, C, M, N, Q), the nopolar residue G, and the aromatic residue, Y. Black are the positively charged residues (K, R, H). The symbols indicate as follows: identical residues (*), complete homology (:), complete charge homology (.).

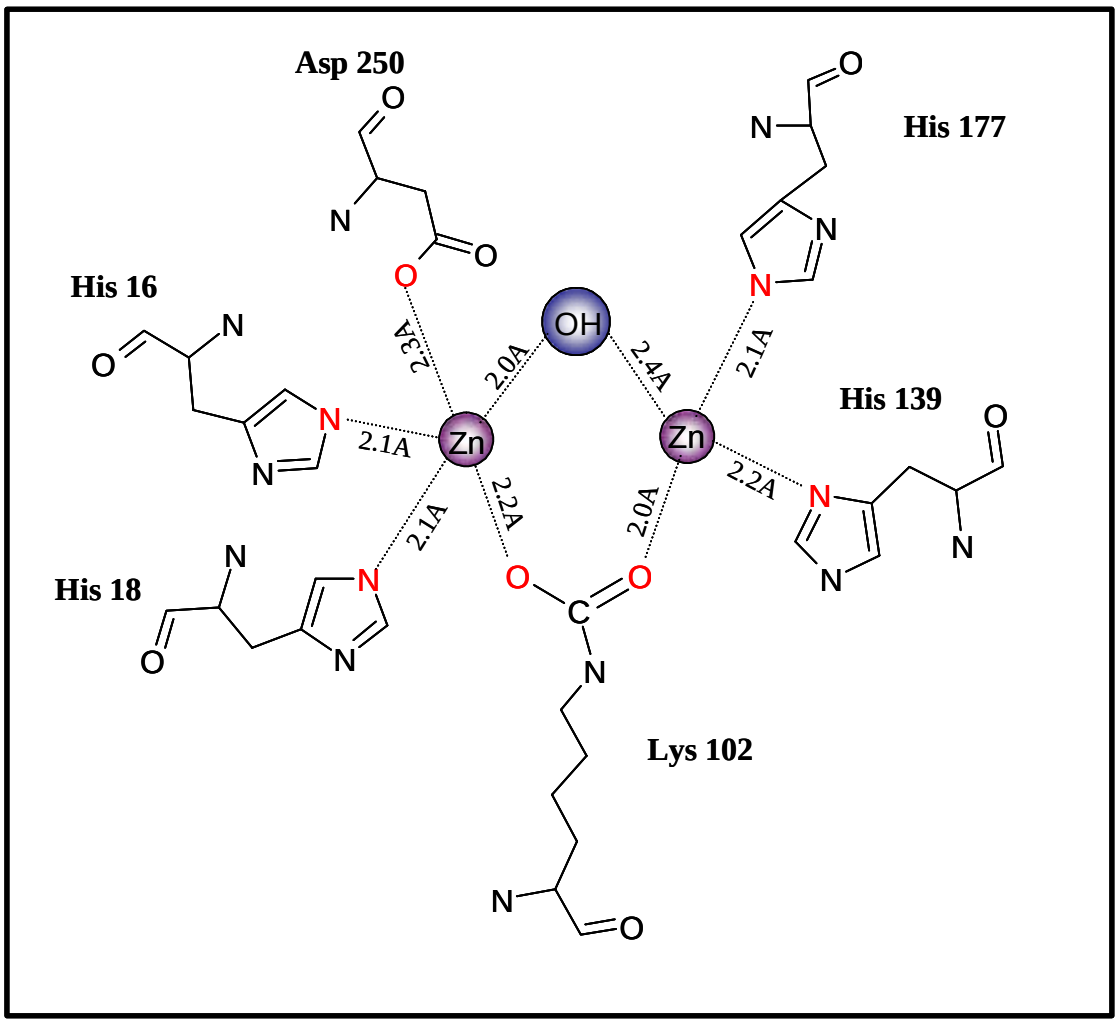

Fig. 12. Binuclear metal center of the *E. coli* DHOase active site. Coordination geometry for the binuclear center at the active site in DHOase. Amino acid numbers are based on the *E. coli* enzyme. Adapted from Thoden, et al., 2000.

group has accepted a proton from the solvent to form a water molecule that resides mainly on the β-metal ion. This possibly explains the observation that the biosynthetic reaction is favored when the pH is less than 7.1 (Christopherson & Jones, 1979).

Pyrimidine biosynthesis is essentially a universal process, thus almost all organisms, with the exception of some parasites, possess the genes encoding the enzymes necessary to carry it out. As a result, several *pyrC* sequences have been reported to date. Comparisons of these sequences show there to be two general types of DHOases (Fig. 13). One group, here designated Type I (the "enteric" type), consists of a homodimer with a polypeptide molecular mass of 37-40 kDa. This form of DHOase has been found in *E. coli* (Brown & Collins, 1991), *Salmonella typhimurium* (Neuhard *et al*., 1986) and *Vibrio cholerae* (GenBank), but has not yet been found in association with any other polypeptides, thus it appears to be monofunctional. The second group, designated here Type II, ("*Bacillus"* type), has a polypeptide molecular mass of 45-55 kDa. This type of DHOase has been isolated as a monofunctional homodimer from *Clostridium oroticum* (Taylor *et al*, 1976), *B. subtilis* (Quinn *et al*., 1991) and *L. leichmannii* (Gröninger *et al*., 1995). Type I DHOases have also been found to associate with ATCase trimers to form the 480 kDa dodecameric enzyme, which has both ATCase and DHOase activities, found in *Thermus* sp (Van de Casteele *et al*., 1997). In *Synechocystis*, and in the pseudomonads, this type of DHOase is not catalytically active, but is maintained because of a structural requirement for the function of the 480 kDa ATCase.

When it was determined that the DHOase-like polypeptides associated with the *P. aeruginosa* ATCase did not have DHOase catalytic activity (Vickery, 1993), the search for the gene encoding DHOase activity was initiated. A cosmid library from

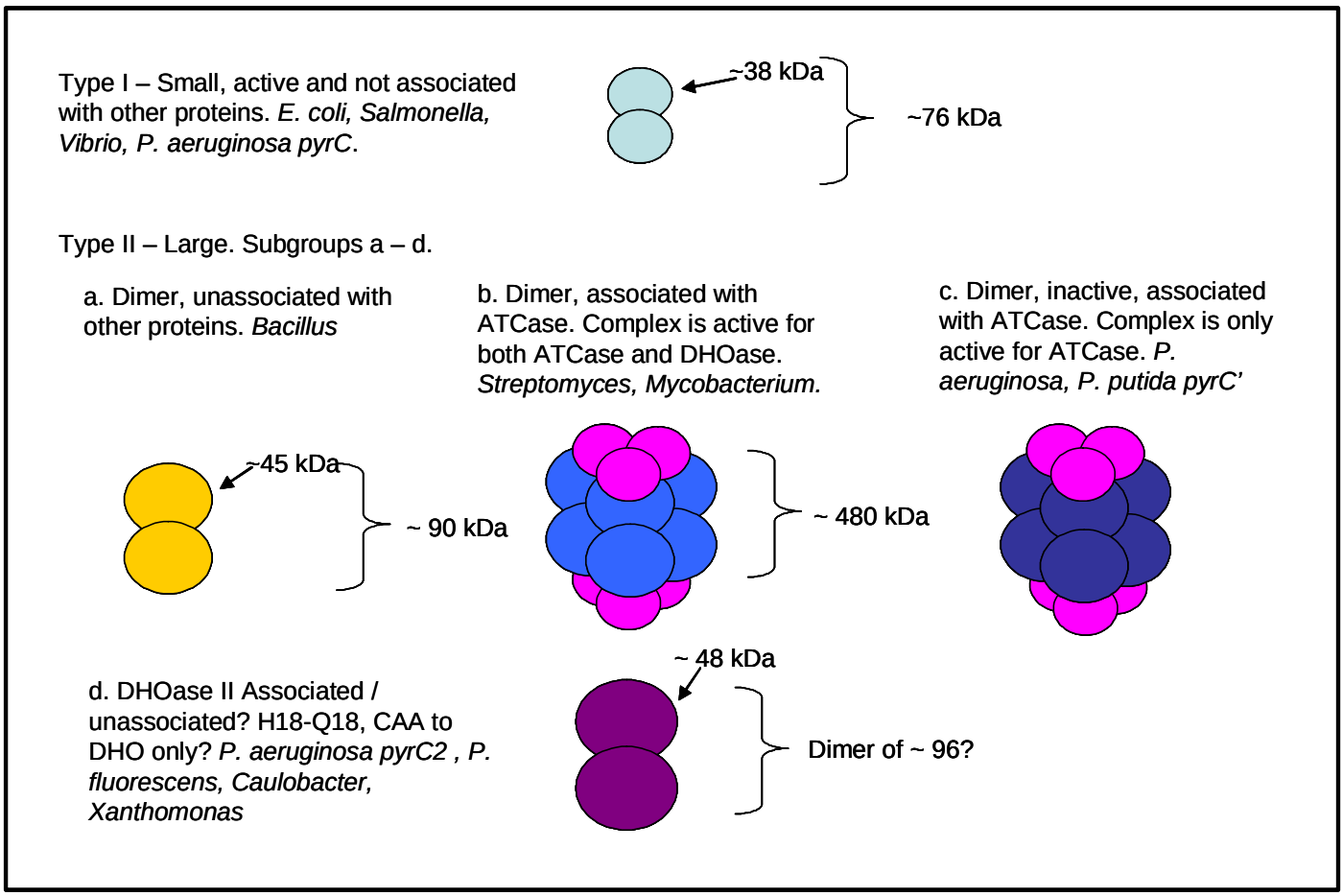

Fig. 13. Description the architecture of bacterial DHOases.

P. aeruginosa, kindly provided by Dr. Abdelal at Georgia State University, was screened by transformation into an *E. coli pyrC* strain, X7014a. Selection for pyrimidine prototrophy resulted in the isolation of a cosmid containing the *pyrC* gene. The *pyrC* gene was isolated from the cosmid and sequenced. It was initially hypothesized that the two *pyrC* genes in *Pseudomonas*, *pyrC* and *pyrC'*, most likely arose as the consequence of a gene duplication event and that, as a result, their DNA and amino acid sequences would be very similar. It was thus a great surprise when the active DHOase was determined to have 64 % amino acid identity and 73 % homology with the DHOase from *V. cholerae*. It thus appears that the contemporary *pyrC* and *pyrC'* genes did not arise from a gene duplication event in *P. aeruginosa*.

The completion of the *Pseudomonas aeruginosa* genome sequence revealed the presence of a third *pyrC* gene in this organism. BLAST analysis of the genome sequence showed this gene, designated *pyrC2*, to encode a polypeptide of 49 kDa (larger than any DHOase described to date) that was most similar to the DHOase from *Xylella fastidiosa*, with 52 % identical and 62 % homologous amino acid residues. The *pyrC2* gene was subsequently isolated by PCR and cloned into pUCP19. The resulting plasmid was able to complement the *E. coli pyrC* auxotroph X7014a.

Thus, the genome of *P. aeruginosa* contains three *pyrC* genes, one inactive but necessary for ATCase activity and designated *pyrC'*, and two *pyrC* genes, *pyrC* and *pyrC2*, encoding active DHOases of greatly different size. In order to determine more about the roles of the two DHOases in *P. aeruginosa*, both the *pyrC* and *pyrC2* genes were knocked out individually. Neither knock-out strain exhibited a requirement for pyrimidines, further demonstrating that both *pyrC* genes encode functional DHOases that

are able to take part in pyrimidine biosynthesis. In addition, a double mutant was created. This strain was blocked in the synthesis of pyrimidines and required uracil for growth on minimal medium, thus, this dissertation represents the first report of a true block in dihydroorotase synthesis for *P. aeruginosa* PAO1.

Recent findings indicate that the pyrimidine biosynthetic pathway and its intermediates may be even more important for bacterial metabolism than originally thought. Maksimova *et al*. (1993) reported that a *P. putida* DHOase mutant failed to produce the siderophore pigment pyoverdin. The *P. aeruginosa* DHOase mutant was also found to produce significantly less pyoverdin than the wild type. In addition, it was observed that the mutant produced only 40 % of the phenazine antibiotic pyocyanin produced by wild type.

Further examination of the *P. aeruginosa* DHOase mutant showed it to be severely impaired in its ability to produce the exoenzymes elastase, casein protease and haemolysin. Moreover, the DHOase mutant was defective for swimming, swarming and twitching forms of motility. Curiously, the addition of uracil did not restore pigment or virulence factor production to wild type levels. Thus, this research demonstrates a potential role for pyrimidine intermediates in the virulence response of *P. aeruginosa* and should lead to the synthesis of novel targets for chemotherapy to thwart infection.

CHAPTER II

METHODS

Bacterial Strains, Plasmids, Media and Growth Conditions.

The bacterial strains and plasmids used in this study are listed in Table 1. *Pseudomonas* strains were cultivated in *Pseudomonas* minimal medium (Psmm) (Ornston & Stanier, 1966) which contains per liter: 25 ml of 0.5 M Na_2HPO_4, 25 ml of 0.5 M KH_2PO_4, 10 ml of 10 % $(NH_4)_2SO_4$ and 10 ml of concentrated base in 930 ml of distilled, deionized H_2O (ddH_2O). The carbon source, either 0.2 % glucose or 0.4 % succinate, was added to the medium when it was cool. When making concentrated base, it is important to add the ingredients in the order in which they are listed and that each ingredient be completely dissolved prior to the addition of the next ingredient. Failure to follow this procedure results in precipitation of the added chemicals. To 600 ml of ddH_2O 14.6 g KOH is added. Next, 20 g of nitriloacetic acid is added. Additional chemicals are added in the following order and amounts: $MgSO_4$ anhydrous (28.9 g), $CaCl_2 \bullet 7\ H_2O$ (6.67 g), $(NH_4^+)_6Mo_7O_{24} \bullet 7H_2O$ (18.5 g), $FeSO_4 \bullet 7H_2O$ (198 mg), and 100 ml "Metals 44." The pH is adjusted to 6.8 prior to bringing the volume to 1000 ml with ddH_2O. "Metals 44" consists of the following components, again added in order and dissolved fully prior to the addition of the next chemical: To 800 ml ddH_2O add 2.5 g EDTA, at pH 8.0 to be soluble, $ZnSO_4 \bullet 7\ H_2O$ (10.95 g), $FeSO_4 \bullet 7\ H_2O$ (5.0 g), $MnSO_4 \bullet H_2O$ (1.54 g) $CuSO_4 \bullet 5\ H_2O$ (392 mg), $CuSO_4$ anhydrous (251 mg), $Co(NO_3)_2 \bullet 6\ H_2O$ (250 mg) or $Na_2B_4O_7 \bullet 10\ H_2O$ (Borax) (177 mg). To further prevent precipitation, a few drops of H_2SO_4 are added. The volume was brought to one liter by the addition of ddH_2O. "Metals 44"

Strain or plasmid	Genotype or relevant characteristic	Source or reference
P. aeruginosa		
PAO1	Prototroph	ATCC
PAODB37	PAO1 *pyrC*Δ	This study
PAODB70	PAO1 *pyrC3::aacCI*	This study
PAODB92	PAO1 *pyrC*Δ *pyrC3::aacCI*	This study
E. coli		
DH5α	*recA1 hsdR17 endA1 supE44 thi-1 relA1 gyrA96* Δ*(argF-lacZYA)U169* ϕ*80lacZ*Δ*M15*	BRL, 1986
X7014a	F^- *pyrC46 purB51 thi-1 lacZ43 or 13 malA1 xyl-7 mtl-2 str-125* λ^R λ^-	J. Beckwith
SM10	Km^R *thi thr leu tonA lacY supE recA*::Rp-2 Tc::Mu	Simon et al., 1983
Plasmids		
pUCP19	Ap^R (Cb^R) source of *lacZ* α *bhr*	Schweizer, 1991
pEX18Gm	Gm^R *oriT sacB*$^+$ gene replacement vector with MCS from pUC18	Hoang et al., 1998
pGMΩ1	Gm^R Ap^R aacC1 gene flanked by Ω transcriptional terminators	Schweizer, 1993
pRTP1	Ap^R *rpsL oriT cps*	Stibitz et al., 1986
pPAC1	pUCP19 with 2.5-kb insert of PAO1 genome containing *pyrC, motY* and partial *argG*	This study
pPACΔ29	*pyrC*Δ in pUCP20	This study
pPAC3-6	pUCP19 with 1.7-kb insert containing *pyrC3* gene	This study
pPAC3:GmΩ	pPAC3-6 with Gm casset inserted into the middle of the *pyrC3* gene	This study
pRTPC3:GmΩ	pRTP1 containing *pyrC3*::Gm	This study
pQF50	Ap^R promoterless *lacZ* transcriptional fusion shuttle vector	Farinha & Kropinski, 1990
pQFC	pQF50 with 788-bp insert in the direction to study *pyrC* promoter activity	This study
pQFM	pQF50 with 788-bp insert in the direction to study *motY* promoter activity	This study
pQF5539	pQF50 with 304-bp insert to study ORF PA5539 promoter activity	This study
pQFCA	pQF50 with 348-bp insert to study putative carbonic anhydrase promoter activity	This study
pQFC3	pQF50 with 469-bp insert to study putative *pyrC3* promoter activity	This study

Table 1. Bacterial strains and plasmids used in this study.

solution is lime green in color and may be stored at 4°C indefinitely, although the solution should be monitored for fungal growth.

Pseudomonas isolation agar (PIA) supplied by Difco, was used as a selective medium for *Pseudomonas* strains in mating experiments. The medium is based on the formulation of King's A medium (King *et al.*, 1954) with slight modification. The medium contains per liter, Bacto peptone (20 g), $MgCl_2$ (1.4 g), K_2SO_4 (10 g), Bacto agar (13.6 g), and Igrasan® (0.025 g) a potent broad-spectrum antimicrobial agent (Furia & Schenkel, 1968), which is not active against *Pseudomonas*. King's A and B media (King *et al.*, 1954), available from Difco as *Pseudomonas* agar P and F respectively, were used to study the pigment production (pyoverdin and pyocyanin specifically) of *P. aeruginosa* wild-type and pyrimidine mutant strains. Difco *Pseudomonas* Agar F, based on King's B medium, contains per liter, Difco proteose peptone No. 3 (10 g), dipotassium phosphate (K_2HPO_4, anhydrous) (1.5 g), $MgSO_4 \bullet 7H_2O$ (1.5 g), Bacto agar (15 g) and is modified from the original King's B medium with the addition of Bacto tryptone (10 g). *Pseudomonas* broth (PB) was used to maximize pyocyanin production in liquid culture for quantitative measurements (Essar *et al.*, 1990). This medium is based on King's A medium with slight modification and contains Bacto peptone (20 g), $MgCl_2$ (1.4 g) and K_2SO_4 (10 g) per liter.

Chrome Azurol Sulfate (CAS) medium (Schwyn & Neilands, 1987) was used to study the iron chelating capacity of *P. aeruginosa* wild-type and pyrimidine mutant strains. The basis of the assay is an iron-dye complex that changes color upon loss of iron. Siderophores have a higher affinity for iron than does the dye, and thus remove iron resulting in a color change from blue to orange. The medium is composed of three

components. 1) 10 x MM9 salts. MM9 salts is a modification of the traditional M9 salts medium (Maniatis *et al.,* 1982) in that it contains a tenth of the KH_2PO_4 component (0.03 %). The 0.1 M phosphate buffer had to be replaced (with PIPES) because of its affinity (albeit low) for iron. This affinity results in "background" iron chelation that interferes with siderophore measurements. One liter of 10 x MM9 salts contains Na_2HPO_4 (60 g)**,** KH_2PO_4 (3 g), NaCl (5 g) and NH_4Cl (10 g) in ddH2O. 2) CAS-HDTMA iron-dye solution. To 500 ml ddH_2O, add CAS (605 mg) and stir until dissolved. Next add 100 ml of iron (III) solution (1 mM $FeCl_3 \bullet 6H_2O$ in 10 mM HCl). Next prepare the hexadecyltrimethylammonium bromide (HDTMA) solution. To 400 ml ddH_2O add 729 mg HDTMA and stir until dissolved. Note that the amount of HDTMA added is crucial as a lesser concentration causes the resulting blue dye of the medium to precipitate while a greater concentration is toxic. When dissolved, and while still stirring, slowly add the 600 ml CAS-iron solution. 3) Deferrated casamino acids (dCAA). Dissolve 10 g of casamino acids in 100 ml ddH_2O. Extract the casamino acids solution with an equal volume of a 3 % (w/w) 8-hydroxyquinoline in chloroform to remove contaminating iron. Extract with an equal volume of chloroform to remove traces of 8-hydroxyquinoline. Note, if using succinate as a carbon and energy source, the succinate solution should also be deferrated. This procedure is not however, necessary for glucose. Each of these solutions should be autoclaved and may then be stored at room temperature for further use. To make one liter of CAS agar plates add PIPES (30.24 g), NaOH (6 g), – to raise the pH of the solution to the pK_a of PIPES which is 6.8, 10 x MM9 salts (100 ml) and agar (15 g) to 750 ml ddH_2O. The pH of the solution should be checked prior to the addition of agar, as a pH greater than 7.0 results in the medium being green instead of

blue. This solution is autoclaved. After cooling to 50°C, add 30 ml of 10 % (w/v) dCAA solution, 10 ml of 20 % glucose or deferrated succinate, 1 ml of 1M $MgSO_4$, 1 ml of 100 mM $CaCl_2$, and any other vitamins or supplements necessary. Finally, slowly add, to avoid foaming, 100 ml of the CAS-HDTMA iron-dye complex and pour plates. The resulting CAS agar plates are sapphire blue in color.

Blood agar (BA) medium, supplied by BBL, (tryptic soy agar (TAS) base and 5 % sheep blood) and brain heart infusion (BHI) medium, supplied by Difco, were used to test the *in vitro* pathogenicity of *P. aeruginosa* wild-type and pyrimidine mutants.

Rhamnolipid plates were prepared according to the method of Siegmund & Wagner, 1991 with modifications by Köhler et al, 2000. This medium was used to test for the production of the biosurfactant, rhamnolipid, which enables pseudomonads to move on solid surfaces. The medium contained M8 salts, a modification of M9 salts without NH_4Cl (Maniatis *et al.*, 1982) and consists of the following per liter: Na_2HPO_4 (6 g), KH_2PO_4 (3 g), and NaCl (0.5 g) supplemented with 0.2 % glucose (instead of 0.2 % glycerol), 2 mM $MgSO_4$, 10 ml of 10 x trace elements per liter, 0.0005 % methylene blue, 0.02 % cetyltrimethylammonium bromide, 0.05 % glutamate as a nitrogen source and agar (1.6 % final concentration). Trace elements (10 x) contained per liter 0.232 g H_3Bo_3, 0.174 g $ZnSO_4 \bullet 7H_2O$, 0.23 g $FeNH_4 (SO_4)_2 \bullet 12 H_2O$, .096 g $CoSO_4 \bullet 7H_2O$, 0.022 g $(NH_4)_6Mo_7O_{24} \bullet 4H_2O$, 8.0 mg $CuSO_4 \bullet 5H_2O$, and 8.0 mg $MnSO_4 \bullet 4H_2O$.

Swarming agar plates contained either M8 salts supplemented with 0.2 % glucose, 2 mM $MgSO_4$, 10 ml of 10 x trace elements per liter, 0.05 % glutamate and 0. 5 % agar (Köhler et al, 2000) or 8 g nutrient broth (Difco), 5 g dextrose and 0.5 % Bacto agar per liter (Rashid & Kornberg, 2000). The medium used to detect swimming motility

(swim medium) contained 1 % tryptone, 0.5 % NaCl, and 0.3 % agarose (not agar). Twitching motility was tested on LB agar plates that were poured such that they were no more than 3 mm thick (Rashid & Kornberg, 2000).

Peptone trypticase soy broth (PTSB) was the liquid medium used to quantitate the production of the exoproducts casein protease and elastase. The medium contained 5 % peptone (Difco) and 0.25 % Trypticase soy broth (Diener *et al.,* 1973). Tryptone broth (TB) contained 10 g of tryptone per liter.

Trypticase soy broth dialysate (TSBD) (Liu, 1973) was used to cultivate *Pseudomonas* strains in low iron conditions. The medium was made by adding 30 g of Trypticase soy broth (Difco) to 90 ml of ddH_2O. Next 10 g of sodium Chelex-100 (Sigma) was added as deferrating agent. This mixture was stirred for 6 hours at room temperature and then dialyzed against 1 liter of ddH_2O at 4°C for 15 hours. The dialysate was supplemented with 0.05 M monosodium glutamate (Sigma) and 1 % glycerol. This TSBD medium had an iron concentration of approximately 0.08 mg/ml (Miller, 1972).

A second low iron medium utilized was the Casamino acids medium (CAA) described by Meyer *et al.,* 1997. The medium contained per liter of ddH_2O, 5 g of Bacto Difco Casamino acids, 1.18 g of $K_2HPO_4 \bullet 3H_2O$, and 0.25 g of $MgSO_4 \bullet 7H_2O$.

Escherichia coli strains were cultivated in *E. coli* minimal medium (Ecmm) with glucose as a carbon and energy source. Ecmm also contained per liter, K_2HPO_4 (10.5 g), KH_2PO_4 (4.5 g), $(NH_4)_2SO_4$ (1.0 g) and, Na_3 Citrate (0.5 g) dissolved in 988 ml ddH_2O. This solution was autoclaved and cooled prior to the addition of sterile solutions of 20 % glucose (w/v) (10 ml, 0.2 % final), 1M $MgSO_4$ (1 ml, 1 mM final) and 0.337 % thiamine (w/v) (5 ml, 0.0015 % final) (Miller, 1972). For the *E. coli* pyrimidine mutant X7014a,

uracil was added at a concentration of 40 μg ml^{-1} and adenine (5 ml of 1.35 % in 0.1 N HCl per liter). *E. coli* strains were also grown in Luria-Bertani (LB) medium, which contained per liter, Bacto tryptone (10 g), Bacto yeast extract (5 g) and NaCl (5 g).

Difco agar was used at 1.5 % when needed for solid medium. When necessary, antibiotics were added in the following concentrations: for *E. coli*, ampicillin (Ap) (100 μg ml^{-1}), gentamicin (Gm) (15 μg ml^{-1}), kanamycin (Km) (25 μg ml^{-1}) and for *P. aeruginosa*, carbenicillin (Cb) (600 μg ml^{-1}), Gm (100 μg ml^{-1}), and 10 % sucrose. Unless stated otherwise, all strains were cultivated at 37ºC, and if liquid culture, with shaking at 250 rpm.

Pyocyanin quantitation assay.

Pyocyanin production was quantified using the method of Essar et al, 1990. The assay is based on the absorbance of pyocyanin at 520 nm (A_{520}) in acidic solution (Kurachi, 1958; MacDonald, 1967). *Pseudomonas* strains were cultured in 125 ml Erlenmeyer flasks containing 30 ml of King's A broth. Cultures were incubated at 37°C for 16 to 20 hours with shaking at 250 rpm. The OD_{600} was recorded for each sample. A 5 ml aliquot was placed in a 15 ml polystyrene conical tube and centrifuged at 1300 x g for 25 minutes at 10°C in a Sorval RT 6000B table top centrifuge. The supernatant was filtered with a 0.45 μm Ambion syringe filter disc and then placed in a 15 ml polypropylene conical tube. Pyocyanin was extracted from the supernatant by the addition of 3 ml of chloroform. This mixture was vortexed for 15 seconds and then centrifuged at 1300 x g for 7 min at 10°C. The organic phase (bottom layer) was removed and placed in a fresh 15 ml polypropylene tube. The pyocyanin was extracted

from the chloroform by the addition of 1 ml of 0.2 N HCl. This mixture was vortexed for 15 seconds and then centrifuged for 7 min at 1300 x g. The resulting pink to deep red HCl solution (top layer) was transferred to a 1.5 ml centrifuge tube and the absorbance was measured at 520 nm. Concentrations, expressed as micrograms of pyocyanin produced per 5 ml of culture supernatant, were determined by multiplying the A_{520} by 17.072 (Kurachi, 1958).

Pyoverdin quantitation assay.

Pyoverdin was measured as a function of growth in King's B medium. The cells were cultured in 30 ml of medium in a 150 ml Erlenmeyer flask, incubated at 37°C with shaking at 250 rpm. At the indicated time points, 1 ml was removed from each culture to be measured. The absorbance of the culture was measured at 600 nm. The sample was then centrifuged for 3 to 5 min at 10,000 rpm in a Sorvall microcentrifuge at 4°C. The supernatant was removed to a cuvette, and the absorance at 405 nm measured. Pyoverdin levels were expressed as the ratio of A_{405}/A_{600} (Stintzi, 1991).

Exoproduct assays.

Elastolysis assay. Elastolytic activity in *P. aeruginosa* culture supernatants was determined by the elastin Congo red (ECR) assay as described by Pearson *et al.,* 1997. Cells were cultivated in 5 ml of PTSB (as described above) for 24 h at 37°C with shaking. Culture supernatants were obtained by centrifuging the 5 ml cultures in 15 ml conical tubes at 3000 rpm and at 4°C for 15 min. The supernatants were filter sterilized (0.45 μM pore size filter) and stored at –70°C. Triplicate 50 μl samples of culture

filtrates were added to tubes containing 20 mg of ECR (Sigma) in 1 ml of buffer (0.1 M Tris pH 7.2, 1 mM $CaCl_2$). Tubes were incubated for 18 h at 37°C with rotation and then were incubated on ice for 10 min after the addition of 0.1 ml of 0.12 mM EDTA. Insoluble ECR was removed by centrifugation, and the absorbance of the supernatant at 495 nm was determined. Absorption due to pigments produced by *P. aeruginosa* was corrected for by subtracting the A_{495} of each sample that had been incubated in the absence of ECR.

Casein protease assay. Proteolytic activity was determined by an azocasein assay described by Kessler *et al.*, 1993. 50 ul of culture supernatant, prepared as above, was added to 1 ml of buffer (0.05 M Tris pH 7.5, 0.5 mM CaCl2) containing 0.3 % azocasein (Sigma). The tubes were incubated at 37°C for 15 min and then the reaction stopped by adding 0.5 ml of a 10 % trichloroacetic acid solution. The samples were then centrifuged and the absorbance of the clarified supernatants was measured at 400 nm.

Cross-streak inhibition assay. *P. aeruginosa* PAO1 has been shown to inhibit the growth of *Burkholderia cepacia* in biofilms. While mixed species biofilms are readily achieved between cystic fibrosis (CF) isolates of *P. aeruginosa* and *B. cepacia*, the laboratory strain of *P. aeruginosa*, PAO1, inhibits mixed biofilm formation. *P. aeruginosa* produces a number of antimicrobial exoproducts such as pyocins, small heat stable microcins (Barberis *et al.,* 1994) and the phenazine pigment pyocyanin. In order to determine if the pyrimidine mutant derivatives of PAO1 generated in this study were as effective at inhibiting the growth of other organisms as the wild-type, a cross-streak inhibition assay was performed (Brock and Madigan 1991). To that end, each mutant (*pyrC*, *pyrC2* and *pyrC*, *pyrC2* double mutant) and the wild-type were streaked to

individual TSA plates. The plates were incubated at 37°C for 18 h to allow exoproduct synthesis. Test organisms were then streaked starting at a fixed-point 5 cm away from and perpendicular to the growth of the *P. aeruginosa* strains. The plates were incubated for 24 h at 37°C and the inhibition determined by measuring the distance between the origin of inoculation and the point of growth.

Preparation of cell extracts.

Cell extracts of *P. aeruginosa* and its isogenic pyrimidine mutant derivatives, were prepared from 30 ml cultures. Cells were collected by centrifugation (25 min at 1300 x g at 10°C) during the mid to late exponential phase (OD_{600} = 0.6 to 1.4) of growth. The cells were washed in minimal medium, collected by centrifugation as above, and resuspended in 2 ml ATCase breaking buffer (2 mM β – mercaptoethanol, 20 μM $ZnSO_4$, 50 mM Tris-HCl pH 8.0 and 20 % glycerol). The suspensions were subjected to ultrasonic disruption using a Branson Cell Disruptor 200 for 6 min intervals at 0°C in 50 ml conical tubes that were submerged in an ethanol-ice water slurry to control heating of the samples. The disrupted cell suspensions were each distributed into two 1.5 ml centrifuge tubes and then centrifuged at 9,000 x g for 4 minutes. An aliquot (300 μl) of the “slow spin” supernatant from each sample, presumably containing a significant portion of the membrane fraction, was removed to a fresh tube for the dihydroorotate dehydrogenase (DHOdehase) assay. The remaining extracts were centrifuged at 12,000 x g for an additional 10 min at 4°C. The cell extracts (including the slow spin fractions) were then dialyzed in 150 volumes of ATCase breaking buffer for 18 to 24 h and then

transferred to fresh microcentrifuge tubes for storage at 4°C until assayed. Assays were performed within 48 h of cell extract preparation.

For the pyrimidine starvation experiments, uracil-requiring mutants or uracil-requiring and gentamicin-resistant mutants were grown, respectively, in *Pseudomonas* minimal medium containing 40 μg uracil ml^{-1} or 40 μg uracil ml^{-1} and 100 μg gentamycin ml^{-1}, to the mid exponential phase of growth (OD_{600} of 0.6). The cells were collected, washed and resuspended in minimal medium lacking only uracil while maintaining sterile conditions. After 4 h of pyrimidine starvation, the OD_{600} was measured, the cells were collected and extracts prepared as described above.

Protein concentration of cell extracts was estimated using the Bradford protein detection assay (Sigma). A standard curve was constructed, using lysozyme ranging in concentration from 0 to 10 μg ml^{-1}, (Fig. 14) and was used to facilitate protein estimation.

Aspartate transcarbamoylase (ATCase) assay.

ATCase activity was measured by quantifying the amount of carbamoylaspartate (CAA) produced in 20 min at 30ºC. This was accomplished using the method of Gerhart & Pardee (1962), with modification, using the color development procedure of Prescott & Jones (1969). Cell extracts were prepared as above in ATCase buffer with 20 % glycerol. The assay mixture contained the following in a 1 ml reaction volume: 40 μl of Tri-buffer pH 9.5 (51mM diethanolamine, 51 mM N-ethylmorpholine and 100 mM MES, adjust pH to 9.5; Ellis & Morrison, 1982), 10 mM potassium aspartate (pH 9.5), 2 mM dilithium carbamoylphosphate and cell extract, usually 20 μl at a concentration of approximately 1 mg ml^{-1}. Assay tubes containing all components, except for

carbamoylphosphate, were prepared in advance and pre-incubated at 30ºC for 5 min. Three control tubes were also prepared. The first contained all components except for cell free extract, the second

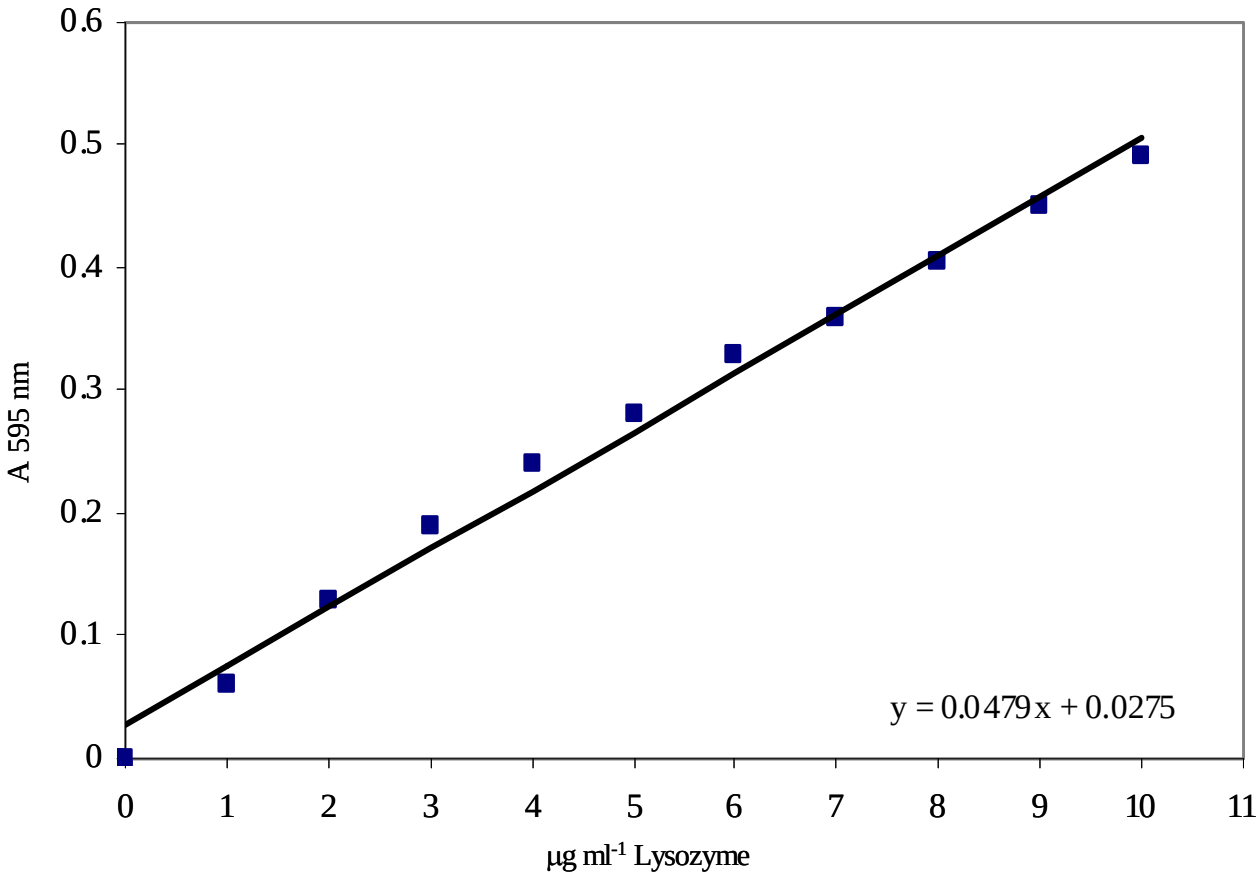

Fig. 14. Bradford protein standard curve. Lysozyme was used at the indicated concentrations. Values reported are the average of three independent determinations. The equation of the line is given in the lower right hand side of the figure.

contained cell extract, but no carbamoylphosphate or aspartate, and the third contained a known concentration of carbamoyl aspartate (1mM final concentration) and buffer, but no cell extract, carbamoylphosphate or aspartate. The reaction was initiated by the addition of carbamoylphosphate.

The reaction was allowed to proceed for a recorded length of time, usually 10 to 30 min, with incubation at 30ºC. The reaction was stopped by the addition of 1 ml of color mix (Prescott & Jones, 1969). The tubes were vortexed for 2-3 seconds and then placed in a 65ºC water bath under fluorescent light for one hour. The tubes were capped with marbles to prevent loss of volume due to evaporation. Color mix was made in an amber flask and contained two parts of 5 mg ml^{-1} antipyrine in 50 % sulfuric acid (v/v) mixed with one part of 8 mg ml^{-1} of 2,3-butanedione monoxime in 5 % acetic acid (v/v). Color mix and CAA should be made up just prior to use, and kept on ice, as both are temperature sensitive compounds.

After incubation at 65ºC, assay tubes were allowed to cool in the dark for 10 to 15 min and then the A_{466} was read and recorded. First the control tubes were read. The control tube containing cell extract but no substrates was used as a blank reference reading. The amount of CAA produced was determined using a CAA standard curve. The standard curve was prepared using the same buffering system and known concentrations of CAA, ranging from 0 to 1.0 mM, in the standard assay mix incubated at the same temperature and for the same amount of time (Fig. 15).

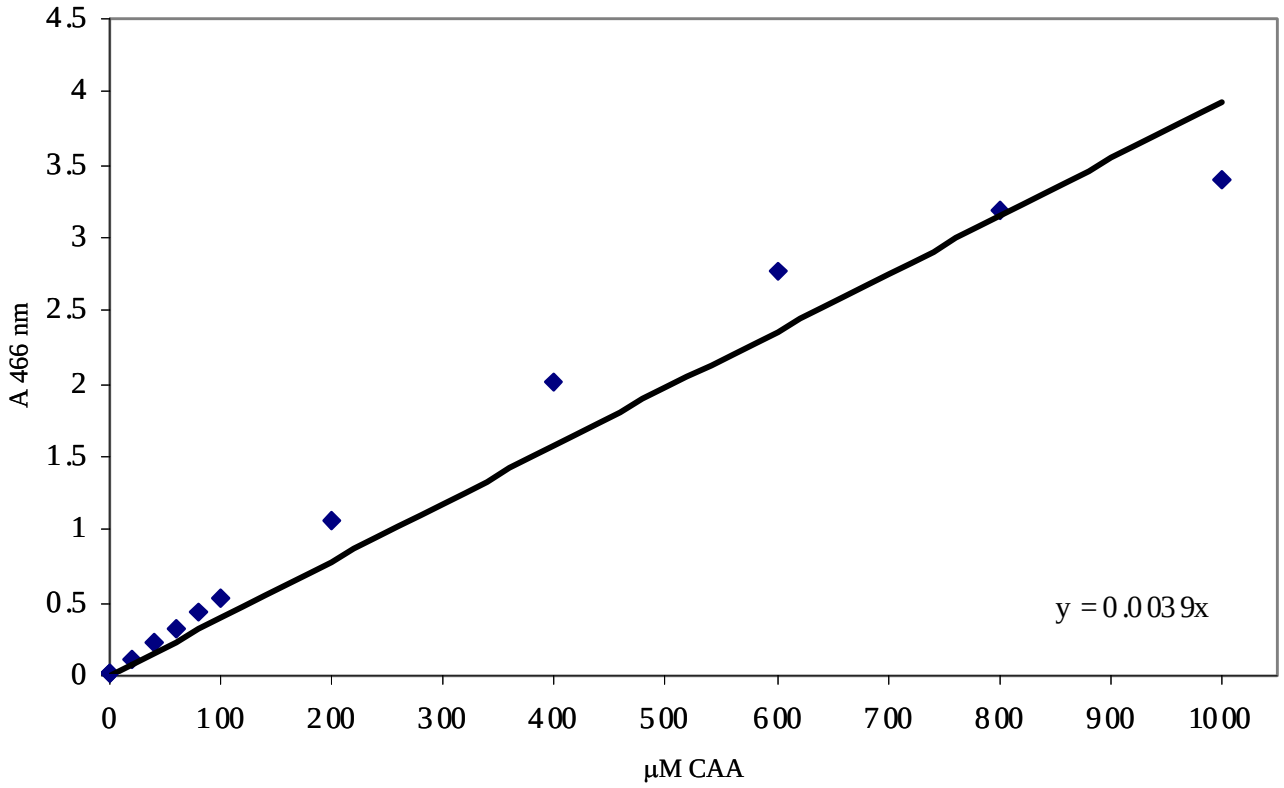

Fig. 15. Carbamoyl aspartate standard curve. The equation of the line is given in the bottom right hand corner Of the figure. The reported values are the average of two separate determinations.

Dihydroorotase assay.

Dihydroorotase was measured using the reverse assay of Beckwith *et al.,* 1962. A 1 ml reaction volume contained 100 mM Tris/HCl buffer, pH 8.5, 1 mM EDTA, 2 mM-L-dihydroorotate and cell extract. Tubes containing buffer and cell-free extract were prepared and incubated at 30°C for 5 min. The reaction was initiated with the addition of dihydroorotate. Assay tubes were incubated at 30°C for an additional 10 to 30 min. The reaction was stopped by the addition of 1 ml of color mix (as above). The tubes were vortexed, capped with marbles and incubated at 65°C for 45 min. The absorbance of each assay tube was measured at 466nm. The amount of DHO converted to CAA was determined with a standard curve. As above, three control assay samples were prepared. The first contained buffer and cell extract but no substrate, the second contained buffer and substrate but no cell extract and the third was a reference sample of CAA. The control tubes are very important in the DHOase assay, as the background tends to be very high. This is due to the tendency for DHO to spontaneously open and form CAA as a result of high temperature and pH.

HPLC assays of DHOase in the biosynthetic and degradative directions.

The formation of DHO from CAA or vice versa was monitored by ion-exchange HPLC. The chromatographic apparatus used was a Waters 510 pump, Waters Model U6K Universal Liquid Chromatography Injector, a SpectroMonitor 5000 Photodiode Array detector, a Waters Model 740 Data Module, and a Partisil SAX column. The mobile phase was 50 mM ammonium phosphate monobasic (Mallinckrodt, HPLC grade), pH 3.5 (HCl) using HPLC grade, filtered water at 10 megaohms cm^{-1} (Millipore, Milli-

Q^{TM} Water System). Samples were injected using a Hamilton syringe and the flow rate was 1 ml min^{-1}. Cell extracts from cultures grown in minimal medium with the appropriate supplements, were prepared as previously described. The assay procedures followed were essentially those of Daniel *et al.,* 1996. For the biosynthetic assay, a 1 ml reaction contained 0.1 M potassium phosphate buffer pH 5.8 and 10 mM CAA. The reaction was initiated by the addition of cell extract (0.2 to 2 μg of total protein) and the sample was incubated at 30°C for 5 min. For the degradative assay, the reaction volume, incubation temperature and time were the same, but the buffer system was 0.05 M Tris phosphate pH 8.0 containing 1 mM DHO. At the indicated time points, 100 μl of the reaction mixture was removed. The sample was filtered using a 0.45 μm Whatman syringe filter and then injected onto the HPLC column. The concentration of DHO was monitored by measuring and recording the A_{220} and A_{230} of the injected reaction mix. The integration of the area under the DHO peak was used as a measurement of DHO produced or consumed over time.

Dihydroorotate dehydrogenase assay.

Dihydroorotate dehydrogenase (DHOdehase) activity was measured spectophotometrically at 290 nm by monitoring the oxidation of dihydroorotate to orotate (Beckwith, *et al.,* 1962; Schwartz & Neuhard, 1975). The reaction volume was 1 ml and was prepared in a quartz cuvette. The reaction mix contained 100 mM Tris/HCl buffer, pH 8.6, 6 mM $MgCl_2$, 1 mM DHO and the “slow spin” fraction of cell extract. It is important to use this fraction of cell extract because DHOdehase is located in the cell membrane. The assay components, except for the DHO substrate, were mixed by

inversion and pre-incubated at 30ºC for 2 min. The reaction was initiated by the addition of DHO, and the A_{290} was recorded at time zero. This reading served as the blank reading and was subtracted from all subsequent readings. The absorbance was measured every 5 min for 15 min. An increase in the A_{290} of the reaction mix by 1.93 is equivalent to a change in substrate concentration of 1mM.

Orotate phosphoribosyltransferase (OPRTase) assay.

OPRTase activity was measured spectophotometrically at 295 nm by monitoring the conversion of orotate to orotidine 5'-monophosphate (OMP) (Beckwith, *et al.,* 1962; Schwartz & Neuhard, 1975). The 1 ml reaction volume was prepared in a quartz cuvette. The reaction mix contained 100 mM Tris/HCl buffer, pH 8.6, 6 mM $MgCl_2$, 0.25 mM orotate, 0.6 mM 5-phosphoribosyl-1-pyrophosphate (PRPP) and cell extract. The assay components, except for orotate, were mixed by inversion and pre-incubated at 30ºC for 2 min. The reaction was initiated by the addition of orotate, and the A_{295} was recorded at time zero. This reading served as the blank reading and was subtracted from all subsequent readings. The absorbance was measured every 5 min for 15 min. A decrease in the A_{295} of the reaction mix by 3.67 is equivalent to an increase in OMP concentration of 1 mM.

OMP decarboxylase assay

OMP decarboxylase activity was measured spectophotometrically at 285 nm by measuring the conversion of OMP to UMP (Beckwith, *et al.,* 1962; Schwartz & Neuhard, 1975). The reaction volume was 1 ml and was prepared in a quartz cuvette. The reaction

mix contained 100 mM Tris/HCl buffer, pH 8.6, 6 mM $MgCl_2$, 0.2 mM OMP and cell extract. The assay components, except for the OMP substrate, were mixed by inversion and pre-incubated at 30ºC for 2 min. The reaction was initiated by the addition of OMP, and the A_{285} was recorded at time zero. This reading served as the blank reading and was subtracted from all subsequent readings. The absorbance was measured every 5 min for 15 min. A decrease in the A_{285} of the reaction mix by 1.38 is equivalent to a decrease in OMP concentration of 1mM.

Competent cell preparation and transformation procedures.

For this study, two types of competent cells were employed, chemically competent and electrocompetent. For the transformation of *E. coli*, cells were made chemically competent by the calcium chloride method of Mandel & Higa, 1970, with slight modification. A 200 ml flask containing 50 ml of LB was inoculated with 500 µl of an overnight culture of *E. coli*. This was incubated at 37°C with shaking at 250 rpm for 2-4 h until the culture reached an OD_{600} of 0.2-0.4 (~ 5 x 10^7 cells ml^{-1}). The culture was aseptically transferred to a 50 ml polypropylene conical tube and placed on ice for 30 min. After the ice incubation step, the culture was then centrifuged at 1300 x g for 20 min at 4°C. The supernatant was removed and the pellet resuspended in 20 ml of a sterile, ice-cold solution of 0.1 M $CaCl_2$. This mixture was incubated on ice for 30 min and then centrifuged at 1300 x g for 10 min. The supernatant was aseptically removed and the pellet gently resuspended in 812 µl of sterile, ice cold 0.1 M $CaCl_2$. This was left on ice and in the refrigerator at 4°C overnight. For maximum transformation efficiency, the bacterial culture must be in the logarithmic phase of growth (the cell density should be

low at the time of treatment with calcium chloride). Also, the cells must be maintained at 4°C for 12-24 h. It has been shown that during this period the efficiency of transformation increases fourfold to six-fold (Dagert & Ehrlich, 1979).

The next morning, 188 μl of sterile 80 % glycerol was aseptically added and the suspension was gently mixed and then dispensed as 0.2 ml aliquots into pre-chilled 1.5 ml Eppendorf tubes. The competent cells were stored at –80°C and were viable for at least 5 months. For transformations, the cells were removed from the –80°C and allowed to thaw on ice. When thawed, plasmid DNA was added, usually between 40 – 500 ng (not more than 1 μg) in a volume of 3 – 20 μl. The plasmid DNA/cell mixture was incubated on ice for 20-30 min. and then "heat shocked" by incubation in a 42°C water bath for 90 s. Next, 1 ml of LB was added to each transformation tube and the cells were incubated at 37°C for 1 h. This allows the cells to recover and begin the expression of antibiotic resistance genes. Finally, 50 μl and a "spin-down" (centrifugation of the remaining transformation mixture and resuspension of the cell pellet in 50 μl of broth) of the transformation mix were plated on to selective medium. If minimal medium plates were to be used, the cells were washed with the same minimal medium broth prior to plating, in order to avoid carry-over of the rich nutrients of the LB medium.

For the transformation of *P. aeruginosa* cells, electroporation was the method of choice. Electrocompetent *P. aeruginosa* cells were made using the method of Enderle & Farwell, 1998. An LB agar plate was inoculated by streaking with 2-3 isolated *P. aeruginosa* colonies. This plate was incubated at 37°C for ~16 h or until the isolated colonies were at least 1 mm in diameter. The authors note that it is important to keep the plate at room temperature as storage at 4°C lowers the transformation efficiency (Enderle

& Farwell, 1998**)**. Next a 1.5 ml Eppendorf tube was filled with 500 µl of sterile ddH_2O and approximately 3 mg of cells (typically three generous swipes across the plate) were resuspended in the ddH_2O. The tube was gently vortexed to make a uniform suspension and then the cells were centrifuged at 12,000 x g for 1 min. The supernatant was removed aseptically and the cells suspended in another 500 µl of ddH_2O by gentle up and down pipetting. The suspension was again centrifuged at 12,000 x g for 1 min and the supernatant removed. The cell pellet was gently resuspended in 40 µl of ddH_2O and the cells kept on ice.

For electroporation, 5 – 50 ng of DNA in 2 – 5 µl was added to the bottom an electroporation cuvette (Gene Pulser Cuvette, 0.2 cm electrode gap, catalog No. 165-2086: BioRad Laboratories, Hercules, CA, USA). The cuvette was placed on ice and then the 40 µl sample of electrocompetent cells added and tapped down to ensure an even suspension of cells and DNA. Next the cuvette was electrically pulsed at 2.5 kV/cm in a Pulse Controller II (BioRad) with settings of 25 µF (capacitance) and 400 Ω (resistance) resulting in a time constant of 8.7 - 9.9 msec. Next, 1 ml of LB was added to the DNA/cell suspension and this mixture was then transferred to a 1.5 ml Eppendorf tube. The cells were incubated at 37°C with shaking for 1 h. After this recovery step, 50 µl and a “spin down” (as above) was plated on selective medium. If minimal medium plates were to be used, the cells were washed, as above, to avoid background growth due to nutrient carry over.

Cloning of the *pyrC'* genes from *P. aeruginosa* and *P. putida* into vector pK184 for ATCase hybrid studies.

In order to study the assembly and enzyme kinetics of the class A ATCases from *P. aeruginosa* and *P. putida*, the *pyrC'* genes from each were isolated and cloned into the vector pK184. This vector is compatible with pUC vectors and encodes Km resistance. Thus, by having *pyrC'* genes in pK184, and *pyrB* genes in pUC19, it was possible to co-transform *E. coli* TB2 *pyr*$^{-}$ with the *pyrB* and *pyrC'* plasmids and to select for the desired transformants with ampicllin and kanamycin. To that end, the *P. aeruginosa pyrC'* gene was isolated from plasmid pA10 (Vickrey, 1993) by restriction digest with *Pst*I and *Pvu*II. This digest released *pyrC'* as a 1.495-kb fragment with 12-bp of the 3' end of *pyrB*. The *pyrC'* DNA fragment was purified from agarose using the Sephaglass™ BandPrep Kit (Pharmacia Biotech) and then directionally ligated into pK184 cut with *Pst*I and *Sma*I. The resulting plasmid, pDBAC', was 3.89-kb in size and expressed the *P. aeruginosa pyrC'* gene and Km resistance (Fig. 16).

The *pyrC'* gene from *P. putida* was isolated from plasmid pMJS29 (Schurr, 1992) by a two step restriction digest. The first digest, using *Pst*I and *Sca*I, released a 2.96-kb *Pst*I DNA fragment containing the *pyrBC'* genes (*Sca*I was used to cut the remaining vector DNA so that the *pyrBC'* fragment could be distinguished from the vector DNA by gel electrophoresis). The *Pst*I fragment was isolated by agarose gel purification, as above, and then digested with *Hin*cII. This digest released a 2.35-kb *Pst*I, *Hin*cII fragment containing the *P. putida pyrC'* gene and 30-bp of the 3' end of *pyrB*. The DNA piece was purified and ligated into pK184 cut with *Pst*I and *Sma*I. The resulting plasmid,

pDBPC', was 4.7-kb in size and encoded the *P. putida pyrC'* and Km resistance (Fig. 17).

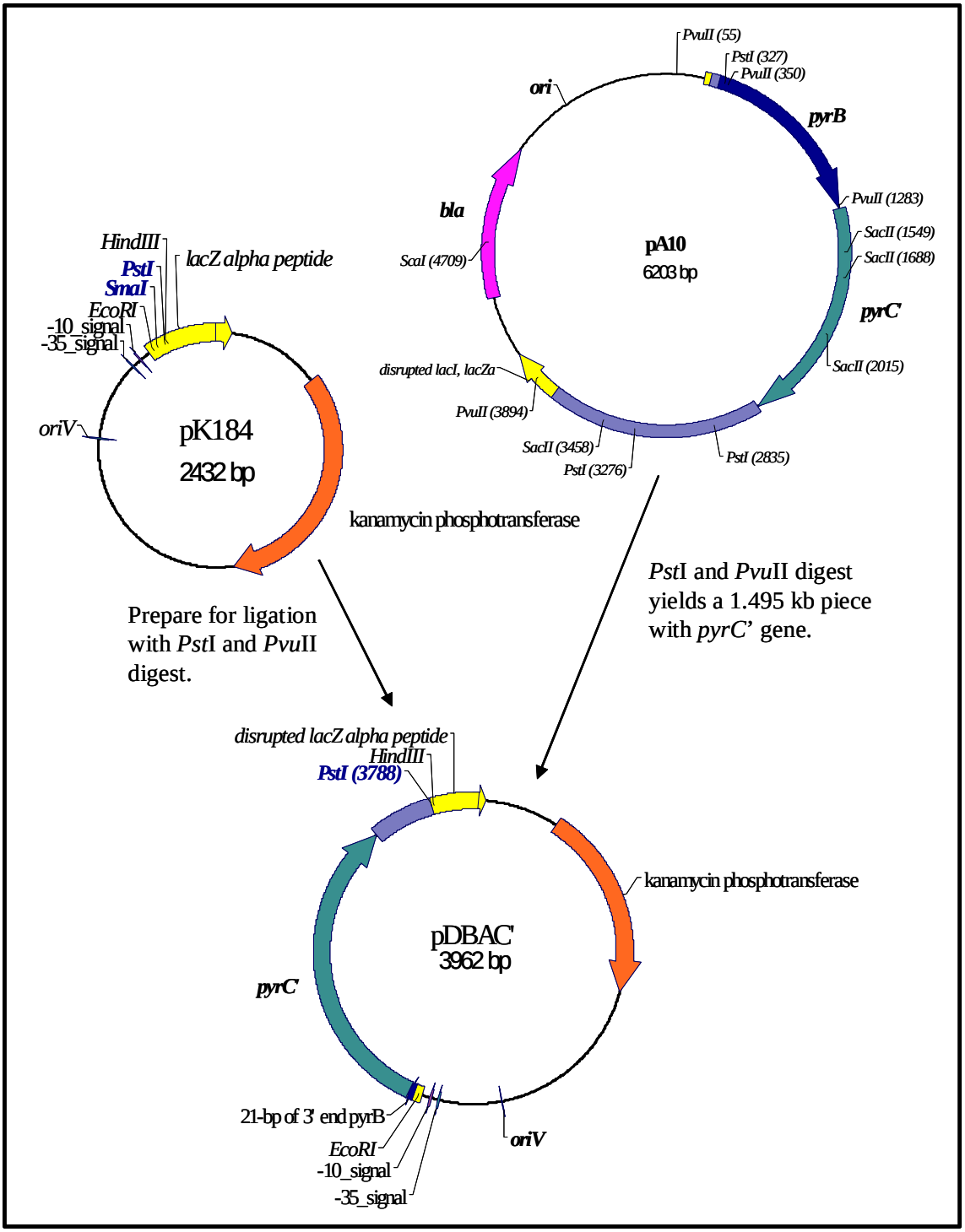

Fig. 16. Construction of plasmid pDBAC'. Contains the *pyrC'* gene from *P. aeruginosa* on plasmid pK184. Used for co-transformation experiments.

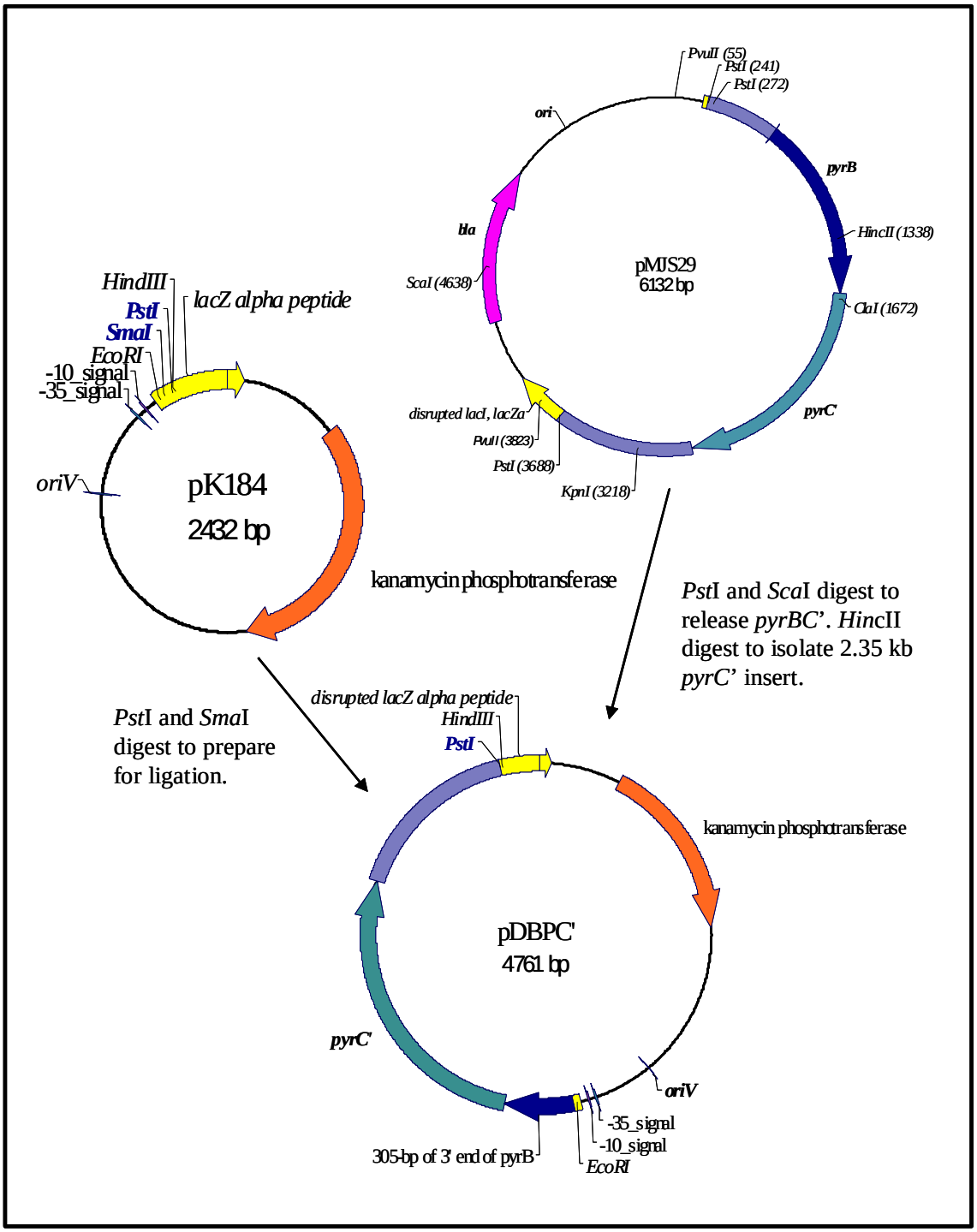

Fig. 17. Construction of plasmid pDBPC'. Contains the *pyrC*' gene from *P. putida* on plasmid pK184. Used for co-transformation experiments.

Cloning of the *pyrB* gene from *P. aeruginosa* for ATCase hybrid studies.

The *pyrB* gene from *P. aeruginosa* was isolated by treating the parent vector, pA10, with the restriction enzyme *Sac*II. pA10 contains the *pyrBC'* genes on a 3.5-kb *Xho*I fragment which was cloned into pUC19 (Vickrey, 1993). A *Sac*II restriction digest of this plasmid results in four cuts, three within the *pyrC'* gene and one downstream of the *pyrC'* gene. Consequently, the result of the *Sac*II digest is that the majority of the *pyrC'* gene is removed, leaving 308-bp of the downstream sequence and 245-bp of the 5' end of *pyrC'*. The 4.1-kb DNA piece containing the *pyrB* gene and the pUC19 plasmid was gel purified and re-ligated. The resulting plasmid, pDBAB (Fig. 18), was used for ATCase hybrid studies. The *P. putida pyrB* plasmid used in these studies was pAKB10 (Kumar, 2000). This plasmid contains the *P. putida pyrB* gene, including 399-bp of upstream sequence and 29-bp of the 5' end of *pyrC'* in pUC19 (Fig. 19).

Co-transformation of *P. aeruginosa* and *P. putida pyrB* and *pyrC'* plasmids into *E. coli* TB2.

P. aeruginosa and *P. putida* ATCases are both subject to inhibition by the effectors ATP, UTP and CTP although to different degrees. It has been shown that effector binding is likely to be on sites associated with the *pyrB* encoded catalytic subunits (Evans, 1993, Schurr et al, 1995 and Kumar, 2000). In order to determine if the *pyrC'* encoded subunits played any role in effector binding, hybrid ATCases were constructed by co-transforming *E. coli* TB2 with the plasmids described above (Fig. 20). The co-transformants were selected on Ecmm containing glycerol (0.4 %) as a carbon

and energy source, arginine and Ap_{100} and Km_{50}, but no uracil. The resulting prototrophs were

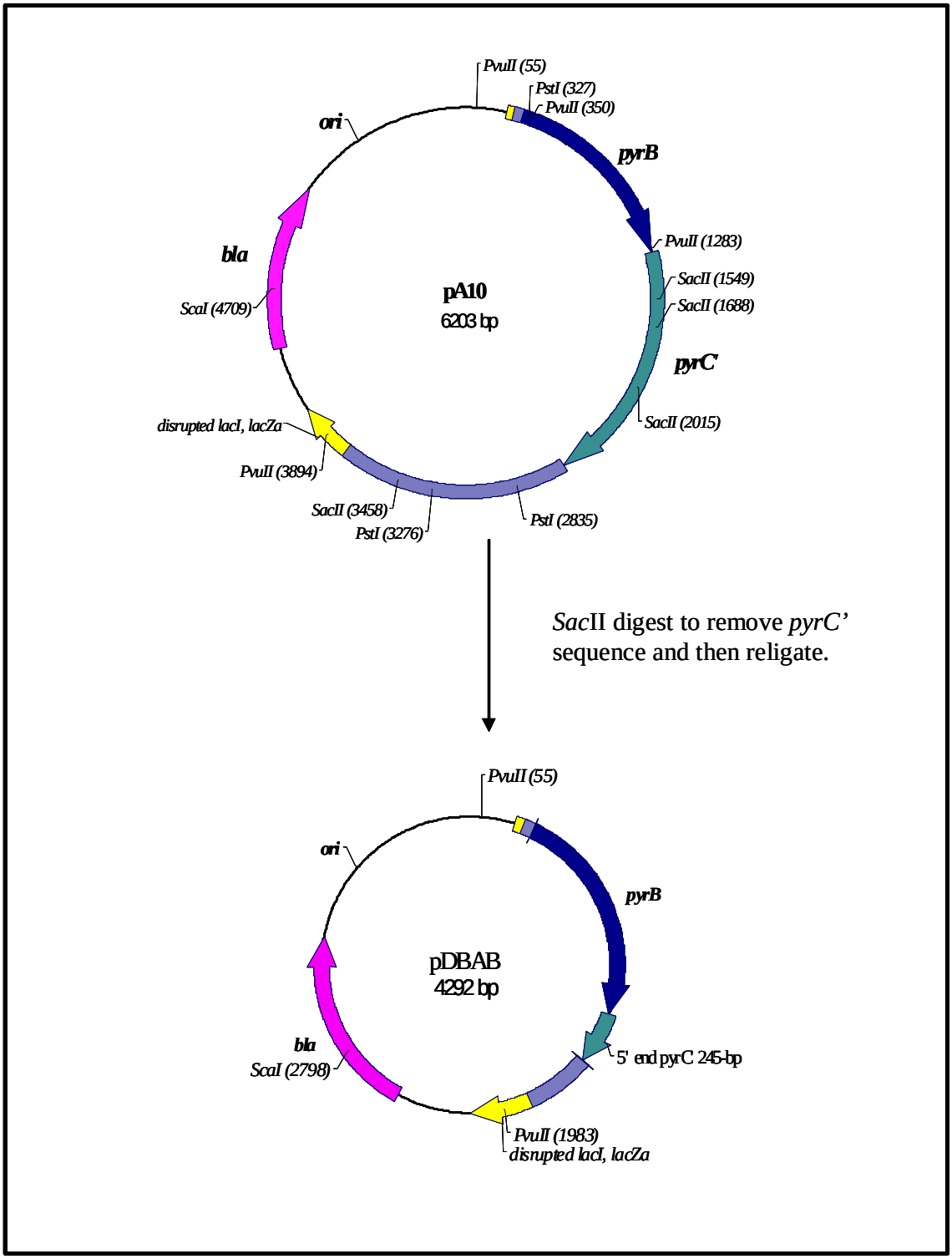

Fig. 18. Construction of plasmid pDBAB. Contains the *P. aeruginosa pyrB* gene in the pUC18 parent vector.

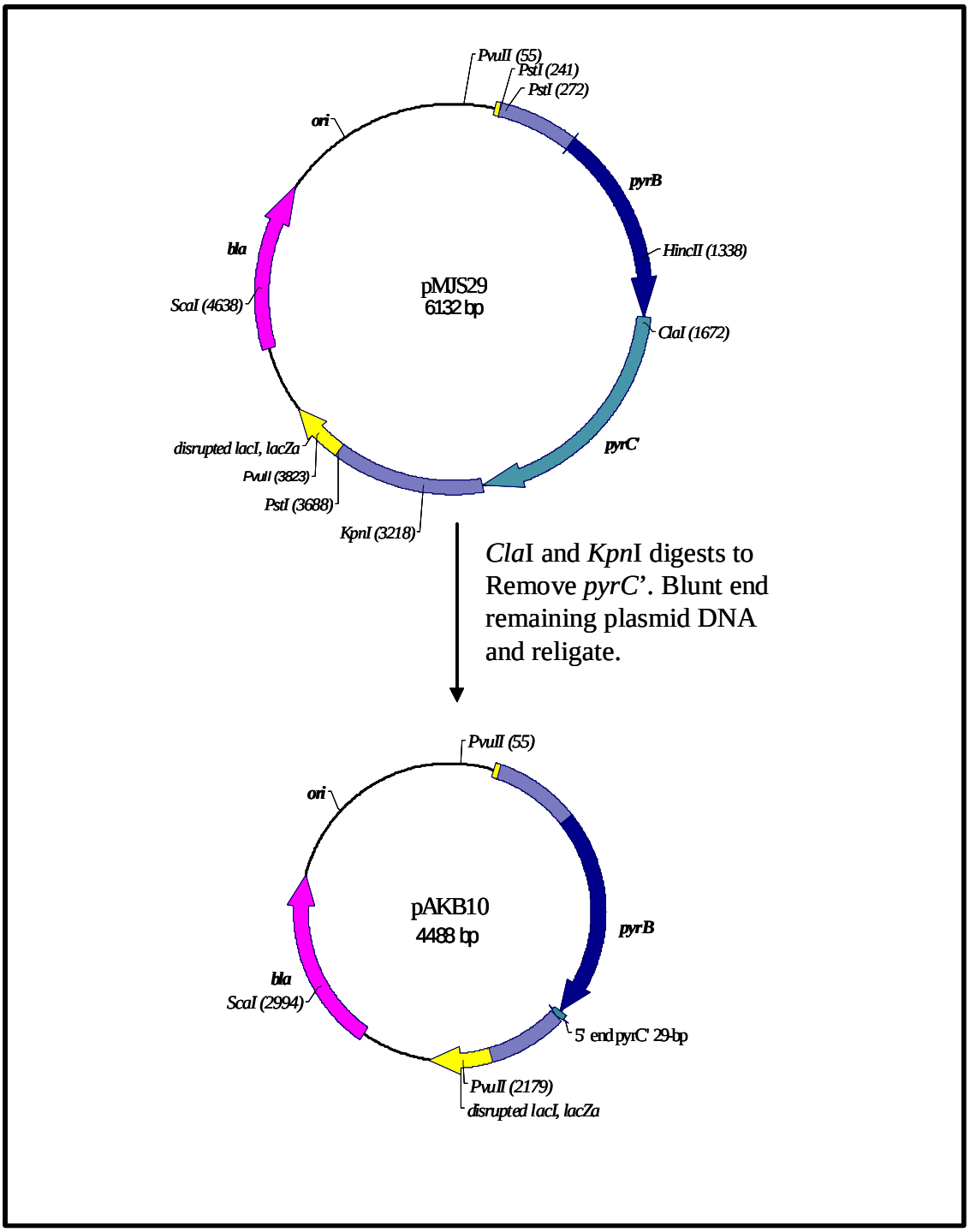

Fig. 19. Construction of plasmid pAKB10. Contains the P. putida pyrB gene in the pUC19 parent vector (Kumar, 2001).

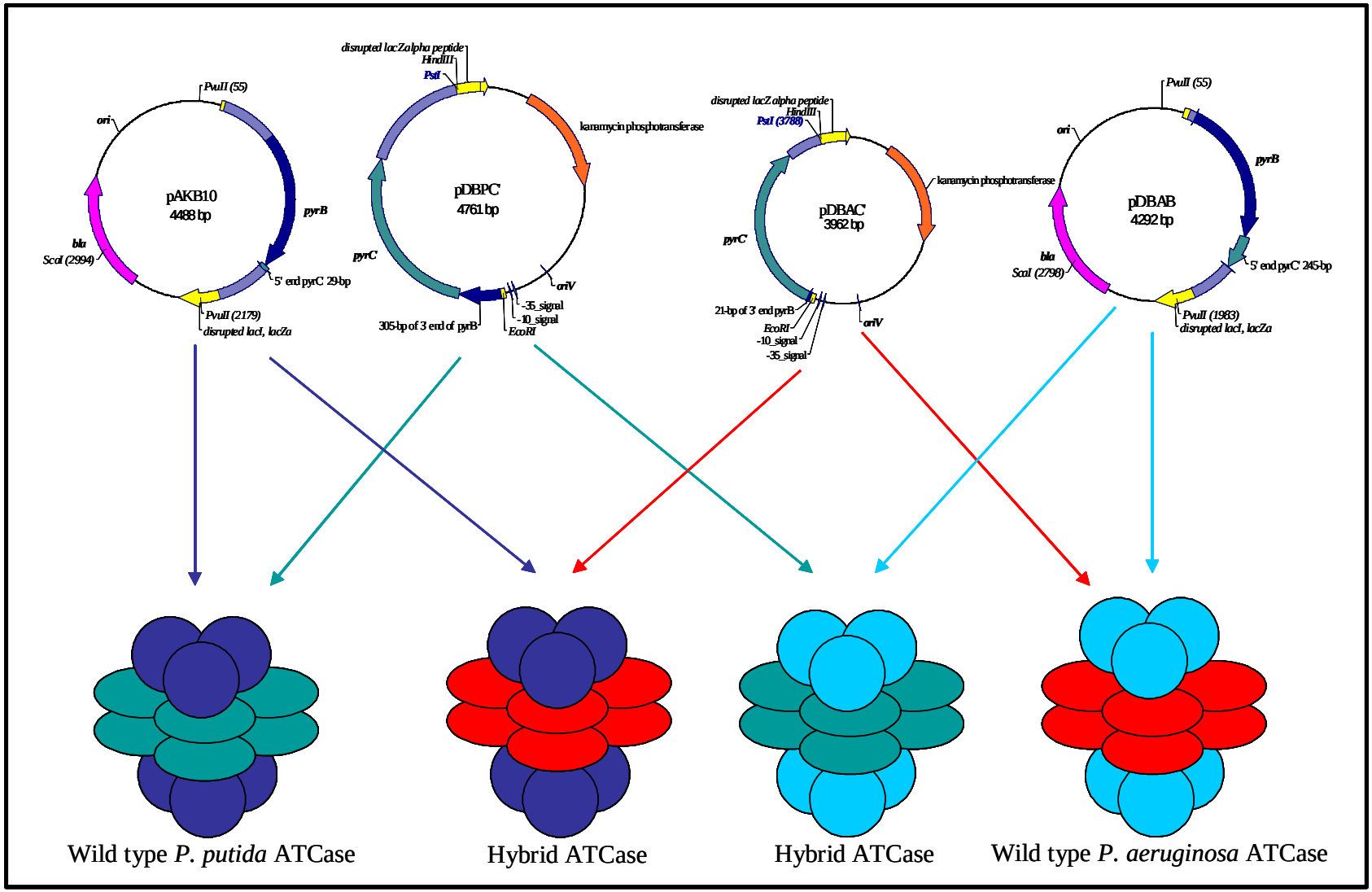

Fig. 20. Co-transformation of the *E. coli* TB2 pyrimidine auxotroph with *P. aeruginosa* and *P. putida pyrB* and *pyrC*' plasmids.

cultivated in 50 ml of Ecmm broth containing the same supplements. The cells were harvested and broken as described above. ATCase assays were conducted with and without effectors. These results were compared with ATCase assays of *P. aeruginosa* and *P. putida* wild-type, cultivated in the same medium, as well as *P. aeruginosa* and *P. putida* ATCases made in *trans,* isolated from *E. coli* TB2 co-transformed with the appropriate plasmids.

Isolation and cloning of *Pseudomonas aeruginosa pyrC* gene.

The *P. aeruginosa pyrC* gene was isolated from a PAO1 SuperCos cosmid library kindly provided by Dr. Ahmed Abdelal at Georgia State University. The library was screened for cosmids containing the *pyrC* gene by transformation into the *E. coli pyrC* auxotrophic strain X7014a (Semple and Silbert, 1975). Ten cosmids were found to complement the *E. coli pyrC* auxotroph. One of these, designated cPA6 (cosmid *P. aeruginosa* no. 6), was selected for further study. The cosmid was amplified using the bulk plasmid preparation described in Maniatis, 1982. The cell lysis method was the SDS method of Godson & Vapnek, 1973, with slight modification. Plasmid DNA was purified using the cesium chloride-ethidium bromide gradient method also described in Maniatis, 1982.

The cosmid DNA was digested with the restriction enzymes *Eco*RI, *Pst*I, *Sca*I and *Hin*dIII. Each digest contained 6 μg of DNA, 10 U of enzyme and the appropriate buffer. The DNA was digested for 3 h at 37°C, and then the restriction enzymes were heat-killed by incubating the digests at 65°C for 30 min. The digested DNA was then ethanol

precipitated and resuspended in ddH_2O, such that the DNA concentration was approximately 100 ng μl^{-1}.

The pUCP19 vector DNA was prepared for ligation by digesting 3 μg of DNA, with 10 U each of the restriction endonucleases listed above, for 3 h at 37°C. The restriction enzymes were heat-killed and then a portion of this mixture (about 2 μg of vector DNA) was treated with 2 U of bacterial alkaline phosphatase (BAP), and the appropriate buffer, in a final volume of 200 μl. This was done in order to remove the 5' phosphate from the ends of the cut vector DNA, preventing vector re-circularization when ligating the insert DNA into the vector DNA.

The BAP-treated vector DNA was extracted with an equal volume of phenol in order to destroy and remove the BAP enzyme. This is a necessary step as it prevents contamination of BAP in the final ligation mixture. The presence of BAP in the ligation mixture could prevent ligation by removing the essential 5' phosphate from the insert DNA. The 200 μl of phenol was back extracted with 100 μl of TE in an attempt to recover any vector DNA that may have been lost in this fraction.

The TE and phenol treated vector fractions were combined for a final volume of 300 μl and then treated with an equal volume of a mixture containing isoamyl alcohol and chloroform in a ratio of 24:1. This was vortexed and then centrifuged at 12,000x g at 4°C for 3 min. The TE, vector containing fraction was removed to a new tube and then ethanol precipitated. The vector DNA was then resuspend in 10 μl ddH_2O and the concentration was calculated to be about 50 μg ml^{-1}. The insert and vector DNA were mixed in ratios of 1:2 for ligation in a final volume of 20 μl.

The ligation mixture was incubated at 16°C overnight and then transformed into *E. coli* X7014a. The resulting transformations were plated onto Ecmm with Ap_{100} and adenine and incubated at 37°C. Colonies, the result of complementation of the *pyrC* auxotroph, were seen on the plates arising from the *Eco*RI digest of cPA6. Rapid plasmid preparation of the plasmid DNA and *Eco*RI restriction analysis showed the resulting plasmid, named pPAC1 (plasmid *P. aeruginosa pyrC* 1), to have a 2.5-kb *Eco*RI insert. Sequence analysis of this insert, with the kind help of John Houghton and Tim Brown at Georgia State University, showed that it contained the entire *pyrC* gene. It was also determined that the orientation of the cloned fragment was such that the *pyrC* gene was in the opposite orientation to the *lacZα* promoter (Fig. 21) and thus was expressed from its own promoter in *E. coli* X7014a. The *pyrC* sequence was submitted to GenBank and the accession number is U75035.

Isolation of Genomic DNA.

Genomic DNA was isolated from 2 ml of a 5 ml overnight culture of nutrient broth. The cells were pelleted in a microcentrifuge tube and the pellet was washed once with normal saline. Next, the pellet was resuspended in 250 μl of a solution containing 0.1 M NaCl, 10 mM Tris pH 8.0 and 10 mM EDTA (at this point the cell suspension can be frozen until the procedure is continued). The cells are broken by the addition of 25 μl of a 10 % solution of SDS and then incubated at 65°C for 10 min. Next, 25 μl of proteinase K (25 mg ml^{-1}) is added and the suspension is incubated at 37°C for 30 min. Proteins and cell debris were removed by two extractions with equal volumes of phenol,

followed by an extraction with an equal volume of water-saturated butanol (butanol is the top layer). The

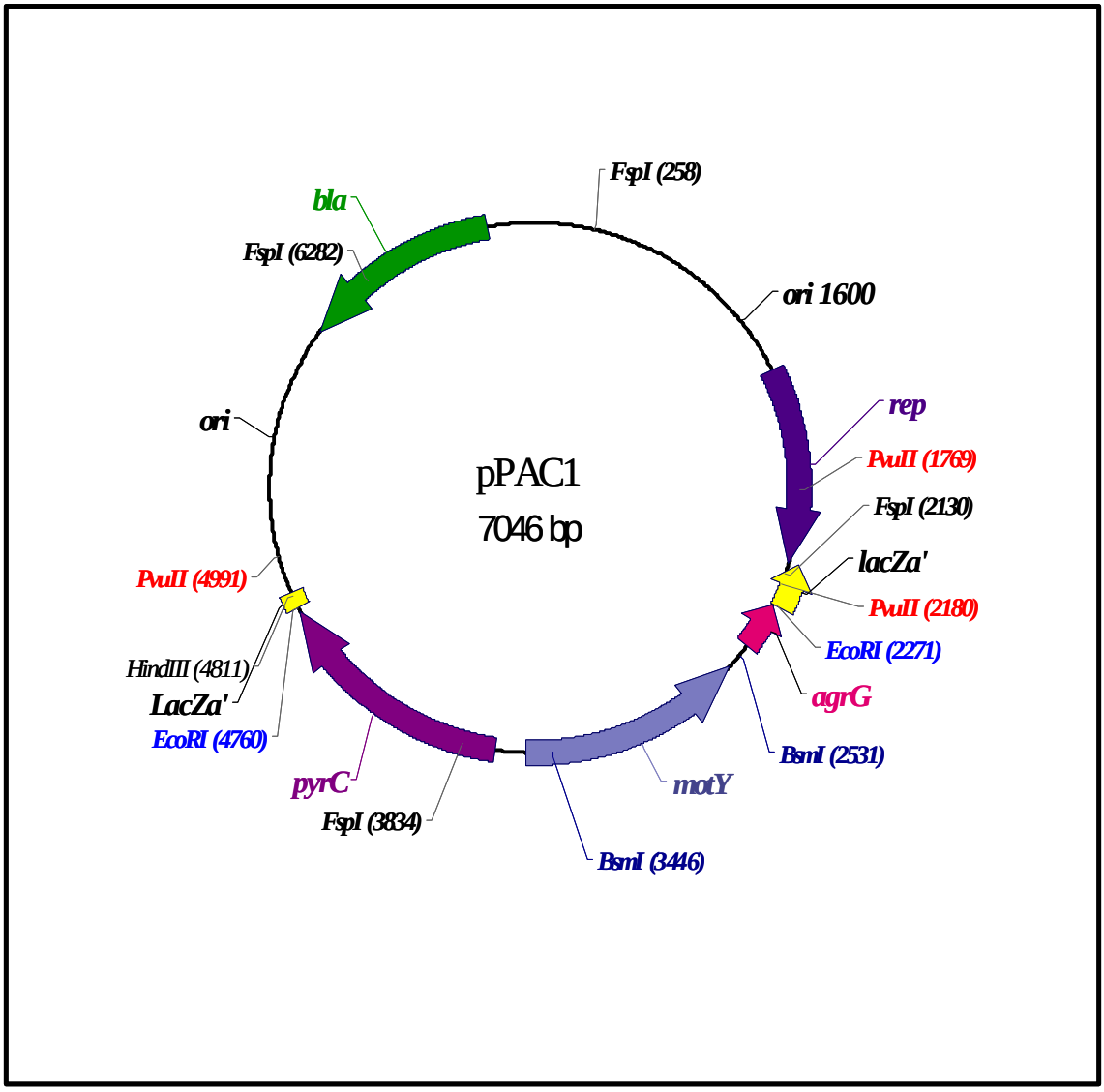

Fig. 21. Plasmid map of pPAC1. Contains the *P. aeruginosa pyrC* gene on a 2.5 kb *Eco*RI insert cloned into the *Eco*RI site of the parent vector pUCP19.

DNA was precipitated by first adding100 ul of 7.5 M ammonium acetate, mixing and then adding 750 μl of ice-cold ethanol. The suspension was gently mixed until the DNA pellet was visible. The suspension was then incubated at –70°C for 5 min. The pellet was then centrifuged at 10,000 rpm for 5 min. The ethanol was poured off and the pellet washed with 1 ml of ice-cold 70 % ethanol by gentle inversion. The sample was centrifuged at 10,000 rpm for 5 min. The ethanol was poured off and the pellet air dried. The DNA pellet was then resuspended in 250 μl of TE containing RNaseI at a concentration of 10 μg ml^{-1} and incubated at 65°C for 30 min. The DNA suspension was gently pulse vortexed in order to minimize sheering. The genomic DNA was stored at 4°C for further use.

PCR screening of various organisms for the presence of small "type I" *pyrC* genes.

Alignments of the amino acid sequence of *pyrC* from *P. aeruginosa* with those of other organisms, indicated that there were strong areas of homology. In an attempt to determine the presence of the small "type I" *pyrC* gene in various organisms, PCR primers were designed based on the *P. aeruginosa* sequence at two of these regions, spaced 658 bp apart (Fig. 22). Genomic DNA was isolated from the organisms of interest as described above and used in PCR reactions with the indicated primers.

Gene replacement of resident *pyrC* gene in PAO1 with Δ*pyrC*.

For the isolation of a PAO1 *pyrC* deletion mutant, a Δ*pyrC* replacement vector was constructed. As seen in Fig. 23, two PCR fragments, CKO1 and CKO2, were generated from PAO1 genomic DNA and the primers listed in Table 2. Fragment CKO1 was 551 bp in length and contained 174 bp upstream of the *pyrC* gene and 377 bp of the

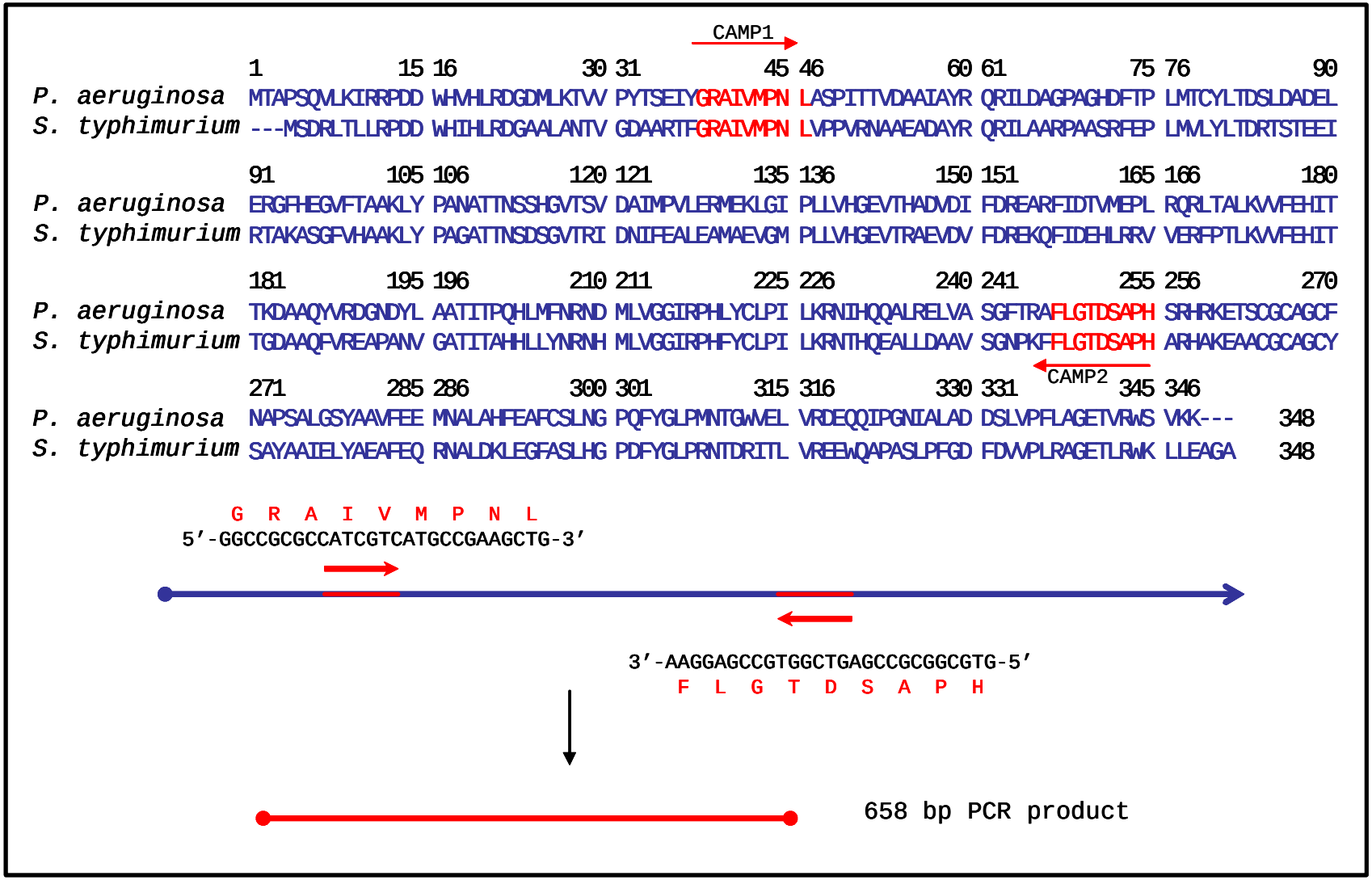

Fig. 22. Primer design for the amplification of the small “type I” *pyrC* genes.

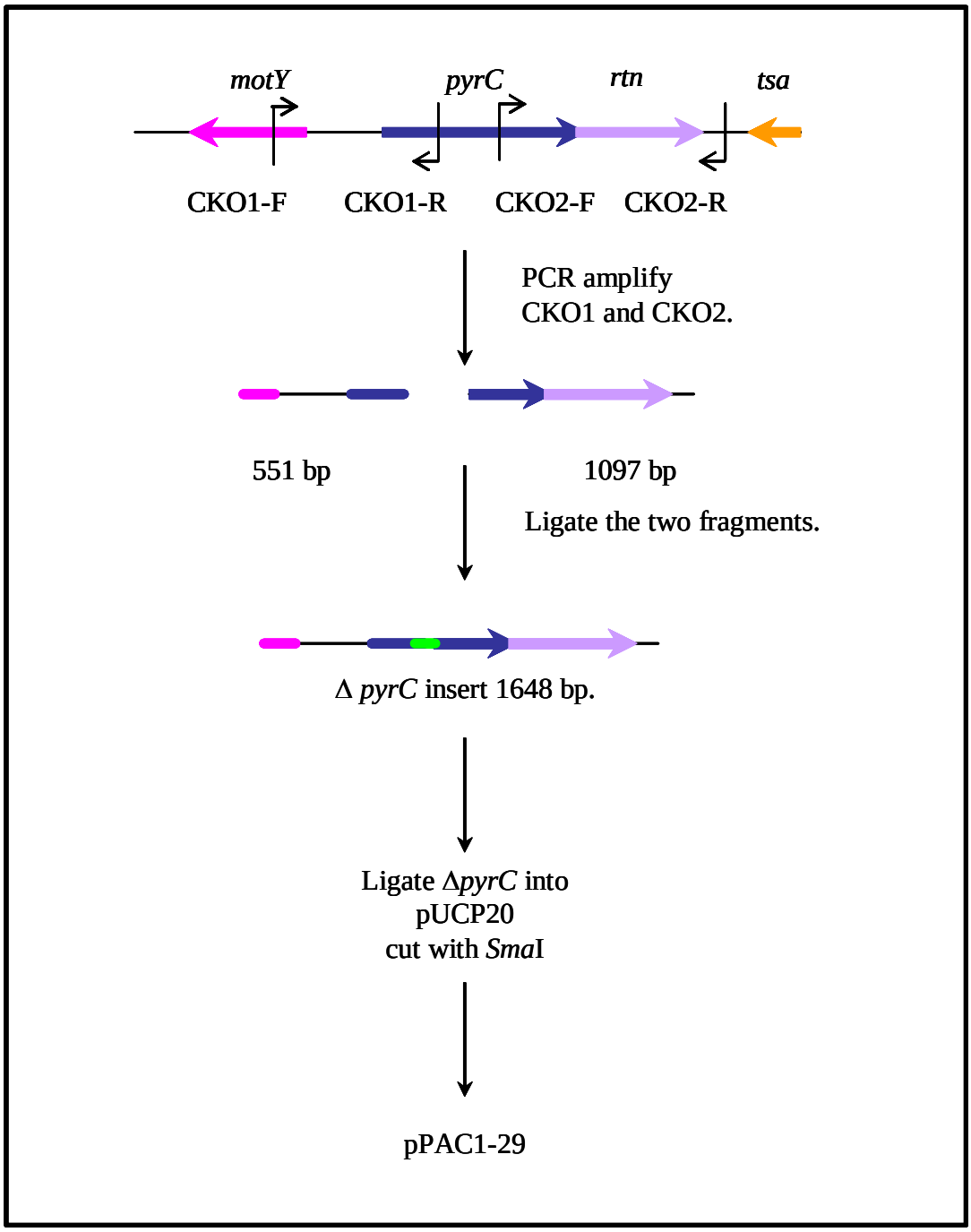

Fig. 23. PCR amplification scheme for the construction of the truncated *pyrC* gene.

Primer	Sequence (5' - 3')[b] (location)	Relevant property (size amplified)	Restriction site
CKO1-F	TGCTCTAGAGGCAGGCTGCTGAGCAGG (located 174-bp upstream from the *pyrC* start)	Outer primer used to amplify *pyrC* knock out fragment 1 (515-bp)	*Xba* I
CKO1-R	CGCGGATCCAGAGTCCGAGTTGGTGG (located 377-bp within the *pyrC* gene)	Inner primer used to amplify *pyrC* knock out fragment 1 (515-bp)	*Bam* HI
CKO2-F	CGCGGATCCGCGCCGCACGCCCGCCAC (located 744-bp within the *pyrC* gene)	Outer primer used to amplify *pyrC* knock out fragment 2 (1097-bp)	*Bam* HI
CKO2-R	ACATGCATGCGGGCTCGCGAGGGCCGGCAG (located 796-bp from the end of the *pyrC* gene; 124-bp from the end of the overlapping *rtn* gene)	Inner primer used to amplify *pyrC* knock out fragment 2 (1097-bp)	*Sph* I
PYRC3-F1	CCCAAGCTTCAACTCGAACATCCAGGACGGC (located 381-bp upstream from the start of the *pyrC3* gene)	Outer primer used to amplify *pyrC3* gene for cloning into pUCP19 (1771-bp)	*Hin* dIII
PYRC3-R	CCGGAATTCCTGCGCTAGGGCCGTGGGCG (located 52-bp downstream from the end of the *pyrC3* gene)	Inner primer used to amplify *pyrC3* gene for cloning into pUCP19 (1771-bp)	*Eco* RI
BAM FC-1	CGCGGATCCGCACCTCGCCGCTACCGA (located 302-bp within the *motY* coding sequence)	Outer primer used to amplify *pyrC* promoter region (788-bp)	*Bam* HI
HINDRC-1	CCCAAGCTTGTCGATGCGGGTCACGCC (located 353-bp within the *pyrC* coding sequence)	Inner primer used to amplify *pyrC* promoter region (788-bp)	*Hin* dIII
HIN MOT-F	CCCAAGCTTGCACCTCGCCGCTACCGA (located 302-bp within the *motY* coding sequence)	Outer primer used to amplify *motY* promoter region (788-bp)	*Hin* dIII
BAM MOT-R	CGCGGATCCGTCGATGCGGGTCACGCC (located 353-bp within the *pyrC* coding sequence)	Inner primer used to amplify *motY* promoter region (788-bp)	*Bam* HI
UKQ50-F	CGCGGATCCGTTCGATAACGCGGCGGG (located 259-bp upstream of the start of ORF PA5539)	Outer primer used to amplify putative promoter region for ORF PA5539 (304-bp)	*Bam* HI
UKQ50-R	CCCAAGCTTGGTGGTGGTCTGGCGGG (located 45-bp within the ORF PA5539 coding sequence)	Inner primer used to amplify putative promoter region for ORF 5539 (304-bp)	*Hin* dIII
CAQ50-F	CGCGGATCCGCATCGGACTGCCCCTGG (located 268-bp upstream from the start of the probable carbonic anhydrase gene)	Outer primer used to amplify putative promoter region for probable carbonic anhydrase (348-bp)	*Bam* HI
CAQ50-R	CCCAAGCTTTTGCCGCAGATGATCGCGG (located 80-bp within the probable carbonic anhydrase coding sequence)	Inner primer used to amplify putative promoter region for probable carbonic anhydrase (348-bp)	*Hin* dIII
C3Q50-F	CGCGGATCCCTCGAACATCCAGGACGGC (located 381-bp upstream of the *pyrC3* ATG start)	Outer primer used to amplify the putative promoter region for *pyrC3* (469-bp)	*Bam* HI
C3Q50-R	CCCAAGCTTTCGATGCGACCGTGGCGG (located 88-bp within the *pyrC3* coding sequence)	Inner primer used to amplify the putative promoter region for *pyrC3* (469-bp)	*Hin* dIII

Table 2. PCR primers used in this study. Primers were purchased from IDT or Biosynthesis. Incorporated restriction sites are underlined.

beginning of the *pyrC* gene. CKO2 was 1097 bp in length and contained the last 301 bp of the *pyrC* gene and the entire 672 bp of the overlapping *tsaA* gene and an additional 124 bp downstream. When ligated, these PCR fragments created a 1.6 kb DNA fragment, containing a Δ*pyrC* that lacked 409 bp from the middle of the gene.

The 1.7 kb blunt-ended DNA fragment was ligated into pUCP20 and cut with *Sma*I, producing plasmid pPAC1-29. The Δ*pyrC* fragment was then excised using *Sac*I and *Sal*I and directionally cloned into pEX18Gm cut with the same enzymes. The resulting plasmid, pEX18Gm-Δ*pyrC* (Fig. 24) was transformed into *E. coli* SM10 and then transferred into PAO1 via conjugation. Briefly, donor cells (d) were cultivated in LB broth with Km_{25} and Gm_{15} at 37°C overnight, while recipient cells (r) were grown in LB at 42°C overnight.

The next morning, the cells were subcultured into fresh LB medium and grown to an OD_{600} of 0.6. Next, donor and recipient cells were mixed in a 1.5ml microcentrifuge tube at ratio of 1:20 (d:r) in a total volume of 200 μl. The cells were pelleted by centrifugation at 10,000 x g for 1 min. The supernatant was removed and the cells were resuspended in 30μl of normal saline by gentle pipetting up and down. The cells were then spotted onto a pre-warmed LB plate and incubated, with the plate face up, at 30°C overnight.

After the overnight mating at 30°C, the cells were scraped into 1 ml of normal saline in a 1.5 ml microcentrifuge tube. Serial dilutions were made with normal saline and plated onto PIA plates containing Gm_{100}. Colonies resulting from single crossovers and plasmid integration were patched to PIA Gm and PIA sucrose, looking for the Gm^r

and Suc^{r} plasmid integrant phenotype. Those with the correct phenotype were picked to LB

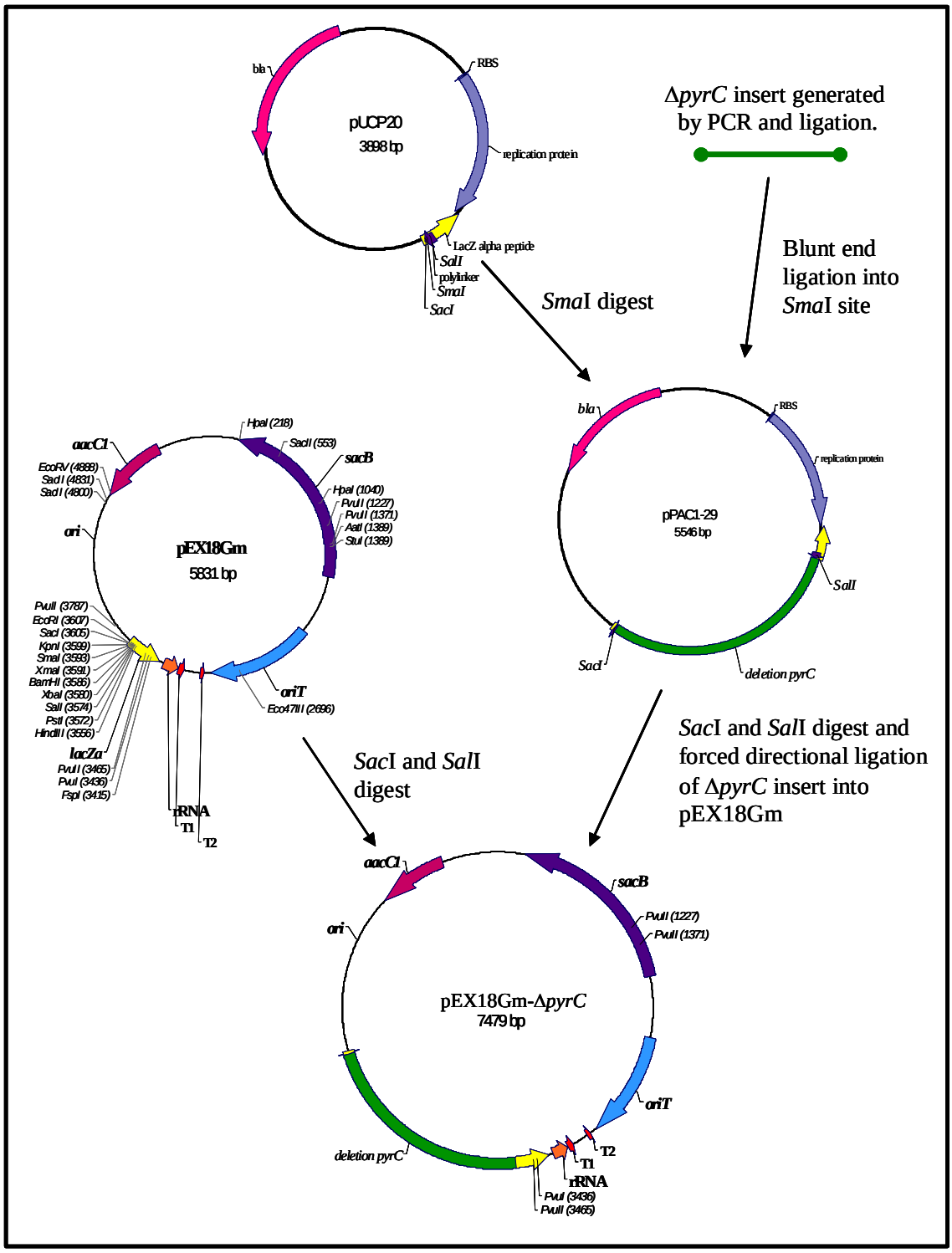

Fig. 24. Construction of plasmid pEX18Gm-Δ*pyrC*. This plasmid was mated into *P. aeruginosa* and the Δ*pyrC* gene was transferred to the chromosome by allelic exchange.

broth tubes without antibiotic, and cultivated at 37°C overnight. Again, serial dilutions were made and plated this time onto PIA containing 10 % sucrose. Resulting colonies were patched to PIA Gm_{100} and PIA sucrose, looking for the double crossover phenotype Gm^s and Suc^r. Resulting colonies that were positive for this phenotype were selected for further analysis.

Insertional inactivation of *pyrC2* gene.

The *pyrC2* gene was cloned as a 1.7 kb DNA fragment which was generated from PAO1 genomic DNA by PCR using *Pfu* polymerase (NEB) and the primers PYRC2F1 and PYRC2R (Table 2). The resulting PCR fragment contained the entire *pyrC2* gene as well as 371 bp of upstream DNA and 52 bp of downstream DNA. The PCR product was digested with *Eco*RI and *Hin*dIII and then ligated using T4 DNA ligase (NEB) into pUCP19 cut with the same restriction enzymes, producing the plasmid pPAC2-6 (Fig. 25). This plasmid expresses the *pyrC2* gene from the *lacZα* promoter.

In order to construct the *pyrC2*::Gm replacement vector, pPAC2-6 was digested with *Eco*47III, which cuts at a unique site 310 bp within the *pyrC2* gene, 691 bp within the cloned DNA fragment, leaving blunt ends. Next, a 1.7 kb gentamycin-omega cassette was isolated from pGMΩ1 (Schweizer, 1993) with *Sma*I. This insert contains the *aacC1* Gm resistance gene flanked by omega cassettes that prevent read-through by RNA polymerase on either side of the *aacC1* gene. This insert was then ligated into the cut pPAC2-6 vector to produce pPAC2-6::GmΩ (Fig. 26). The *pyrC2*::GmΩ insert was isolated by restriction digest with *Pvu*II, which leaves blunt-ends. The resulting 3.6-kb fragment was ligated into the shuttle vector pRTP1 (Stibitz *et al.,* 1986) cut with *Hin*dIII

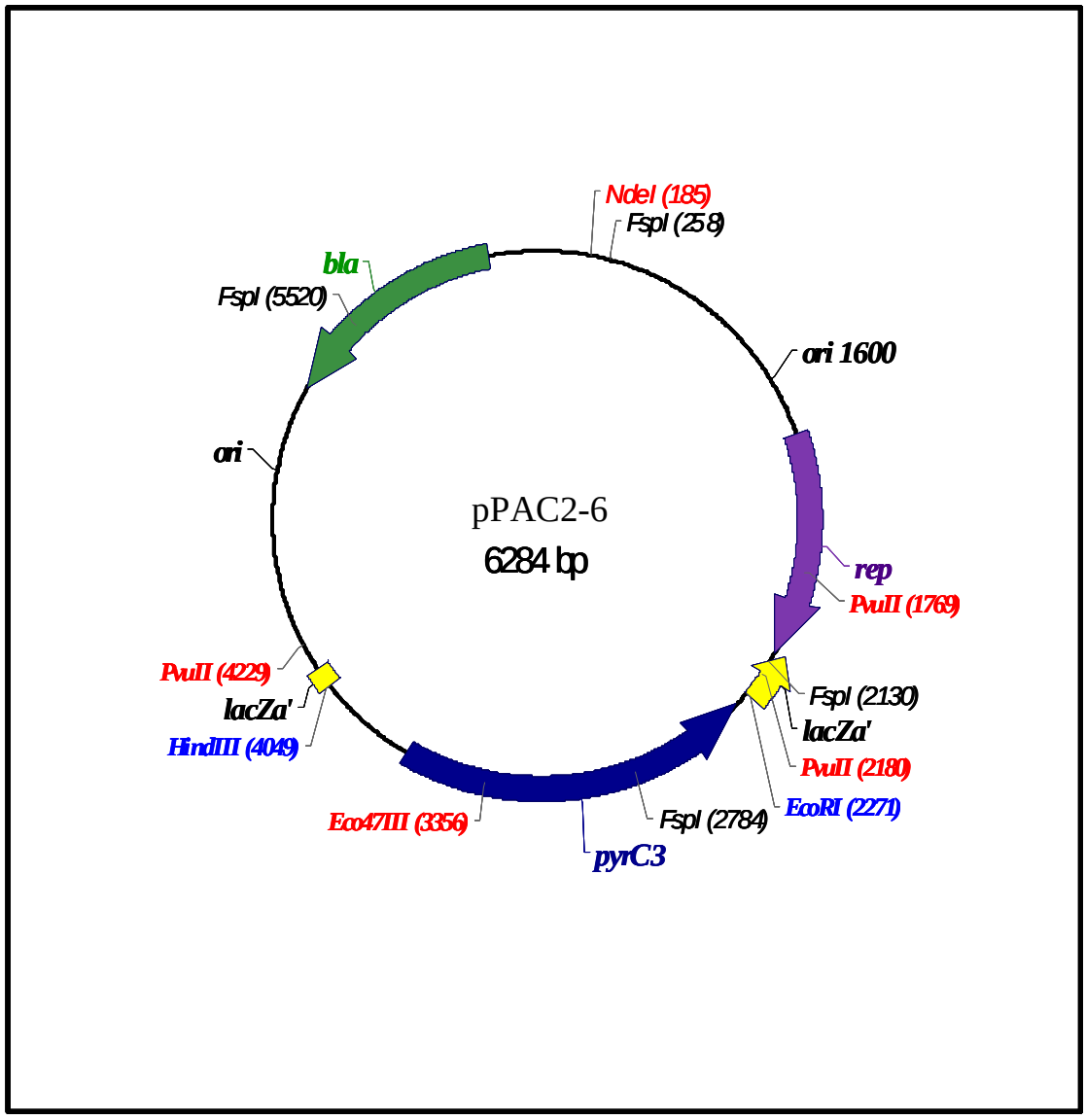

Fig. 25. Plasmid map of pPAC2-6. The *pyrC2* gene was PCR amplified from PAO1 genomic DNA. The primers used for PCR contained the restriction sites *Eco*RI and *Hin*dIII (see Table 2). The PCR product was digested with *Eco*RI and *Hin*dII and the insert was forced directionally ligated into the parent vector pUCP19 digested with the same restriction enzymes.

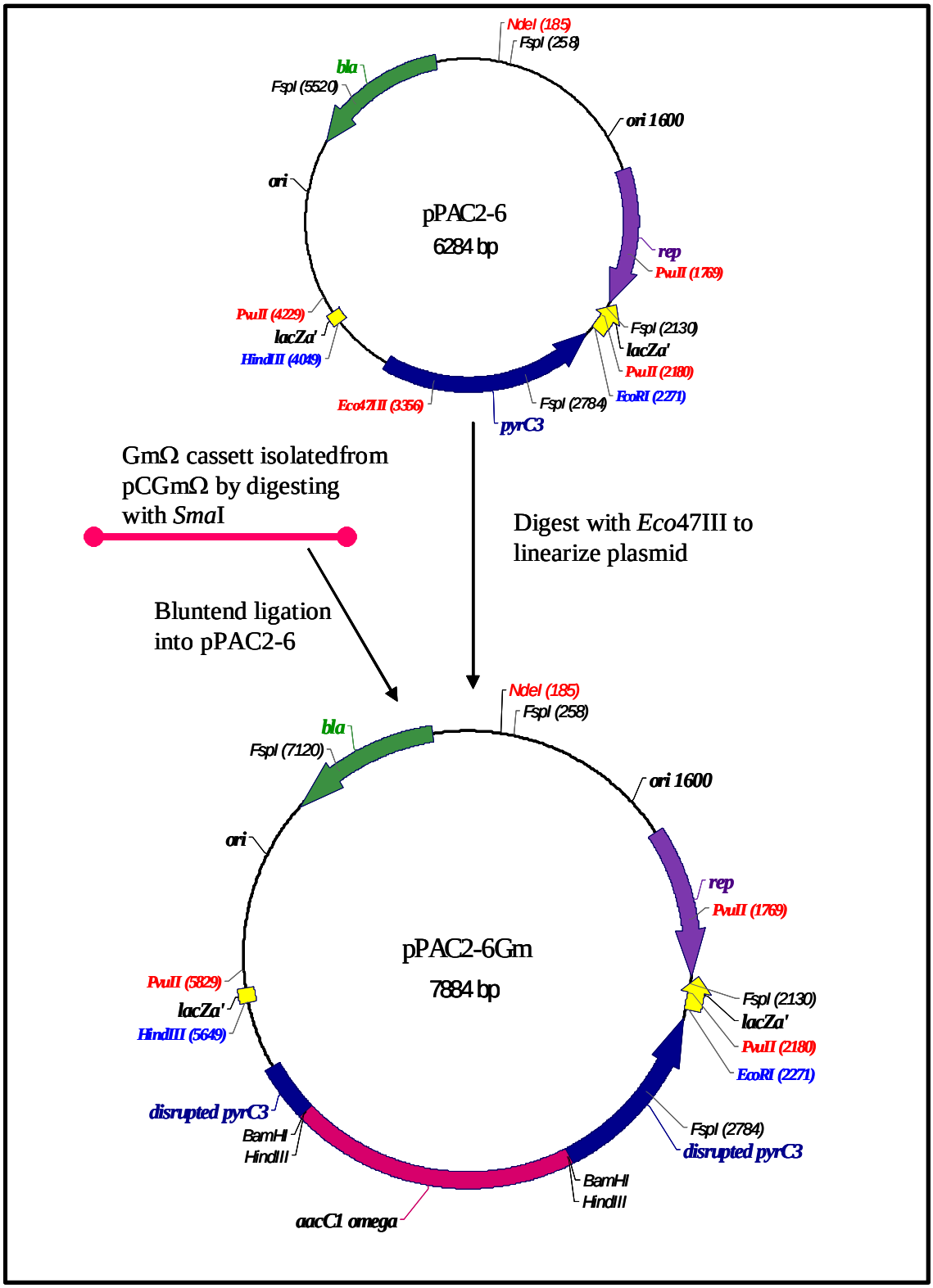

Fig. 26. Construction of plasmid pPAC2-6Gm. The Gm resistance cassett, *aacC*1, was isolated from pCGmΩ and ligated into the *pyrC2* gene in plasmid pPAC2-6.

and blunt ended with Klenow fragment. The resulting plasmid, pRTPC3::GmΩ (Fig. 27), was transformed into *E. coli* SM10 and then transferred into *Pseudomonas* PAO1 and PAODB37, the *pyrC* deletion mutant, by conjugation. Recipients carrying integrated pRTPC2::GmΩ were selected on PIA containing Gm_{100} and Cb_{300}. Colonies appearing after 24 h of growth were grown over-night in LB broth containing Gm_{100} at 37°C. Serial dilutions were plated on PIA Gm_{100} and the resulting colonies were patched to PIA Gm_{100} and PIA Gm_{100}, Cb_{300} plates. Those growing only on PIA Gm_{100}, representing potential double cross-overs, were selected for further analysis.

Southern hybridization to confirm the genotype of the *pyrC* deletion mutant.

As mentioned above, the *pyrC* gene of *P. aeruginosa* was inactivated by gene replacement with a defective copy of the *pyrC* gene that lacked 409 bp from the middle of the coding sequence. A Southern blot of the genomic DNA from the resulting mutants and wild-type was used to confirm that the *pyrC* gene was actually replaced with the defective version, and not merely inserted elsewhere on the chromosome. To that end, 10 μg of genomic DNA from PAO1 wild-type, PAO1 *pyrC*, PAO1 *pyrC2*, and the PAO1 double mutant was digested with 10 U of *Eco*RI in a total volume of 100 μl for 5 h at 37° C. Half of each of the digests was loaded and electrophoresed on a 1 % TRIS-acetate-EDTA (TAE) agarose gel at 30 volts for 17 h, while the remaining digested DNA was stored at –20°C. The gel was stained with ethidium bromide and then photographed.

In order to prepare the gel for DNA transfer, it was soaked in 1 L (10 x the gel volume, which was 100 ml) of denaturation solution (0.5 M NaOH and 1.0 M NaCl) for 1 h and 30 min. The gel was then rinsed two times with 200 ml of sterile ddH_2O. Next, the

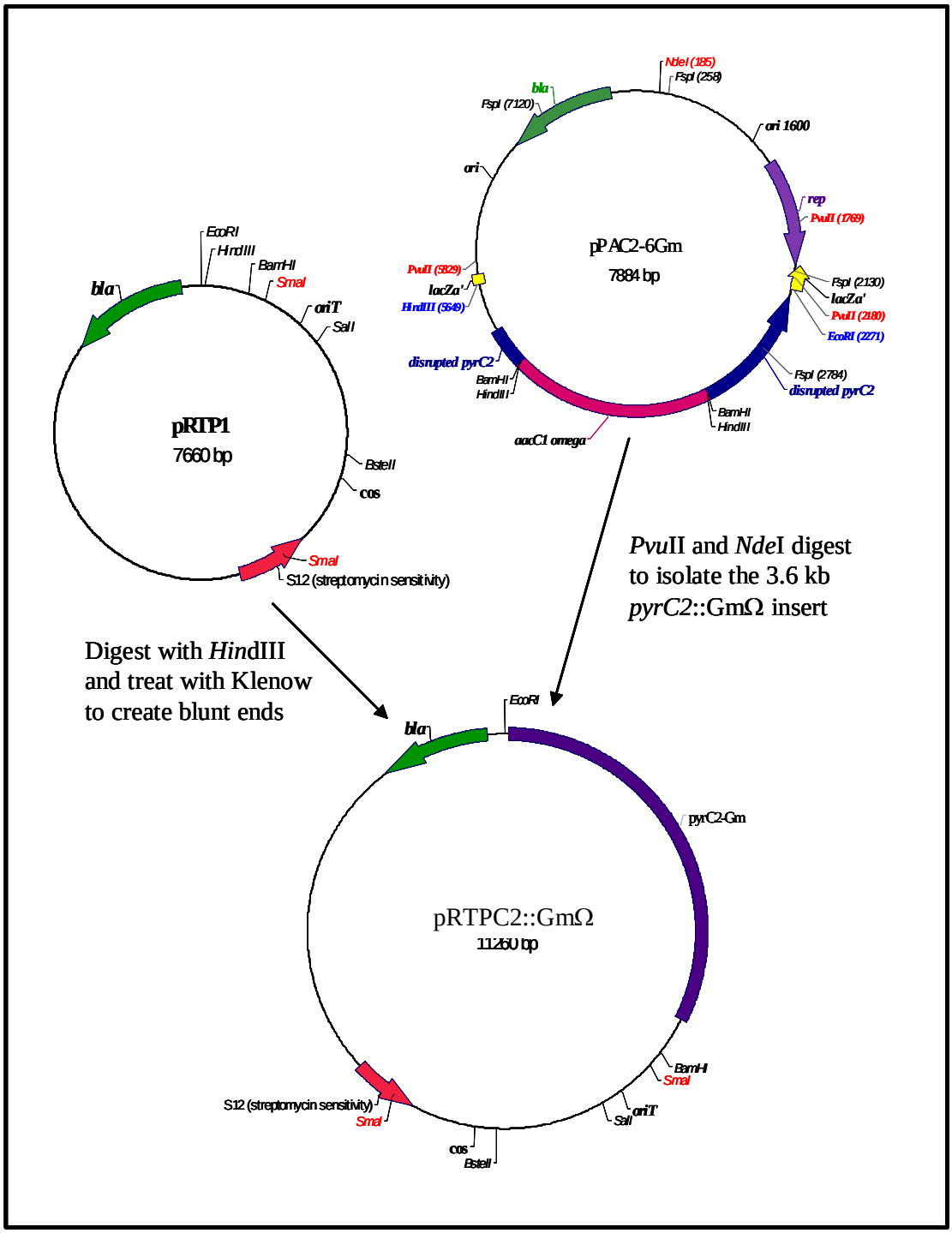

Fig. 27. Construction of plasmid pRTPC2::GmΩ. This plasmid was mated into *P. aeruginosa* and the interrupted *pyrC2* gene was transferred onto the chromosome by allelic exchange.

gel was soaked in 1 L of neutralization solution (0.5 M Tris pH 7.0 and 1.5 M NaCl), for 30 min. The neutralization solution was poured off and 1 L of fresh neutralization solution added and the gel was soaked for an additional 30 min. The gel was then ready for transfer. The DNA was transferred to a neutral nylon membrane, (Hybond©) supplied by Quiagen, that had been cut such that it was 1 cm longer than the gel on any side. Neutral transfer buffer is used to transfer DNA to uncharged membranes, therefore, neutral 10 x SSC (standard sodium citrate containing 3 M NaCl, 0.3 M Na_3Citrate dihydrate, and HCl to bring the pH to 7.0) was used. The wick transfer apparatus was set up as described in Sambrook *et al.*, 1999, and the transfer was allowed to proceed overnight.

When the DNA transfer was complete, the apparatus was disassembled, and then the membrane soaked in 6 x SSC for 5 min at room temperature. The membrane was then dried on 3MM Whatman paper for 30 min at room temperature. Next, the DNA was fixed to the membrane by baking. The dry membrane was sandwiched between two sheets of Whatman paper and then placed in a 70°C incubator for 1 h. The membrane was then ready for hybridization.

The membrane was first incubated at 65°C in a prehybridization solution, in order to block any areas that could bind probe DNA nonspecifically. The prehybridization solution contained 6 x SSC, 5 x Denhardts solution, 0.5 % SDS and denatured salmon sperm DNA at a concentration of 100 μg ml^{-1}. A 50 x Denhardts stock was prepared as described in Sambrook *et al.*, 2000 and contains 1 % Ficoll 400, 1 % polyvinyl pyrolidone (PVP) and 1 % bovine serum albumin (BSA). The prehybridization step was

allowed to proceed overnight while the probe DNA was labeled and readied for hybridization.

For this experiment, the entire 2.49 kb insert from pPAC1 was used as a probe. The insert was excised from 10 μg of pPAC1 using the enzyme *Eco*RI in a 5 h digest with 10 U of enzyme. This resulted in a theoretical yield of 3.57 μg of insert DNA which was electrophoresed and excised from an agarose gel using the Sephaglass™ BandPrep Kit (Pharmacia Biotech). The probe DNA was labeled with α^{32}P-dATP (6000 Ci mmol $^{-1}$; 20 mCi ml^{-1}) which was supplied by New England Nuclear (NEN), using the fill-in activity of Klenow DNA polymerase (Fig. 28). Probe DNA (500-750 ng) was combined with 50 μCi α^{32}P-dATP. Next, a cocktail of dNTPs (-dATP) at a final concentration of 0.1mM, NEB buffer # 2 and 1.25 U of Klenow enzyme, supplied by NEB, was added. The final volume of the reaction was 50 μl. Note that the Klenow enzyme is only 50 % effective in NEB buffers 1-4, but only 0.5 U was required for the reaction (0.5 U per 0.5 μg DNA). The fill-in reaction was allowed to proceed at room temperature for 15 min. Next, a mixture of "cold" (non-radioactive) dNTPs (including dATP) was added at a concentration of 0.2 mM, as a chase step. The reaction continued for another 5 min and was then terminated by incubation at 75°C for 10 min. The unincorporated dNTPs were removed using the Microselect-D G-25 spin column supplied by 5'- 3'.

In order to assess the level of ^{32}P-ATP incorporation into the probe DNA, 1 μl was placed on a piece of 3MM Whatman paper and the counts per minute (cpm) were measured using a scintillation counter. The labeled probe DNA was now ready for hybridization with the membrane bound genomic DNA. Prior to its addition, the probe

DNA was boiled for 5 min and then quick cooled by placing it in an ice-water bath. This was done in order to ensure that the probe DNA was denatured (single stranded) and

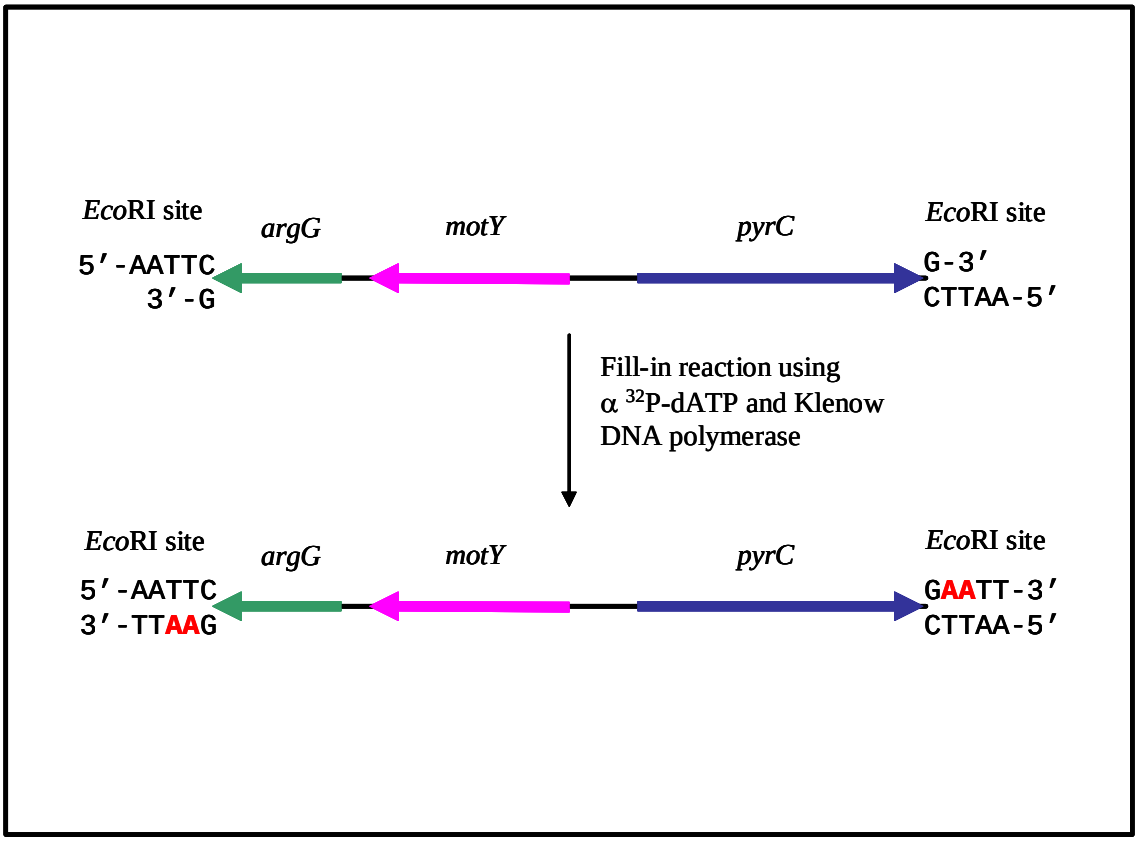

Fig. 28. Fill-in reaction of the *pyrC* probe DNA. The 2.5 kb insert from pPAC1 was isolated by restriction digest with *Eco*RI. The 3' recessed ends were filled in using α^{32}P-dATP and the Klenow DNA polymerase. The incorporated radioactive residues are depicted in red.

would bind to its area of identity on the membrane. The prehybridization solution was removed and 11 ml of new hybridization solution (the same formula as the prehybridization solution) was added (0.1 ml $(cm^2)^{-1}$). The boiled, quick-cooled probe DNA was added and the membrane was hybridized at 50°C for 14 h.

After the hybridization step, unbound probe was removed by washing the membrane. The membrane was first washed with a solution containing 2 x SSC and 0.5 % SDS (1 ml $(cm^2)^{-1}$ of membrane) at room temperature for 5 min. Next the membrane was washed with 2 x SSC and 0.1 % SDS for 15 min, again at room temperature. After this wash step, the background counts were checked with a Geiger counter. The background was still high so the membrane was washed further, this time in 0.1 x SSC and 0.1 % SDS for 30 min at room temperature. After this step, the background was found to be lower, so the membrane was subjected to a final wash of 0.1 x SSC for 3 min at room temperature. After this, the membrane was placed on 3MM paper and allowed to dry briefly but not completely (less than 5 min). The membrane was then sandwiched between two pieces of suran wrap and the labeled DNA bands, resulting from hybridization, were visualized by autoradiography using Kodak film and a 24 – 36 h exposure in the freezer at -70°C.

Construction of pQF50 promoter fusion vectors.

In order to study the putative promoter regions for the *pyrC* and *pyrC2* genes, each upstream region was amplified using *pfu* polymerase and a primer pair with engineered *Bam*HI and *Hin*dIII ends (Table 2). The PCR products were then digested, agarose gel purified and directionally cloned into the *lacZ* promoter fusion vector, pQF50, which had been cut by the same enzymes, as seen in Fig. 29. Three regions were

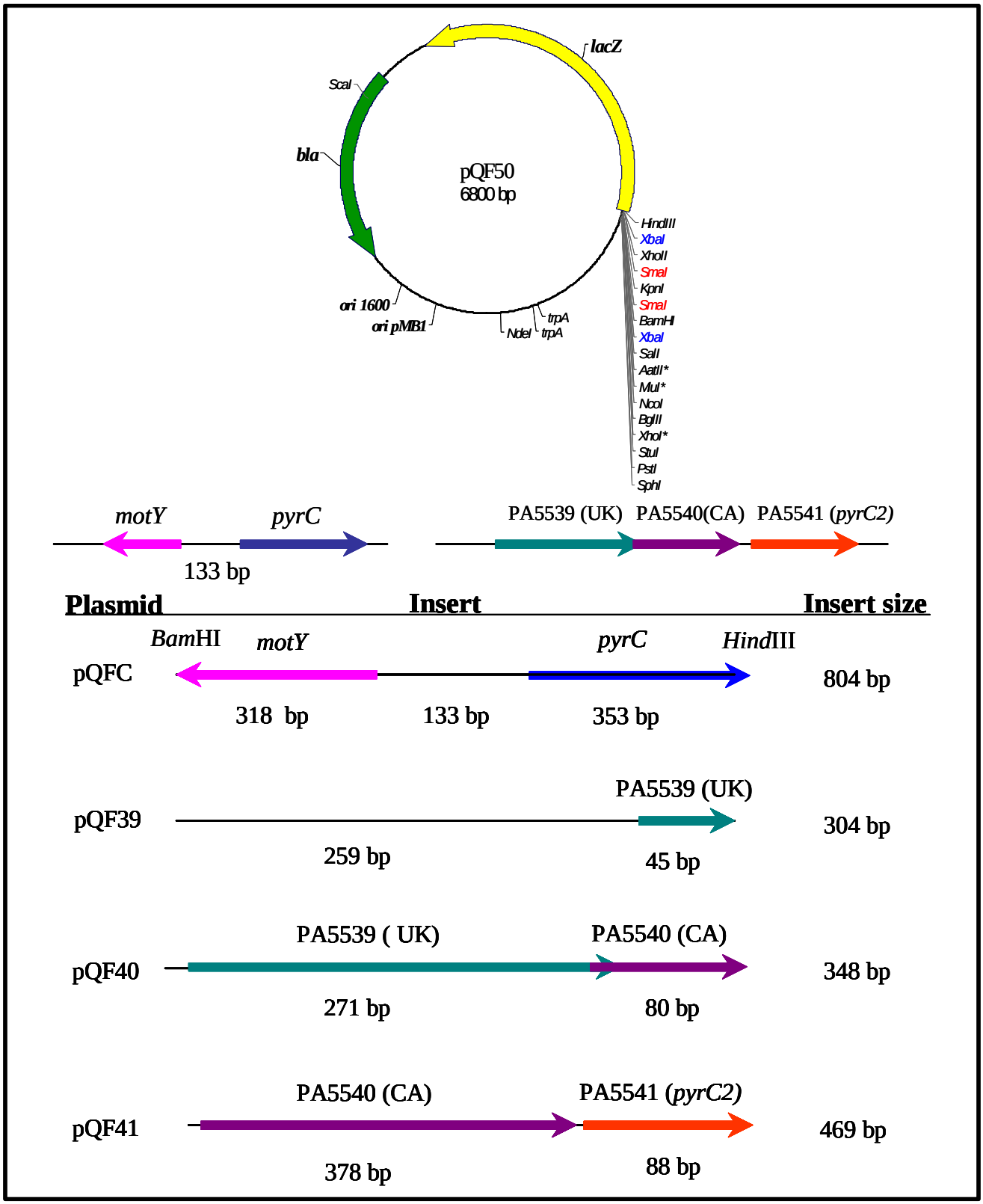

Fig. 29. Construction of pQF50 transcriptional promoter fusion plasmids containing the upstream regions of *pyrC* and *pyrC2*. The promoter regions were isolated by PCR amplification using PAO1 genomic DNA. The PCR products contained *Eco*RI and *Hin*dIII ends and were directionally ligated into pQF50 digested with the same enzymes. The restriction enzymes in the MCS of pQF50 marked with an (*) are not unique sites within the plasmid.

amplified for the study of the *pyrC2* promoter as the *pyrC2* gene is apparently the last of a three-gene operon, and it was not known definitively where transcription was initiated. The resulting plasmids were electroporated into PAO1 and its pyrimidine mutant derivatives.

β-galactosidase assays.

P. aeruginosa harboring the pQF50 promoter fusion vectors containing the promoter regions for *pyrC, motY* and the three potential promoter regions for *pyrC2* were cultivated in various media containing Cb_{300}. The cells were grown to mid log (OD_{600} = 0.6 - 1.0) or to stationary phase and the OD_{600} was measured and recorded. The β-galactosidase assay procedure of Miller (1992) was followed. To that end, 0.1 to 0.5 ml of culture was combined with Z buffer in a 15 ml test tube, to a final volume of 1 ml. Z buffer contains 60 mM $Na_2HPO_4 \bullet 7H_2O$, 40 mM $NaH_2PO_4 \bullet H_2O$, 10 mM KCl, 1 mM $MgSO_4 \bullet 7H_2O$ and 50 mM β-mercaptoethanol. The solution was adjusted to pH 7.0 and then not autoclaved but instead stored at 4°C. Cells were disrupted to release β-galactosidase enzyme by adding 100 μl chloroform and 50 μl 0.1 % SDS to each 1ml sample. Tubes were vortexed vigorously for 10 sec. The tubes were then placed in a 28°C water bath for 5 min. The reaction was initiated with the addition of 0.2 ml of *o*-nitrophenyl-β-D-galactoside (ONPG) (4 mg ml^{-1}) to each tube. The tubes were mixed by shaking for a few seconds and then placed back into the water bath. The reaction was allowed to proceed for 7 to 15 min.

The reaction time was recorded and the reaction stopped by the addition of 0.5 ml of 1 M Na_2CO_3. The tubes were vortexed briefly and a 1 ml aliquot of each tube was

removed to a 1.5 ml Eppendorf tube. The samples were centrifuged at 12,000 x g for 5 min at 4°C in order to pellet the cellular debris. The A_{420} of the clarified yellow solution was measured and recorded. Preferred readings are those in the range of 0.6 to 0.9. β-galactosidase enzyme units (Miller units) were calculated by the following equation:

$$\frac{1000 \times A_{420}}{t \times v \times A_{600}} = \text{units of } \beta\text{-galactosidase}$$

where *t* is the reaction time in minutes, and *v* is the volume of culture used in the assay in milliliters. Miller units are proportional to an increase in *o*-nitrophenol per minute, per bacterium, as determined for *E. coli* (Miller, 1992).

Growth curve studies.

Growth curves of each of the pyrimidine mutant strains, and PAO1 wild-type, were initiated by first inoculating a 5 ml starter culture of the appropriate medium, the same as that to be used in the growth curve study, and incubating overnight. This overnight culture (15 – 20 h) was used to inoculate 30 ml of medium in a 125 ml Erlenmeyer flask. The bacteria were diluted 1:1000 (300 µl inoculum for a 30 ml culture) and the OD_{600} measured and recorded for time zero. The cultures were incubated at 37°C with shaking at 250 rpm. At the indicated time points, 1 ml of each culture was aseptically removed and the OD_{600} recorded.

Partial purification of *P. aeruginosa* DHOase.

In order to purify the DHOase encoded by *pyrC*, the *E. coli pyrC* strain, X7014a, was transformed with the *pyrC* containing plasmid, pPAC1. The resulting prototrophic

transformants were cultivated in 1 L of Ecmm with Ap_{100} and adenine for 36 h (since the *pyrC* gene is expressed from its own *P. aeruginosa* promoter, it takes a while for pPAC1 to complement and for the culture to reach the mid-log growth phase). Cells were harvested by centrifugation in a Sorval centrifuge at 12,000 x g for 10 min at 4°C using the GS-3 rotor. The supernatant was removed and the cell pellet (5 g) was resuspended in 10 ml of DHOase breaking buffer as described by Zimmerman and Evans (1993). DHOase breaking buffer contains 50 mM Tris-acetate pH 8.3, 10 % glycerol, 50 mM NaCl, 50 μM $ZnCl_2$ and 1 mM DTT. The cells (17 ml final volume) were broken by French press and then the cell extract was centrifuged at 16,000 rpm using the SA600 rotor, for 30 min at 4°C to pellet the cell debris.

Nucleic acids were removed by from the cell extract by streptomycin sulfate precipitation with the addition of 5 ml of a 10 % solution of streptomycin sulfate, to a final concentration of 3 %. This mixture was stirred slowly at 4°C and allowed to equilibrate for 2 h, after which, the solution was centrifuged at 15,000 rpm for 40 min in the SA600 rotor at 4°C. The supernatant was removed and placed into a dialysis bag and the sample was dialyzed against 4 liters of DHOase breaking buffer overnight. The sample was then centrifuged as above and the supernatant subjected to ammonium sulfate fractionation using the following percent (w/v) cuts: 35 %, 45 %, 50 %, 55 %, 60 % and 65 %. Solid ammonium sulfate was slowly added at each fraction step, and this mixture was stirred at 4°C and allowed to equilibrate in the cold for 1 h. The mixture was then centrifuged at 16,000 rpm, using the SA600 rotor, for 30 min at 4°C. Samples of the supernatant (0.5 ml) were collected at each step and stored at 4°C. Also, each pellet was resuspended in 1 ml of DHOase breaking buffer and stored at 4°C. All samples were

assayed for DHOase activity to determine the ammonium sulfate fraction at which DHOase precipitates.

The fractions containing the peak DHOase activities were pooled and subjected to a “heat purification step” adapted from a method described by Washabaugh and Collins**,** 1986. To that end, the volume of the pooled ammonium sulfate fractions was increased to 50 ml with DHOase breaking buffer in a 150 ml Erlenmeyer flask. A rubber stopper with a thermometer was placed into the mouth of the flask in order to monitor the temperature of the liquid with in. The flask was placed into a 90°C water bath until the temperature of the liquid reached 71°C (this took about 3 min). Then the flask was transferred to a 72°C water bath in order to maintain the temperature of the cell extract at 72°C for an additional 3 min. The flask was swirled continuously during this incubation step.

Next the solution was rapidly cooled to 4°C in an ice bath (approximately 5 min). The solution was then centrifuged at 16,000 rpm, using the SA600 rotor, for 30 min at 4°C, which pelleted the white, fluffy, denatured extraneous proteins. The supernatant was collected and the soluble DHOase was precipitated by the addition of 65 % (w/v) ammonium sulfate as described above. The resulting pellet was resuspended in 1 ml of DHOase breaking buffer and stored at 4°C. The sample was assayed for DHOase activity and analyzed on SDS and non-denaturing PAGE gels in order to determine purity and size of the partially purified DHOase.

Zubay Analysis of *pyrC* and *pyrC2* gene products.

The *pyrC* and *pyrC2* gene products were identified and characterized from pPAC1 and pPAC2-6, respectively, using the *E. coli* S30 Extract System (Promega)

which is an *in vitro* transcription/translation system. This method of expressing plasmid encoded genes using *E. coli* cell extract, free of its own DNA, was originally described by Zubay, 1973. An *E. coli* strain B is used to isolate the expression machinery. This strain B is deficient in OmpT endoproteinase and ion protease activity, thus the stability of the expressed proteins is greater than if the proteins were expressed *in vivo* and subject to degradation by these proteases.

The *E. coli* S30 expression system includes an S30 Premix, which contains rNTPs, tRNAs, an ATP-regenerating system, IPTG and appropriate salts but no amino acids, and the S30 Extract, which contains the *E. coli* strain B expression machinery, including RNA polymerase and ribosomes. An amino acid mixture is provided which lacks methionine, so that ^{35}S methionine may be added separately and incorporated into the translation products. This allows detection of the translated proteins using autoradiography. A strong limitation of the system is that expression of cloned DNA fragments requires that they be under the control of a good *E. coli* promoter. Examples of such promoters include the lambda P_R, lambda P_L, *tac*, *trc* and *lac*UV5. The *pyrC2* gene was cloned in pPAC2-6 such that it would be expressed from the *lacZ*α promoter, which is equivalent to the *tac* promoter. However, expression of the *pyrC* gene in pPAC1 using *E. coli* S30 system was questionable, since the *pyrC* gene was ligated in the opposite orientation to the *lacZ*α promoter and expressed off of its own *P. aeruginosa* promoter. Never-the-less, this plasmid is capable of complementing an *E. coli pyrC* auxotroph, thus it was likely that the *E. coli* S30 transcription/translation machinery would also be able to express the *pyrC* gene and therefore pPAC1 was used in the expression system. As a control, the parent plasmids pUCP20, pUCP19 and the plasmid pPAC2-25, containing

the *pyrC2* gene cloned in the opposite orientation to the *lacZα* promoter (Fig. 30), were also used in the *in vitro* expression system. The protocol entails combining 1 – 4 μg of cesium chloride purified plasmid DNA with 5 μl of the amino acid mixture minus methionine, 20 μl of the S30 premix without amino acids, 1 μl of ^{35}S methionine (1,200 Ci mmol^{-1} at 15 mCi ml^{-1}), 15 μl of the S30 extract and nuclease-free water to a final volume of 50 μl. The components were mixed in a 1.5 ml microcentrifuge tube and centrifuged briefly to bring the reaction mixture to the bottom of the tube. The reaction was then incubated at 37°C for 2 h and then stopped by placing the tubes in an ice bath for 5 min.

The results were analyzed by electrophoresis on an SDS PAGE gel. Prior to SDS PAGE gel analysis, 5 μl of the 50 μl sample was mixed with 20 μl of acetone and incubated on ice for 15 min. This acetone precipitation step is required to remove PEG 8000, which is included in the reaction mix (the presence of PEG will result in background salting and wavy banding patterns on the SDS gel). The acetone-precipitated S30 sample was centrifuged at 12,000 x g for 5 min. Next, the supernatant was removed and the pellet was dried in a "speed vac" for 15 min. The dry pellet was then resuspended in 20 μl of SDS PAGE sample buffer (see below) and heated at 100°C for 2-5 min. A 10 μl aliquot of the sample was loaded onto SDS PAGE gels and the remaining sample was stored at –20°C.

Before the radiolabeled bands could be visualized, the gels first had to be dried. The gels were dried in one of two ways. One method involved placing the gels on Whatman® 3MM paper, with a piece of plastic wrap on top, and drying on a vacuum gel

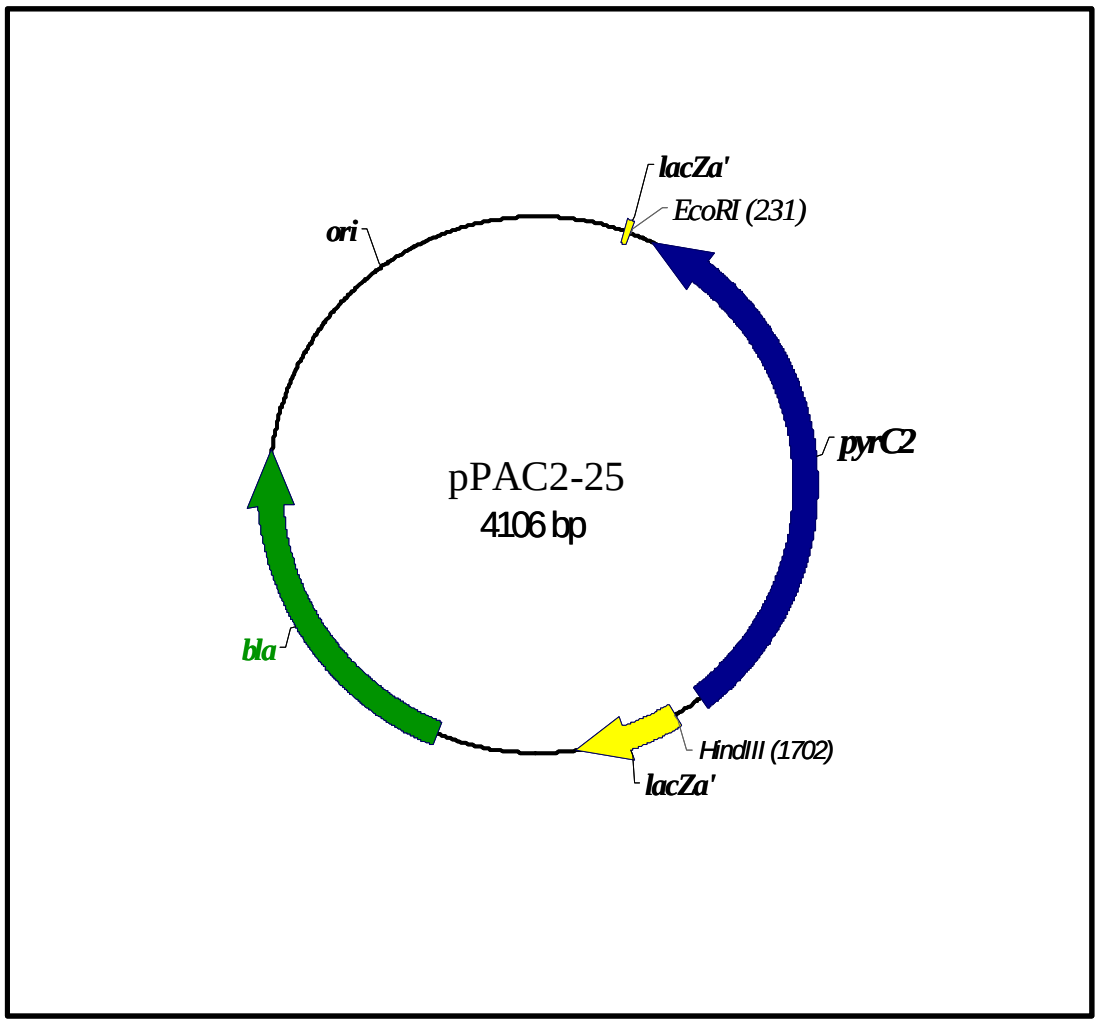

Fig. 30. Plasmid map of pPAC2-25. The parent vector, pUC18, was digested with *Eco*RI and *Hin*dIII and the *pyrC2* insert was directionally cloned into these sites. This results in the *pyrC2* gene being in the opposite orientation to the *lacZα* promoter.

drier at 60°C for 1 h followed by 1 h of drying at room temperature. The second method involved air- drying the gels using Promega's Gel Drying Kit (Cat.# V7120). The gels were soaked in 10 % glycerol for 30 min (to prevent cracking while drying) and then placed in between two sheets of thoroughly moistened cellulose gel drying film. The gel and drying sheets were then clamped into the drying frame and allowed to dry overnight. Following electrophoresis and drying, labeled protein bands were visualized by autoradiography using Kodak film and an overnight exposure in the freezer at -70°C.

Sodium dodecyl sulfate denaturing polyacrylamide gel electrophoresis (SDS PAGE).

Samples of partially purified cell extract, or from the *E. coli* S30 expression system, were analyzed on SDS PAGE gels in order to estimate enzyme subunits size. Typically, 12 % polyacrylamide separating gels with a 5 % staking gel were utilized. The 12 % gel was prepared in a 15 ml conical tube, by mixing 4 ml of acrylamide stock solution (solution A: 29 % (w/v) acrylamide, 0.8 % (w/v) bis-acrylamide in ddH_2O), 2.5 ml denaturing buffer B (1.5 M Tris-HCl, pH 8.8, 0.4 % (w/v) SDS in ddH_2O) and 3.5 ml of ddH_2O for a final volume of 10 ml. The solution was mixed gently by inversion, so that no bubbles were introduced. To this, 20 mg of ammonium persulfate (APS) was added. Just prior to pouring, 5 μl of N,N,N',N'-tetramethylene-ethylenediamine (TEMED) was added and the solution gently mixed by inversion. The gel was poured, using a Pasteur pipette, into the gel sandwich (two glass plates separated by spacers and fixed into the gel pouring apparatus for BioRad Mini-Protean gels). A 2 cm gap was left at the top for the stacking gel. N-butanol was added to the top of the gel to prevent drying, and the gel was allowed to polymerize at room temperature for 1 h.

Next, the butanol layer was later poured off and the remaining butanol rinsed away with ddH_2O. Kimwipes were used to remove any excess water and then the 5 % stacking gel was added. The stacking gel contained 2.3 ml ddH_2O, 0.67 ml of solution A, and 1.0 ml of the 4 x stacking gel buffer (solution C). Solution C contained 0.5 M Tris-HCl, pH 6.8 and 0. 4 % (w/v) SDS. APS (10 mg) and TEMED were each mixed into the solution by gentle inversion. The stacking layer was then poured into the gel sandwich and the comb was inserted to form the wells for sample loading. The stacking gel was allowed to polymerize for about 30 min.

The comb was carefully removed and the gel was attached to the electrode assembly (if running only one gel, a spacer plate was used on the other side of the electrode assembly so that an inner chamber was formed). The gel assembly was inserted into the electrophoresis tank and SDS denaturing electrode buffer was added to the inner and outer reservoir, making sure that the both the top and the bottom of the gel were immersed in buffer. SDS denaturing electrode buffer contains 25 mM Tris, 192 mM glycine and 0.1 % (w/v) SDS. The pH of the buffer should be approximately 8.3. After preparing and loading the samples, the gel was electrophoresed at 200V for 1 h 25 min or until the dye front was 1 cm or less from the bottom of the gel.

Samples were prepared by mixing 4 parts sample protein with 1 part of 5 x loading dye (60 mM Tris-HCl, 25 % (v/v) glycerol, 2 % (w/v) SDS, 14.4 mM β-mercaptoethanol and 0.1 % (w/v) bromophenol blue) to the desired volume (usually 20 μl) in a sterile microcentrifuge tube. Promega mid-range protein markers pre-mixed in loading dye (5 μl) were used as standards. The samples, including the standards, were

placed in boiling water for 5 min. Finally, the samples were cooled and loaded onto the gel.

After electrophoresis, the proteins were stained, using Coomassie Blue staining solution (45 % (v/v) methanol, 10 % (v/v) glacial acetic acid, and 0.1 % (w/v) Coomassie Brilliant Blue R-250 in ddH_2O), for 15 min while gently shaking. The stained gels were then destained for 2-4 h (overnight is not too long) using a solution of 10 % (v/v) methanol and 10 % (v/v) acetic acid in ddH_2O. Molecular masses of the samples were estimated by comparing the sample bands with those of the known Promega mid-range marker bands. These standards have molecular masses of 97.4 kDa, 66.2 kDa, 55.0 kDa, 42.7 kDa, 40.0 kDa, 31.0 kDa, 21.5 kDa, and 14.4 kDa.

Non-denaturing polyacrylamide gel electrophoresis and ATCase activity gels.

Non-denaturing polyacrylamide gels and standard protein markers were used to estimate the native sizes of the hybrid ATCases and DHOases I. The cell extracts analyzed were prepared as previously described. An 8 % separating gel was prepared in a 15 ml conical tube by combining 2.67 ml of a stock solution of acrylamide, solution A (29 % (w/v) acrylamide and 0.8 % bis-acrylamide in ddH_2O), with 2.5 ml of solution B (4 x separating buffer containing 1.5 M Tris-HCl, pH 8.8) and 4.83 ml of ddH_2O. APS was added (20 mg) and the solution was mixed gently by inversion. Just prior to pouring the gel, 5 μl of TEMED was added and the solution again mixed by gentle inversion. The gel was poured into a glass plate sandwich, using a Pasteur pipette, leaving a 2 cm gap for the stacking gel. N-butanol was layered on top of the separating gel, to prevent

drying, and a piece of plastic wrap was placed over the gel while it polymerized at room temperature for 1 h.

The butanol layer was poured off and ddH_2O used to rinse off any remaining butanol. Kimwipes were used to remove residual ddH_2O and then the stacking gel was prepared. The stacking gel contained 0.67 ml of solution A, 1 ml of solution C (4 x stacking buffer composed of 0.5 M Tris-HCl, pH 6.8) and 2.3 ml of ddH_2O. APS (10 mg) was added and the solution was mixed by inversion. TEMED (5 μl) was added and the solution mixed prior to pouring the stacking gel layer. After the stacking gel was poured, a comb was quickly inserted to form the wells for loading the samples. The gel was wrapped with plastic wrap and allowed to polymerize for 30 min.

The polymerized gel was inserted, as above, into the electrode apparatus and then placed into the buffer chamber. The running buffer contained 25 mM Tris-HCl and 192 mM glycine and the final pH was 8.8. The cell extract samples, typically 24 μl, were mixed with 6 μl of 5 x loading buffer (312.5 mM Tris-HCl, pH 6.8, 50 % (v/v) glycerol, and 0.05 % bromophenol blue in ddH_2O). The samples were loaded into the wells, and the gel was electrophoresed at 150 V for 1-2 h, or until the dye front was 1 cm or less from the bottom of the gel, at 4°C. After electrophoresis, the gel was stained and destained as described previously. Alternatively, the gels were stained specifically for ATCase activity, using the method previously described by Bothwell (Bothwell, 1975) and later modified by Kedzie (Kedzie, 1987) who used histidine instead of imidazole.

The gel to be stained was first soaked in 250 ml of ice-cold 50 mM histidine buffer, pH 7.0 for 5 min with gentle shaking. Next, 5 ml of 1 M aspartate and 10 ml of 0.1 M carbamoylphosphate were added to the histidine buffer and allowed to react for 20

min with continued gentle shaking. The gel was then rinsed 3 times with 100 ml of ice-cold ddH_2O to remove the reactants. Orthophosphate released enzymatically and trapped in the gel was precipitated by the addition of 3 mM lead nitrate dissolved in ice-cold 50 mM histidine, pH 7.0. After a 10 min incubation step with gentle shaking, the lead nitrate was removed with 3 changes of ice-cold ddH_2O. ATCase activity was visible as white bands at the site of lead phosphate precipitation. Intensity of the bands generally increased with storage of the gel overnight at 4°C in ddH_2O. The gel was counter stained with 1 % sodium sulfide for 3 min so that the white ATCase bands were better visualized. Incubating longer than 3 min results in the entire gel turning dark brown, making none of the ATCase bands visible. Brown lead sulfide replaces the white lead phosphate bands while the remaining gel turns tan in color. The gel was destained in ddH_2O to remove some of this background color. Gels were saved for scanning and documentation by drying in either of the two ways previously described.

CHAPTER III

RESULTS

Characterization of the three *pyrC* genes from *Pseudomonas aeruginosa*. *P. aeruginosa* has been found to possess three homologous *pyrC* genes. The first to be identified was named *pyrC'* (Vickrey, 1993). The other two *pyrC* genes, isolated and characterized in this research, have been designated *pyrC* and *pyrC2*. In order to determine if each encoded an active DHOase enzyme, each of these genes was cloned, and the resulting plasmids were transformed into the *E. coli pyrC* mutant X7014a. As seen in Table 3, the *pyrC* and *pyrC2* plasmids were able to complement the *E. coli pyrC* mutant, while the *pyrC'* plasmid could not. Thus, *pyrC'* does not appear to encode a catalytically active DHOase enzyme, which begs the question, what is its role in pyrimidine biosynthesis?

Vickery (1993) established that the PyrC' polypeptide is an integral part of the ATCase holoenzyme in *P. aeruginosa*. In fact, the PyrB and PyrC' subunits rely on each other to such an extent that when the *pyrB* gene, encoding the ATCase catalytic subunit, is isolated on a plasmid and transformed into the *E. coli pyrB* auxotroph TB2, it is not able to complement the mutation. Only when the *pyrB* and *pyrC'* genes are co-transformed on compatible plasmids, into *E. coli* TB2, is prototrophy observed. Thus, the PyrC' polypeptide is necessary for the architecture and function of the ATCase holoenzyme. The two remaining *pyrC* genes in *P. aeruginosa* are located in separate regions of the chromosome (Fig. 31) and encode active DHOases that differ significantly

Plasmid	Medium	Result
pPAC1	*E. coli* minimal medium with added adenine and ampicillin (100 μg ml^{-1})	Complementation
pPAC2-6	*E. coli* minimal medium with added adenine and ampicillin (100 μg ml^{-1})	Complementation
pPAC2-25	*E. coli* minimal medium with added adenine and ampicillin (100 μg ml^{-1})	No growth; *pyrC2* insert orientation opposite to *lacZ*α promoter.
pUCP20	*E. coli* minimal medium with added adenine and ampicillin (100 μg ml^{-1})	No growth; Confirmation of phenotype.
	E. coli minimal medium with added adenine and ampicillin (100 μg ml^{-1})and uracil (40 μg ml^{-1})	Growth; Confirmation of phenotype.
No Plasmid	*E. coli* minimal medium with added adenine	No growth; Confirmation of phenotype.
	E. coli minimal medium with added adenine and ampicillin (100 μg ml^{-1})	No growth; Confirmation of phenotype and competent cells not contaminated.
	E. coli minimal medium with added adenine and ampicillin (100 μg ml^{-1}) and uracil (40 μg ml^{-1})	No growth; Confirmation of phenotype and competent cells not contaminated.
	E. coli minimal medium with added adenine and uracil 40 μg ml^{-1}	Growth; Confirmation of phenotype.

Table 3. Complementation studies of *E. coli pyrC*$^-$ strain, X7014a. The indicated plasmids were transformed into X7014a. Transformants were selected by plating on the stated media. Adenine was added at a concentration of 0.0067% to the samples indicated. The results observed are listed.

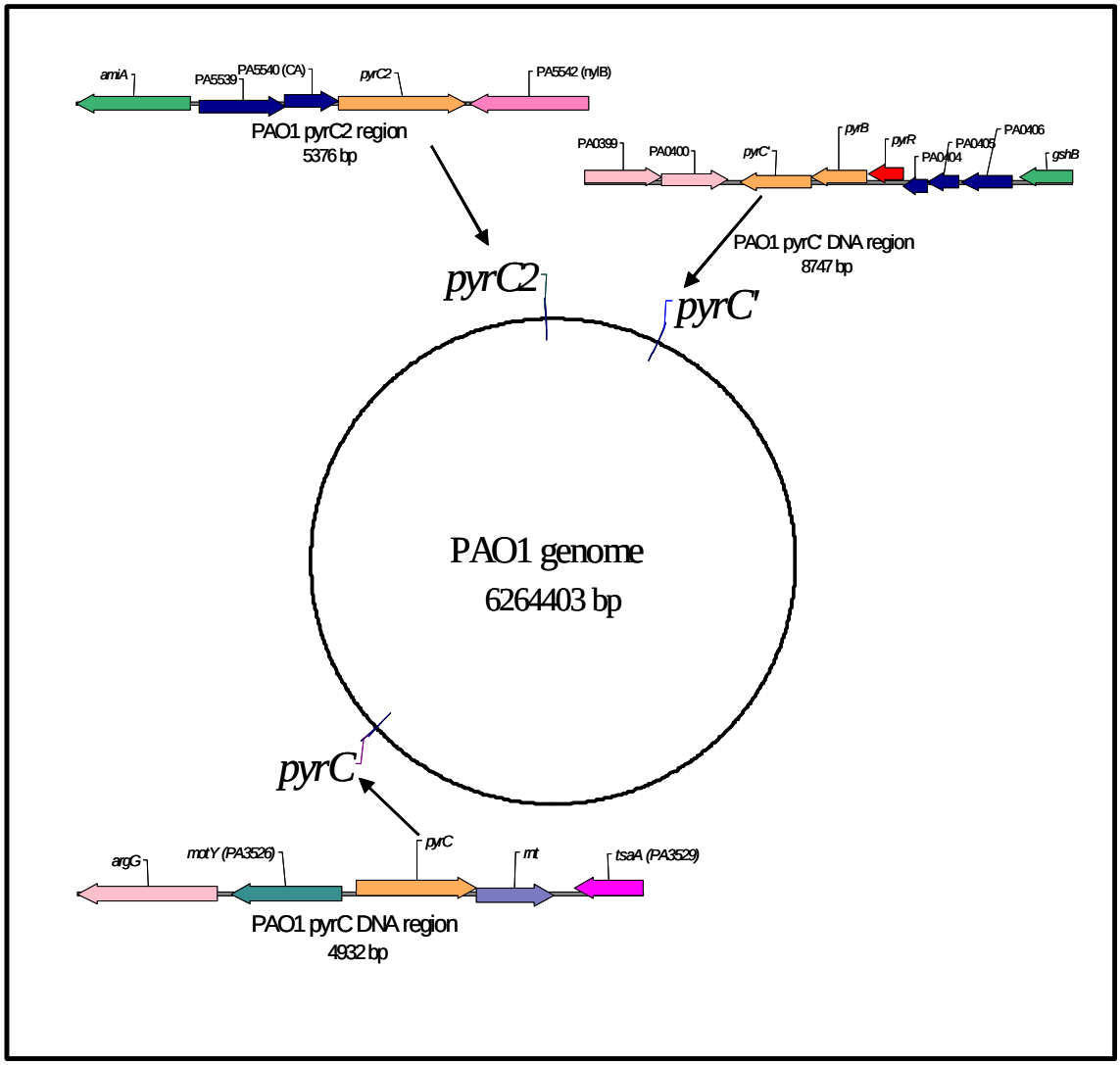

Fig. 31. Location of the three *pyrC* gene on the *P. aeruginosa* chromosome. The location of each of the *pyrC* genes is indicated. In addition, the identity of the surrounding genes is given when known. Sequence data was obtained from the *Pseudomonas* genome web site (www.pseudomonas.com).

in size. The *pyrC* gene, encoding the smaller of the two DHOases, was isolated from a *P. aeruginosa* cosmid library by screening for complementation of *E. coli* X7014a. One of the isolated cosmids, designated cPA6, was chosen for further study. In order to isolate the *pyrC* gene, this cosmid was digested with several restriction enzymes (Fig. 32) and the resulting fragments were ligated into pUCP19 digested with the same enzymes. The *Eco*RI digest of cPA6 yielded a plasmid designated pPAC1, with a 2.5 kb insert that could complement the *E. coli pyrC* mutant strain.

The DHOase encoded by pPAC1 was expressed in *E. coli* X7014a and partially purified (see Methods). SDS-PAGE analysis showed a polypeptide of ~40 kDa (Fig. 33) which agrees with the theoretical molecular mass of 38 kDa, calculated from the predicted amino acid sequence. As seen in Table 4, the *pyrC* encoded DHOase has greatest amino acid identity with the *pyrC* found in *P. fluorescens* strain PFO1. Curiously, the *pyrC* sequence from the Gram negative enteric organism, *Vibrio cholerae*, is also very similar (64% identity and 73% homology) to the *pyrC* gene of *P. aeruginosa*. This will be addressed further elsewhere, but it is worthy of mention here, that while analyzing the DNA sequence surrounding the *pyrC* gene in *P. aeruginosa*, a cluster of similar genes was found to be present in *V. parahaemolyticus*. This observation makes it tempting to suggest that the *pyrC* gene in *P. aeruginosa* is the product of horizontal gene transfer.

The *pyrC2* gene, encoding the second DHOase designated DHOase II, was isolated by PCR amplification from PAO1 genomic DNA using *pfu* polymerase in order to minimize the chance of error during replication. The PCR product was then cloned into

pUCP19 and pUC18, resulting in the plasmids pPAC2-6 and pPAC2-25, respectively. As seen in Table 3, pPAC2-6 is able to complement the *E. coli pyrC* strain, while pPAC2-25

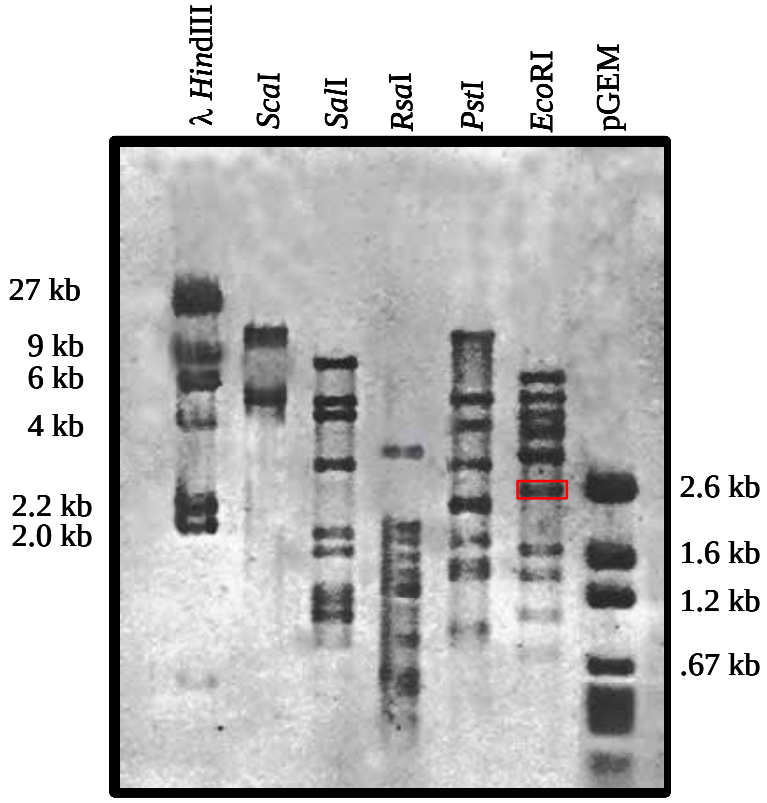

Fig. 32. Agarose gel of restriction digests of cosmid cPA6. The highlighted 2.5 kb band from the *Eco*RI digest, contains the *pyrC* gene. This was ultimately subcloned into pUCP19 resulting in plasmid pPAC1. The DNA markers used and sizes are indicated.

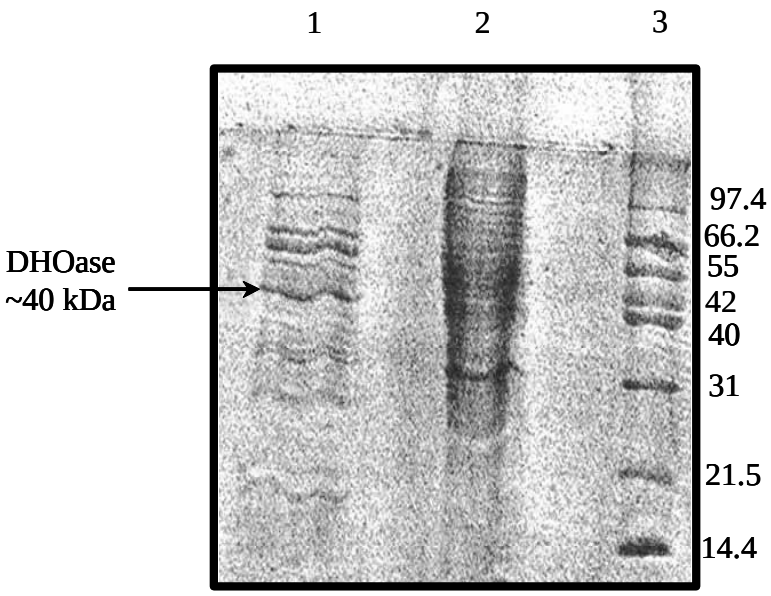

Fig. 33. SDS gel of partially purified *pyrC* encoded DHOase from *P. aeruginosa*. Lane 1 contains *P. aeruginosa* partially purified cell extract treated with ammonium sulfate followed by the heat step as described in the Methods. Lane 2 contains a sample of the combined 55% and 65% ammonium sulfate pellets, prior to the heat step. Lane 3 contains SDS molecular weight markers from Promega. The marker sizes in kDa are indicated to the right.

	P. aeruginosa pyrC'	*P. aeruginosa pyrC2*	*P. aeruginosa pyrC*
P. fluorescens PFO1	79 / 87	68 / 78	83 / 86
P. putida KT44	79 / 86		83 / 87
Ralstonia solanocarum	41 / 61		66 / 76
Synechocystis sp. PCC 6803	31 / 44		60 / 72
Xylella fastidiosa		52 / 62	
Xanthomonas campestris		50 / 62	
Vibrio cholerae			64 / 73
P. aeruginosa pyrC'	100	26 / 40	12 / 22
P. aeruginosa pyrC2		100	15 / 23
P. aeruginosa pyrC			100

Table 4. Comparison of the three PyrC amino acid sequences of *P. aeruginosa* with each other and those of other organisms. The values listed are percentages identity / homology determined by BLAST analysis. No reported value indicates that the corresponding protein is not present in that organism.

is not. This is because *pyrC2* is expressed from the *lacZ*α promoter in pPAC2-6, but is in the opposite orientation of the promoter in pPAC2-25. Thus, the cloned *pyrC2* insert either does not contain a promoter for its expression, or a promoter is present but unrecognizable to the *E. coli* expression machinery. The former seems to be the more likely scenario, as the *pyrC2* gene appears to be the last of a three gene operon (Fig. 31). Further evidence for this will be presented shortly.

The *pyrC2* gene is 1335 bp in length and encodes a polypeptide of 445 amino acids. *In vitro* transcriptional analysis of pPAC2-6 using the Zubay method (1973) showed that the expressed polypeptide was approximately 47 kDa in size (Fig. 34). This is in agreement with its predicted molecular mass of 48 kDa. Most DHOases characterized to date fall into one of two size categories, type I at 45 kDa and type II at 38 kDa. Thus, at 48 kDa, DHOase II represents the largest active DHOase characterized to date. BLAST analysis of DHOase II showed it to have several homologs in other bacterial genera. The strongest similarity observed was with its homolog in *P. fluorescens* (Table 4). Aside from its large size, several other interesting features of DHOase II are evident. An amino acid alignment of DHOase II with other DHOase sequences shows that one of the key histidine residues required for the coordination of the zinc atoms at the active site (His 16) is replaced with a glutamine residue (Fig. 11). This glutamine residue is conserved in all DHOase II homologs observed to date.

Another curious feature of the DHOase II enzyme is that DHOase activity cannot be measured by the traditional reverse assay of Beckwith *et al.,* 1962. This was first discovered when cell extracts from *E. coli* X7014a expressing DHOase II from pPAC2-6, were prepared and assayed for DHOase activity. Several modifications of the enzyme

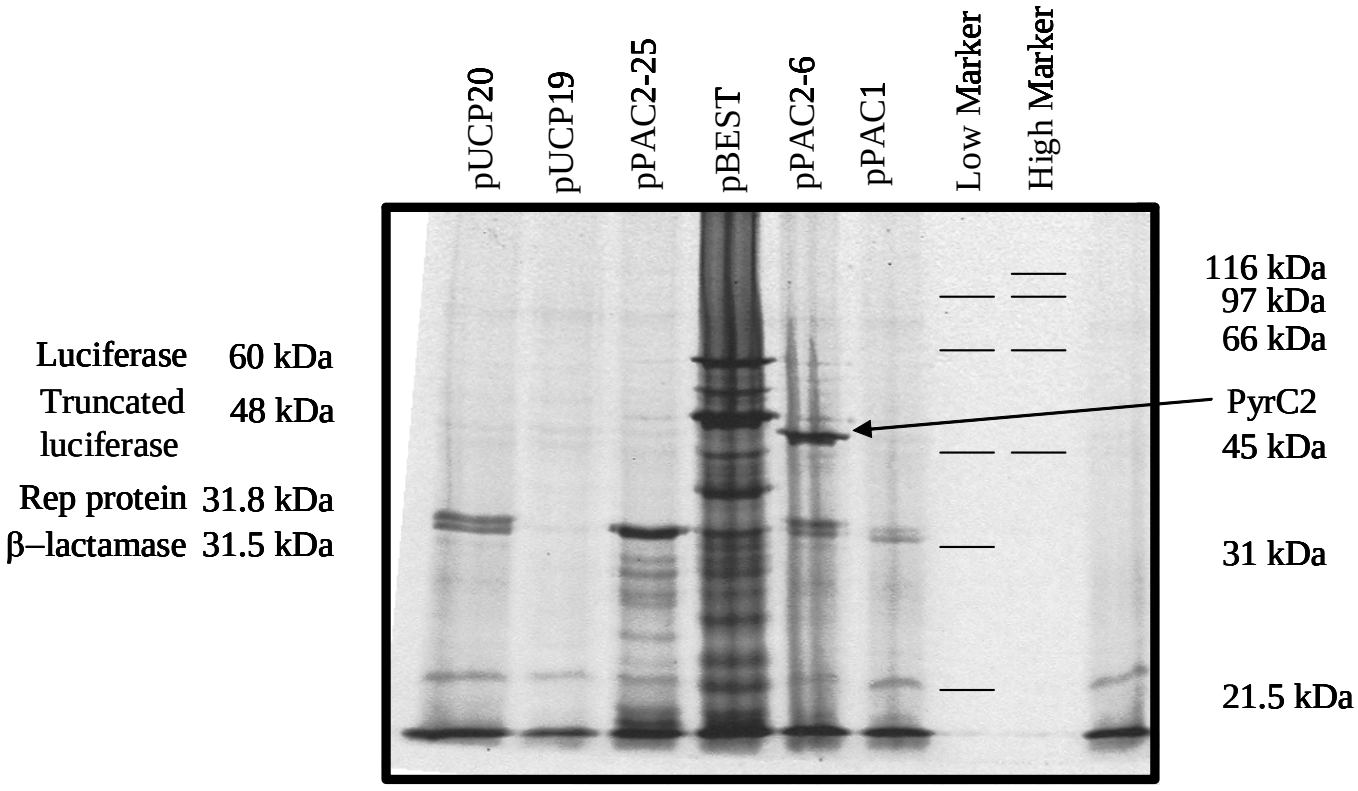

Fig. 34. *In vitro* translational analysis (Zubay) of *pyrC2*. Autoradiograph of a 12% SDS gel, showing proteins expressed from the indicated plasmids. The sizes and locations of the molecular weight markers are shown. The positive control lane (pBEST) expresses β-lactamase and luciferase. Also present is a protein product resulting from an internal start codon of the luciferase gene which is 48 kDa in size. The DHOase II subunit expressed from pPAC2-6 is indicated. Note that the *pyrC2* insert in pPAC2-25, in the opposite orientation to the *lacZα* promoter, does not make a protein product.

assay, including varying pH, temperature and substrate concentration, were tested to see if DHOase II could convert DHO to CAA, but none were found. However, it was shown that DHOase II could convert CAA to DHO. This was measured by the HPLC assay described in the Methods and illustrated in Fig. 35a. Thus, while it is evident that the DHOase II enzyme is capable of catalyzing the conversion of CAA to DHO, and that it can serve in the *E. coli pyrC* mutant as a functional part of the pyrimidine biosynthetic pathway, there is something unique and different about the way this enzyme works. Further experimentation in this area is needed to determine if there are assay conditions in which the conversion of DHO to CAA by this enzyme can be detected.

With the knowledge that *P. aeruginosa* contains two DHOase enzymes, we were curious to know the role that each played in pyrimidine metabolism. To that end, the location of each gene on the PAO1 chromosome and the identity of proximal genes were investigated. It was hypothesized that examining genes in the vicinity of *pyrC* and *pyrC2* may lend clues to the regulation of their expression. As seen in Fig. 31, the three *pyrC* genes are separated by considerable distances on the chromosome. The *pyrC'* is the distal gene of the *pyrRBC'* operon, where it is flanked by the gene encoding the putative cystathione *gamma* lyase (*metBC*) and the gene encoding glutathione synthetase (*gshB*). The *pyrC* gene is divergently transcribed from the *motY* gene, encoding the sodium ion specific stator for flagellar movement, and is overlapping the *rnt* gene. This gene encodes an exoribonuclease which is a tRNA regeneration protein, necessary for protein synthesis (Kelly & Deutscher, 1992). Also found in the region surrounding *pyrC* are the genes *argG* encoding arginino-succinate synthetase, and *tsaA***,** a homolog for *ahpC*, which

encodes the small subunit of alkylhydroperoxide reductase. This protein has been shown to be

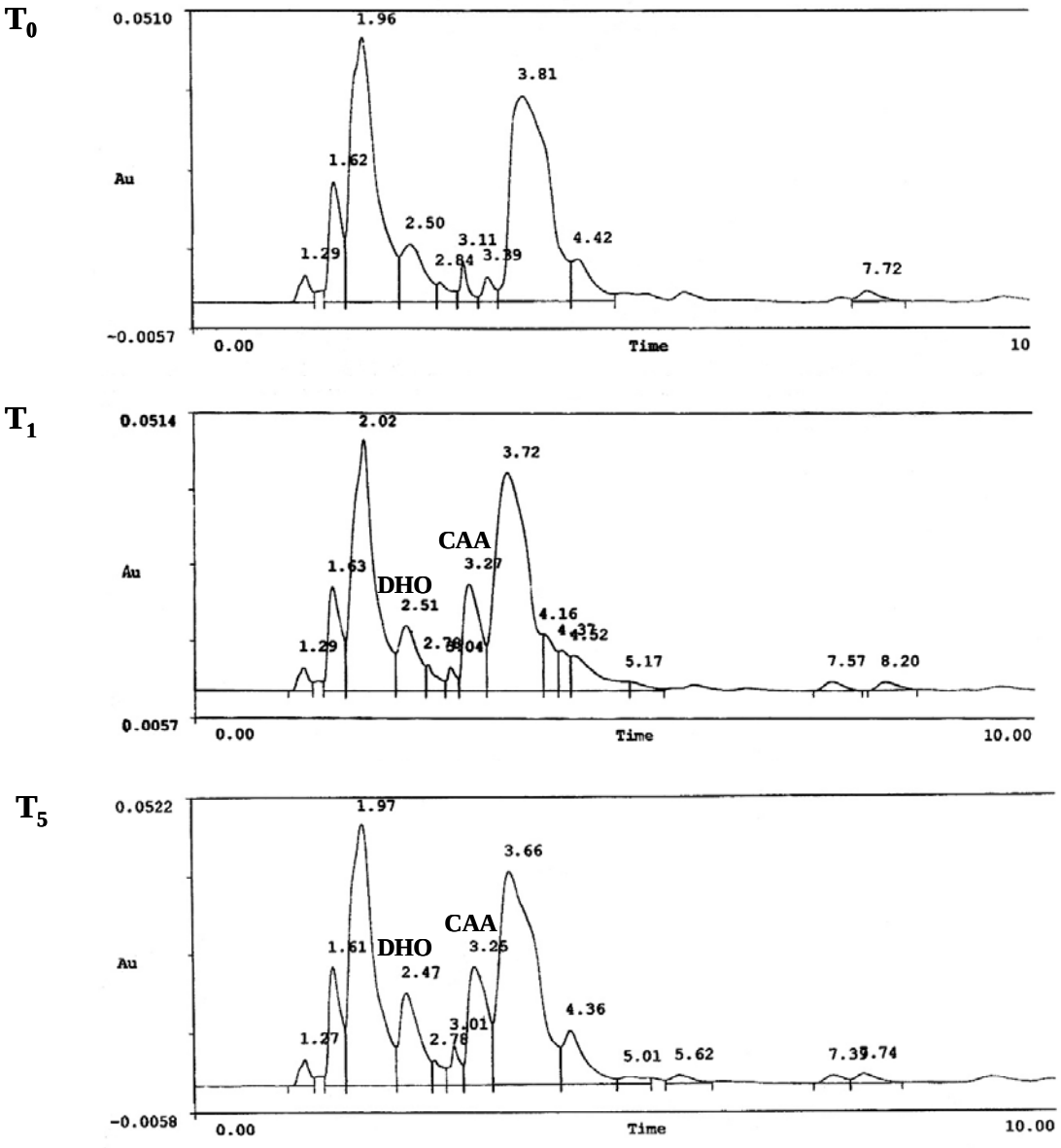

Percent area under the peaks with time in minutes

Compound	T_0	T_1	T_5
DHO	6.89	6.29	8.32
CAA	1.36	8.89	9.89

Fig. 35a. HPLC chromatograph of the conversion of CAA to DHO by cell extract from *E. coli* X7014a expressing DHOase II from the *pyrC2* gene on pPAC2-6.

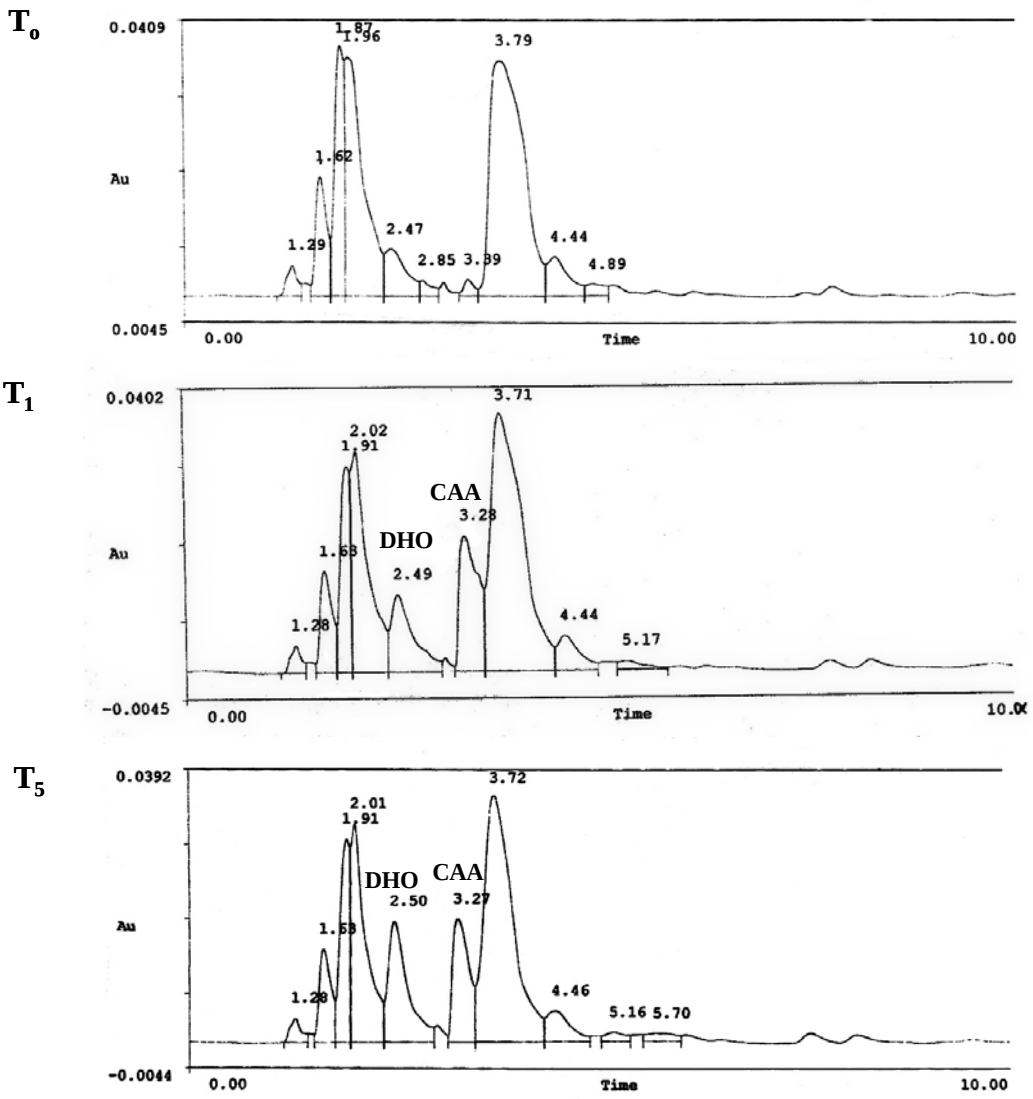

Percent area under the peak with time in minutes.

Compound	T_0	T_1	T_5
DHO	5.32	8.32	12.45
CAA	0.89	12.33	10.30

Fig. 35b. HPLC chromatograph of the conversion of CAA to DHO by cell extract from *E. coli* X7014a expressing DHOase from the *pyrC* gene in pPAC1.

important in the defense against oxidative stress, specifically conferring resistance to alkyl hydroperoxides by reducing them to alcohols (Jacobson *et al.,* 1989).

While seeking the identity of the coding sequences surrounding *pyrC*, it was discovered that the same gene cluster, with the exception of the *pyrC* gene itself, exists in *V. parahaemolyticus*. An alignment of the two regions is depicted in Fig. 36. Given the strong homology between the translated *pyrC* genes of *P. aeruginosa* and *V. parahaemolyticus* (73% homology, 64 % identity), it is tempting to hypothesize that a horizontal transfer event occurred between ancestors of these two organisms at some point in the past. Additional support for this hypothesis was found by analyzing the *P. aeruginosa* intergenic DNA regions and calculating the percent GC ratio. As seen in Fig. 36, two of the intergenic regions have GC content values between 54 and 60%. The average GC content of *P. aeruginosa* is 67% while that of *V. parahaemolyticus* is 53%. These observations, in conjunction with the fact that the *P. aeruginosa pyrC* gene was expressed from its native promoter in the *E. coli* background, strongly suggests that this region was adopted from *Vibrio* or a *Vibrio* ancestor.

The *pyrC2* gene is located near, to what has been designated in the *P. aeruginosa* annotation project as, the end of the PAO1 genome sequence (Fig. 31). It appears to be the distal gene of a three gene operon. The other two genes encode sequences that have been identified as a putative carbonic anhydrase and a highly conserved unknown protein. The *pyrC2* operon is surrounded by the *amiA* gene, encoding N-acetyl muramoyl-L-alanine amidase and *nylB,* encoding 6-aminohexanoate-dimerhydrolase, each of which is transcribed separately, in the opposite orientation relative to the operon containing *pyrC2* (Fig. 31).

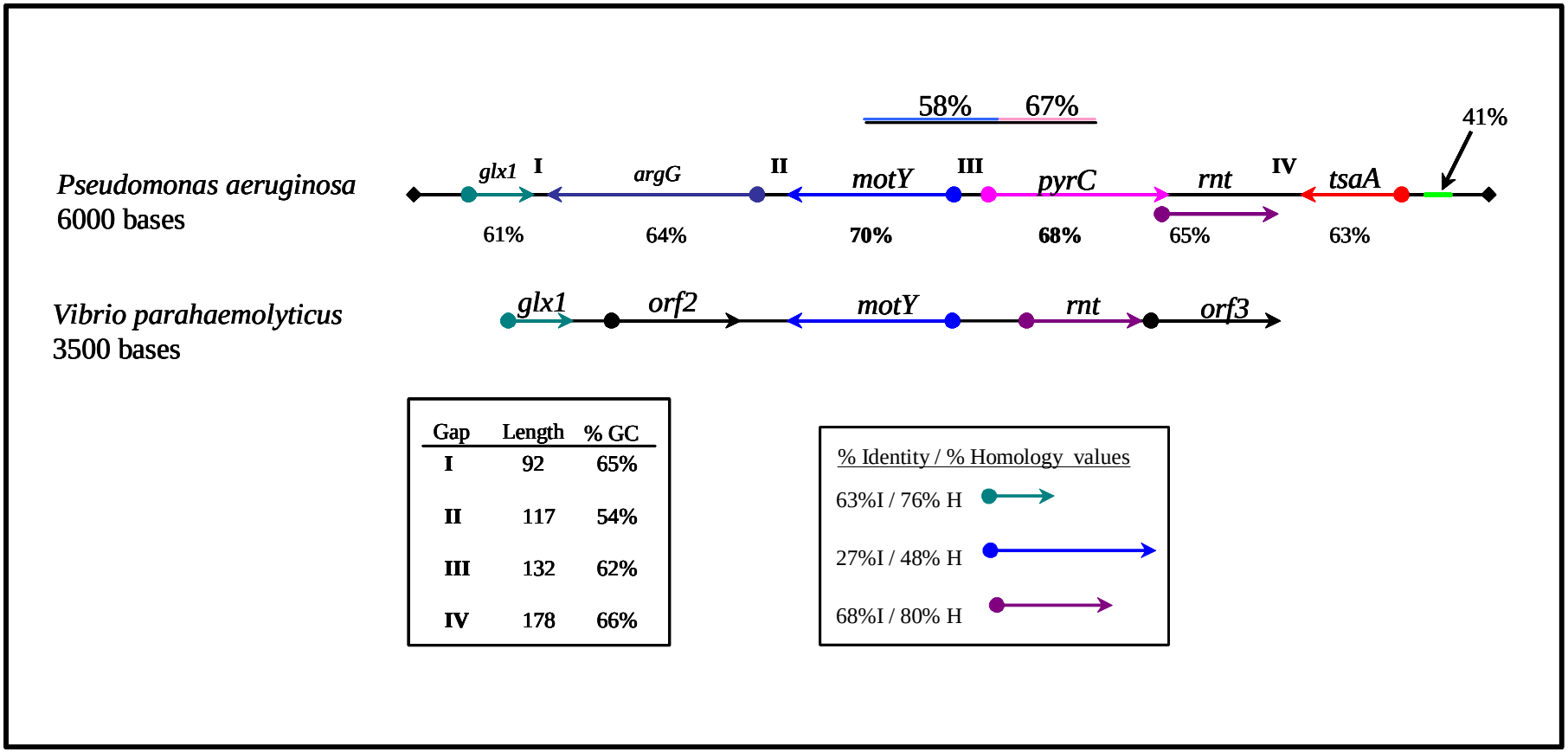

Fig. 36. Comparison of the gene cluster surrounding *pyrC* in *P. aeruginosa* with a similar cluster from *V. parahaemolyticus*. Note that the gene order and orientation is conserved for the *glx1*, *motY* and *rnt* genes. Also note the decreased GC content in the indicated areas.

A study of the locations of the *pyrC* genes in the *P. aeruginosa* genome, in itself, gave limited information regarding their differential roles, if any, in pyrimidine metabolism. Another approach to determining if a particular *pyrC* gene encodes a DHOase enzyme uniquely suited to a specific environment was to conduct a survey of all known DHOases in order to establish what organisms possessed which types, and then search for a trend. This was initially accomplished by screening for the *pyrC* gene using PCR primers as described in Methods. The results of the PCR screening are depicted in Fig 37. However, as more bacterial genomic DNA sequence became available, and BLAST search engines more user-friendly, computational screening methods were used instead. As seen in Table 5, we found that several organisms maintained more than one type of *pyrC* gene.

One explanation for the multiple *pyrC* gene phenomenon is that DHOase enzymes may be unusually sensitive to environmental conditions, thus organisms, which routinely occupy disparate niches, such as *P. aeruginosa*, may require more than one type of DHOase in order to retain their viability and versatility. One way to experimentally test the hypothesis that the different *pyrC* genes in *P. aeruginosa* allow it to survive in varying conditions, was to individually inactivate each *pyrC* gene and then examine the differences in growth capabilities. To that end, three *P. aeruginosa* strains were created.

Construction of *pyrC* mutant strains. The first strain, PAODB37, is a *pyrC*$^-$ mutant. The native *pyrC* gene was replaced with a truncated version of the gene by allelic exchange as described in Methods. A Southern blot of the genomic DNA digested with *Eco*RI shows that the *pyrC* gene was successfully replaced with the inactive version. As

seen in Fig. 38, the 2.5 kb *Eco*RI fragment "shifts down" to 2.1 kb as a result of the insertion of the truncated *pyrC* gene. This mutant strain is capable of growing on minimal

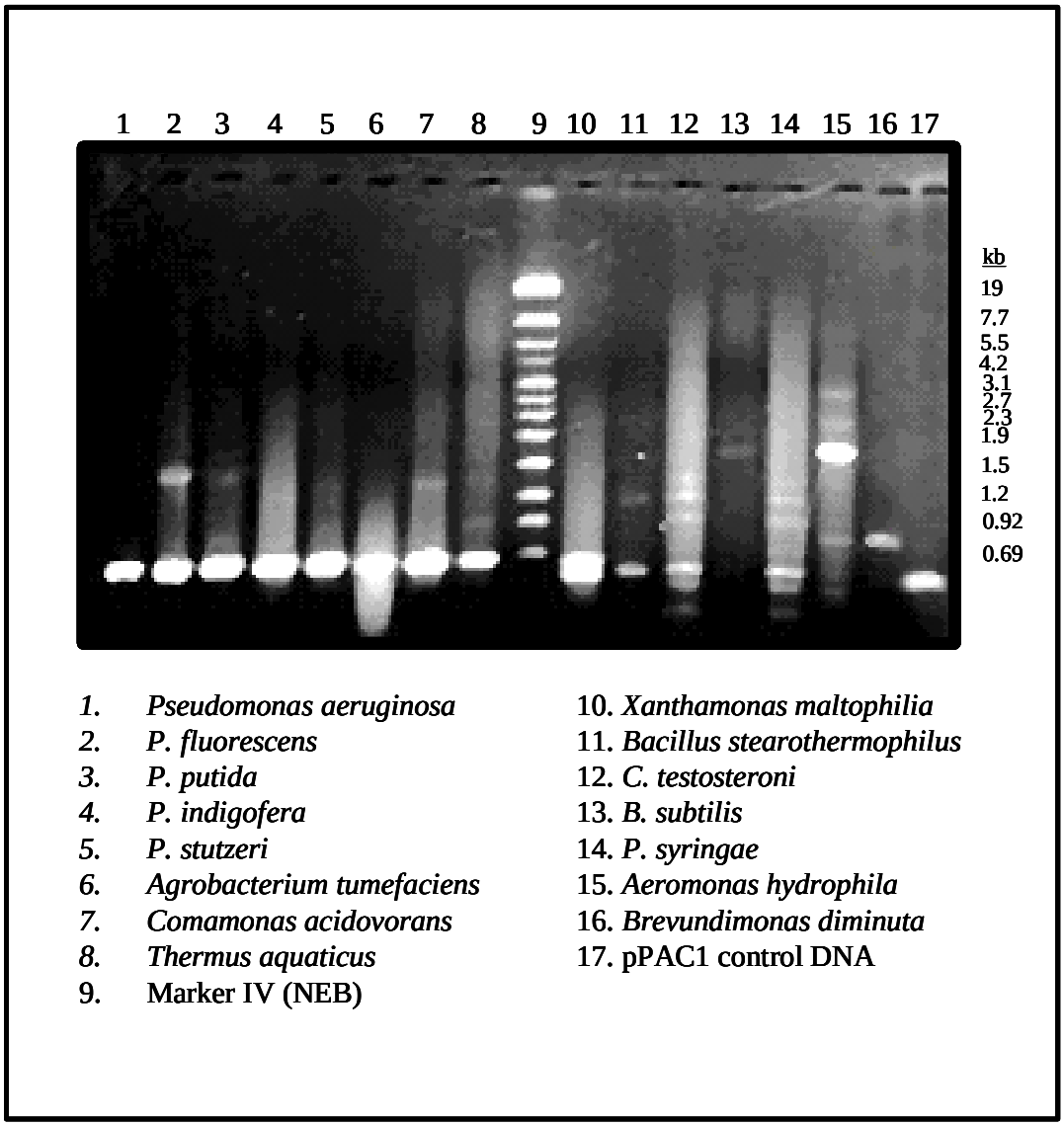

Fig. 37. PCR amplification of the small type II DHOase from various organisms. Genomic DNA was isolated from the organisms listed above and PCR primers specific for the *pyrC* gene encoding the type II DHOase were used to amplify a 658 bp fragment. The presence of a PCR product of the appropriate size is a strong indication that the organism has a *pyrC* gene in its genome.

	Organism	45 kDa *pyrC*	38 kDa *pyrC*	48 kDa *pyrC2*	45 kDa *pyrC'*	*huyA*
γ	***Pseudomonas aeruginosa***		+	+	+	+
γ	*Pseudomonas fluorescens*		+	+	+	+
β	*Ralstonia metallidurans*		+	+	+	+
γ	*Acidithiobacillus ferrooxidans*		+	+	+	
β	***Ralstonia solanacearum***		+	+	+	
β	*Burkholderia pseudomallei*		+	+	+	
γ	*Pseudomonas putida*		+		+	+
β	*Bordetella parapertussis*	+	+		+	
γ	*Colwellia* sp.	+	+			+
α	***Mesorhizobium loti***			+	+	+
α	***Caulobacter cresentus***			+	+	
	Mycobacterium smegmatis	+				+
γ	*Pseudomonas syringae*		+		+	
γ	*Methylococcus capsulatus*		+		+	
	***Synechocystis* sp.**		+		+	
γ	***Salmonella typhimurium***		+			+
γ	***Escherichia coli***		+			+
	Clostridium difficile	+				
γ	***Xanthomonas campestris***			+		
γ	***Xylella fastidiosa***			+		
	Porphyromonas gingivalis			+		
γ	*Vibrio cholerae*		+			
γ	*Shewanella putrefaciens*		+			

Table 5. Distribution of the three different DHOases, and the related hydantoinase encoded by *huyA*, among various bacterial organisms. Greek letters indicate the division of proteobacteria where applicable. Organism names in bold represent those for which the entire genome sequence has been elucidated.

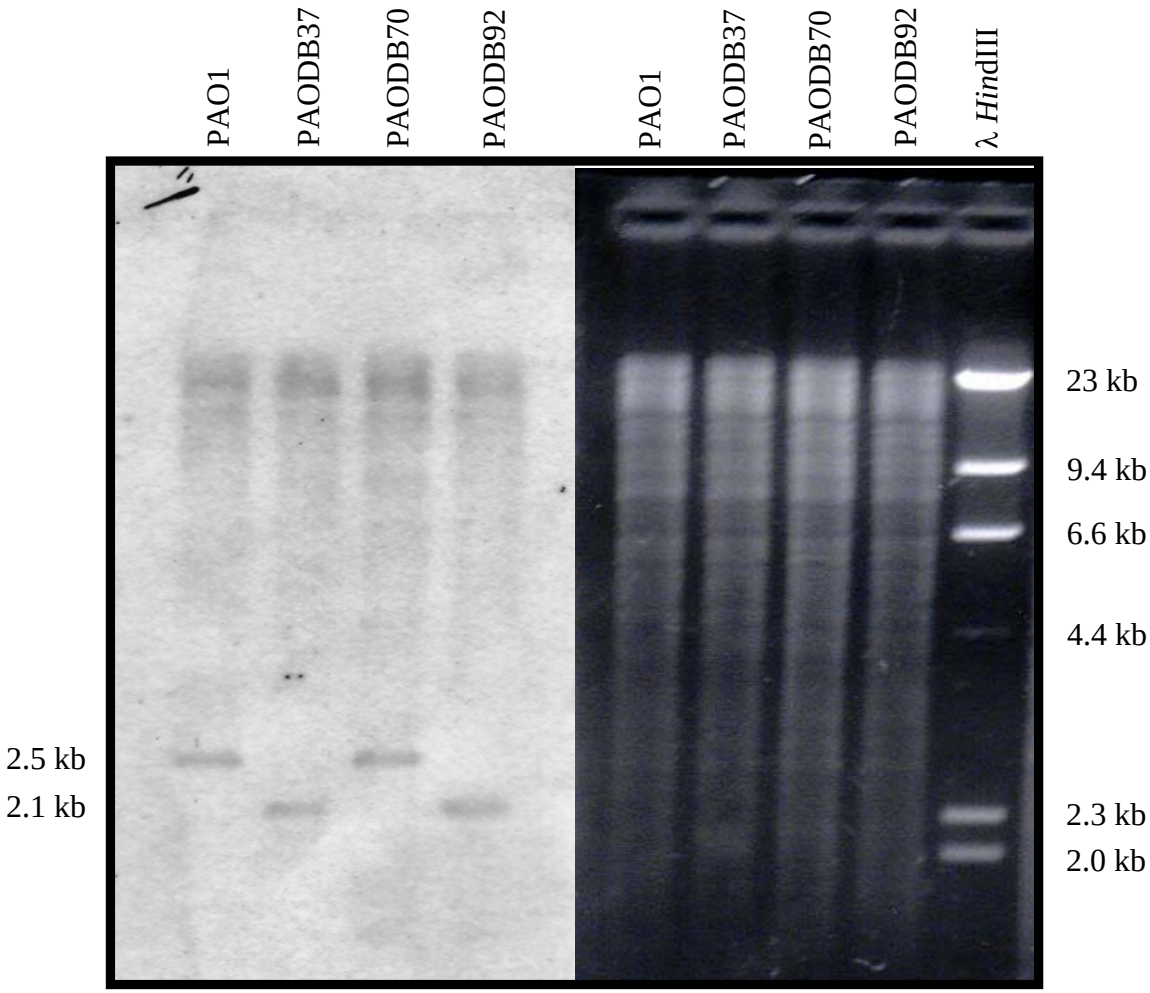

Fig. 38. Southern hybridization of the 2.5 kb *Eco*RI *pyrC* probe with genomic DNA digested with *Eco*RI. Digested genomic DNA was loaded as indicated. The marker sizes are listed as well as the size of the hybridized bands.

medium without the addition of uracil. The strain is a pyrimidine prototroph because the DHOase encoded by *pyrC2* is providing the necessary activity for pyrimidine biosynthesis. When cell extracts of this strain were assayed for DHOase activity by the reverse reaction of Beckwith *et al.*, 1962, no activity was observed. This is in keeping with previous assays of *E. coli* X7014a expressing the DHOase II, in which the conversion of DHO to CAA could not be detected.

The second strain, PAODB70, was produced by the insertional inactivation of the *pyrC2* gene using the gentamicin omega cassette isolated from pCGmΩ1 (Schweitzer *et al.*, 1996). To accomplish this, the *aacC1* gene was inserted into the middle of the cloned *pyrC2*, as described in Methods. The inactivated *pyrC2*::GmΩ gene was subcloned into pRTP1, resulting in plasmid pRTC2:: GmΩ, as seen in Methods. This plasmid was mated into *P. aeruginosa*, and the inactivated *pyrC2* gene inserted into the chromosome by homologous recombination. The resulting mutant was a pyrimidine prototroph, resistant to gentamicin.

The third strain, PAODB92 was created by mating the *pyrC2*::GmΩ construct into PAODB37, resulting in a *pyrC* double knockout, henceforth designated DKO. This mutant requires uracil or orotate for growth on minimal medium and is resistant to gentamicin. This research represents the first report of a true block in the third step of pyrimidine biosynthesis in *P. aeruginosa*. As such, this is also the first study on the effects of the accumulation of the pyrimidine intermediate carbamoyl aspartate (CAA) within the *P. aeruginosa* cytoplasm. In order to update the study of pyrimidine metabolism in *P. aeruginosa* initiated by Issac and Holloway (1968), the pyrimidine enzymes ATCase, DHOase, DHODHase, OPRTase and OMPdecase were assayed in the

individual *pyrC* and *pyrC2* mutants and in the DKO mutant and these findings were compared with enzyme activities in wild-type *P. aeruginosa*.

Effect of a complete block in DHOase on the other pyrimidine enzymes in the biosynthetic pathway. *P. aeruginosa* wild-type and *pyrC* mutant strains, were cultivated in *Pseudomonas* minimal medium in the presence or absence of uracil, as described in Methods. This was done in order to determine the effect of the accumulation of the pyrimidine biosynthetic intermediate, carbamoyl aspartate, on the specific activity of *de novo* pathway enzymes. This study represents a continuation of a similar study conducted by Isaac and Holloway in 1968. These researchers sought to detect repression, derepression, induction or feedback inhibition of the pyrimidine biosynthetic enzymes as had been previously demonstrated in *E. coli* and *Serratia* and later in *Salmonella* (Beckwith *et al.*, 1962; Hayward & Belser, 1965; Williams & O'Donovan, 1973). To that end, they generated pyrimidine mutants of *P. aeruginosa* by using Tn5 transposon mutagenesis and ethylmethane sulfonate (EMS) chemical mutagenesis. Using these techniques, they were able to isolate *pyrB*, *pyrD*, *pyrE* and *pyrF* mutants. Notably absent were *pyrC* mutants.

In order to determine if the pyrimidine biosynthetic enzymes in *P. aeruginosa* were subject to mechanisms of repression, Isaac and Holloway cultivated wild-type PAO1 in minimal medium with and without the addition of uracil and then assayed the pyrimidine enzymes. It has been shown previously in many organisms, that the rate of production of the enzymes involved in the biosynthesis of a compound is markedly decreased by the presence of that compound in the growth medium (Isaac & Holloway, 1968). For example, in *E. coli* it has been shown that cultivation of the cells in the

presence of 0.9 mM uracil causes a six-fold decrease in the level of ATCase and a two-fold decrease in the levels of DHOase, DHODHase, OPRTase and OMPdecase (Beckwith *et al.*, 1962). In contrast, Isaac and Holloway found no evidence for the repression of pyrimidine enzyme synthesis in *P. aeruginosa* when grown in uracil (Isaac & Holloway, 1968). The data presented in Table 6 for the most part confirm their initial observations, as little difference in pyrimidine enzyme specific activity is observed when *P. aeruginosa* is grown in the presence or absence of uracil. On average, a 1.3 fold decrease in pyrimidine enzyme specific activity is observed when the cells are cultivated in uracil, but this pales in comparison to the levels of repression observed in *E. coli*. Thus pyrimidine enzymes in *P. aeruginosa* do not appear to be subject to repression.

The pyrimidine mutants generated by Isaac and Holloway were also tested for their ability to grow on pyrimidine intermediates. Previous studies in *E. coli* and *Serratia* had shown that pyrimidine mutants of these organisms could utilize intermediates of the pathway to satisfy their pyrimidine requirement (Beckwith *et al.*, 1962; Hayward & Belser, 1965). However, Isaac and Holloway found in *P. aeruginosa*, that while mutants of the pyrimidine pathway could readily use uracil as a pyrimidine source, they were unable to use the pathway intermediates CAA, DHO, OA or OMP to satisfy their pyrimidine requirement. As seen in Table 7, the data reported here are at odds with their observations. Here it is shown that when the *P. aeruginosa* dihydroorotase mutant is grown in minimal medium with glucose as the carbon and energy source, either uracil or orotate can be utilized as a source of pyrimidines. The same was also found to be true for the *pyrD* mutant but not for the *pyrF*, which because of a later block, regardless, could not use orotate. Orotate did not satisfy the mutants when succinate was used as the

	PAO1 (WT)		PAODB37 (*pyrC*⁻)		PAODB70 (*pyrC2*⁻)		PAODB92 (DKO)	
Enzyme	+U	-U	+U	-U	+U	-U	+U	-U
Aspartate transcarbamoylase	581 (28)	779 (14)	615 (22)	863 (41)	493 (42)	681 (26)	**557 (3)**	**1317 (7)**
Dihydroorotase	207 (1)	281 (46)	54 (2)	123 (42)	183 (3)	285 (39)	46 (3)	94 (26)
Dihydroorotate dehydrogenase	63 (4)	44 (4)	54 (2)	78 (1)	40	61 (7)	**80 (4)**	**146 (9)**
Orotate phosphoribosyl transferase	38 (2)	34	28 (1)	43 (7)	17 (3)	34 (4)	31 (7)	38 (2)
OMP decarboxylase	6	23 (12)	17 (2)	13 (8)	19	37 (2)	11 (6)	23 (1)

Table 6. Activities of pyrimidine biosynthetic enzymes in *P. aeruginosa* PAO1 wild type and mutant strains. Specific activity units are nmol min^{-1} mg^{-1}. The numbers in parentheses are the standard deviation from the average. Assays were repeated in triplicate from three independent cultures. The cells were cultivated in *Pseudomonas* minimal medium with glucose as the carbon and energy source. +U indicates that uracil was added to the culture medium at a concentration of 40 μg ml^{-1} while -U indicates that the cells were "starved" for uracil for 4 h prior to harvesting. Starvation conditions are detailed in the Methods. Specific activity numbers in bold are those were a significant change is observed.

Mutant strain	Uracil	CAA	DHO	OA	OMP
PAODB92 (*pyrC* DKO)	+	-	-	+	-
PAO114 (*pyrD*-)	+	-	-	+	-
PAO161 (*pyrF*-)	+	-	-	-	-

Table 7. Growth of *P. aeruginosa* mutant strains in the presence of uracil and Pathway intermediates. The *P. aeruginosa* mutant strains listed were cultivated in 50 ml of *Pseudomonas* minimal medium with 0.2% glucose as a carbon and energy source and the indicated pathway intermediate as a pyrimidine source. Intermediates were added at a concentration of 50 μg ml^{-1}. The flasks were incubated at 37°C, while shaking at 250 rpm for 48 h. The (+) indicates growth, while the (-) indicates no growth.

carbon and energy source. Under these conditions, only uracil was able to serve as a source of pyrimidines. An explanation for this observation may be that the entry of orotate is under some form of catabolite repression control mechanism mediated by succinate. It has been previously demonstrated that *P. aeruginosa* preferentially utilizes TCA cycle intermediates, such as succinate, as carbon and energy sources and that growth in the presence of these intermediates causes catabolite repression of many other systems (Phibbs *et al.,* 1996). It is however curious that Isaac and Holloway did not also find that orotate could satisfy the pyrimidine requirement of their mutants, as they too reported using glucose as a carbon source, and the *pyrD* mutant studied here was generated in their initial study.

Derepression is another well-known level of control of pyrimidine biosynthetic enzymes. According to the model of repression, if uracil or a derivative of uracil represses the formation of pyrimidine enzymes, then, in a uracil mutant, the system should be derepressed and the level of pyrimidine biosynthetic enzymes should rise when the external supply of uracil has been exhausted (Isaac & Holloway, 1968). The derepression of pyrimidine biosynthetic enzymes has been demonstrated in pyrimidine mutants of *E. coli*, *Serratia* and *Salmonella* (Beckwith *et al.,* 1962; Hayward & Belser, 1965; Williams & O'Donovan, 1973; Kelln *et al.,* 1975). Isaac and Holloway generated pyrimidine mutants of PAO1 in order to determine if derepression mechanisms existed in this organism. They cultivated the mutants in minimal medium in the presence of uracil or under conditions of uracil starvation and then assayed the cell extracts of these cultures for pyrimidine enzyme activity. They reported that derepression of pyrimidine enzymes synthesis was not observed in any of the *P. aeruginosa* pyrimidine mutants

studied. Since repression of pyrimidine enzymes was not observed when grown in uracil, it makes sense that derepression was not detected in the *P. aeruginosa* pyrimidine mutants. However, the data reported here disagree somewhat with their findings.

A major difference between the initial study in 1968 on *P. aeruginosa* pyrimidine metabolism and the present work, is the acquisition here of a true block in the DHOase step of the biosynthetic pathway. As can be seen in Table 6, when compared with wild-type PAO1 cultivated under the same conditions, the specific activity of ATCase in the *pyrC* DKO appears to increase two-fold. In addition, DHOdehase and OMPdecase activities in the *pyrC* DKO are also approximately two-fold greater when starved for uracil. Thus it appears that the accumulation of the intermediate CAA may cause a stimulatory effect on the enzymes ATCase, DHOdehase and OMPdecase. Also studied were the *pyrD* and *pyrF* mutants of PAO1. As seen in Table 8, the specific activity of ATCase in the *pyrD* mutant, which presumably accumulates DHO, is decreased eight-fold, in both the presence **and** absence of uracil. Thus it is possible, that the DHO intermediate somehow decreases the synthesis or the activity of the ATCase enzyme when it reaches a particular concentration within the cell. Moreover, the *pyrF* mutant, which likely accumulates OMP, appears to have a major stimulatory effect on the DHOdehase enzyme, as the specific activity increases 10-fold when this mutant is starved for uracil (Table 8). Thus, the concentration of OMP within the cell appears to increase the synthesis or the activity of the DHOdehase enzyme.

Analysis of the data in Tables 6 and 8 leads to the synthesis of a revised model for the regulation of pyrimidine biosynthetic enzymes in *P. aeruginosa* (Fig. 39). Unlike the

enteric bacteria, here it is not simply a matter of the pyrimidine end product controlling all

	pyrD-		*pyrF-*	
Enzyme	+U	-U	+U	-U
Aspartate transcarbamoylase	**66 (8)**	**97 (27)**	**748 (22)**	**570 (12)**
Dihydroorotase	278 (29)	373 (54)	215 (4)	305 (3)
Dihydroorotate dehydrogenase	1	3	**11 (1)**	**118 (8)**
Orotate phosphoribosyl transferase	26 (3)	30 (1)	25 (7)	26 (1)
OMP decarboxylase	14 (2)	30 (10)	0	0

Table 8. Activities of pyrimidine biosynthetic enzymes in *P. aeruginosa pyrD* and *pyrF* mutant strains. Specific activity units are nmol min^{-1} mg^{-1}. The numbers in parentheses are the standard deviation from the average. Assays were repeated in triplicate from three independent cultures. The cells were cultivated in *Pseudomonas* minimal medium with glucose as the carbon and energy source. +U indicates that uracil was added to the culture medium at a concentration of 40 μg ml^{-1} while –U indicates that the cells were "starved" for uracil for 4 h prior to harvesting. Starvation conditions are detailed in the Methods. Specific activity numbers in bold are those where a significant change is observed.

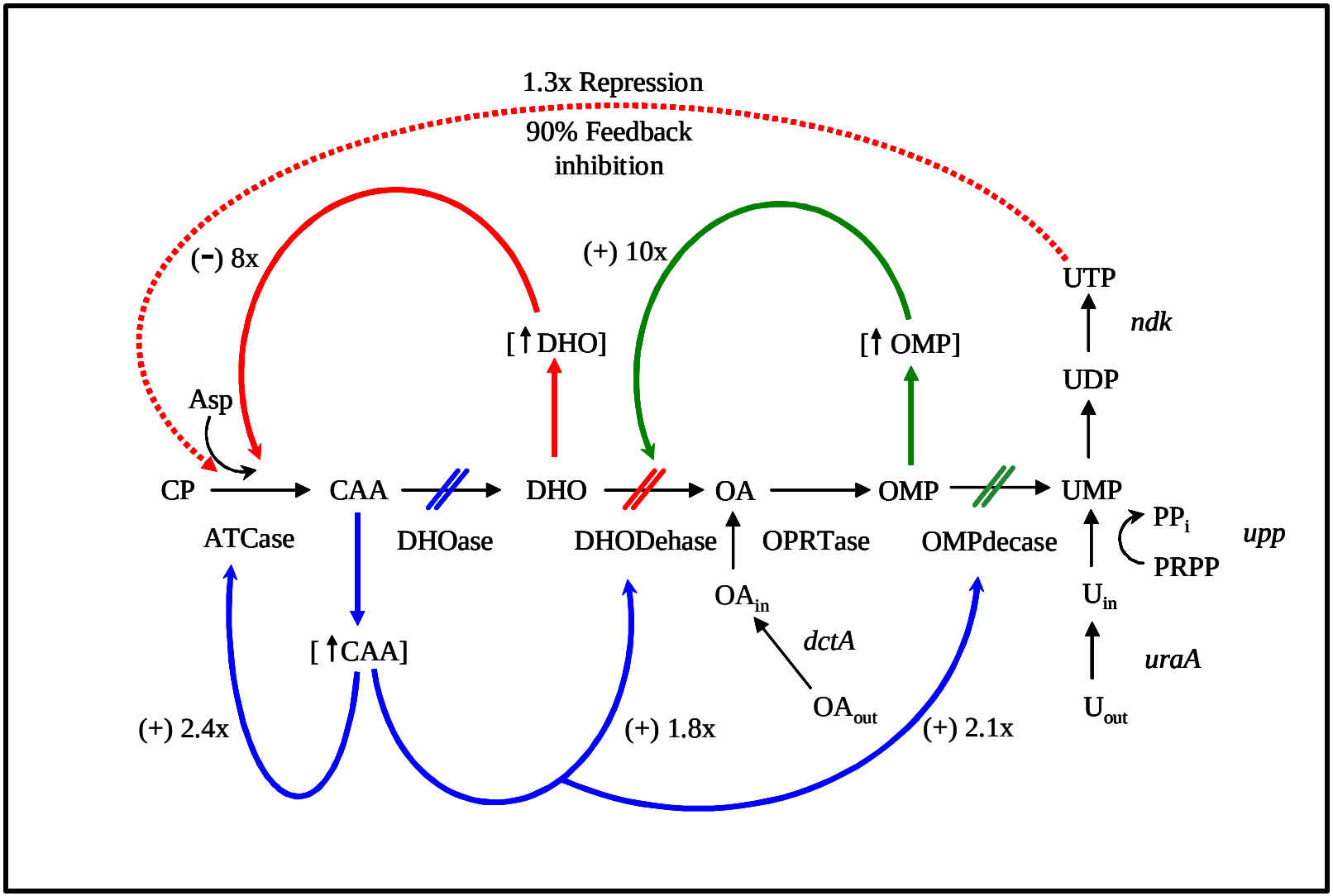

Fig. 39. Proposed model for the regulation of pyrimidine *de novo* enzymes in *P. aeruginosa* by pathway intermediates. Abreviations are as follows: CP- carbamoyl phosphate; CAA- carbamoyl aspartate; DHO- dihydroorotate; OA- orotic acid; OMP- orotidine monophosphate; UMP- uridine monophosphate; PRPP- phosphoribosyl pyrophosphate; *uraA*- uracil permease; *dctA*- dicarboxylic acid transport protein; *upp*- uracil pyrophosphatase; *ndk*- nucleotide diphosphate kinase.

of the enzymes involved in its synthesis. On the contrary, the regulatory scheme in *P. aeruginosa* appears to be a fluid system in which the accumulation of various substrates within the pathway affects key steps, which in turn stimulate the synthesis of particular intermediates. These intermediates then act as signals controlling the flow of compounds through the pathway. And it does not appear that this control mechanism is unique to *P. aeruginosa*. A comparison of the assay data from a *pyrC* mutant of *P. fluorescens* strain A126 shows the same stimulatory affect, a two to three fold increase, in the specific activities of the enzymes ATCase, DHOdehase and OMPdecase (Chu & West, 1990). The finer details and the implications of this regulatory model are addressed further in the discussion.

Promoter fusion studies. When it was discovered that the *P. aeruginosa* genome contained three *pyrC* genes, and that two of these encoded active DHOase enzymes, the next logical question focused on their expression. Were they both constitutively expressed, or did conditions exist in which the expression of one *pyrC* gene was favored over the other? In order to address these questions, the upstream regions of each of the *pyrC* genes were cloned into the transcriptional *lacZ* fusion vector, pQF50. As seen in Fig. 29 (Methods), five clones were created for this study. Two clones included the promoter regions for the divergently transcribed *pyrC* and *motY* genes. Thus an 804 bp piece of DNA was PCR amplified from pPAC1 and cloned into pQF50 in either direction in order to study the differential regulation, if any, of these two genes. The other three clones contained the upstream regions of each of the three genes in the potential three gene operon encompassing the *pyrC2* gene (Figs 29 and 31). Each of these promoter fusion vectors, along with the parent vector, was electroporated into wild-type *P.*

aeruginosa. The resulting transformants were cultivated on various media containing carbenicllin and then assayed for β-galactosidase activity.

As seen in Fig. 40, the *pyrC* promoter was highly active under all tested conditions. Limited expression was observed from any of the three potential *pyrC2* promoters. It seems apparent that *pyrC* is constituitively expressed, while *pyrC2* is under some form of transcriptional control. In an attempt to determine which of the three *pyrC2* potential promoter regions directed transcription, all three fusion vectors were electroporated into the *pyrC* strain, which grows without uracil and thus must be expressing *pyrC2* for prototrophy. As shown in Fig. 41, considerable β-galactosidase activity was obtained from clone pQF39, which contains the upstream region of the PA5539 orf, the first gene in the operon. Substantial activity was also observed for the *pyrC* promoter in this strain, indicating that *pyrC* expression was not turned off at the expense of *pyrC2* expression.

The *pyrC* strain, harboring either the pQFC or the pQF39 promoter fusion constructs, was cultivated in *Pseudomonas* minimal medium containing either glucose or succinate, as a source of carbon and energy, and in the presence or absence of uracil or orotate, as a means of testing the differential expression of the two *pyrC* genes. The cell extracts were assayed for β-galactosidase activity and the results are shown in Fig. 42. The expression from either promoter appears to be about the same when the cells are grown in glucose, but in succinate, expression of the pQF39 promoter (that governing *pyrC2*) is about 31% greater than that of the *pyrC* promoter. Also, the addition of uracil to the glucose medium seemed to have a stimulatory effect on the expression from the *pyrC2* promoter, as β-galactosidase production is 33% greater than that observed from

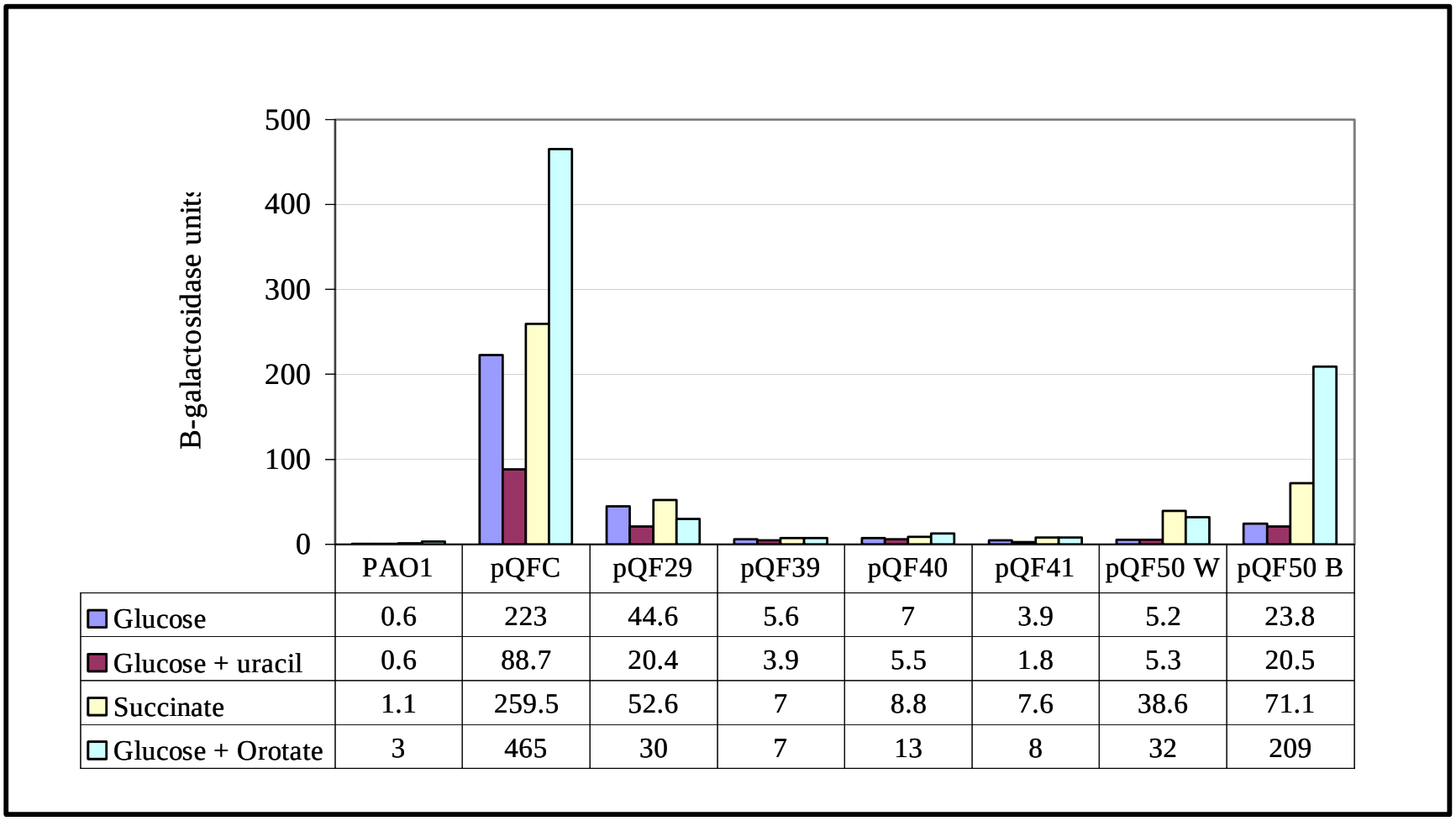

	PAO1	pQFC	pQF29	pQF39	pQF40	pQF41	pQF50 W	pQF50 B
Glucose	0.6	223	44.6	5.6	7	3.9	5.2	23.8
Glucose + uracil	0.6	88.7	20.4	3.9	5.5	1.8	5.3	20.5
Succinate	1.1	259.5	52.6	7	8.8	7.6	38.6	71.1
Glucose + Orotate	3	465	30	7	13	8	32	209

Fig. 40. Promoter expression studies in *P. aeruginosa* wild type, cultivated in *Pseudomonas* minimal medium.

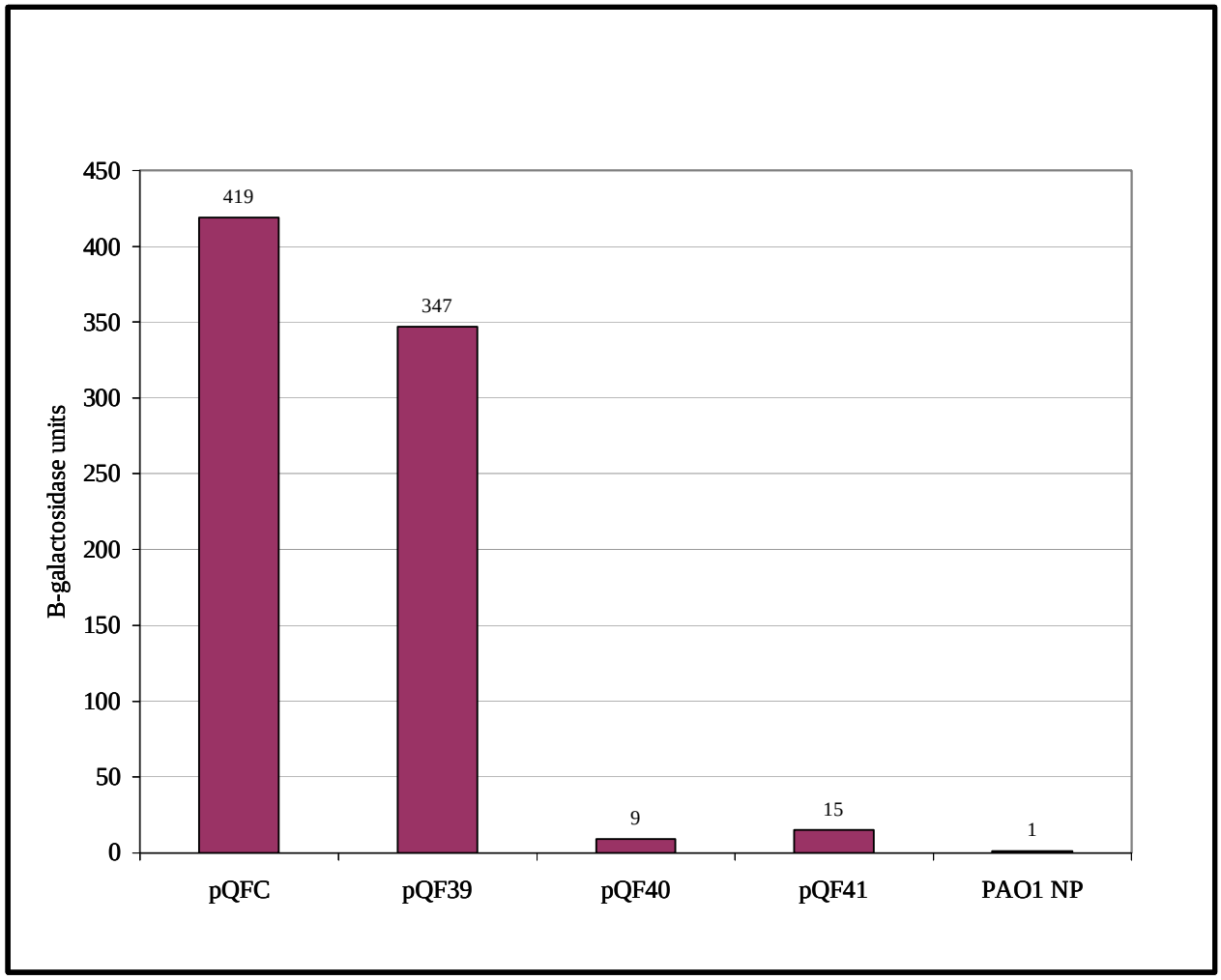

Fig. 41. pQF50 promoter fusion studies in *P. aeruginosa pyrC* strain, PAODB37. Cells were cultivated in *Pseudomonas* minimal medium with glucose as the carbon and energy source. β-galactosidase was measured from PAO1 without plasmid DNA (PAO1 NP) to demonstrate the low background of β-galactosidase activity.

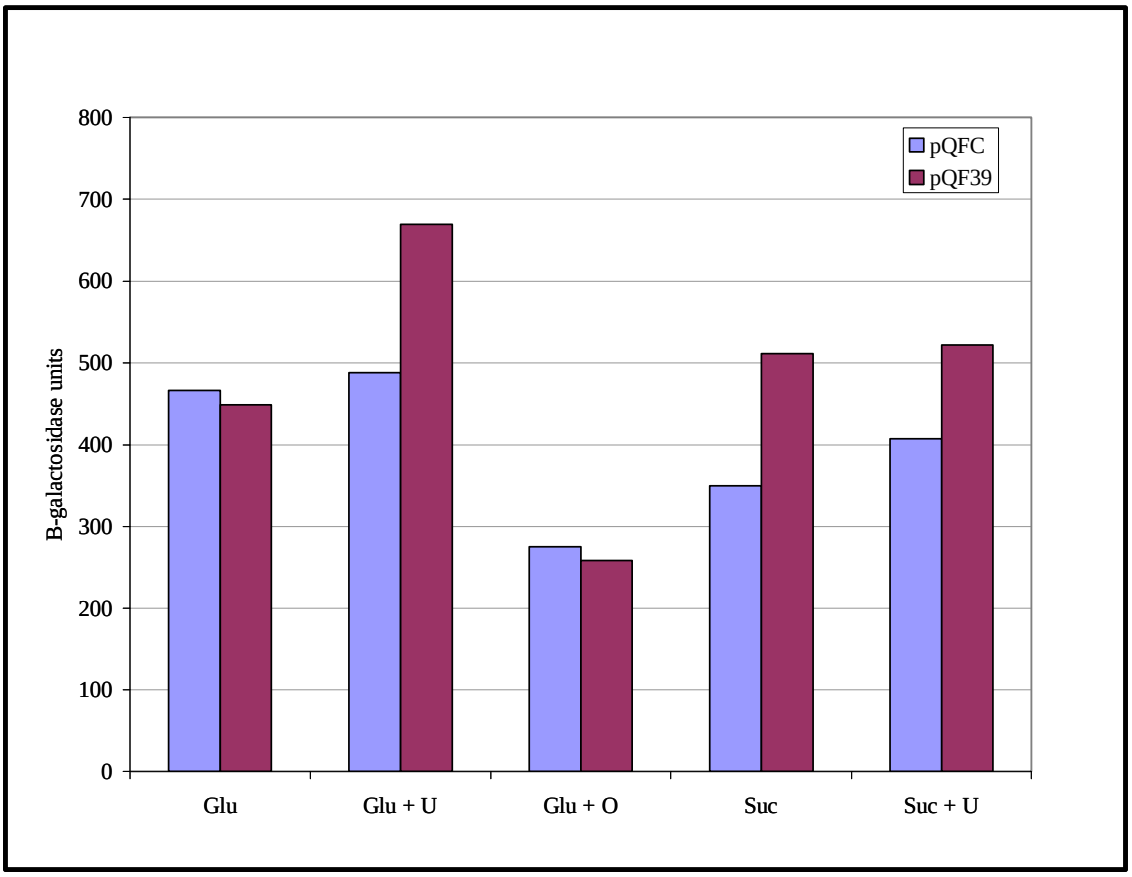

Fig. 42. Promoter expression studies of the *pyrC* and *pyrC2* promoter regions expressed in the PAO1wild type and the *pyrC* strain, PAODB37. The cells were grown in *Pseudomonas* minimal medium that contained glucose (Glu) or succinate (Suc). Uracil (U) and orotate (O) were added as indicated at concentrations of 40 μg ml^{-1} and 100 μg ml^{-1} respectively.

the *pyrC* promoter. The addition of orotate to the glucose medium apparently decreased the expression from both the *pyrC* and the *pyrC2* promoters, as β-galactosidase levels were 41% lower than when the cells were cultivated in glucose alone (Fig. 42).

It is well known that *P. aeruginosa* is capable of growing anaerobically using a form of respiration called anaerobic respiration, where nitrate serves as a final electron acceptor instead of oxygen. Conditions within the cell are likely to be radically different when *P. aeruginosa* is growing anaerobically. Thus, it seemed logical to test for the differential expression of either *pyrC* gene when the cells were grown in the absence of oxygen. To that end, wild-type PAO1 harboring the pQFC or the pQF39 promoter fusion vectors was cultivated in a yeast nitrate medium in a sealed Erlenmeyer flask. The cultures were incubated at 37ºC with shaking (to avoid clumping) for 20 h. The cells were then assayed for β-galactosidase activity. As can be seen in Fig. 43, no activity was observed from the *pyrC2* promoter. The picture thus emerges, that the *pyrC* gene is constitutively expressed and is the "work horse" of the pyrimidine pathway. Many questions still exist concerning the function of the *pyrC2* gene and its role in *P. aeruginosa* pyrimidine metabolism. These will be addressed further in the Discussion.

Growth Curve analysis. In order to identify any metabolic differences between the individual *pyrC* knockout strains, the *pyrC* double knockout (DKO) and wild-type *P. aeruginosa*, the strains were cultivated in several different media and growth was spectrophotometrically measured. The calculated growth rates are summarized in Table 9. Here it is clearly demonstrated that succinate is the preferred carbon source, as the generation time for wild-type *P. aeruginosa* is 57 min, while that for glucose is 67 min. This can also be seen in the graph of the growth curves in Figs 44 and 45. As seen in Fig

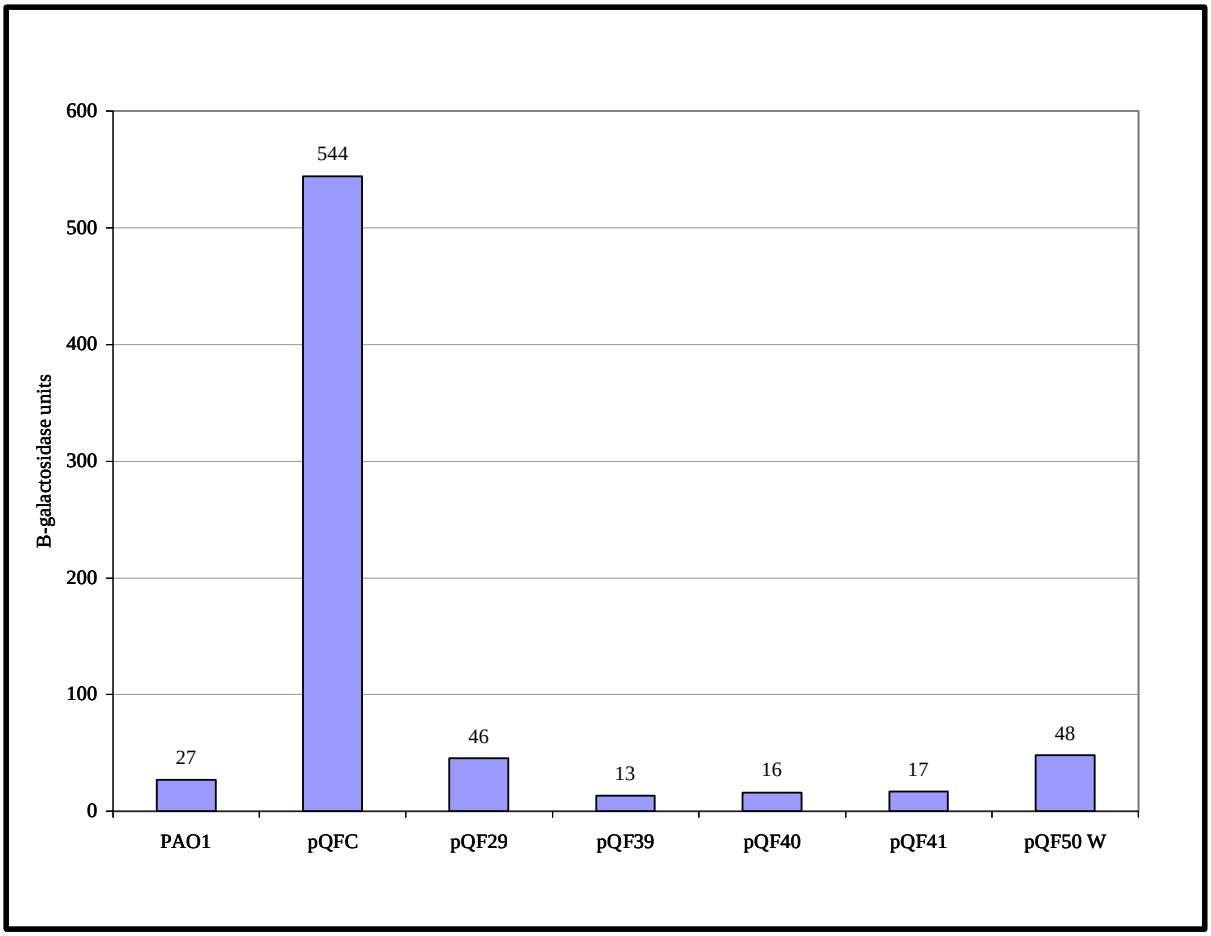

Fig. 43. Promoter fusion studies in *P. aeruginosa* wild type grown anaerobically.

Strain	Glu	Suc	Glu + U	Suc + U	King' A	King's B	BHI
PAO1 WT	67	57			60	60	60
PAODB37 (*pyrC*⁻)	75	62			60	60	60
PAODB70 (*pyrC2*⁻)	71	62			60	60	65
PAODB92 (DKO)			85	70	72/72*	84/84*	84/84*

Table 9. Growth rates of PAO1 wild type and the *pyrC* mutants. The reported generation times are in minutes. Strains were cultivated in *Pseudomonas* minimal medium containing either glucose (Glu) or succinate (Suc). When necessary, uracil was added at a concentration of 40 μg ml^{-1}. Strains were also cultivated in the following rich media: King's A, King's B and brain heart infusion (BHI) broth. The (*) indicates that the reported doubling times are from cells grown in the absence or presence of uracil (-U/+U). The reported values are the average of three separate determinations.

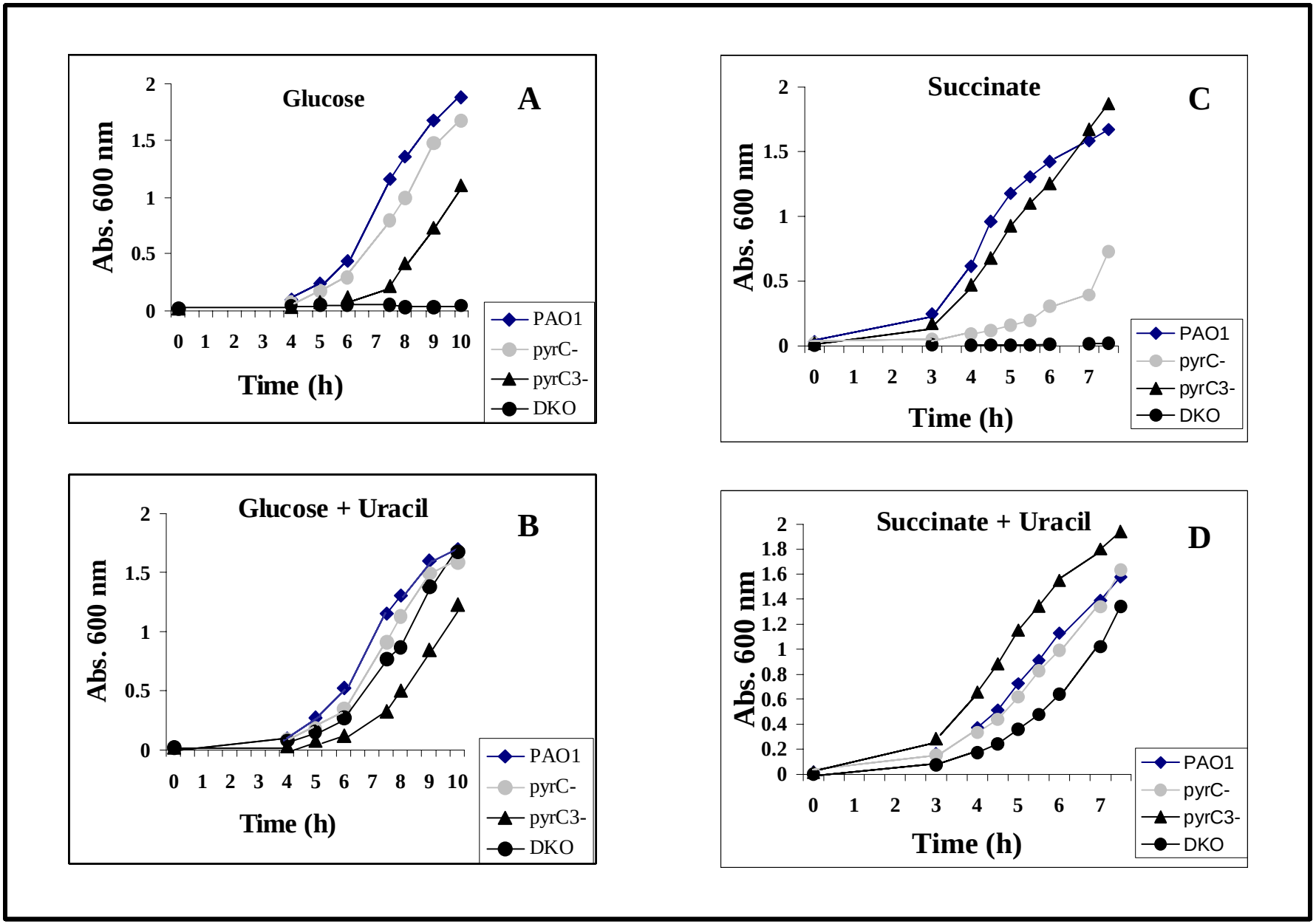

Fig. 44. Growth curves of *P. aeruginosa* wild type and *pyrC* mutants in *Pseudomonas* minimal medium with the indicated carbon and energy source. When necessary, uracil was added at a concentration of 40 μg ml^{-1}.

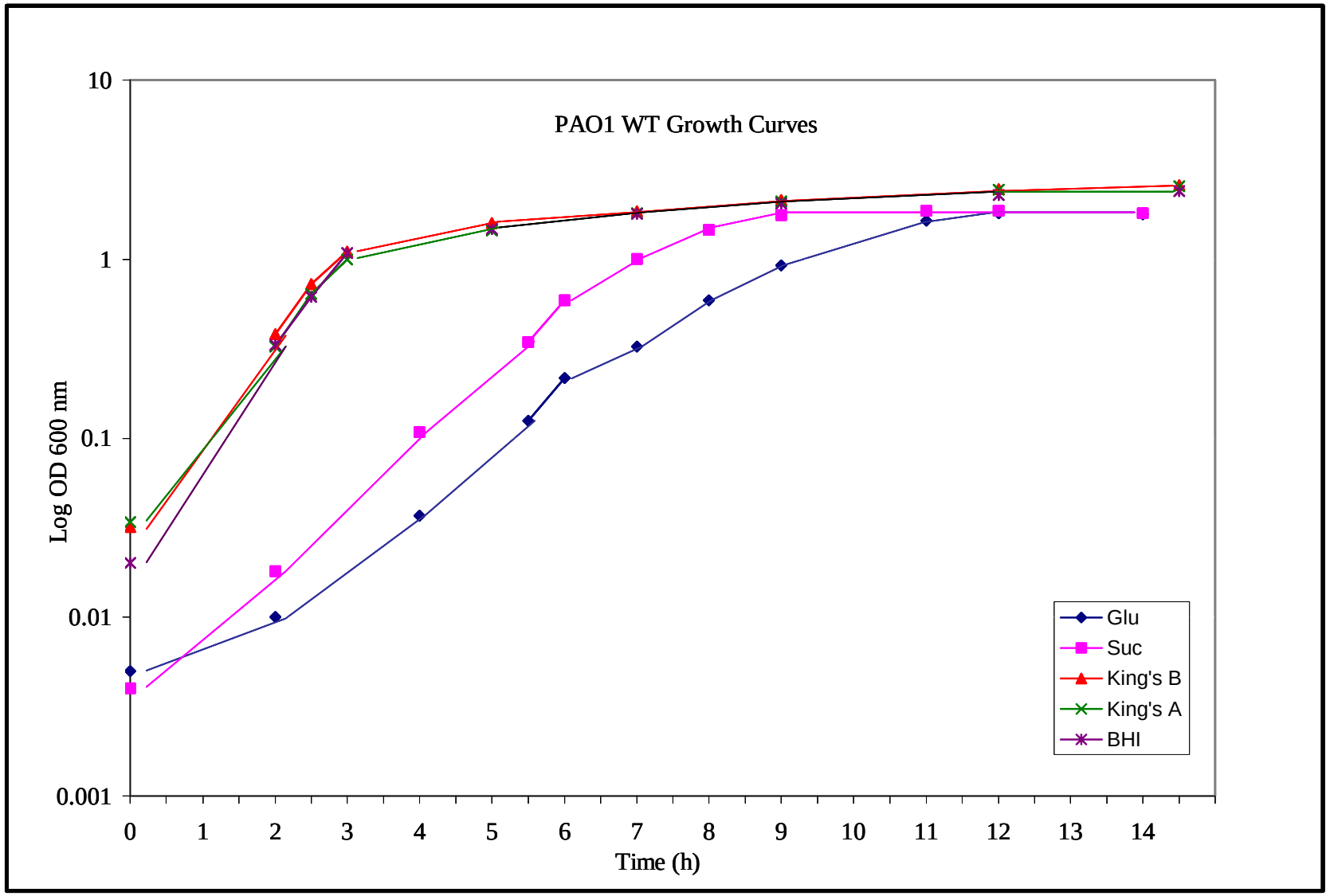

Fig. 45. Growth curves of *P. aeruginosa* wild type cultivated in rich and minimal media.

44a and 44c, the *pyrC* DKO has an absolute requirement for uracil when grown in minimal medium. Even with the addition of uracil to minimal medium, the growth rate of the *pyrC* DKO is considerably slower than that of wild-type PAO1 (Table 9). Note that the addition of uracil to the rich media (King's A and B media and brain heart infusion (BHI) broth) did not increase the growth rate of the DKO strain. The strain grew best in King's A medium, followed by *Pseudomonas* minimal medium with succinate and uracil (Fig. 46). In contrast, the DKO strain grew 25 to 40% more slowly in *Pseudomonas* minimal medium with glucose and uracil and in the King's B and BHI rich media, than the wild-type (Table 9).

Growth curves of the *pyrC* and *pyrC2* strains showed many similarities, especially in rich media (Table 9). As seen in Figs 44a and 44c, neither strain is uracil requiring, and both grow best in King's A and King's B media (Figs 47 and 48). The two strains also have comparable growth rates in *Pseudomonas* minimal medium with succinate or glucose as the carbon source. There are however, intriguing differences between the two strains. For example, the *pyrC2* strain has a slightly slower growth rate in BHI medium as seen in Table 9 and Fig. 48. Also, the *pyrC2* strain shows a consistent three to five hour lag when grown in *Pseudomonas* minimal medium containing glucose (Figs 44 and 48). The possible reasons for the observed differences in growth rate are addressed in the Discussion.

Quantitation of pigment production by *P. aeruginosa* wild-type and *pyrC* mutants. When grown on PIA medium, which is noted for enhancing the pigment

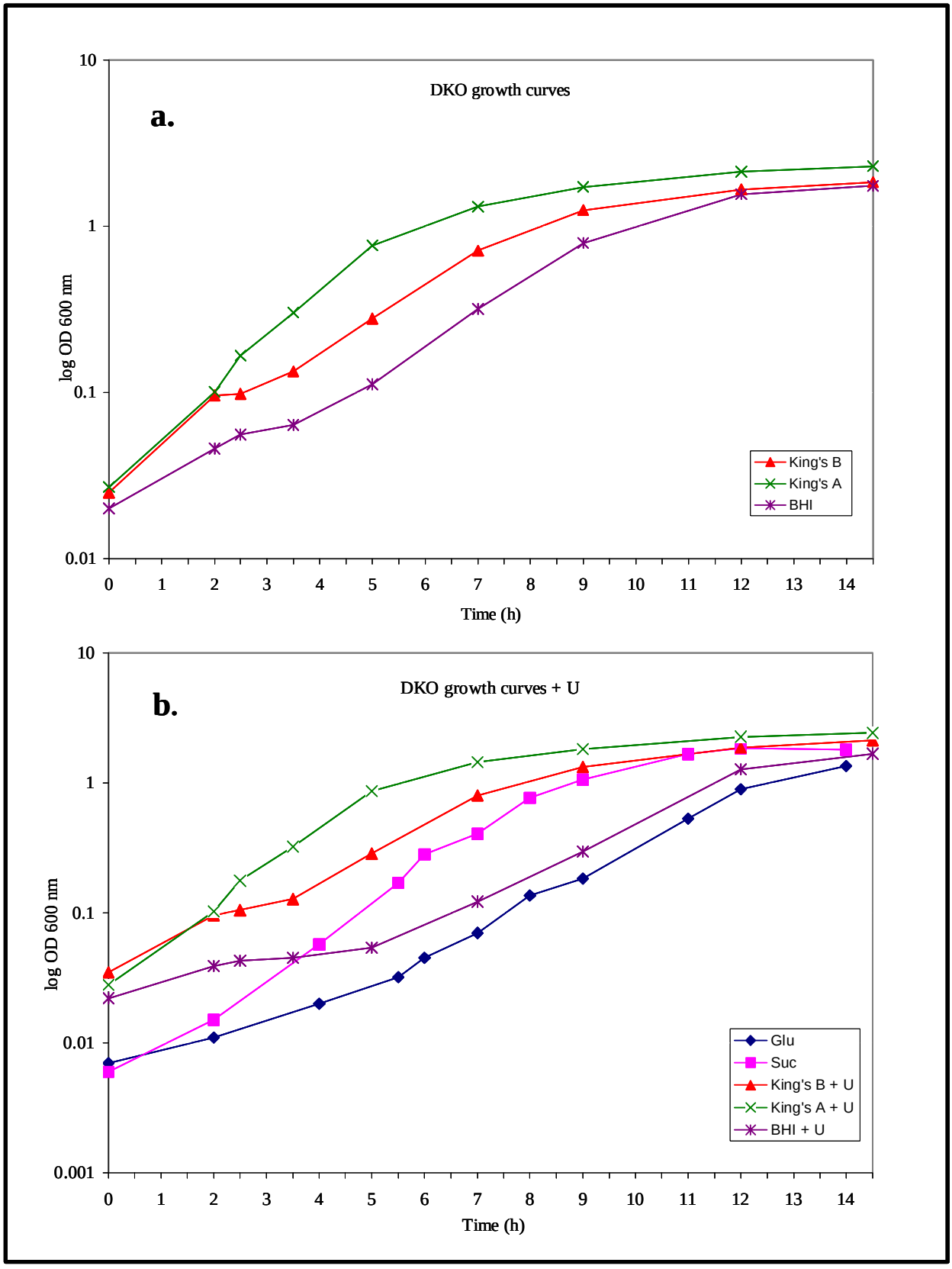

Fig. 46. Growth curves of *P. aeruginosa* DHOase mutant strain (*pyrC* DKO) in rich and minimal media, with and without the addition of uracil.

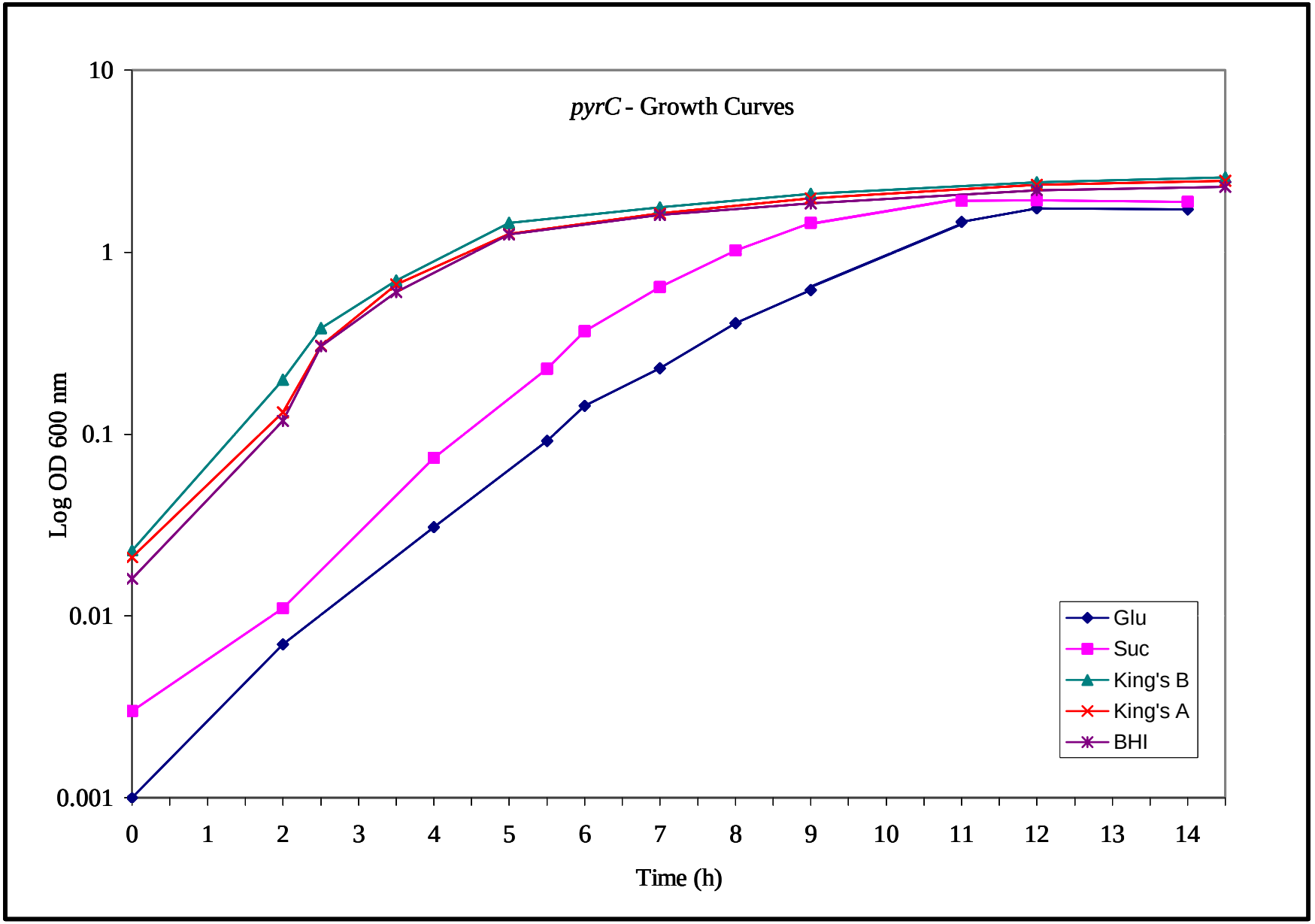

Fig. 47. Growth curves of the *P. aeruginosa pyrC* strain in rich and minimal media.

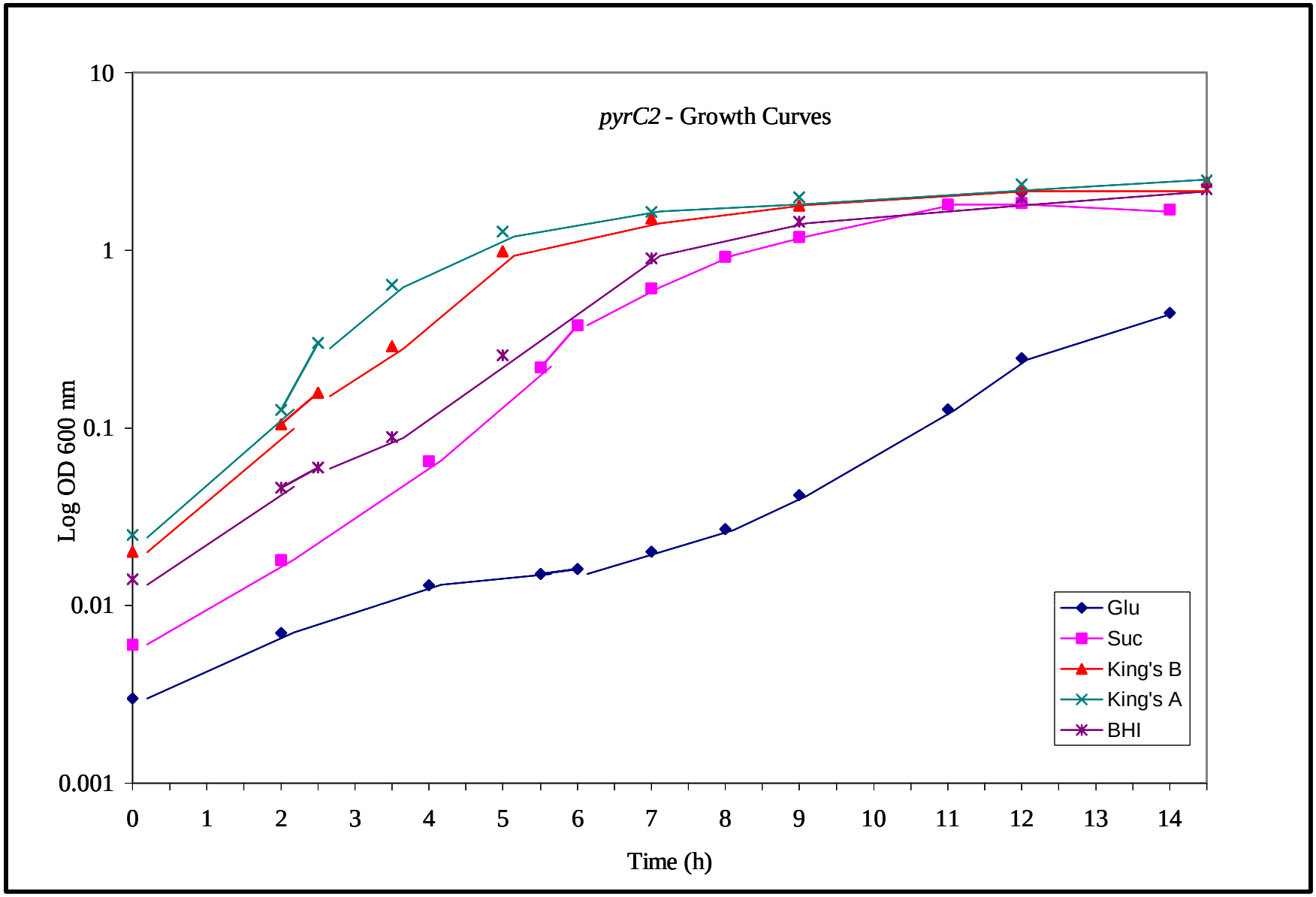

Fig. 48. Growth curves of the *P. aeruginosa pyrC2* strain in rich and minimal media.

production of *P. aeruginosa*, the *pyrC* double mutant exhibited phenotypic characteristics not readily attributed to its inability to convert CAA to DHO. Specifically, a marked decrease in the production of the pigments, pyoverdin and pyocyanin, was observed. In order to quantitate and compare pigment production in wild-type and mutant *P. aeruginosa* strains, cells were cultivated in King's A and King's B media which enhance the production of the pigments pyocyanin and pyoverdin respectively. The pigments were isolated and measured as described in Methods.

As seen in Fig. 49a, after 12 h of growth in King's B medium, the amount of pyoverdin produced by the *pyrC* double mutant (DKO) was only 10 % of the level produced by wild-type PAO1. The addition of uracil to the medium had only a slight effect, as the level increased to 18 % of wild-type. In order to see if pigment production increased over time, samples were also taken after 30 h of growth. Here it was found that the *pyrC* DKO produced 50 % of the pyoverdin produced by wild-type in medium without uracil, but with uracil it produced wild-type levels of pyoverdin (Fig. 49b). The ability to produce pyoverdin was also tested by growing the *P. aeruginosa* wild-type and mutant strains on CAS medium. As described in Methods, CAS medium detects the production of siderophores (iron-chelating compounds). When a siderophore, such as pyoverdin, is excreted into the medium, a yellow-orange halo appears around the bacterial growth. As seen in Fig. 50, without the addition of uracil to the CAS medium, the *pyrC* DKO is unable to grow, but with the addition of uracil, a small halo, a fraction of the size produced by wild-type, is visible.

The *pyrC* and *pyrC2* strains show some difference in pyoverdin production from the wild-type. After 12 h of growth, the *pyrC2* produces only 45 % of the pyoverdin

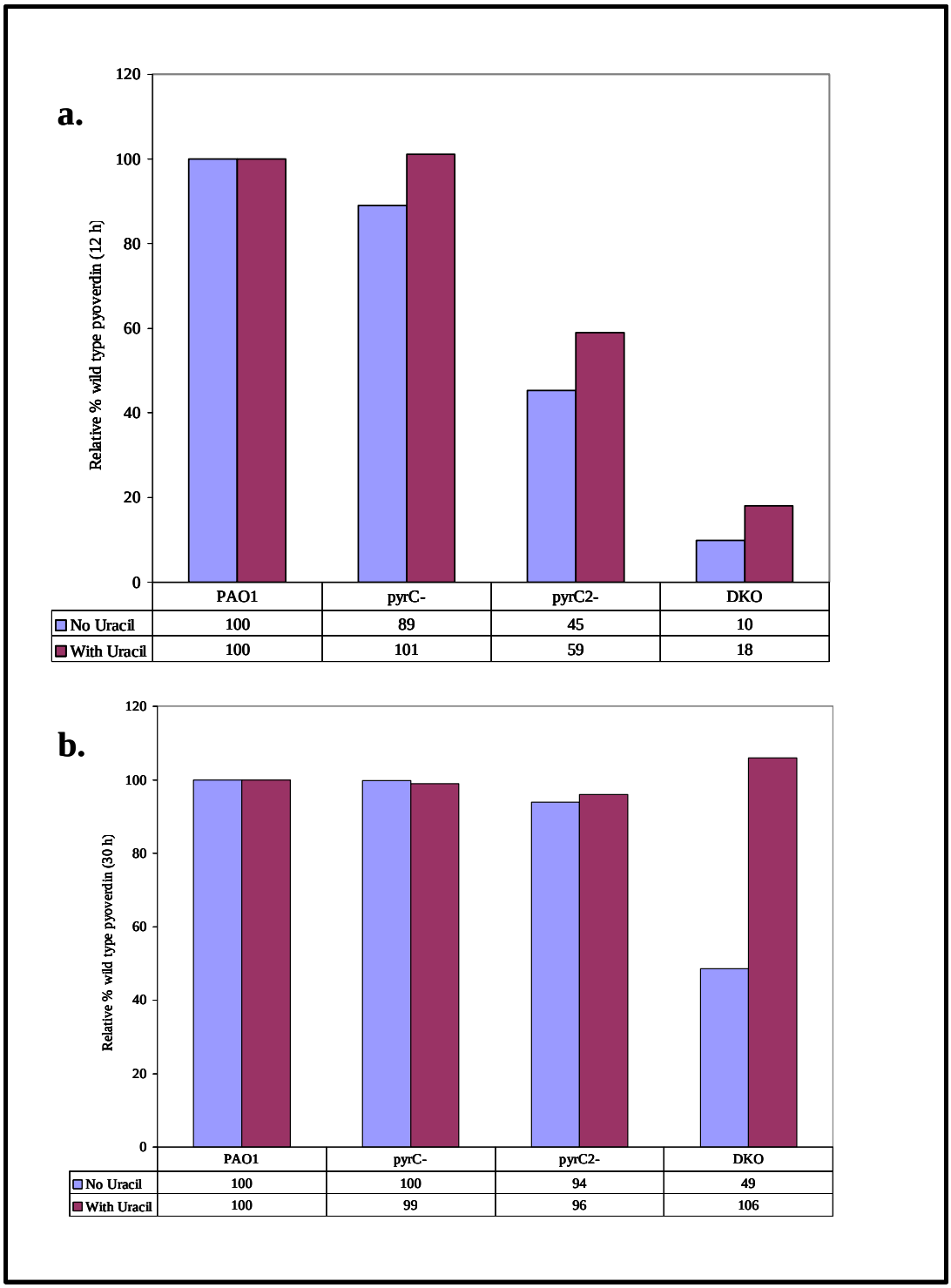

Fig. 49. Pyoverdin production of the *P. aeruginosa* wild type and *pyrC* mutant strains in King's B medium. Samples were collected at 12 and 30 h and the pyoverdin was measured spectrophotometrically by reading the absorbance at 405 nm. The absorbance at 405 nm was normalized by dividing by the optical density of the culture (OD 600 nm) and then expressed as a percentage of the wild type level. Wild type values (405/600) were 1.192 (no U) and 1.077 (U) at 12 h and 0.9 (no U) and 0.911 (U) at 30 h.

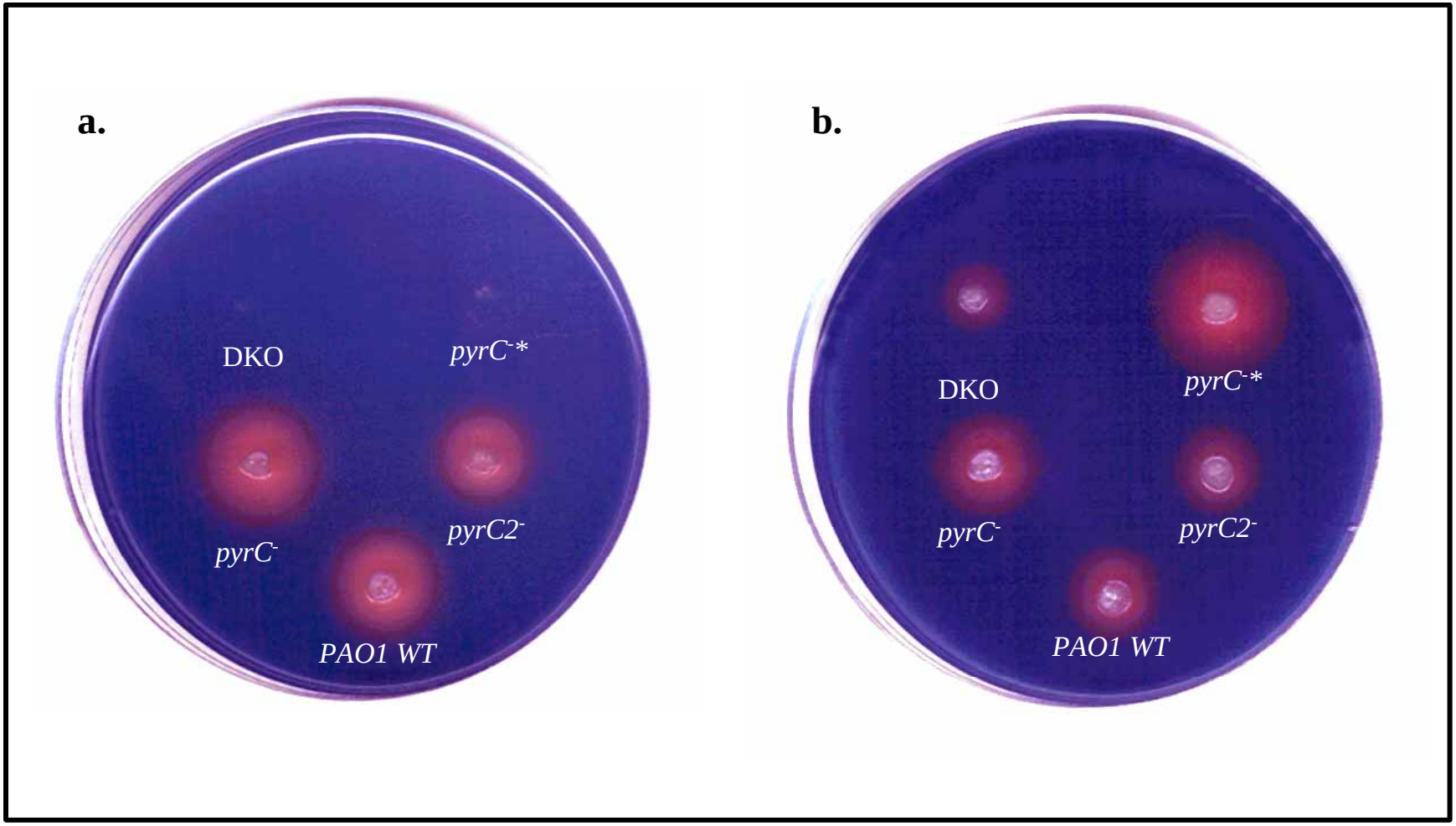

Fig. 50. *P. aeruginosa* wild type and *pyrC* mutant strains growing on CAS medium. The plates were inoculated with bacteria by toothpick and then incubated at 37°C for 20 h. Plate (a) contains no uracil while plate (b) contains uracil at a concentration of 5 μg ml^{-1}. The designation DKO stands for the *pyrC* double knockout, while *pyrC*-* is the *pyrC* strain that has not yet turned on the expression of *pyrC2* (see Discussion).

produced by wild-type, while with uracil the level increases slightly to 59 % (Fig. 49). On the other hand, the *pyrC* produced 89 % of the wild-type level. After 30 h of growth however, both of the *pyrC* mutant strains produced pyoverdin at wild-type levels, regardless of the addition of uracil (Fig. 49b).

Production of the phenazine pigment, pyocyanin, was also measured as described in Methods. As seen in Fig. 51, the *pyrC* DKO produced 59 % less pyocyanin than the wild-type when cultivated in King's A medium for 20 h. When uracil was added to King's A medium, slightly more pyocyanin was produced, but the level was still 51 % less than that produced by PAO1, cultivated in the same conditions. Note that the addition of uracil to King's A medium caused a slight increase in pyocyanin production from both the wild-type and the *pyrC* DKO. This increase was not however, observed for the individual *pyrC* mutants (Fig. 51).

Although the *pyrC* and *pyrC2* strains are not pyrimidine auxotrophs, the level of pyocyanin produced by these two strains was not identical to that of wild-type. As seen in Fig. 51, the *pyrC* strain produced 24 % less pyocyanin than wild-type when cultivated in King's A medium without uracil and 39 % less when uracil was added to the culture medium. Conversely, the *pyrC2* strain consistently produced more pyocyanin (on average 30 % more) than did the wild-type when cultivated in King's A medium with or without uracil (Fig. 51). The possible explanations for these differences are explored in the Discussion.

Virulence factor production. As mentioned previously, the *P. aeruginosa pyrC* DKO strain grew poorly on BHI medium, even with the addition of uracil (Fig. 46).

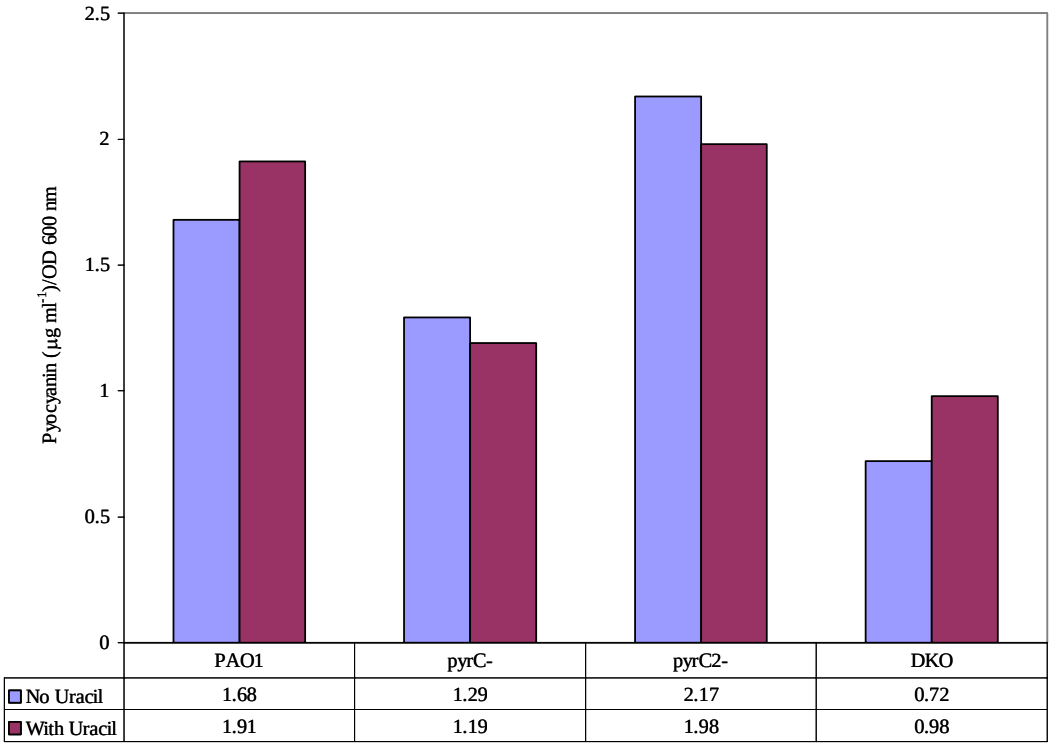

OD_{600} after 20 h of growth in PB medium.

	PAO1 WT	*pyrC*⁻	*pyrC2*⁻	*pyrC* DKO
No Uracil	2.68	2.63	2.71	2.57
With Uracil	2.68	2.62	2.66	2.57

Fig. 51. Measurement of the pyocyanin produced by *P. aeruginosa* wild type and the *pyrC* mutant strains when cultivated for 20 h in PB medium. Reported values are the average of three separate determinations and were normalized by dividing the µg of pyocyanin produced by the OD_{600} of the culture.

Growth of bacterial organisms in BHI medium is a standard test for *in vitro* pathogenicity. The slow growth rate of the DKO in this medium, combined with its inability to produce wild-type levels of pyoverdin and pyocyanin (a noted virulence factor), lead to the hypothesis that the DHOase minus mutant may be impaired in the production of other virulence factors as well. A search of the literature brought to light several reports of *P. aeruginosa* mutants with so called "pleiotropic phenotypes" (Latifi, *et al.*, 1995; Reimmann, *et al.*, 1997). These mutants, while containing single genetic lesions, demonstrated several phenotypic defects. The genes mutated in these studies included a number of those involved in the *P. aeruginosa* quorum sensing cascade, namely *gacA*, *lasRI* and *rhlRI*. When certain genes in the quorum sensing system were inactivated, the resulting pleiotropic phenotype consisted of decreased production of virulence determinants such as pyocyanin, haemolysin, elastase, casein protease, exotoxin A, stapholytic lyase and phospholipase C. In order to determine the extent to which the *P. aeruginosa pyrC* DKO mutant phenotype mirrored the phenotypes of quorum sensing mutants, the production of elastase, casein protease and the haemolysis of blood agar were measured.

As seen in Fig. 52a, after 20 h of growth in peptone trypticase soy broth (PTSB), the level of elastase produced by the *pyrC* DKO was only 23 % of wild-type. Similarly, when casein protease production was measured at 20 h in PTSB, the amount produced by the *pyrC* DKO was 36 % of that produced by wild-type (Fig. 53a). It is noteworthy that while the *pyrC* and *pyrC2* strains are not pyrimidine auxotrophs, they too exhibit decreased elastase and casein protease levels. The *pyrC* produces 52 % less elastase and

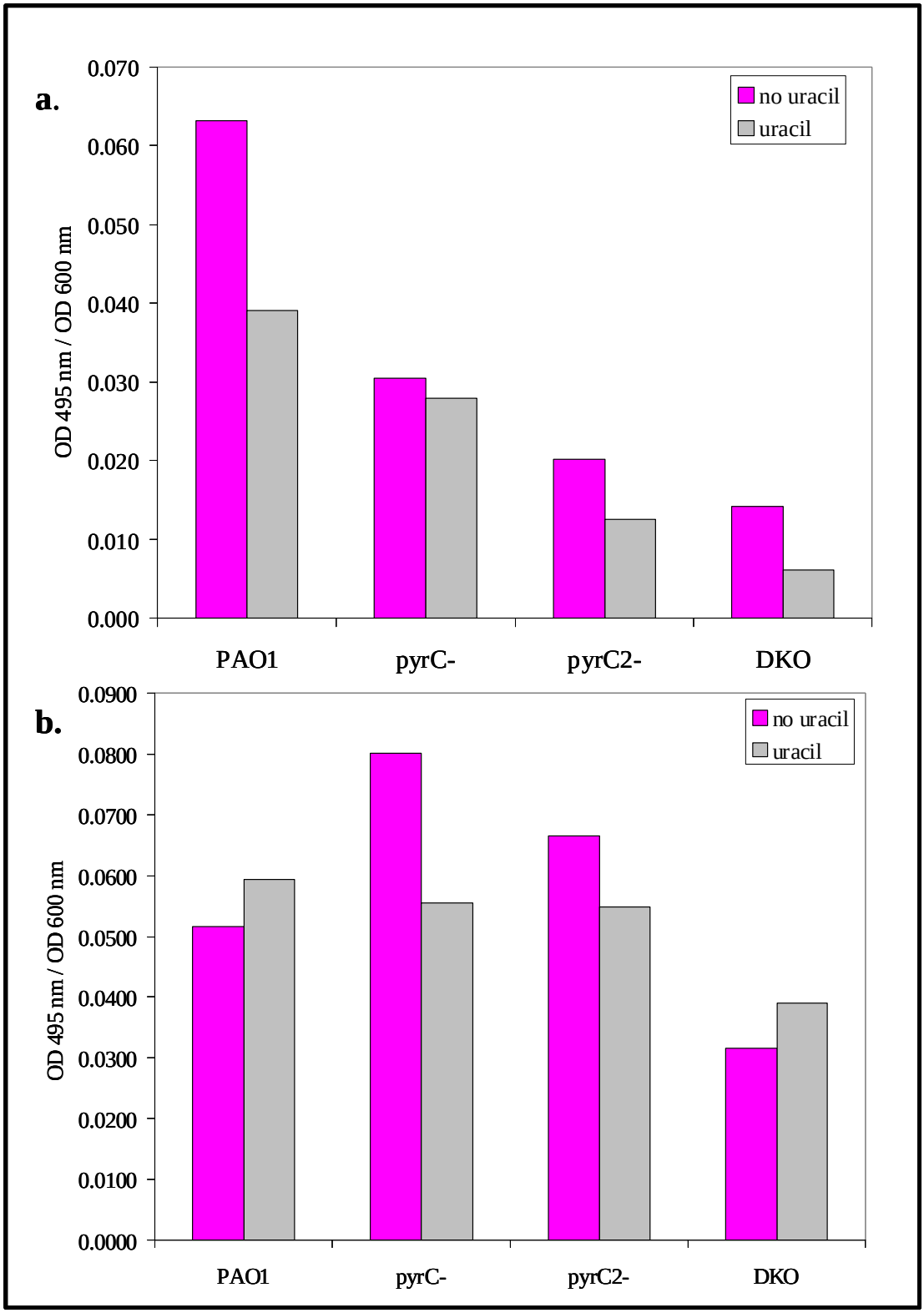

Fig. 52. Elastase production by *P. aeruginosa* wild type and *pyrC* mutant strains. Samples were collected in triplicate at 20 h (a) and 42 h (b) and elastase was measured as described in Methods. The results were normalized by dividing the A_{495} nm by the OD 600 of the culture.

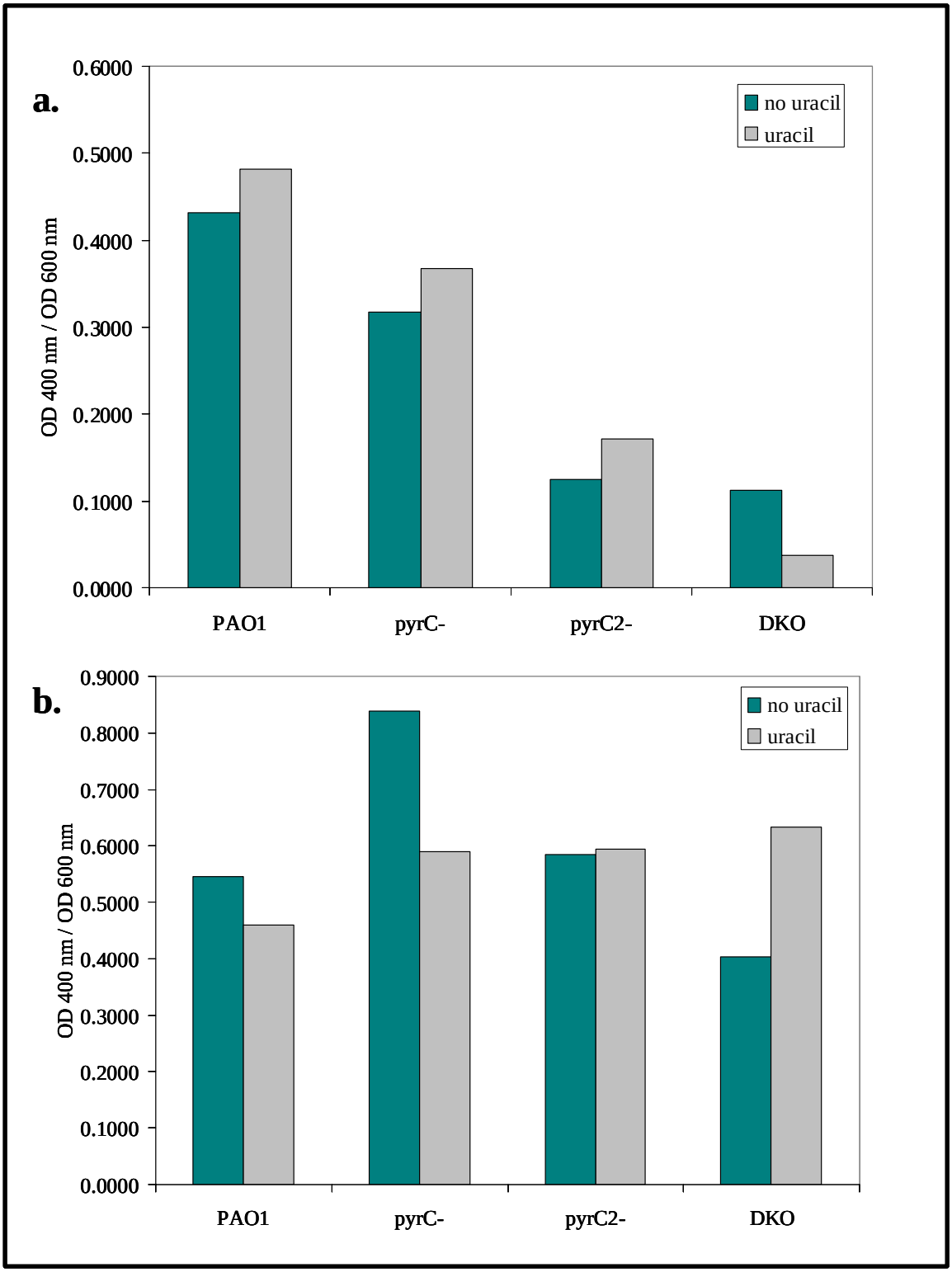

Fig. 53. Measurement of casein protease production by *P. aeruginosa* and *pyrC* mutant strains. Samples were collected in triplicate at 20 h (a) and 42 h (b) and casein protease was measured as described in Methods. The results were normalized by dividing the A_{400} by the OD_{600} of the appropriate culture.

26 % less casein protease, while the *pyrC2* produces 68 % less elastase and 66 % less casein protease than the wild-type at the 20 h time point (Figs 52a and 53a).

In order to be certain that the observed decrease in virulence factor production was not simply due to a growth defect in response to a change in the pyrimidine biosynthetic machinery, additional uracil was provided in the PTSB medium. Rather unexpectedly, it was discovered that when uracil was added to the culture medium, elastase production, in most cases, actually dropped (Fig. 52a). The *pyrC* DKO mutant produced 84 % less elastase than wild-type. The elastase produced by the *pyrC* and *pyrC2* strains was also less by 28 % and 68 % respectively. Even the wild-type level of elastase was reduced by 38 % in the presence of uracil at the 20 h time point (Figs 52a). The addition of uracil did not have the same negative effect on casein protease production, and in fact it actually slightly stimulated production of the exoenzyme in all strains except the *pyrC* DKO (Fig. 53a).

In addition, the culture incubation time, prior to sample collection for virulence factor assays, was extended from 20 h to 42 h. Although 20 h is the standard time point used in virulence assay reports, here, the incubation time was increased in order to determine if growth phase played a factor. As seen in Figs 52b and 53b, even after 42 h of growth, the *pyrC* DKO did not produce elastase or casein protease at wild-type levels (61 % and 69 % of wild-type respectively). Curiously, the *pyrC* strain produced more elastase and casein protease than wild-type at this time point (55 % and 54% greater, respectively), while the *pyrC2* strain produced enzyme levels very near to those of wild-type. The addition of uracil had slightly different effects after 42 h of growth as compared

to the results obtained at 20 h. When grown in uracil, the *pyrC* and *pyrC2* strains showed decreased elastase production. On the contrary, a slight increase in elastase was observed for the wild-type and the *pyrC* DKO strains (Fig. 52b). Casein protease production was also negatively affected by uracil at this time point, in all cases except the *pyrC* DKO. Here, it was found that the addition of uracil actually increased casein protease production to a level 15 % greater than that observed for the wild-type (Fig. 53b).

Production of haemolysin was measured by growth on blood agar (BA). *P. aeruginosa* wild-type and the *pyrC* mutant strains were inoculated on to BA medium, with and without uracil. The plates were incubated at 37ºC for 24 h and 48 h and the growth and haemolysis patterns were noted. The *pyrC* DKO was found to grow moderately on BA (without added uracil) after 24 h of incubation (Fig. 54a). After 48 h, the zone of growth was larger, but little haemolysis was observed (Fig. 54c). However, the addition of uracil to the BA medium allowed the mutant to grow to approximately the same extent as wild-type, producing almost the same size zone of haemolysis, albeit less intense (Fig. 54d). The *pyrC* strain appeared to have a very slight growth defect, as its color and zone of haemolysis was decreased in comparison to wild-type on the BA plate without uracil (Fig. 54c). The *pyrC2* strains showed essentially no growth defect on BA and appeared essentially as wild-type (Figs 54c and 54d).

Another measurement of the pathogenicity of *P. aeruginosa*, or rather its ability to produce virulence factors, is the assessment of its capacity to inhibit the growth of other bacterial organisms growing in the vicinity. The cross streak inhibition assay is a common method of testing the virulence of an organism. To that end, *P. aeruginosa* and each of the *pyrC* mutant strains were tested for their ability to inhibit the growth of

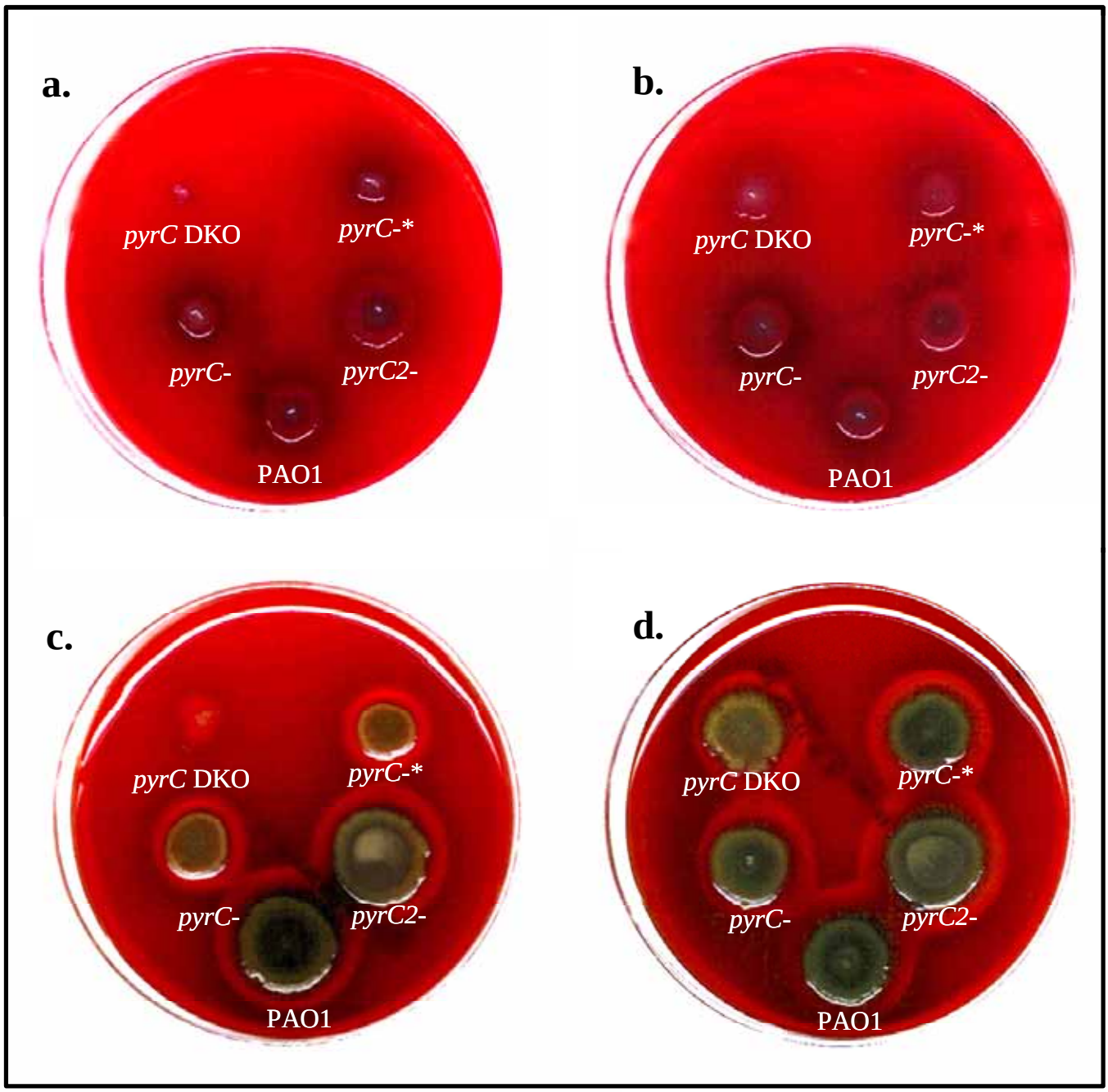

Fig. 54. Detection of haemolysis on blood agar by *P. aeruginosa* wild type and *pyrC* mutant strains. The blood agar plates were inoculated as described in Methods. The plates were incubated at 37°C for 24 (a and b) and 48 h (c and d). To test the effect of uracil on the ability of the strains to haemolyse blood, uracil was spread plated at a concentration of 40 μg ml^{-1} (b and d). The locations of the strains tested are indicated below the area of growth. The *pyrC*-* designation indicates that in this *pyrC*- strain, the expression of *pyrC2* has not yet been initiated.

Burkholderia cepacia 25416, *B. cepacia* 17616, *Staphylococcus aureus* and *E. coli*. As seen in Fig. 55a, *P. aeruginosa* wild-type inhibited the growth of all organisms tested, *E. coli* to the greatest extent, followed by *S. aureus, B. cepacia* 17616 and finally *B. cepacia* 25416. The individual *pyrC* mutants exhibited essentially the same virulence pattern as the wild-type (Figs 55b and 55d). The *pyrC* DKO however, failed to inhibit the growth of any of the organisms tested, again demonstrating its inability to produce virulence factors (Fig 55c).

Motility assays. Yet another aspect of the virulence arsenal of *P. aeruginosa* is its ability to move. *P. aeruginosa* has been found to be capable of three types of motility, namely swimming, swarming and twitching. Swimming and swarming (a process aided by rhamnolipid production) both involve the use of polar flagella, while twitching motility is mediated by surface pili. These surface structures are also involved in the attachment of *P. aeruginosa* on surfaces such as tissues or plastics. It has been demonstrated that *P. aeruginosa* strains that are deficient in virulence factor production are also often impaired in motility (Hazlett, *et al.*, 1999). In order to test the hypothesis that the *pyrC* DKO strain was also impaired in its ability to move, the swimming, swarming and twitching capabilities, and rhamnolipid production, of the *pyrC* mutant strains were assessed and compared to wild-type *P. aeruginosa*.

The swimming motility test showed that the zone of growth was much smaller for the *pyrC* DKO than for the individual *pyrC* mutant strains and the wild-type (Fig. 56a). The swim agar medium is tryptone based and fairly rich, thus the *pyrC* DKO was able to grow without additional uracil. However, in order to test the effect of added uracil on swimming motility, uracil was added to the medium at a concentration of 40 μg ml^{-1}. As

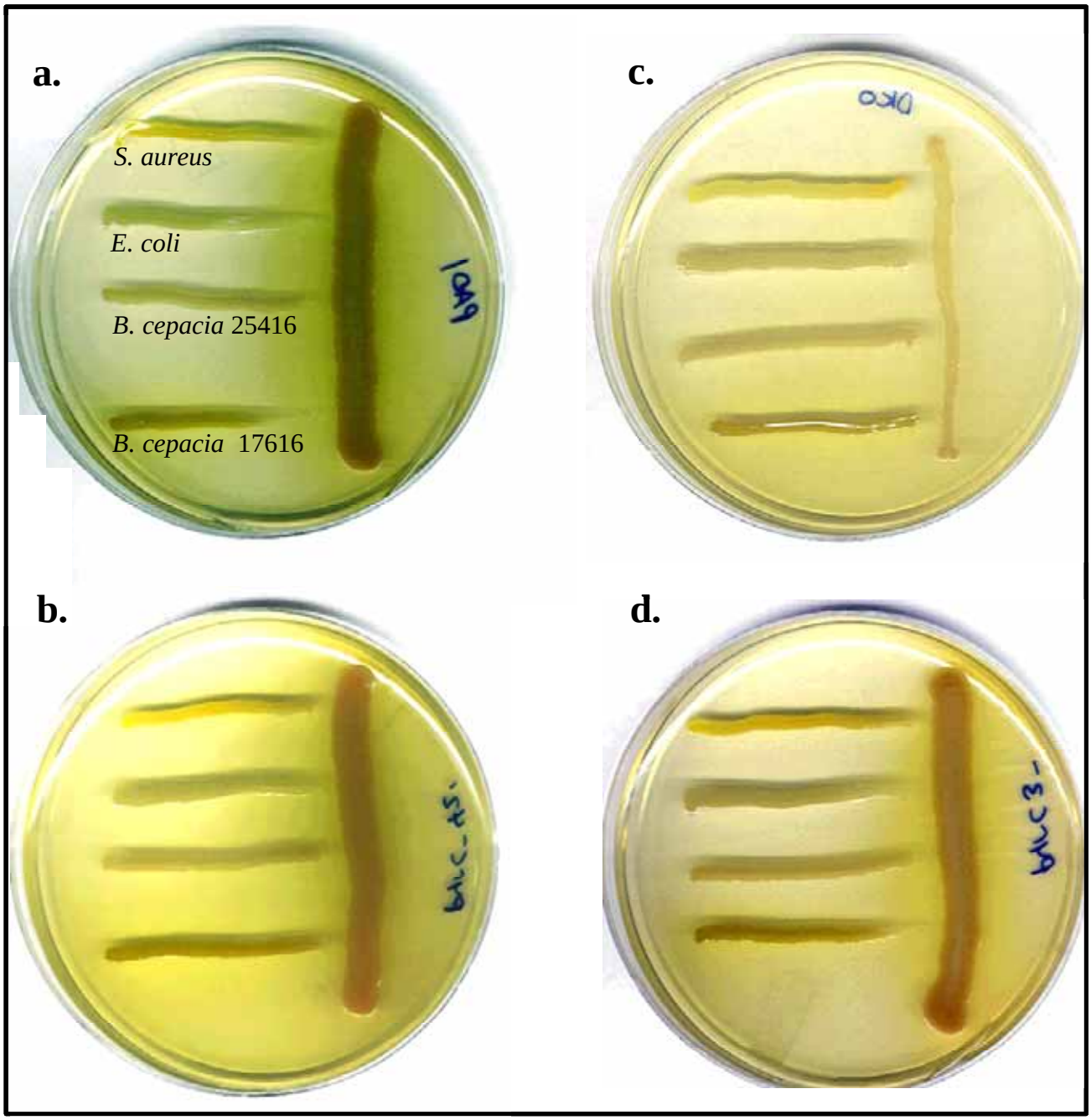

Fig. 55. Cross streak inhibition assays of *P. aeruginosa* wild type and the *pyrC* mutant strains. The tryptic soy agar plates were inoculated as described in Methods. The *P. aeruginosa* strains tested are the vertical line of growth on each plate and are as follows: (a) PAO1, (b) *pyrC* ¯, (c) *pyrC* DKO and, (d) *pyrC2*¯. The bacterial organisms tested against the PAO1 strains are listed on plate (a) and follow the same order on all plates shown.

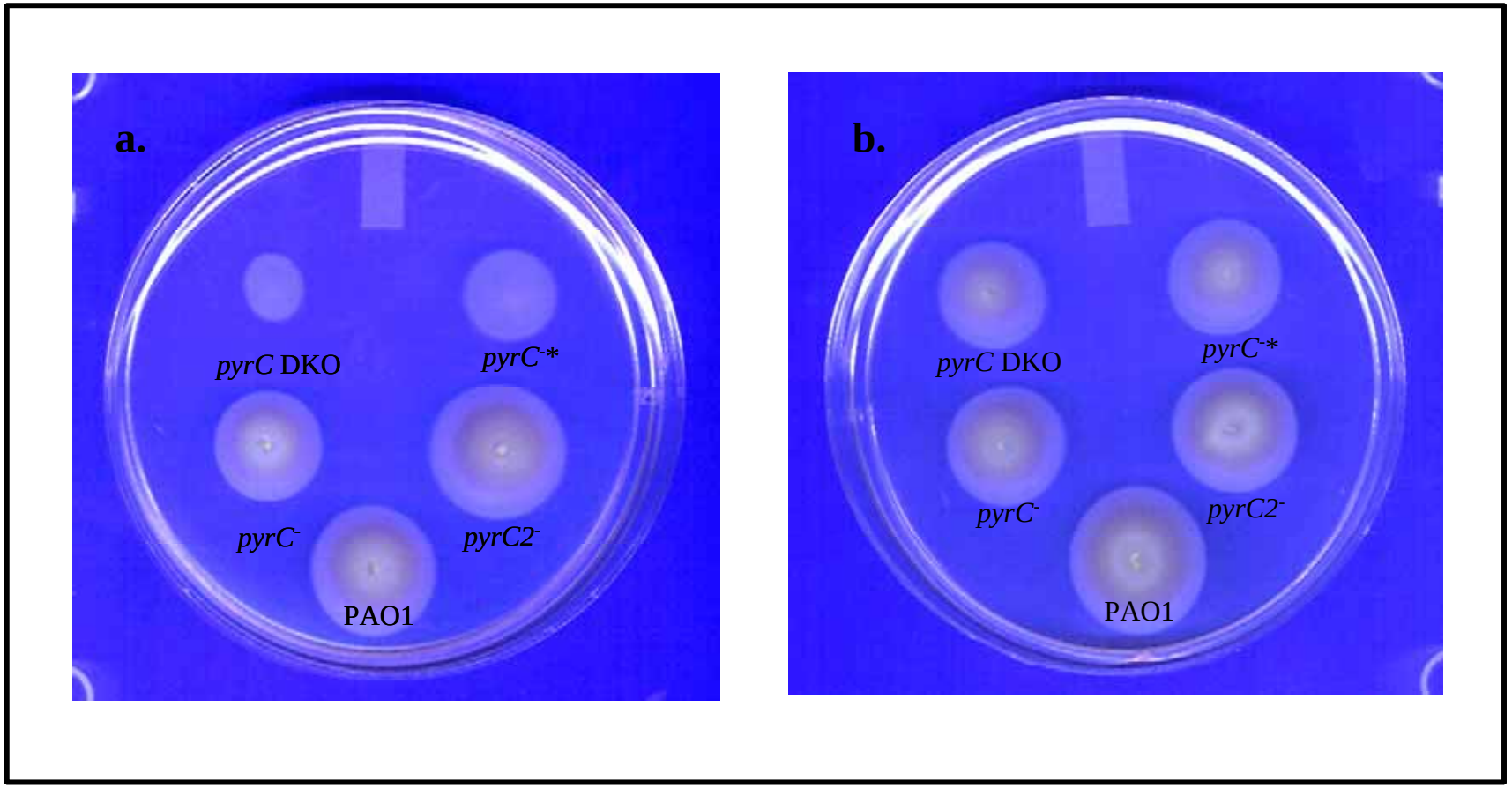

Fig. 56. Swimming motility test of *P. aeruginosa* wild type and *pyrC* mutant strains. The strains were inoculated on to swim medium as described in Methods. The plates were incubated at 25°C for 16 h and then inspected for growth. Although the medium is rich, uracil was added to plate (b) at a concentration of 40 μg ml^{-1} to test its effect on swimming motility. The strains tested are indicated under the area of growth.

seen in Fig. 56b, additional uracil increased the growth and swimming zone of the *pyrC* DKO mutant, although it was still less than that observed for wild-type and the individual *pyrC* mutant strains. No major difference was observed between the growth of the wild-type, *pyrC* or *pyrC2* strains on medium with or without added uracil.

A test of the capacity of the *P. aeruginosa* mutant strains to swarm showed that the *pyrC* DKO was severely impaired in this form of motility (Fig. 57a). The addition of uracil did increase the growth observed on the plate, but no real increase in the undulating pattern, characteristic of swarming, was observed. The *pyrC* mutant grew well on the swarming medium with or without uracil, but again, the growth pattern, characteristic of swarming, was not seen (Figs 57a and 57b). Conversely, the *pyrC2* strain was clearly positive for swarming motility, whether uracil was added or not (Figs 57a and 57b), perhaps to even a greater extent than wild-type. These data correlate well with the results of the rhamnolipid detection assay, as rhamnolipid production has been found to be required for swarming motility. As seen in Table 10, the *pyrC* DKO did not produce rhamnolipid when cultivated in low uracil, and additional uracil increased growth on the medium, but still showed little rhamnolipid production. The *pyrC* mutant grew well, but produced little rhamnolipid when grown in either low or high uracil. Finally, the *pyrC2* and *P. aeruginosa* wild-type both grew copiously and produced large halos of rhamnolipid.

The twitching motility test indicated that the *pyrC* DKO strain was also deficient in this form of motility, as the zone of twitching is only a fraction of that seen for wild-type (Fig. 58a). The addition of uracil increased the size of the twitching zone, but the

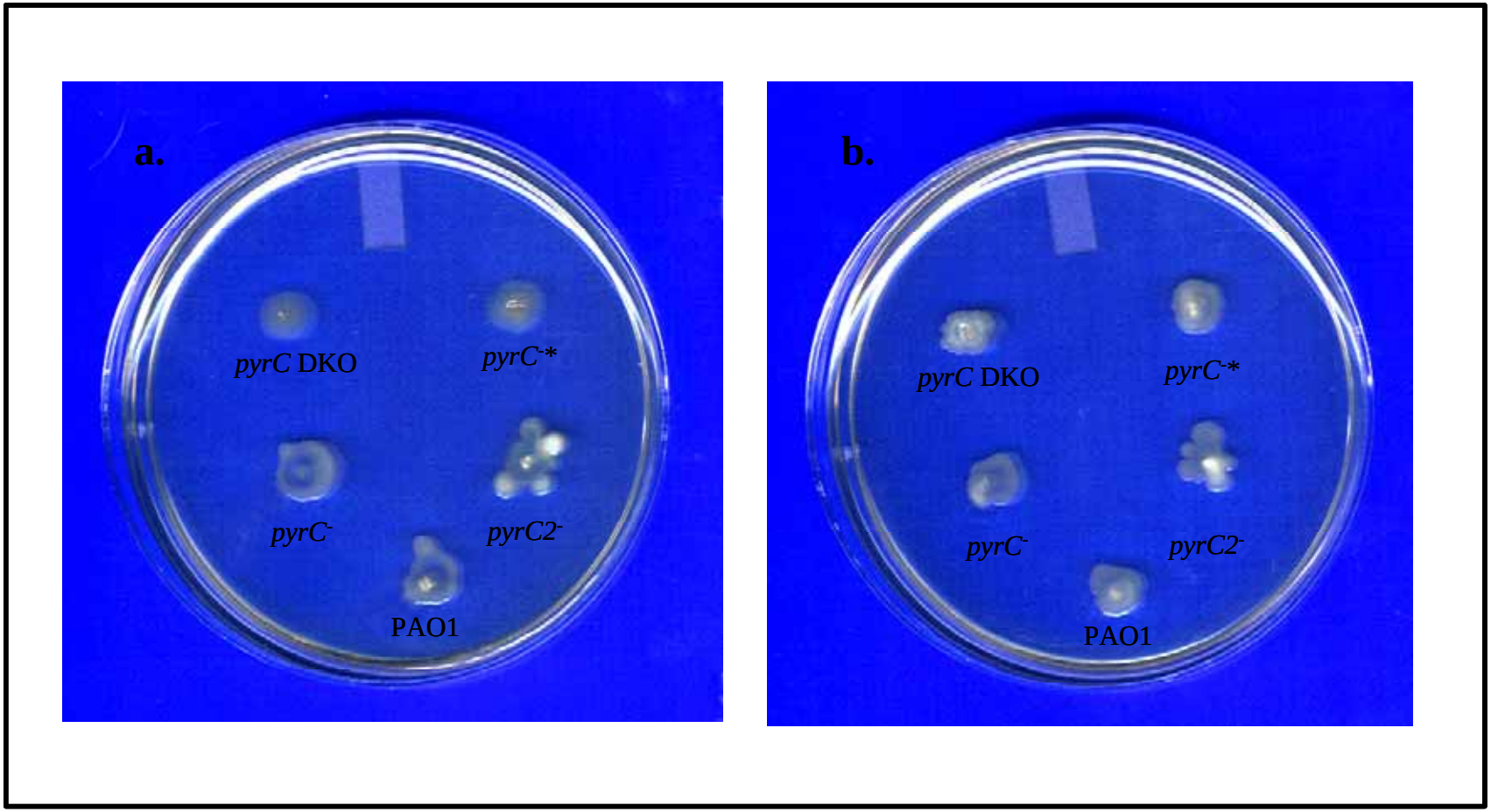

Fig. 57. Swarming motility test of *P. aeruginosa* wild type and *pyrC* mutant strains. The strains were inoculated on to swim medium as described in Methods. The plates were incubated at 30°C for 24 h and then inspected for growth. Although the medium is rich, uracil was added to plate (b) at a concentration of 40 μg ml^{-1} to test its effect on swarming motility. The strains tested are indicated under the area of growth.

	Rhamnolipid production	
Strain	Low uracil (5 μg ml^{-1})	High uracil (40 μg ml^{-1})
P. aeruginosa WT	++	++
PAODB37 (*pyrC*⁻)	+	+
PAODB70 (*pyrC2*⁻)	++	++
PAODB92 (*pyrC* DKO)	-	+

Table 10. Assessment of rhamnolipid production by *P. aeruginosa* wild type and the *pyrC* mutant strains. The strains were cultivated on rhamnolipid test plates, containing low or high uracil, as described in Methods and incubated at 37°C for 22 h. Rhamnolipid production was observed as a pink halo around the bacterial growth on the medium. The symbols used indicate the following: (++), large colony of growth and a large pink rhamnolipid halo; (+), large colony of growth, small rhamnolipid halo; (-), little to no growth and no rhamnolipid production.

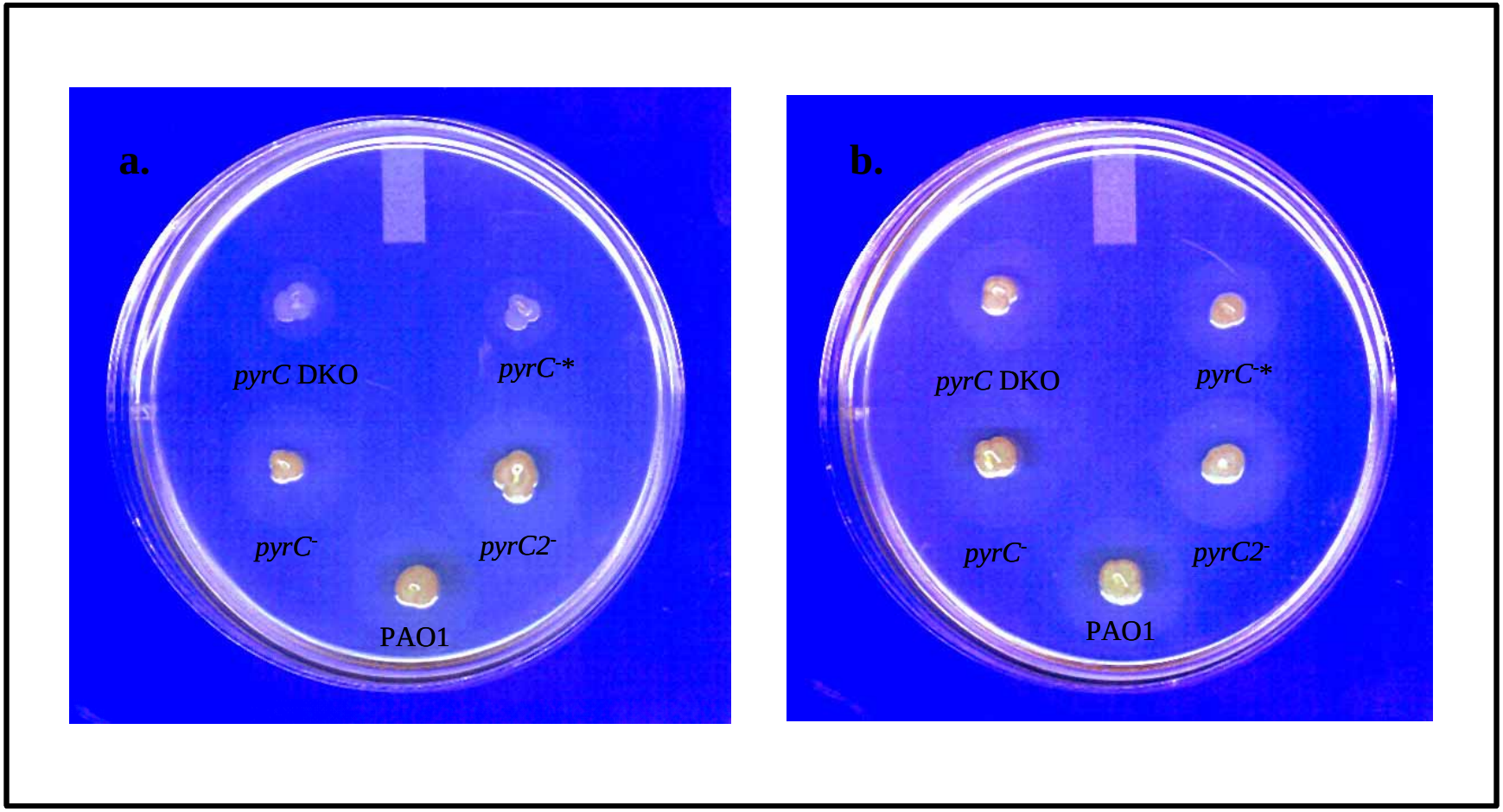

Fig. 58. Twitching motility test of *P. aeruginosa* wild type and *pyrC* mutant strains. The strains were inoculated on to twitch medium as described in Methods. The plates were incubated at 30°C for 24-48 h and then inspected for growth. Although the medium is rich, uracil was added to plate (b) at a concentration of 40 μg ml^{-1} to test its effect on twitching motility. The strains tested are indicated under the area of growth.

zone still did not reach the diameter of the wild-type zone (Fig. 58b). The individual *pyrC* mutant strains both appeared to be capable of twitching motility, in the presence or absence of uracil, as the twitching zones appear similar to those seen for wild-type. The second half of the twitching test is the test for adherence. The twitching medium agar layer is removed and the plate is washed with a gentle stream of water. Any bacteria that remain attached to the plate are stained with crystal violet. As seen in Figs 59a and 59b, the *pyrC* DKO was completely deficient in its ability to adhere, whether uracil was added to the medium or not. The *pyrC* strain appeared to adhere slightly better when grown in uracil, as did the wild-type (Figs 59a and 59b). Interestingly, the *pyrC2* strain appeared to adhere to the greatest extent, whether uracil was present or not.

CAA measurements inside and outside of the cell. As this study represents the first report of a true block in the DHOase step in *P. aeruginosa*, it is also the first analysis of the accumulation of the pathway intermediate carbamoyl aspartate (CAA) within the cell. It has been shown previously in *S. typhimurium*, that the growth of *pyrC* or *pyrD* auxotrophs was severely inhibited in media that caused derepressed pyrimidine gene expression (Turnbough & Bochner, 1985). This growth inhibition was not observed for *pyrA* or *pyrB* mutants. These researchers concluded that the accumulation of CAA was toxic to the cell. They also determined that conditions that decreased CAA production, such as growth in the presence of uracil, concomitantly decreased the toxicity, thus the cells grew better. Conversely, conditions that resulted in pyrimidine limitation, such as growth of the *pyrC* or *pyrD* auxotrophs in orotate, resulted in the derepression of ATCase and exacerbated the growth defect.

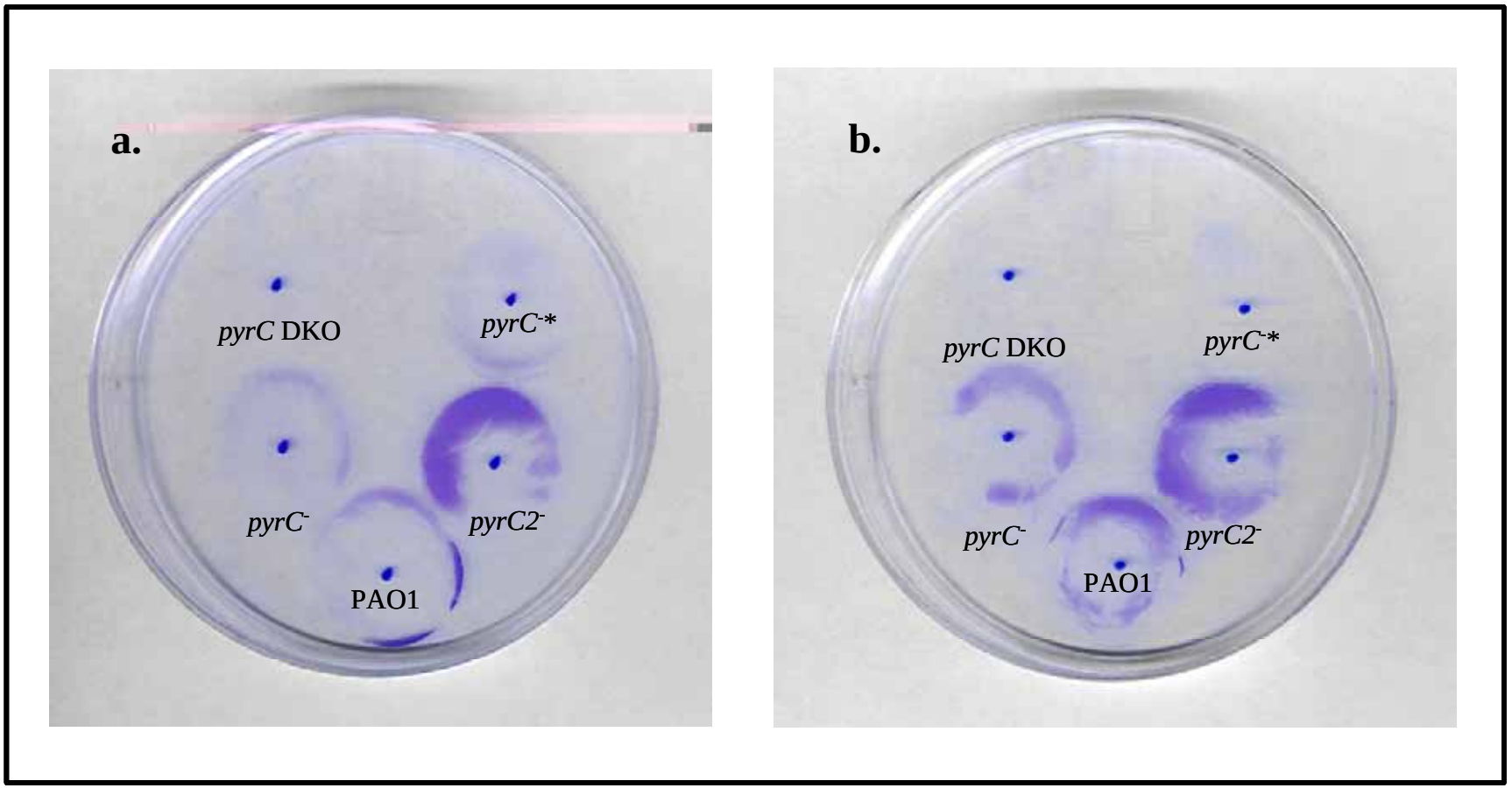

Fig. 59. Adherence test of *P. aeruginosa* wild type and *pyrC* mutant strains. The strains were inoculated on to twitch medium as described in Methods. The plates were incubated at 30°C for 24 to 48 h. The agar layer was then removed and the twitching zones that remained attached to the polystyrene surface, after washing with water, were stained with crystal violet. Although twitching medium is rich, uracil was added to plate (b) at a concentration of 40 μg ml^{-1} to test its effect on twitching motility and adherence. The strains tested are indicated under the stained areas.

In order to determine the extent to which the CAA toxicity phenomenon played a role in the metabolism of the *P. aeruginosa pyrC* DKO strain, the amount of CAA that accumulates within the cell was measured and compared to PAO1 wild-type and the individual *pyrC* mutant strains. As seen in Fig. 60, the wild-type and the individual *pyrC* mutant strains were about the same, and contained on average 0.37 mM CAA when the cells were grown without uracil. When supplied uracil, the cells grew better and to a higher concentration, thus the CAA was found to be higher at about 0.42 mM. In comparison, the *pyrC* DKO mutant accumulated three times the amount of CAA when starved for uracil (1.1 mM) and about 26 % more CAA (0.53 mM) when grown with uracil in the medium (Fig. 60).

In order to further quantitate the effect of pyrimidine limiting or replete conditions on the growth of the *pyrC* DKO strain, the DKO was cultivated in tryptone broth (TB), a moderately rich medium, with and without orotate at a concentration of 0.5 mM or 1.5 mM and growth was monitored spectrophotometrically. After seven hours of growth, 0.4 mM uracil was added to all samples, except for one of the samples containing 0.5 mM orotate, and growth was monitored for another 5 h. Additionally, samples were collected at the 7 h (t_7) and 12 h (t_{12}) time points for determination of the CAA concentration in the spent medium as well as within cell extracts.

As seen in Fig. 61, the addition of 0.5 mM orotate to the medium increases the growth rate of the *pyrC* DKO in TB medium, as the generation time decreases from 168 min, without orotate, to 84 min with orotate. Curiously, the addition of 1.5 mM orotate did not further enhance growth as expected, but instead stunted the *pyrC* DKO growth rate. After 7 h of growth, the generation time was 200 min, and after 12 h of growth, the

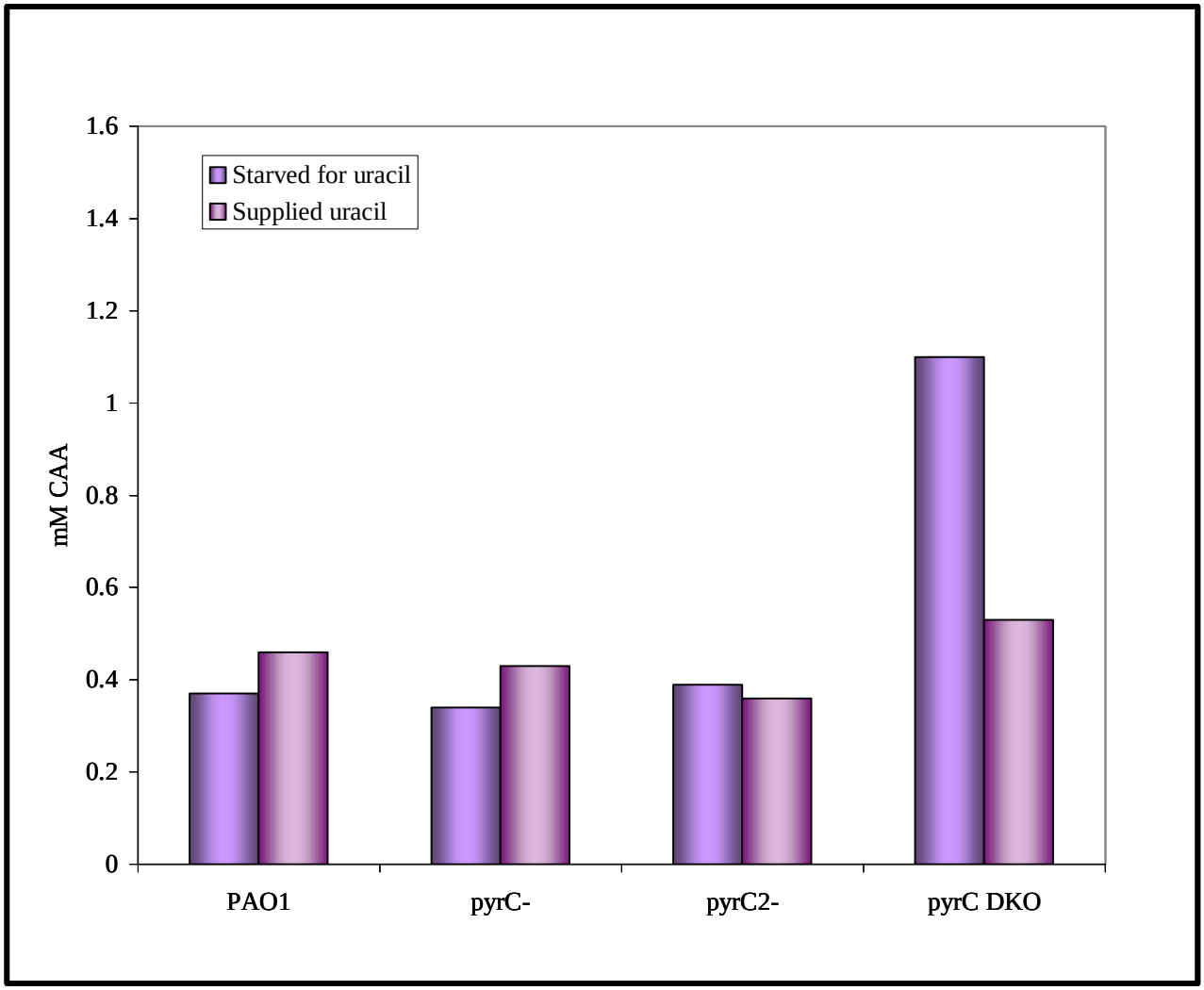

Fig. 60. Concentration of CAA in the cell extracts of *P. aeruginosa* wild type and *pyrC* mutant strains. The strains were cultivated in 50 ml of *Pseudomonas* minimal medium with 0.2% glucose and uracil at a concentration of 40 μg ml^{-1}, until they reached an OD_{600} of 0.4-0.6. The cells were then collected by centrifugation, washed and resuspended in the same medium either with or without (= starved) uracil. The cells were grown for another 4 h and then harvested.

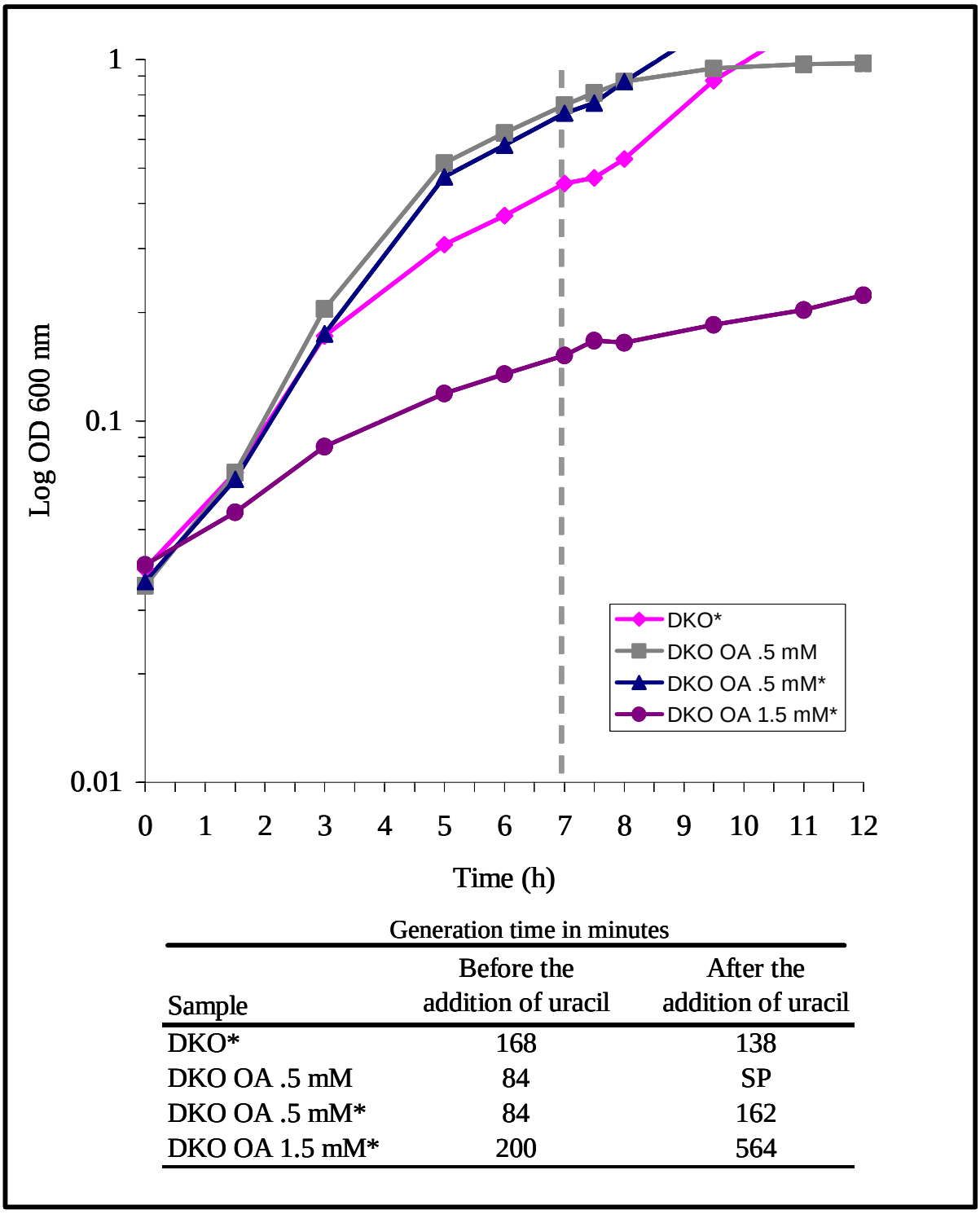

Generation time in minutes

Sample	Before the addition of uracil	After the addition of uracil
DKO*	168	138
DKO OA .5 mM	84	SP
DKO OA .5 mM*	84	162
DKO OA 1.5 mM*	200	564

Fig. 61. Growth curve of the *P. aeruginosa pyrC* DKO strain in tryptone broth (TB) with and without orotate (OA) and/or uracil. SP stands for stationary phase and the (*) indicates that uracil was added at a concentration of 0.4 mM or 40 μg ml^{-1} at t_7.

culture reached an OD 600 of only 0.22. Addition of uracil at t_7 resulted in a spike of growth in all cases except for the sample containing 1.5 mM orotate, where uracil showed no effect.

Analysis of the CAA concentration in the cell extracts and the spent medium from the TB cultures at the t_7 and t_{12} time points, confirms that CAA does accumulate within the cell under conditions of pyrimidine limitation and that the addition of uracil curtails this accumulation (Fig. 62). The effect of uracil on CAA accumulation can perhaps best be appreciated when the calculated CAA concentration is normalized by dividing by the OD 600 of the sample culture (Fig. 63). Analysis of these data show that, relatively speaking, the *pyrC* DKO grown without pyrimidine supplement demonstrated the highest CAA concentration within the cell at t_7. After the addition of uracil, the CAA concentration within the *pyrC* DKO sample dropped by almost half.

Perhaps most striking was the difference observed between the two *pyrC* DKO samples cultivated with 0.5 mM orotate. Prior to t_7, the concentration of CAA measured within the cell and in the spent medium, was about the same for the two cultures (Fig. 63a). However, the addition of uracil to one of the sample cultures at t_7 caused a significant drop in the CAA measured at t_{12}. As seen in Fig. 63b, the sample to which uracil was added accumulated 3.3-fold less CAA within the cell, than the sample that did not receive uracil. In addition, comparison of the CAA measured in the spent medium of the two cultures, showed there to be a 4.5-fold decrease in the sample that received uracil. Finally, examination of the CAA measured in the cell extract and spent medium of the *pyrC* DKO sample cultivated in 1.5 mM orotate shows, that although the culture OD 600 only reached 0.23 after 12 h of growth, relatively speaking, the highest amount of

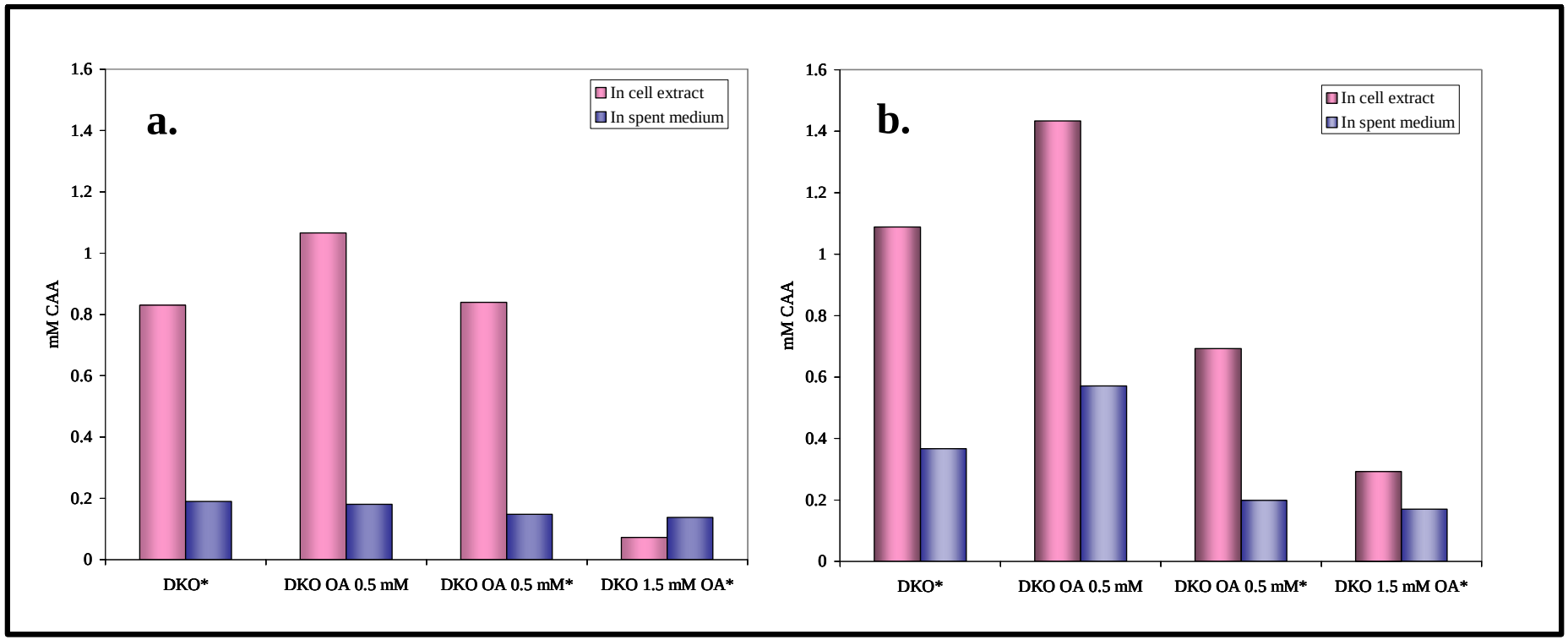

Fig. 62. Concentration of carbamoyl aspartate (CAA) measured from cell extracts and supernatants of the *P. aeruginosa pyrC* DKO strain cultivated in TB medium (correlates with Fig. 60). The (*) indicates those samples to which uracil was added after 7 h of growth. Panel (a) represents measurements taken after 7 h of growth and prior to the addition of Uracil. Panel (b) shows the values obtained after 12 h of growth, 5 h in the presence of uracil

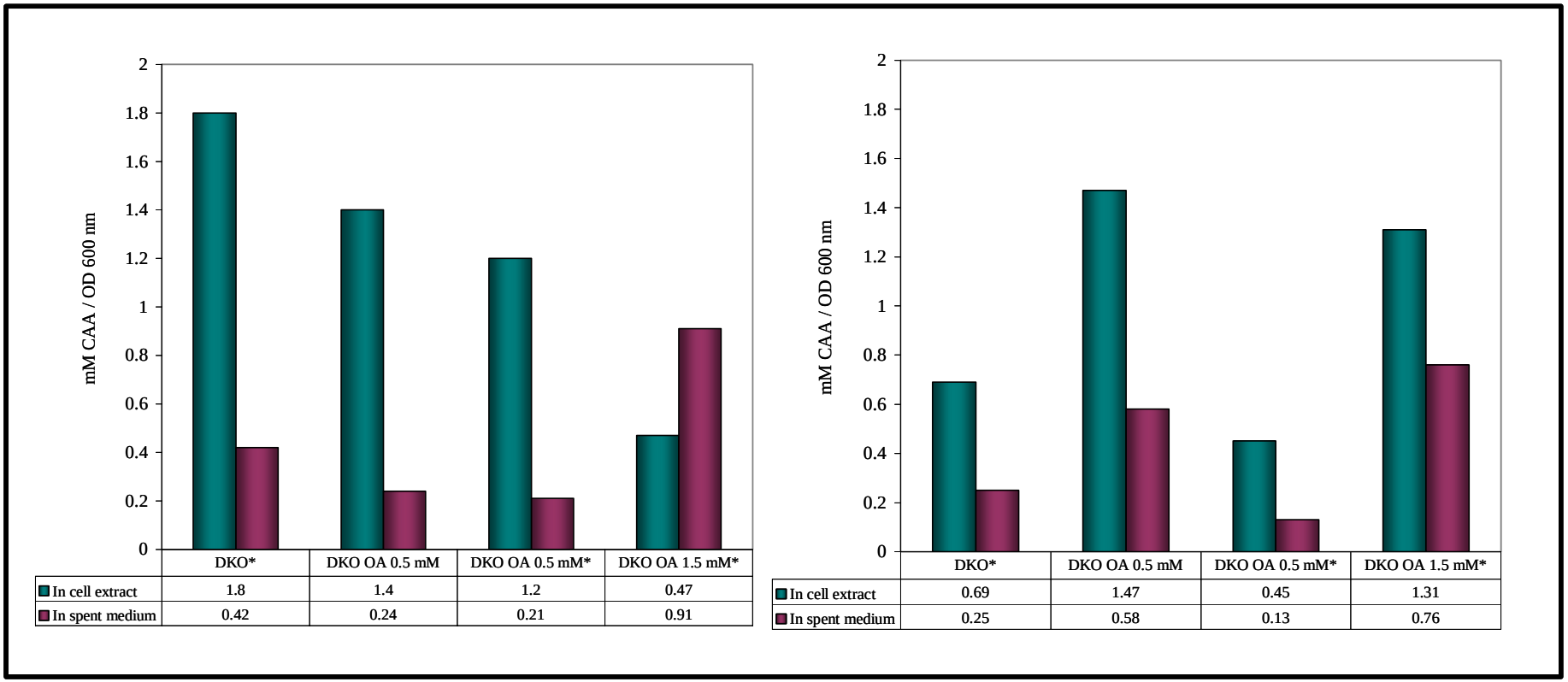

Fig. 63. Concentration of CAA measured from cell extracts and supernatant of *P. aeruginosa pyrC* DKO cultivated in TB with and without orotate and/or uracil (correlates with Fig. 62). The values presented here are normalized by dividing each CAA concentration by the OD_{600} of the sample from which it was obtained.

extracellular CAA was found here at both t_7 and t_{12}. Also, the second highest level of CAA within the cell was found in this sample at t_{12} (Fig. 63a and 63b).

Anaerobic growth in the presence of nitrate. While searching the literature for reports of other *P. aeruginosa* virulence pleiotropic mutants, it was discovered that a mutant in the Sec-independent secretion apparatus known as TAT (twin-arginine translocase) had many phenotypic characteristics in common with the *pyrC* DKO mutant. Ochsner and co-workers, studying the TAT system in *P. aeruginosa*, created a TAT mutant by deleting one of the essential genes of the translocation apparatus, *tatC* (Ochsner *et al.*, 2002). These scientists also reported that one of the proteins found to be secreted by TAT apparatus is nitrate reductase (NapA). Thus, the *tatC* mutant that they created was unable to grow anaerobically in the presence of nitrate. In order to determine the extent to which the *pryC* DKO mutant mimicked the *tatC* mutant, the *pyrC* DKO mutant was cultivated anaerobically, with 1 % KNO_3 and 0.5 mM uracil or orotate, as described in Methods. As seen in Fig. 64, the *pyrC* DKO strain was unable to grow anaerobically using nitrate, when orotate served as the pyrimidine source. Growth in the presence of uracil, however, was almost the same as the wild-type or the individual *pyrC* mutant strains.

Other growth deficiencies of the *pyrC* DKO strain. The growth capabilities of the *pyrC* DKO on three additional carbon sources was further tested and compared to PAO1 wild-type and the individual *pyrC* mutant strains. The growth tests determined that that the *pyrC* DKO was unable to use *p*-hydroxybenzoate, or choline as carbon and energy sources when orotate, at 5 μg ml^{-1}, served as the pyrimidine source. Moderate growth was observed when uracil was used at a concentration of 5 μg ml^{-1}. In addition,

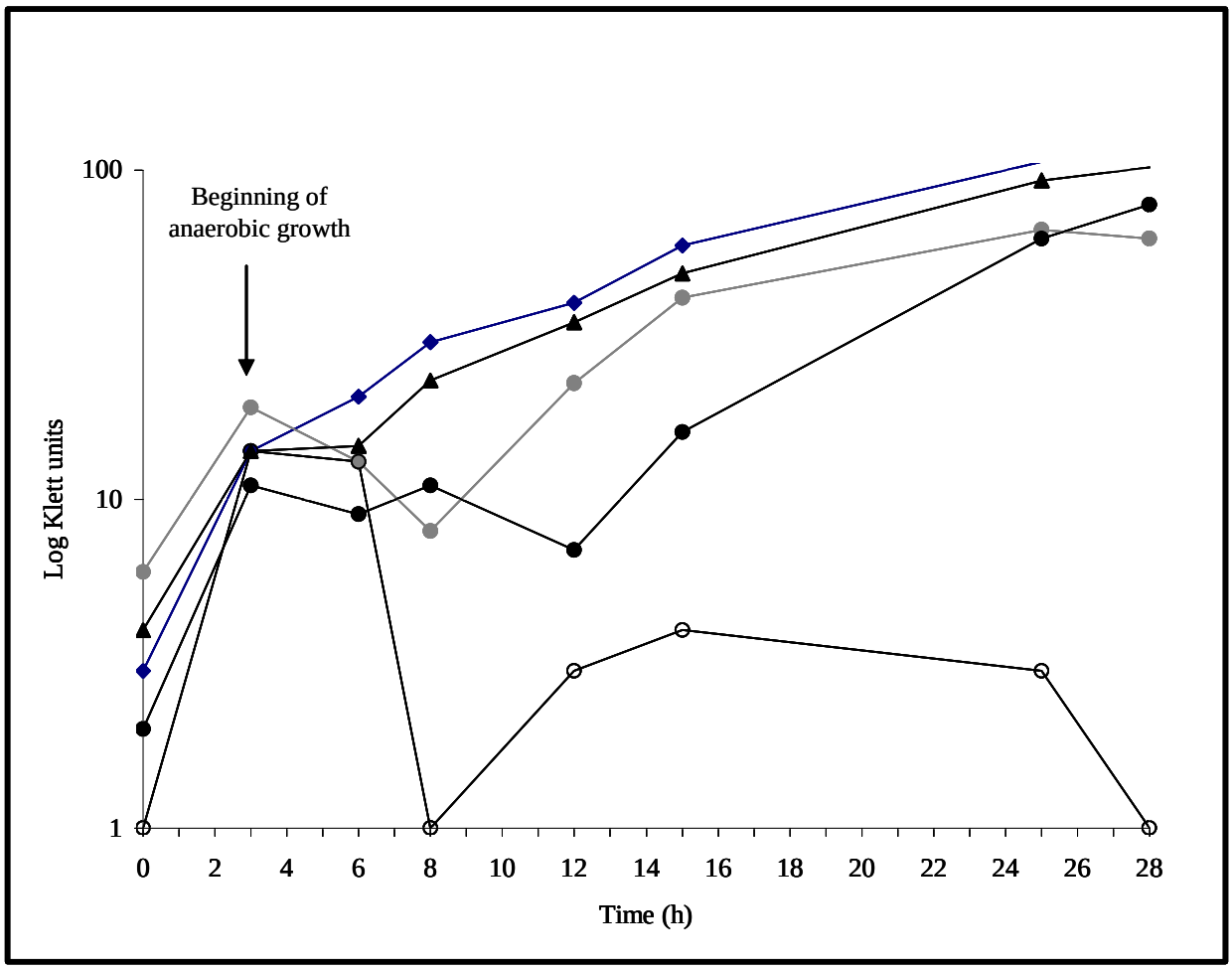

Fig. 64. Anaerobic growth of *P. aeruginosa* wild type and the *pyrC* mutant strains in MM9 medium With 1% KNO_3 and glucose. Samples were cultivated as described in Methods, in triplicate, and the graph shown is representative of the data obtained. The symbols used represent the following: (◆), PAO1 wild type; (●), pyrC-; (▲), pyrC2-; (●), pyrC DKO + U; (○) pyrC DKO + OA. Uracil and orotate were both added at concentrations of 0.5 mM.

the *pyrC* DKO was unable to use citrate as a carbon source, as the organism grew on the citrate slant, but did not cause the color of the slant to turn blue, as is characteristic of *P. aeruginosa* wild-type.

Antibiotic susceptibility. As the *pyrC* DKO strain exhibited so many other defects, it seemed logical to test its susceptibility to antibiotics. *P. aeruginosa* wild-type is notorious for its resistance to antibiotic therapy. One of the mechanisms that enables *P. aeruginosa* to be so remarkably drug resistant is the Mex transport system. The Mex, or multi drug efflux system, allows the export of many antibiotics that make their way into the cell. Other resistance mechanisms involve the modification of various catabolic pathways, so that certain antibiotics are recognized as carbon and energy sources. In order to determine the antibiotic susceptibility of the *pyrC* DKO strain in comparison with wild-type and the individual *pyrC* mutant strains, the strains were tested using the Kirby Bauer method as described in Methods. As seen in Table 11, the zones of inhibition observed for the *pyrC* DKO, when present, were always larger than those seen for wild-type or the individual *pyrC* mutant strains. The most striking result however, was that found for the antibiotic sulfamethoxizol trimethoprim (SXT). Whereas the wild-type is strongly resistant to this antibiotic, the *pyrC* DKO strain is shown here, to be susceptible to its effects. The implications of this discovery will be discussed shortly.

a.

Strain	C 30	CAZ 30	CIP 5	FOX 30	NA 30	PB 300	SXT	Te 30
PAO1 WT	15	**28**	**28**	NZ	9	**14**	10	9
PAODB37 (*pyrC*⁻)	17.5	**27**	**30**	7 (NZ)	10	**15**	10	10
PAODB70 (*pyrC2*⁻)	17	**28**	**26**	NZ	10	**15.5**	11	10
PAODB92 (*pyrC* DKO)	17.5	**37**	**31**	11(NZ)*	10.5	**20**	**18**	13

b.

Disc	Antibiotic and concentration	Resistant (less than or equal to)	Intermediate	Susceptible (greater than or equal to)
C 30	Chloramphenicol 30 ug	12	13-17	18
CAZ 30	Ceftazidime 30 ug	14	15-17	18
CIP 5	Ciprofloxacin 5 ug	15	16-20	21
FOX 30	Cefoxitin 30 ug	14	15-17	18
NA 30	Nalidixic acid 30 ug	12	18-21	22
PB 300	Polymixin B 300U	8	9-11	12
SXT	Trimethoprim / Sulfamethoxazole	10	11-15	16
Te 30	Tetracycline 30 ug	14	15-18	19

Table 11. Antibiotic susceptibility test of the *P. aeruginosa* wild type and *pyrC* mutant strains using the Kirby Bauer method. PAO1 strains were grown at 37°C ON on LB medium. A sterile swab was used to transfer bacteria to an LB broth tube until the turbidity was 0.5 McFarland (OD_{600} of 0.6). A new sterile swab was used to inoculate the Mueller Hinton agar plates by the three quadrant streak method. The antibiotic discs were aseptically placed on the plates and the plates incubated at 37°C for 20 h. The diameter of the zones of inhibition were measured in mm and are reported in table (a). The code names for the antibiotic discs, their concentrations and the resistant, intermediate and susceptible zone sizes are given in table (b).

CHAPTER IV

DISCUSSION

"The most beautiful thing we can experience is the mysterious, it is the source of all true art and science. He to whom this emotion is a stranger, who can no longer wonder and stand rapt in awe, is as good as dead: his eyes are closed."

Albert Einstein

What I Believe, 1930.

For every endeavor, there is a first step. The path to understanding the mysteries of pyrimidine biosynthesis in *Pseudomonas aeruginosa* began in 1968, when Isaac and Holloway isolated various mutants of the pyrimidine biosynthetic pathway, in an attempt to understand the relationship between gene distribution and control mechanisms. The course of knowledge was continued, some 20 years later, in our laboratory, with the cloning and sequencing of the genes encoding the enzyme aspartate transcarbamoylase (ATCase). Vickrey (1993) discovered that the *P. aeruginosa* ATCase was composed of two types of polypeptides, a 35 kDa PyrB subunit and a 45 kDa PyrC subunit. These findings gave support to an emerging model of the architecture of ATCase in the pseudomonads. The structure was reminiscent of the *E. coli* ATCase, which is dodecameric with six catalytic PyrB polypeptides and six regulatory PyrI polypeptides, but instead of the regulatory subunits, the *Pseudomonas* enzyme contained six PyrC polypeptides.

It was soon discovered however, that the PyrC polypeptides in the ATCase complex, despite strong amino acid homology to other known PyrC sequences, were not capable of catalyzing the DHOase reaction. Assays of the purified ATCase holoenzyme did not exhibit DHOase activity. Thus, the gene encoding the PyrC-like polypeptide was designated *pyrC'*, and the search for the gene encoding the DHOase activity of *P. aeruginosa* was initiated. This is where my involvement in this venture began, as I set out to clone and sequence the gene encoding DHOase activity in *P. aeruginosa*. Here it is shown that the *P. aeruginosa* genome actually contains two *pyrC* genes, in addition to the *pyrC'*, and that each encodes an active DHOase.

A comparison of the two *pyrC* genes reveals several pertinent differences. The most obvious is a substantial difference in size, as partial purification of the *pyrC* encoded polypeptide was shown to be approximately 40 kDa (Fig. 33), while Zubay analysis of the *pyrC2* encoded polypeptide showed it to be about 47 kDa (Fig. 34). Both of these experimentally determined molecular mass values are in keeping with the theoretically predicted values of 38 kDa for the PyrC, and 48 kDa for the PyrC2. The two *pyrC* genes are located on separate regions of the chromosome (Fig. 31), and an amino acid alignment of the polypeptides shows that they share little homology (15 % identity and 23 % homology). Curiously, the PyrC2 polypeptide has higher homology with the inactive PyrC' polypeptide (26 % identity and 40 % homology). These homology values, despite the fact that the PyrC' polypeptide is inactive and has been accumulating mutations (that do not interfere with its ability to function in the ATCase holoenzyme) make it tempting to hypothesize that the *pyrC'* and *pyrC2* genes arose from an ancient gene duplication event. Another observation in support of this hypothesis is the fact that

almost all organisms discovered to date to possess the *pyrC2* gene, also have the *pyrC'* gene (Table 5).

On the other hand, the *pyrC* gene may reside in the *P. aeruginosa* chromosome as the result of an ancient, horizontal gene transfer event. Analysis of the DNA surrounding the *pyrC* sequence using the BLAST algorithim, showed that a similar gene cluster existed in *Vibrio parahaemolyticus* (Fig. 36). Although the *pyrC* gene itself is no longer contained in this cluster in *V. parahaemolyticus*, the gene order and orientation of three other genes is maintained, and the homology is significant for two of these (*glx1*, 63 % identity and 76 % homology, and *rnt*, 68 % identity and 80 % homology). In addition, several of the intergenic regions of the *P. aeruginosa* cluster do not reflect the overall GC content of the genome, which is 67 %, as they are between 41 to 62 % GC. Also, the *pyrC* gene from *P. aeruginosa* was expressed from its own promoter on pPAC1 in the *E. coli pyrC* mutant strain, X7014a. As a general rule, *E. coli* promoters are easily recognized by *P. aeruginosa* expression machinery, while the converse is rarely true (Deretic *et al.*, 1989). This, in combination with the strong homology between the *P. aeruginosa pyrC* and the *V. cholerae pyrC* (64 % identity and 73 % homology), builds a strong case that the *pyrC* gene in *P. aeruginosa* came from elsewhere.

Promoter fusion vectors, containing the promoter regions of the different *pyrC* genes, were used to establish any differences in their expression patterns. The *pyrC* promoter was found to be active in all conditions tested and thus appears to be constitutively expressed. Expression of the *motY* gene, which is separated from the *pyrC* gene by 120 bp and divergently transcribed, was also tested, as the two putative promoter regions, predicted by computer analysis, appear to overlap slightly. The data indicate that

expression from the *motY* promoter is also constitutive but about four to five times less active than is the *pyrC* promoter region (Fig. 40). The *pyrC2* gene was found to be the last gene of a three gene cluster. Accordingly, three promoter fusion vectors were created in order to test the expression of each. However, no β-galactosidase activity was observed when the promoter fusion vectors were introduced into *P. aeruginosa* wild-type (Figs 40 and 43).

The promoter fusion vectors were also introduced into the *P. aeruginosa pyrC* strain, which is a prototroph as a result of the expression of *pyrC2*. Here, β-galactosidase activity was observed from the promoter region belonging to the first of the three gene cluster containing *pyrC2* (Fig. 41). Thus, it is apparent that *pyrC2* is the distal gene of a three gene operon, and that this operon is expressed in the *pyrC* strain. The observation that no β-galactosidase activity was detected when the vectors resided in the *P. aeruginosa* wild-type background, indicates that the operon is not constitutively expressed, rather it is under some form of control. However, the mechanism governing the expression of *pyrC2* remains unclear. Analysis of the promoter region of the *pyrC2* operon, using a statistical promoter prediction program (University of California Berkeley Drosophila Genome Project - UCBDGP) indicates the presence of a strong promoter sequence that may be controlled by RpoS. Examination of the –10 region reveals the presence of several features that are commonly found in RpoS binding sites (Fig. 65) (Becker & Hengge-Aronis, 2001). Entertaining the possibility that *pyrC2* expression could be under the control of RpoS, allows the development on an interesting hypothesis. Lets say that *pyrC* is constitutively expressed, and that DHOase I functions predominantly in pyrimidine biosynthesis during growth. It has been established that

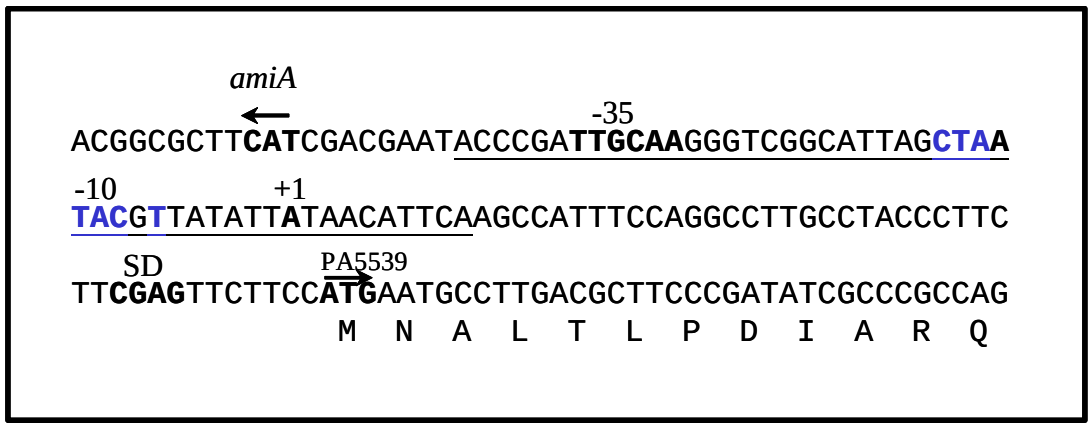

Fig. 65. Promoter region governing the expression of the operon containing the *P. aeruginosa pyrC2* gene. The 100 bp separating the *amiA* gene and the first gene in the *pyrC2* operon were analyzed using the UCBDGB promoter analysis program. Underlined is the putative promoter which was determined to have the highest probability of functioning in the expression of the operon (0.92 where 1.0 is the highest probable value). The putative -10 and -35 regions are indicated as well as the +1 and the Shine Delgarno (SD) region. In addition, a potential RpoS binding sequence was identified and is depicted with blue text. RpoS consensus sequence is CTATACT.

DHOase I catalyzes the biosynthetic reaction (CAA to DHO) when the ambient pH is 6 to 7. If conditions arise that cause the cytoplasm to become more basic, then DHOaseI begins to catalyze the reverse reaction (DHO to CAA) (Christopherson & Jones, 1979). This would result in an increase in CAA and a decrease in pyrimidine nucleotides, as the momentum of the pathway would no longer be in the forward direction. The ensuing stress upon the cell could trigger an increase in the level of transcription of *rpoS*, which in turn could stimulate the expression of the operon containing *pyrC2*, either directly or indirectly, through the activation of other regulatory proteins. The DHOase II encoded by *pyrC2*, may be capable of performing the biosynthetic reaction under conditions that the DHOase I cannot. However, further studies are necessary (such as the cultivation of PAO1 containing the promoter fusion vectors under stationary-phase and stress response conditions) in order to strengthen this hypothesis.

One of the most perplexing discoveries of this research was the observation that while molecular evidence showed the *pyrC2* encoded DHOase II to be catalytically active, traditional enzyme assays, which measure the reverse reaction which is the conversion of DHO to CAA (Beckwith *et al.*, 1962), did not detect enzyme activity. The data supporting the assertion that DHOase II is catalytically active are strong. First, the *pyrC2* gene is able to complement the *E. coli pyrC* auxotroph, X7014a, when expressed from the *lacZ*α promoter on pUCP19, as the cells can grow on minimal medium without uracil. However, DHOase assays of the complemented *E. coli* cells do not detect activity, as measured by the conversion of DHO to CAA. Second, the *P. aeruginosa pyrC* strain is a prototroph as a result of the activity of the *pyrC2* encoded enzyme, and yet enzyme assays of cell extracts from this strain, do not detect DHOase activity. Third, a complete

block in pyrimidine biosynthesis, at the DHOase step, is achieved only when **both** the *pyrC* and *pyrC2* genes are inactivated. And fourth, the promoter fusion vector containing the promoter of the *pyrC2* operon, only shows activity when expressed in the *P. aeruginosa pyrC* strain (although it should be noted that this vector was not tested in wild-type PAO1 cultivated to stationary phase or under stress response conditions). Additionally, HPLC assays, measuring the conversion of CAA to DHO, show that the DHOase II enzyme is capable of the biosynthetic reaction (Fig. 35a). All DHOase enzymes studied to date are readily reversible and have the ability to bind either CAA or DHO and catalyze the condensation or hydrolysis reactions respectively. This preliminary analysis of the DHOase II enzyme indicates that it is different from any DHOase studied previously, and further comparisons of the PyrC2 polypeptide with the PyrC sequence from *E. coli*, pinpoints some of these differences.

Recently, the DHOase from *E. coli* has been crystalized and the three-dimensional structure determined and refined to a resolution of 1.7 Å (Thoden *et al.*, 2001). A multiple alignment of the PyrC and PyrC2 polypeptides from *P. aeruginosa*, with the *E. coli* PyrC sequence, reveals that many of the amino acids found to be essential for substrate binding and subunit-subunit interactions, remain conserved in all three peptides (Fig. 66). For example, in *E. coli*, the amino acids determined to be important for the coordination of the binuclear metal center (His 16, His 18, Lys 102, His 139, His 177 and Asp 250) are essentially conserved in the *P. aeruginosa* PyrC2 polypeptide. The only exception is the first residue, where His 16 is replaced with Gln (position 60 in PyrC2). The amino acids found to participate in key salt bridges that serve to stabilize the subunit-subunit interface are conserved as well (Fig. 66). There are however, certain

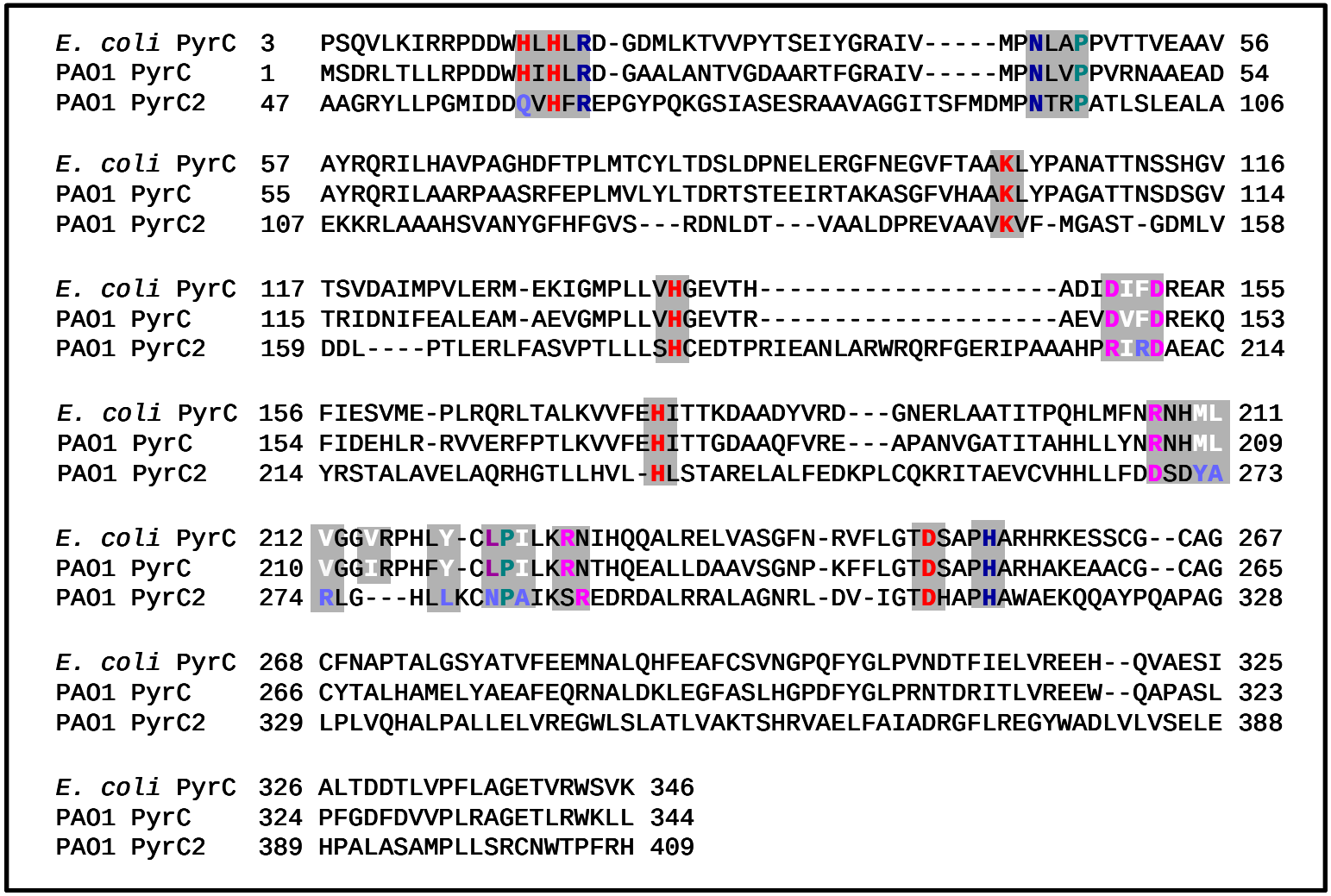

Fig. 66. Alignment of the *P. aeruginosa* PyrC and PyrC2 polypeptides with the *E. coli* PyrC amino acid sequence. The alignment shows the key amino acid residues present in each sequence, and the differences observed for the PyrC2 polypeptide. Residues in color represent the following: Red, active site; pink, salt bridges that stabilize subunit interaction; white, "sticky" patch between subunits; aqua, essential proline residues; dark blue, anchor carboxylate group of DHO within the active site; purple, important leucine residue that hydrogen bonds with DHO or CAA in active site; light blue, residues of PyrC2 that differ significantly from PyrC.

differences between the PyrC and PyrC2 sequences that could conceivably alter the catalytic mechanism of DHOase II.

In the *E. coli* PyrC, Leu 222 is defined as playing a significant role in substrate binding. The carbonyl oxygen of leucine reportedly forms a hydrogen bond with the N3 of either DHO or CAA (Thoden *et al.*, 2001). In PyrC2, Leu 222 is replaced with asparagine. Whether asparagine would perform the same function as leucine is unknown, however, asparagine in this position is not unique to the *P. aeruginosa* PyrC2, as all DHOase IIs and large DHOases (Type II as in *Bacillus*) were found to have asparagine in this position (Table 12). A BLAST search using the *P. aeruginosa* PyrC2 amino acid sequence resulted in the identification of 16 other organisms that contain the *pyrC2* gene. An alignment of these 16 sequences revealed many amino acid residues that were conserved in all sequences. A comparison of these residues, and their positions, with alignments of the small PyrC sequences (Type I, DHOase I) and the large Type II PyrC sequences (as seen in *Bacillus*), results in a list of the amino acids that are completely conserved, but also unique for PyrC2. As seen in Table 12, there are 14 amino acids for which this is the case. It is difficult to predict how any of these differences in amino acid sequence effect PyrC2 activity, but the data presented here clearly show, that while *pyrC2* does encode a polypeptide with DHOase activity, the catalytic parameters are different from any DHOase studied to date.

Once it was established that *P. aeruginosa* contained two *pyrC* genes, and that both encoded active DHOase enzymes, it became obvious that in order to create a block in the third step of the pyrimidine biosynthetic pathway, both genes would need to be inactivated. Accordingly, the *pyrC* and *pyrC2* genes were inactivated individually in

E. coli PyrC	*P. aeruginosa* PyrC2
H 16	**Q 60**
V 48	**T 99**
R 59	K 109
L 75	G 125
83	N 130
A 106	**M 149**
G 115	L 157
F 175	L 234
M 210	**Y 272**
L 222	**N 282***
C 263	**Y 322**
C 265	**P 326**
A 271	V 332
272	Q 333
F 282	V 343
285	G 346

Table 12. Conserved amino acid differences between DHOaseI and DHOaseII. Single letter amino acid designations are used. The amino acid number for *E. coli* is given and its equivalent, based on alignment, is given for DHOaseII. The (*) indicates that this amino acid is present in all large DHOases, not just the DHOaseII enzymes. The amino acids in bold represent significant changes.

P. aeruginosa. In addition, the *pyrC* double knock-out (DKO) was created by inactivating the *pyrC2* gene in the *pyrC* strain. The genotypes of these mutant strains were confirmed by Southern hybridization (Fig. 38), and when necessary, by growth in the presence of gentamicin, and their phenotypes confirmed by biochemical analyses. Here it is worth while to mention a curious phenomenon encountered during the isolation of the *pyrC* strain.

In order to create the *pyrC* strain, the *pyrC* gene was replaced by allelic exchange with a truncated version of this gene as described in Methods. The putative *pyrC* mutants were screened for pyrimidine auxotrophy by plating onto minimal medium with and without uracil. Of the one hundred colonies screened, one was found to be uracil-requiring. This was unexpected, because at that time it was hypothesized that both *pyrC* and *pyrC2* genes were constitutively expressed. It was anticipated that the only way to accurately screen for the replacement of *pyrC* with Δ*pyrC* would be with PCR, where allelic exchange would be demonstrated by the presence of a shortened PCR product.

The *pyrC* pyrimidine auxotroph was further characterized by streaking for isolation on *Pseudomonas* minimal medium with and without uracil, and on *Pseudomonas* isolation agar (PIA) medium. After 24 h of growth at 37ºC, the *pyrC* strain showed no growth on the plate without uracil, good growth on the plate with uracil, and moderate but transparent growth on PIA, with little pigment production. When these plates were allowed to sit on the bench top at room temperature for 3 to 4 days, a number of colonies began to appear on the plate without uracil. And on the PIA plates, a number of colonies appeared that were more opaque and produced more pigment than the initial growth. It was first thought that these colonies represented revertants of some form.

However, DHOase assays of the cell extracts obtained from these cells showed no activity, despite the ability of the cells to grow on without uracil. Thus, it was determined that here, the *pyrC2* was being expressed, and DHOase II activity was allowing the cells to grow as prototrophs.

The observation that the inactivation of *pyrC* causes temporary auxotrophy until the expression of *pyrC2* is initiated, combined with the data obtained from the promoter fusion studies, strongly suggests that the *pyrC* is constitutively expressed, while the *pyrC2* gene is under some form of transcriptional control. And the control mechanism is not likely straightforward, as it does not seem that *pyrC2* is turned on in all *pyrC* strains. Plate count studies on minimal medium, with and without uracil, have determined that the appearance of the *pyrC* pyrimidine prototrophs occurs at a frequencey of about 1.6 x 10^{-5}. The occurrence of these so called “pseudo-revertants” is not unique to the *pyrC* mutant described here, as Essar and co-workers (1990) reported a similar phenomenon for the genes involved in anthranilate biosynthesis in *P. aeruginosa*. A brief summary of their observations follows.

In *P. aeruginosa,* anthranilate is required for the synthesis of the amino acid tryptophan. Esser and co-workers have reported that anthranilate is also essential for the synthesis of the phenazine pigment, pyocyanin, a product of secondary metabolism. These researchers discovered that *P. aeruginosa* has two anthranilate synthase enzymes and the genes encoding them were designated *phnAB* and *trpEG*. The *phnAB* encoded synthase was found to supply anthranilate for pyocyanin biosynthesis, as *phnA* mutants produced 66 to 78 % less pyocyanin than did wild-type PAO1. The *trpEG* encoded synthase was determined to provide anthranilate specifically for tryptophan biosynthesis

as *trpE* mutants were tryptophan auxotrophs. Curiously however, they discovered that upon further characterization, the *trpE* auxotrophs gave rise to spontaneous tryptophan-independent colonies at a frequency of 10^{-5} to 10^{-6} (Esser *et al.*, 1990). After confirming that *trpE* was truly inactivated in the "pseudo-revertants", the researchers determined that the anthranilate synthase activity was being provided by the *phnAB*-encoded anthranilate synthase. It was also discovered that the level of *phnA* mRNA was eight times greater in the pseudo-revertants than in wild-type, when measured in early log phase cells. Finally, it was determined that in order to make a true Trp^- mutant, it was necessary to inactivate both *trpE* and *phnA* (Esser *et al.*, 1990).

The parallels between these studies on anthranilate synthase and the research presented here, on DHOase in *P. aeruginosa*, are intriguing. Taken a step further, an even stronger analogy can be made, as it would appear that anthranilate synthase and dihydroorotase both represent biosynthetically essential enzymes that, through duplication and adaptation, have apparently been recruited as enzymes that also function in secondary metabolism. In the case of anthranilate, the *phnAB*-encoded enzyme synthesizes this compound specifically for the biosynthesis of pyocyanin, which is not produced until the onset of stationary phase. As for the potential role of DHOase in secondary metabolism, Maksimova and co-workers (1994) have reported that a *P. putida* DHOase mutant produces significantly less pyoverdin (also a secondary metabolite) as compared to wild-type. The biosynthetic pathway for the synthesis of the pyoverdin chromophore, as proposed by this research group (Maksimova *et al.*, 1994), is initiated by a reaction involving phenylalanine and DHO as substrates (Fig. 67). In accordance with their findings, it is shown here that a *P. aeruginosa* DHOase mutant (*pyrC* DKO)

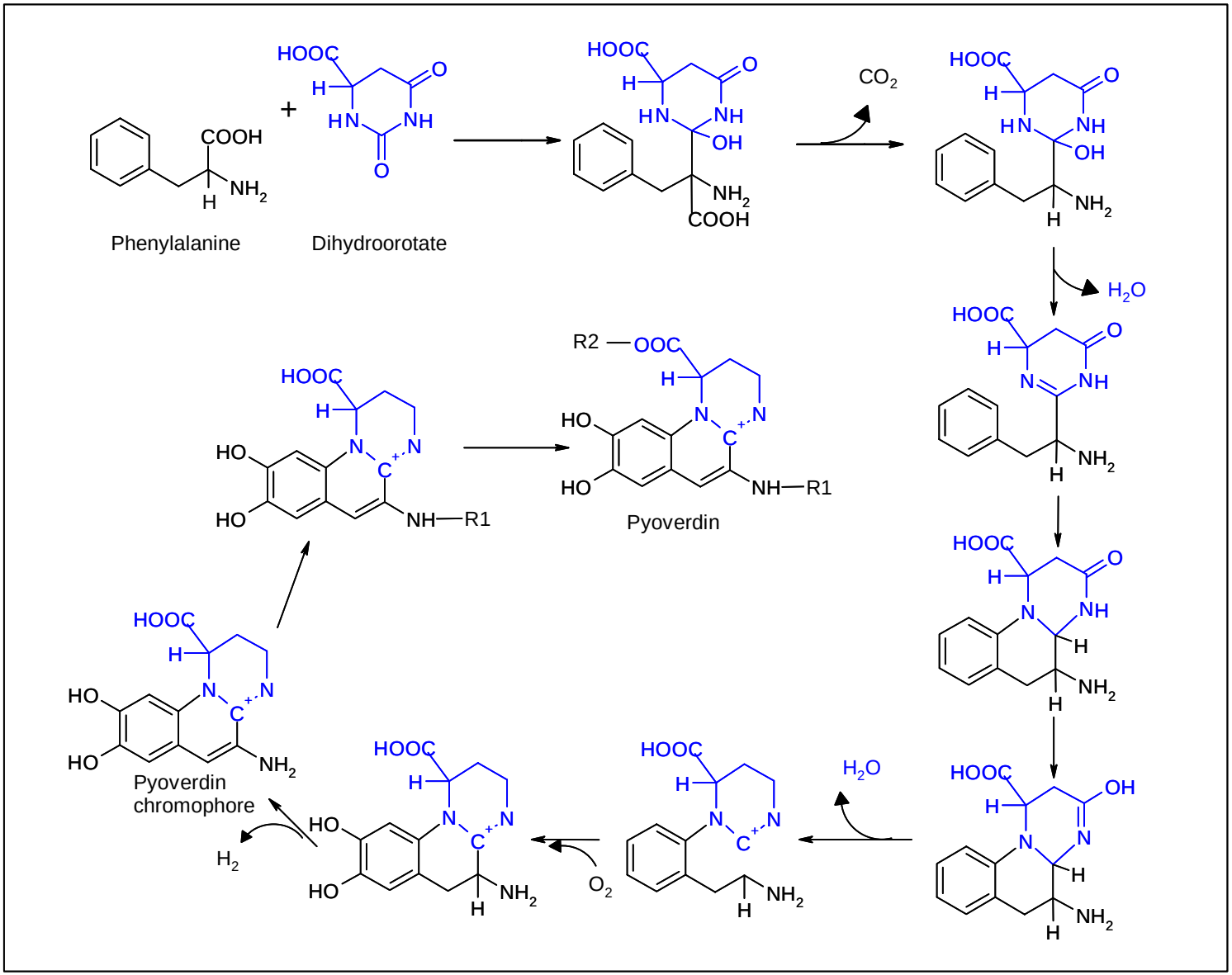

Fig. 67. Proposed pathway for the synthesis of the pyroverdin chromophore using phenylalanine and dihydroorotate as substrates. Adapted from Maksimaova et al., 1994.

produced 90 % less pyoverdin as compared to wild-type after 12 h of growth. Also, the addition of uracil to the medium did not restore pyoverdin production, as the level was still 82 % less than that produced by the wild-type (Fig. 49a). It is interesting to note that the *pyrC2* strain also exhibited decreased pyoverdin production, as the measured levels were 60 % less (without uracil) and 40 % less (with uracil) than those of wild-type (Fig. 49a).

Thus it is possible, that while the *pyrC* encoded DHOase I provides the DHO necessary during exponential growth, the *pyrC2* encoded DHOase II, may function in the stationary phase or when *P. aeruginosa* is growing in an environment that induces the stress response. As previously mentioned, the predicted promoter region that governs the expression of *pyrC2* contains several elements that are consistent with what has been defined as an activated RpoS promoter (Becker & Hengee-Aronis, 2001). As seen in Fig. 65, these elements include a poorly defined –35 region, a T residue in position –14, a hexameric sequence in the –10 region that is in keeping with other activated RpoS promoters, and an AT rich region between the –10 and the +1 sites.

If the transcription of *pyrC2* were governed by RpoS, it might explain why *pyrC2* expression is detected, on average, in only one out of every 160,000 *pyrC* mutants. For the *pyrC2* encoded DHOase II to function in the *pyrC* cell, it would have to be expressed early in the cells growth phase. It has been shown in *E. coli* that RpoS is highly unstable in exponential phase. One of the possible reasons for this instability is that RpoS is subject to degradation by the negative response regulator RssB and the serine protease ClpXP (Matin, 1996). Thus, one way of maintaining stable RpoS early in the growth phase, is by mutating the genes encoding RssB and ClpXP (Wösten, 1998).

An alignment of the RpoS polypeptides from *E. coli* and *P. aeruginosa* reveals that they are nearly identical in regions 2.3, 2.4 and 2.5. Region 2.4 has been reported as being responsible for interaction with the core –10 region of the promoter (Gross *et al.*, 1996) and Lys 173, in this region, has been found to be absolutely required for binding of the proteolysis recognition factor RssB (Becker *et al.*, 1999). In addition, there are homologs present in the *P. aeruginosa* genome for RssB and ClpXP, designated PA4776 and PA1801 respectively (www.pseudomonas.com). Thus, it is possible that similar mechanisms may influence the stability of RpoS in *P. aeruginosa*. If this were the case, only cells that had incurred mutations in the proteins that destabilize RpoS would have the capacity to express *pyrC2* early in the growth phase, and these would be expected to be only a fraction of the population. This mode of diversity is consistent with the persistent theme of variation seen in the life style of *P. aeruginosa*. In fact, it is likely that "hot spots" for genetic mutation exist in the genes encoding proteins that destabilize RpoS in the exponential phase. General mechanisms of modification, such as this, would only serve to ensure the long-term survival of the species in a multitude of growth conditions (Dorman, 1995).

One of the major goals at the outset of this research project, was to reappraise the control mechanisms of the enzymes involved in pyrimidine biosynthesis in *P. aeruginosa*. As previously mentioned, Isaac and Holloway (1968) initially undertook this task, by isolating several mutants in the pyrimidine pathway. They cultivated these pyrimidine mutants in the presence and absence of uracil, and then studied the effect of pyrimidine limitation on the other biosynthetic enzymes. Specifically, they were trying to determine if the mechanisms of repression and derepression, observed for the pyrimidine

enzymes in *E. coli* and *Salmonella*, were also present in *P. aeruginosa*. But the great differences in pyrimidine enzyme specific activity observed for the enterics, were not found to exist in *P. aeruginosa*. Rather, it seemed that the enzymes in the pathway were constitutively expressed, at a moderate level, regardless of the concentration of exogenous or endogenous pyrimidines. They also tested the ability of pyrimidine mutants to utilize intermediates of the pathway to satisfy their pyrimidine requirement, and found that only uracil could serve as the pyrimidine source for the mutant strains. The research presented here agrees with their initial findings in many respects. For example, repression of the pyrimidine enzymes is observed only slightly, as a 1.3-fold decrease is seen in the specific activity of pyrimidine enzymes assayed from cells grown in the presence of uracil. However, some noteworthy differences between the results of these two studies were found.

Isaac and Holloway (1968) reported that only uracil could serve as a pyrimidine source for the mutants they had isolated. Here it is shown that the pathway intermediate orotate was also able to satisfy the pyrimidine requirement of the DHOase and DHODehase mutants tested, but only when the cells were cultivated in glucose as a carbon source. This was not the case when mutant strains were cultivated with succinate as a carbon source. *P. aeruginosa* preferentially uses tricarboxylic acid (TCA) cycle intermediates, such as succinate, as carbon sources over other carbohydrates such as glucose or mannitol (O'Toole *et al.,* 2000). The dicarboxylate transport protein (DctA) is responsible for the transport of the TCA intermediates into the cell. In *Sinorhizobium meliloti* and in *Salmonella typhimurium*, it has been shown that orotate is also transported by DctA (Yurgel *et al.,* 2000; Baker *et al.,* 1996). Inhibition studies of the uptake of

orotate by DctA in *S. meliloti*, showed that 0.1 mM succinate inhibited the transport of orotate by 80 %. It will be important to note later, that orotate uptake was also inhibited 46 %, 76 %, 79 % and 94 % by carbamoyl aspartate at concentrations of 0.1 mM, 0.5 mM, 1.0 mM and 10 mM, respectively (Yurgel *et al.*, 2000).

The *P. aeruginosa* genome was searched using the *S. meliloti* DctA sequence and two homologs of this protein were found. The two DctA sequences whose genes are in the same region of the genome (PA0119 and PA1183) are 49 % identical and 83 % homolgous overall with each other. A comparison of the *S. meliloti* DctA with the two *P. aeruginosa* DctA homologs, shows 38 % of the residues to be identical for the three sequences. The DctA sequence designated PA1189 shows the greatest similarity to the *S. meliloti* sequence, as 60 % of the residues are identical between them, while the sequence designated PA0119 has 46 % identity with the *S. meliloti* sequence.

Given the strong homology between the *S. meliloti* and *P. aeruginosa* DctA sequences, it does not seem too great a stretch to suggest that the *P. aeruginosa* DctA transports orotate into the cell and that this transport is likely inhibited by both succinate and carbamoyl aspartate, as observed in *S. meliloti*. What is curious however, is that Isaac and Holloway (1968) reported that orotate could not satisfy the pyrimidine requirement of *pyrB* or *pyrD* mutants of *P. aeruginosa*, and they state that glucose was used as the carbon source. In keeping with the data reported here, orotate has also been found to satisfy the pyrimidine requirement of ATCase mutants in *P. fluorescens* (Chu & West, 1990). It remains unclear as to why Isaac and Holloway (1968) did not report the same result, especially since the *pyrD* mutant (PAO114) studied here was isolated in their initial study.

Another aspect where the study by Isaac and Holloway and the data reported here differ, is the capacity of the pyrimidine enzymes in *P. aeruginosa* to be derepressed, or elevated, in the absence of pyrimidines. The concept behind derepression is that, if enzymes in a biosynthetic pathway are repressed by the endproduct of the pathway, then in the absence of the endproduct, the enzyme activities should be augmented or derepressed. Isaac and Holloway (1968) reported that when they starved their pyrimidine mutants for uracil and then assayed the enzyme activities, no difference in activity was detected. They concluded that the *P. aeruginosa* pyrimidine biosynthetic enzymes were not subject to derepression. Here it is shown however, that derepression or repression of pyrimidine enzymes does exist in *P. aeruginosa*, but rather than being mediated by the endproduct of the pathway, the intermediates of the pathway dictate the flow of substrates.

Three pyrimidine mutants were utilized in this study and they included a DHOase mutant (PAODB92), a DHODehase mutant (PAO114) and an OMP decarboxylase mutant (PAO161). As previously mentioned, this is the first report of a true block in the DHOase step in *P. aeruginosa*, the difficulty in isolating such a mutant in the past was a consequence of the fact that the organism contains two functional genes encoding this enzyme activity. The mutant strains were cultivated in Psmm, in the presence or absence of uracil, using glucose as a carbon source as described in Methods. The specific activities of the various pyrimidine enzymes were measured and reported in Tables 6 and 8 of the Results. The diagram in Fig. 39 summarizes the results of this study.

As seen in Fig. 39, a block in DHOase results in a 1.8 to 2.4-fold increase in the specific activity of the enzymes ATCase, DHODehase and OMP decarboxylase. When

starved for uracil, this mutant accumulates the intermediate carbamoyl aspartate (CAA), which has been shown in *S. typhimurium* DHOase mutants to be toxic (Turnbough & Bochner, 1985). The mechanism by which this intermediate stimulates the enzyme activities mentioned is unclear. It seems logical though, in a "metabolic sense," that if an intermediate early in the pathway is building up, especially a potentially toxic intermediate, one course of action might be to increase the activity of enzymes further down the pathway, in order to "pull" the pathway forward. The observation that CAA stimulated ATCase activity, the very enzyme that produces it, seems contradictory, and it may actually be an artifact. Although the cell extracts used in these assays were dialyzed, it is still possible that the elevated specific activity value reported is due to the detection of residual CAA in combination with that being produced in the assay by the ATCase enzyme. Regardless, the same increases in specific activity were observed in a *P. fluorescens* DHOase mutant (Chu & West, 1990), thus it seems that this mechanism of activation by CAA is not unique to *P. aeruginosa*.

Assays of the pyrimidine enzymes in the DHOdehase mutant showed a significant change in activity for ATCase, as its specific activity was decreased eight-fold, whether the cells were starved for uracil or not (Table 8). A DHOdehase mutant would be expected to build up the pathway intermediate dihydroorotate (DHO), and due to the reversibility of the DHOase enzyme, some of this DHO would be expected to be converted to CAA, depending on the pH of the cytoplasm. It may be that, in order to prevent CAA and DHO build up in the cell, DHO inhibits the first step unique to the pyrimidine biosynthetic pathway, namely ATCase. One theory as to how this inhibition might be mediated is that DHO may be able to bind to the PyrC' subunits of the ATCase

holoenzyme, and then decrease enzyme activity by a change in conformation. Further studies will need to be conducted however, such as *P. aeruginosa* ATCase enzyme assays in the presence of various concentrations of DHO, in order to test this hypothesis.

Perhaps the most curious result in the derepression studies was obtained when the OMP decarboxylase mutant was assayed. Here it was discovered that a block in the conversion of OMP to UMP caused a 10-fold increase in the activity of the DHOdehase enzyme (Table 8). At first glance, this mechanism seems counter productive, because the OMP intermediate would essentially be activating the synthesis of its precursor, orotic acid (OA). A closer look at the activity of the OPRTase enzyme however, sheds some light on how this form of activation could actually be beneficial to the cell.

OPRTase is a bireactant biproduct enzyme following a random sequential mechanism of catalysis that has been thoroughly studied in *S. typhimurium* (Wang *et al.*, 1999). The two reactants, OA and phosphoribosyl pyrophosphate (PRPP), are combined to form OMP and PP_i. The reaction is reversible but the forward reaction is favored, as the unliganded enzyme binds the biosynthetic substrates PRPP and OA preferentially. Binding measurements for each of the substrates were determined and provide clues to a potentially larger role for this enzyme in the control of the concentration of various pyrimidine intermediates in the cell.

The dissociation constant (K_D) for each of the ligands was determined and reported to be 33 μM for PRPP, 3.1 μM for OMP, 283 μM for orotate and 960 μM for PP_i. Interestingly, Wang and co-workers (1999) reported that the binding of PP_i was significantly altered in the presence of 1.5 mM orotate such that the K_D in these conditions was decreased almost 4-fold to 230 μM. When the concentration of the ligand

is less than the K_D then very little binding occurs. But when the ligand concentration equals the K_D then half of the protein has bound the ligand and in order for 90 % of the protein to be bound, the concentration of the ligand must be nine-times greater than the K_D. The K_M of each substrate was also determined and reported to be 18 μM for PRPP, 3.4 μM for OMP, 19 μM for OA and 31 μM for PPi (Wang *et al.*, 1999). An alignment of the OPRTase sequences from *P. aeruginosa* and *S. typhimurium* shows that they are 69 % identical and 85 % similar. Thus, it is possible that many of the kinetic parameters determined for *S. typhimurium*, may also apply to *P. aeruginosa*. If this is the case, then an intriguing hypothesis can be developed regarding the stimulatory effect of OMP on DHOdehase activity.

Nucleotide monophosphates, such as OMP, are noted as being toxic in the bacterial cytoplasm. As such, the cell has evolved mechansims for quickly depleting the pools of these monophosphates, by either converting them to diphosphates by the action of kinases or to the base level *via* 5'-nucleotidase activity (Hammer-Jespersen, 1983). In the case of OMP, the OMP decarboxylase has a very high affinity for its substrate and quickly and irreversibly converts it to UMP which is then rapidly phosphorylated to UDP and UTP. The OMP decarboxylase step is noted as the step in the pathway that "pulls" all the intermediates to the synthesis of UMP.

In the case of the OMP decarboxylase mutant however, the driving force of the pathway has been blocked and this results in the accumulation of various pyrimidine intermediates. As previously mentioned, two of these intermediates are noted for being toxic, CAA and OMP (Turnbough & Bochner, 1985; Hammer-Jespersen, 1983). As both of these compounds are charged, they can not readily cross the cell membrane without

the aid of a permease, thus, in order to deal with this type of scenario in nature, the cell must have devised a way of detoxifying these compounds. It should be noted that inhibitors of OMP decarboxylase do exist, such as 6-azauracil, and are likely employed in the constant warfare that occurs in the soil between bacteria, plants and fungi, thus a mode of selection for this type of by-pass is conceivable.

A build up of OMP would signal a surplus of all pyrimidine intermediates and that the flow through the pathway had ceased. In order to deplete the toxic compounds OMP and CAA, the activity of the middle step of the pathway, the DHOdehase, is stimulated. This accomplishes at least two things. First, it depletes any CAA that may be accumulating by drawing it to DHO and then to OA. Second, it aids in increasing the OA concentration in the cell, which enhances PPi binding to OPRTase in order to help drive the backward reaction. This would aid in depleting the toxic OMP pool by converting it to OA and PRPP. OA is not toxic and is readily excreted out into the medium, as it has been shown previously that *pyrE* and *pyrF* mutants of *E. coli* excrete large amounts of OA into the medium (Womack & O'Donovan, 1978).

Thus it would appear, that the accumulation of certain intermediates in the pyrimidine pathway of *P. aeruginosa* affects the activity of key enzymes, that in turn modify the flow of substrates when the end product UMP is not being formed. The mechanism by which substrate concentrations affect enzyme activity, whether by interaction with regulatory proteins that alter transcription or translation or by activation or inhibition through direct binding to the enzyme of interest, remains unclear. One way to address this question would be to construct promoter fusion vectors, both transcriptional and translational, containing the promoter regions of the pyrimidine genes

of interest and then introduce these vectors into *P. aeruginosa* wild-type and pyrimidine mutant strains. The transformed cells could then be cultivated in pyrimidine replete and deplete conditions and the β-galactosidase levels compared. The data obtained would serve as a springboard for further studies into the regulatory mechanisms employed by *P. aeruginosa* to control pyrimidine biosynthesis.

While the *P. aeruginosa* DHOase mutant strain described in this research afforded a new look into the mechanisms of pyrimidine regulation in this organism, it also unearthed an incredible discovery. Here it is shown that a block in the third step of the pyrimidine biosynthetic pathway results in a marked decrease in the ability of *P. aeruginosa* to produce virulence factors. To our knowledge this it the first report of a link between pyrimidine biosynthetic intermediates and virulence in bacterial systems.

As mentioned previously, the *pyrC* DKO strain produced considerably less pyoverdin than did wild-type PAO1, and the addition of uracil to the medium did not restore pyoverdin production to wild-type levels (Fig. 49). Furthermore, a marked decrease in the production of the phenazine pigment pyocyanin was also observed, and again, supplementary uracil did not amend the pigment production defect (Fig. 50). The decrease in pyoverdin production was somewhat anticipated because of the report that a *P. putida* DHOase mutant was defective in pyoverdin production (Maksimova *et al.*, 1994). This research group also proposed a pathway for the synthesis of the pyoverdin chromophore that implicates DHO as one of the starting substrates (Fig. 67). The negative effect of the block in DHOase on pyocyanin production was unanticipated however, and the cause for this defect not readily apparent, as the structure of pyocyanin does not bear resemblance to DHO (Fig. 4).

P. aeruginosa strains deficient in pyoverdin production, were also reported to be less virulent as a result of their decreased ability to obtain iron from serum (Ankenbauer *et al.*, 1985; Visca *et al.*, 1992). The *pyrC* DKO mutant was cultivated on blood agar (BA) in order to determine if it also demonstrated this growth defect. Indeed, as seen in Fig. 54a, the *pyrC* DKO showed very little growth on BA after 24 h incubation at 37ºC. After 48 h, a small amount of growth is observed but only a fraction of that seen for wild-type (Fig. 54c). The addition of uracil to the BA medium increased the growth and haemolysis observed for the *pyrC* DKO, but it still did not reach the level of wild-type (Fig 54b and 54d). Thus it would appear that blocking the conversion of CAA to DHO in *P. aeruginosa* results in a decreased ability of the organism to produce haemolysin and to lyse blood cells.

A search of the literature brought to light several reports of *P. aeruginosa* mutants that were impaired in pyocyanin production and showed decreased haemolysis when grown on blood agar (Latifi *et al.*, 1995; Brint & Ohman, 1995). The mutations that resulted in this phenotype were in the quorum sensing regulators LasRI or RhlRI. As previously mentioned, these two-component systems function by producing homoserine lactone signals (HSLs) that increase in concentration as the bacterial population increases in density. When the concentration is great enough, the regulatory proteins bind to their appropriate signal molecule and then turn on the transcription of many genes that are important for affecting a virulence response. Thus, mutations in the quorum sensing system impair the production virulence factors, including the exo-enzymes, elastase and casein protease. The level of these exo-enzymes from the *pyrC* DKO mutant was tested in order to determine the extent to which the DKO phenotype mirrored the quorum

sensing mutant phenotype in *P. aeruginosa*.

Indeed this was found to be the case, as analysis showed that the *pyrC* DKO was impaired in its ability to produce elastase and casein protease (Figs 52 and 53). Further confirmation that the virulence response of the *pyrC* DKO was altered, could be seen in the cross-streak inhibition assays performed with wild-type *P. aeruginosa* and the *pyrC* mutant strains (Fig. 55). The *pyrC* DKO strain was found to be completely ineffective at inhibiting the growth of any of the bacterial strains tested. Thus it is apparent, that the *P. aeruginosa pyrC* DKO mutant is substantially impaired in its ability to produce pyocyanin, pyoverdin, haemolysin, elastase and casein protease. All of these defects are consistent with those observed for quorum sensing mutants (Latifi *et al.*, 1995; Brint & Ohman, 1995; Pearson *et al.*, 1997; Stintzi *et al.*, 1998). Could this mean that the *pyrC* DKO is also a quorum-sensing mutant? Quorum-sensing mutants are generally able to be restored to wild-type phenotype by supplying exogenous HSLs in cross feeding experiments (Latifi *et al.*, 1995; Brint & Ohman, 1995). However, in the case of the *pyrC* DKO, no cross feeding is observed, as *P. aeruginosa* wild-type growing near the *pyrC* DKO strain does not enhance pigment production or augment the growth of this strain. Therefore, whereas the *pyrC* DKO strain mirrors the pleiotropic phenotype of quorum sensing mutants, cross feeding does not ameliorate the defect. Thus it is unlikely that a defect in the production or sensing of HSLs is the mechanism causing the observed phenotype.

P. aeruginosa strains that are deficient in virulence factor production are frequently deficient in motility as well (Hazzlet, 1999). As seen in Results, the ability of the *pyrC* DKO to swim, swarm or twitch was also found to be impaired (Figs 56-58). The

production of rhamnolipid, which aids in swarming motility, was also lacking, as the *pyrC* DKO strain did not produce this compound when grown on medium with low uracil (5 μg ml^{-1}) (Table 10). When uracil was added at a concentration of 40 μg ml^{-1}, rhamnolipid production of the DKO strain increased, but still did not reach that of wild-type. In addition, the ability to adhere, which is mediated by type IV pili, was also found to be lacking in the *pyrC* DKO stain (Fig. 59). It is difficult to imagine how a block in the conversion of CAA to DHO could cause such a pleiotropic phenotype and the results described above were somewhat unexpected. Somehow a block in the conversion of CAA is causing a much larger effect then anticipated. The question is, what is mediating this broad affect?

One way to address this question was to search for mutants with similar phenotypes and then, by comparison, look for a common element that could be mediating the observed defects. In the course of this search, it was discovered that a *P. aeruginosa ppk* mutant was defective in all forms of motility (Rashid & Kornberg, 2000). In addition, this mutant was also impaired in biofilm formation, quorum sensing and virulence (Rashid *et al.,* 2000). The parallels between the *P. aeruginosa ppk* and *pyrC* DKO mutants are astonishing. But biochemically speaking, what do they have in common? One possibility is that in both mutant strains there is an increase in negative charge in the cytoplasm from the accumulation of their respective enzyme blocks, namely inorgainc phosphate and carbamoyl aspartate (Fig. 68). I believe that this increase in negativity could adversely affect the energetics of these mutant strains such that their ability to export virulence factors and to move is significantly impaired.

Another *P. aeruginosa* mutant that has been found to share a similar phenotype

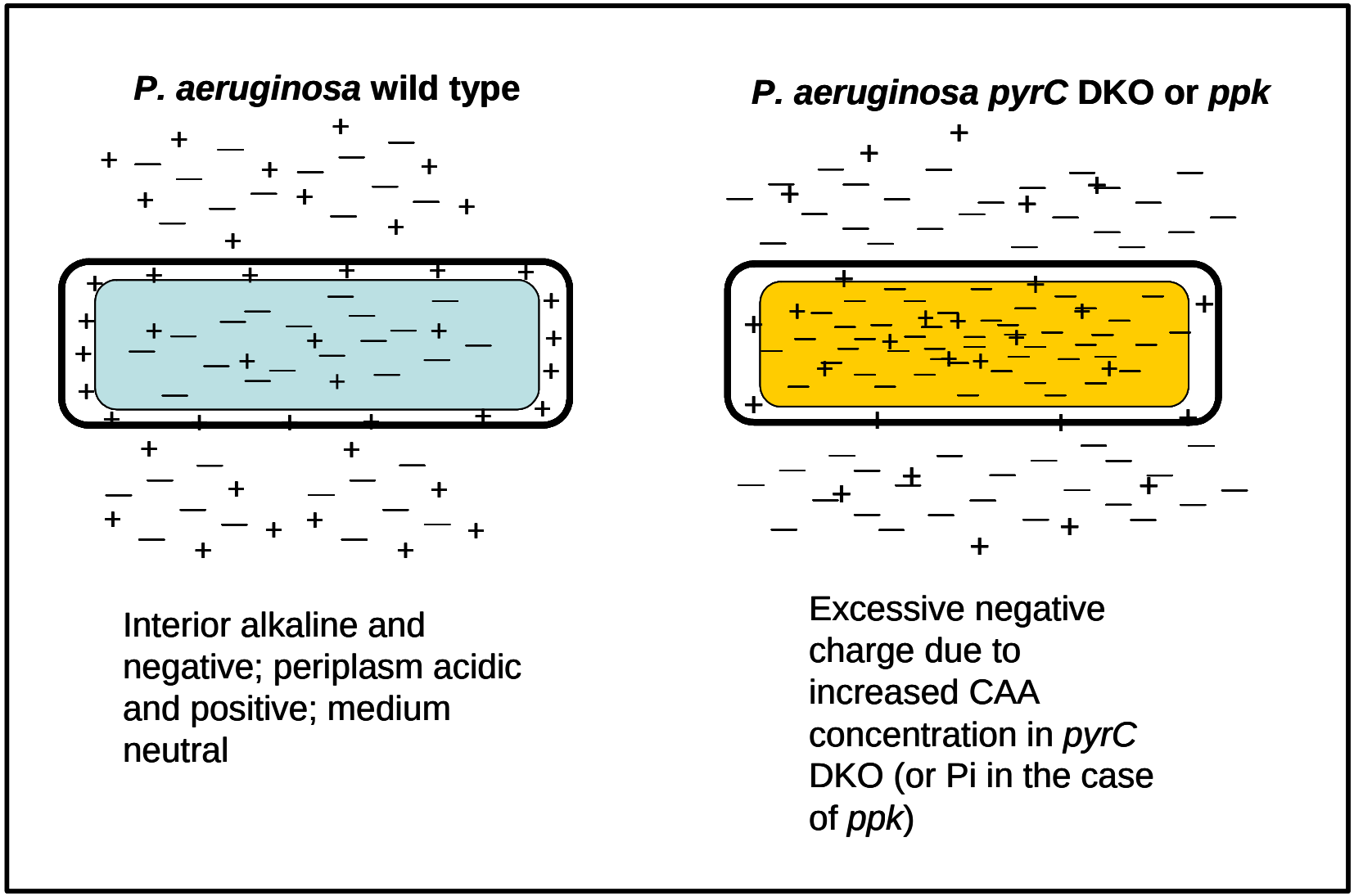

Fig. 68. Depiction of the possible mechanism of action and effect of increased negative charge within the P. aeruginosa cell.

with the *pyrC* DKO is the *tatC* mutant constructed by Ochsner and co-workers (Ochsner *et al.*, 2002). These researchers reported that a mutation in the twin arginine translocase (TAT) apparatus resulted in diminished production of virulence determinants such as pyoverdin, exotoxin A, and casein protease. The mutant was also impaired in swimming, swarming and twitching motility and was unable to adhere to polystyrene surfaces. In addition, they found that the *tatC* mutant was unable to grow anaerobically with nitrate as the final electron acceptor because the nitrate reductase protein, which is normally transported to the periplasm by the TAT system, is not transported in this mutant. The *pyrC* DKO strain was also unable grow anaerobically in nitrate when orotate served as the pyrimidine source. On the other hand when uracil was the pyrimidine source, the *pyrC* DKO grew at about the same rate as wild-type.

An additional common feature of the *pyrC* DKO strain and the *tatC* mutant was the observed inability to use choline as a carbon and energy source. In the case of the *pyrC* DKO, when orotate served as the pyrimidine source, choline could not be used as a carbon source, whereas when uracil was the pyrimidine source, choline could be used as a carbon source. It is noteworthy that the TAT system is driven by the proton motive force and that the translocated proteins are secreted by an antiport mechanism (protein out, hydrogen ion in) (Chaddock *et al.*, 1995). One could envision that in a DHOase mutant, an excessive accumulation of negative charge resulting from an increase in CAA within the cytoplasm, could result in a disruption of the proton motive force (pmf) such that systems that use the energy of the pmf are impaired in their function (Fig. 68).

With all of the numerous defects exhibited by the *pyrC* DKO strain, it seemed appropriate to test its susceptibility to antibiotics. The resistance of *P. aeruginosa* to

antibiotic therapy is well known and one of the mechanisms that allows for this resistance is the Mex transport system. As with the TAT system, it has been shown that the Mex system is driven by the proton motive force (Paulsen, *et al.,* 1996). Here we show that the zones of growth inhibition from the antibiotic susceptibility test (Table 11) demonstrated by the *pyrC* DKO were always greater than those seen for wild-type. The antibiotic sulfamethoxizole trimethoprim (SXT) gave the most striking result, as the *pyrC* DKO was shown to be susceptible to this combination of antibiotics, while wild-type was resistant. The MexAB-OprM efflux system is known to be primarily responsible for the export of SXT (Köhler *et al.,* 1996). Thus, if the *pyrC* DKO strain is susceptible to this combination of antibiotics, it is likely because of a defect in the MexAB-OprM efflux system. This is yet another example of a pmf driven system (Paulsen *et al.,* 1996) whose activity is diminished in the *pyrC* DKO mutant strain.

This body of work has led to the idea that the accumulation of the negatively charged CAA wreaked havok on the energetics of the *P. aeruginosa* DHOase mutant strain (Fig. 68). It was therefore important to assess the internal and external concentrations of the offending molecule. Assays of the cell extracts and supernatants obtained from the *pyrC* DKO strain, grown in various conditions, showed that indeed the CAA was significantly higher (Figs 60 and 62). That the concentration of CAA in the supernatant would also be increased was unanticipated, however as seen in Fig 62, this was the case. The mechanism by which CAA exits the cell however, is currently unknown.

As mentioned in Results, the accumulation of CAA in a *pyrC* mutant of *Salmonella typhimurium* has been reported as being toxic to the cell (Turnbough &

Bochner, 1985). These researchers found that conditions resulting in pyrimidine limitation,

such as growth of the *pyrC* mutant in orotate, which allows only a trickle of substrate through the pyrimidine pathway to UTP, resulted in the derepression of ATCase and thus a substantial increase in CAA in the cell. Conversely, growth in uracil resulted in a swelling of the UTP pool and, through feed back inhibition, caused a decrease in the ATCase activity and consequently deminished the level of CAA in the cell. One of the experiments used to further explore the growth defect caused by CAA accumulation involved growing the *pyrC* mutant strain in minimal medium with varying concentrations of orotate (0.5 to 5.0 mM). After 7 h of growth, uracil was added to the samples with low orotate. The addition of uracil resulted in a decrease in CAA and consequently the cells grew better.

This experiment, with slight modification, was used to test the effect of CAA on the growth of the *pyrC* DKO mutant. As seen in Fig. 61, the *pyrC* DKO mutant actually demonstrated the strongest growth defect when cultivated in tryptone broth (TB) with 1.5 mM orotate, while growth in 0.5 mM orotate was better than that without supplement. Measurement of CAA from cell extracts and supernatants, showed that growth in orotate resulted in an increased CAA concentration and that the addition of uracil caused a concomitant decrease in the CAA concentration (Fig 62). When the CAA measurements are normalized, the dramatic decrease in CAA concentration, after the addition of uracil, can more readily be seen (Fig. 63). One possible reason for the poor growth observed for the *pyrC* DKO in 1.5 mM orotate, could be due to the effective CAA concentration blocking the transport of orotate by DctA. As previously mentioned, CAA at

concentrations of 0.1 – 0.5 mM, has been found to inhibit DctA uptake of orotate by 46 – 76 % in *S. meliloti* (Yurgel *et al.,* 2000).

Thus, while increasing orotate concentration augments the growth of the *S. typhimurium pyrC* mutant, the opposite is the case for the *P. aeruginosa pyrC* DKO mutant. Since both organisms use DctA to transport orotate into the cell, it is not readily obvious why this difference is observed, unless the mechanisms for utilizing orotate are more adept in *S. typhimurium* than in *P. aeruginosa*, and increasing orotate actually swells the UTP pool in this organism. As Turnbough and Bochner (1985) did not however, report measurements of the concentration of CAA in the cell extracts or supernatants, it is difficult to make further comparisons between the two mutant strains.

In summary, it is reported here that *P. aeruginosa* contains two *pyrC* genes, both of which encode active DHOase enzymes. The *pyrC* gene encoding DHOase I is constitutively expressed while the larger *pyrC2* encoding DHOase II is under a form of transcriptional control. The parameters for the catalytic mechanism of the DHOase II are unlike that of any DHOase studied to date, and for good reason. The *pyrC2* gene and DHOase II protein have been "hidden" from scientific view. Only the completion of the *P. aeruginosa* genome sequence and the inactivation of the constitutive *pyrC* gene, allowed the study of the *pyrC2* gene and the protein it encodes.

When both *pyrC* genes are inactivated, the concomitant block in the conversion of CAA to DHO results in a pleiotropic phenotype that is deficient in virulence factor production, motility and adherence. Additionally, the *pyrC* DKO is unable to grow anaerobically using nitrate as a final electron acceptor, when orotate is supplied as the pyrimidine source. The *P. aeruginosa* DHOase mutant is also susceptible to the antibiotic

SXT, while the wild-type is resistant. The exact mechanism mediating these observed defects is unknown. However, comparison of other *P. aeruginosa* mutants with similar pleiotropic defects reveals a possible explanation (Table 13).

Virulence factor	*P. aeruginosa* *pyrC* DKO	*P. aeruginosa* *ppk* mutant	*P. aeruginosa* *tatC* mutant
Pyoverdin	-		-
Pyocyanin	-		
Elastase	-	-	
Casein protease	-	-	-
Haemolysin	-	-	-
Swimming	-	-	-
Swarming	-	-	-
Twitching	-	-	-
Adherence	-	-	-
Choline c-source respiration using KNO_3	-		-

Table 13. Common phenotypic characteristics between the DHOase, *ppk* and *tatC* mutants of *P. aeruginosa*. The (-) symbol indicates that the organism demonstrates a defect in this attribute. No symbol indicates that the characteristic was not tested.

As the majority of the affected systems have some connection with the proton motive force, it is tempting to suggest that the accumulation of negative charge, either from CAA in a DHOase mutant, or inorganic phosphate, in the case of the *ppk* mutant, disrupts the membrane energetics, resulting in the observed phenotype (Fig. 68). As for the *tatC* mutant, the observed defects here result from an actual mutation in the transport machinery, as opposed to the *ppk* and *pyrC* DKO mutants, where the "fuel" that runs the transport machinery (the proton motive force) is affected.

The link between the pyrimidine intermediate CAA and the virulence response was unanticipated, however it affords an exciting avenue for chemotherapy to potentially thwart *P. aeruginosa* infection. Ogawa and co-workers (1996) tested several DHOase inhibitors *in vitro* while studying the DHOase of *P. putida*. Some of the compounds that they found to inhibit the enzyme (when used at a concentration of 2 mM) and the percents inhibition were: *p*-chloromercuribenzoate (76 %), phenlyhdrazine (86 %), semicarbazide (43 %) and diisopropyl fluorophospahte (66 %). If an inhibitor, that is taken up by the cell, and capable of inhibiting the function of both DHOases can be found, then subjecting *P. aeruginosa* to both this DHOaes inhibitor and traditional antibiotic therapy could be more effective at killing the organism, since the Mex systems used to export traditional antibiotics would potentially be ineffective.

The Mex system is likely a good target for attacking *P. aeruginosa*, as it appears to rely on it heavily. Analysis of the genome sequence has revealed that *P. aeruginosa* contains a greater number of predicted pmf driven multidurg efflux systems (10) than *E. coli* (4), *Bacillus subtilis* (1) or *Mycobacterium tuberculosis* (0) (Stover *et al.*, 2000).

And it is likely that the Mex systems export more than antibiotics, as it has recently been shown that the HSL produced by LasI ($3OC_{12}$-HSL) is transported in part by MexAB-OprM (Pearson *et al.*, 1999). This is also the case for the *Pseudomonas* quinolone signal (PQS) molecule which has been shown to be a substrate for the MexEF-OprN system (Köhler et al, 2001). The Mex transport systems are known for exporting toxic substances; continued research will undoubtedly reveal additional natural substrates, such as $3OC_{12}$-HSL and PQS, for these transport systems. Consequently, any mechanism that adversely affects the activity of these transport systems, will have far reaching affects on the survival of this organism in the host or in the environment.

While considering the multi layered control mechanisms employed by *P. aeruginosa* to regulate its lifestyle, there is a feeling of nostalgia for the days when not so much was known…things seemed simpler. Now, in the information age, surfing the internet and trying to keep up with the current state of knowledge is actually like attempting to traverse an intricate maze or spider web; you think you've found a good path, but at the next turn you are blocked or tangled up. Perhaps the sentiment is best conveyed as stated by F.M. Harold and D. L. Heefner, prominent scientists in the field of bacterial membrane energetics. Looking at the scientific horizon in 1981, and predicting the boon of information to come, they lamented over the increasing complexity of energetic systems with the following:

"*One feels some sense of loss for the elegant simplicities of ion transport as we saw it a decade ago, but we might have anticipated the outcome: by their very nature, the forces that shape evolution will create architecture that is baroque, if not downright rococo*."

The twists, turns and intricacies of the regulatory schemes employed by *P. aeruginosa*, in the control of its virulence and stress responses, are a testament to how very right they were.

REFERENCES

1. **Albus, A.M., Pesci, E.C., Runyen-Janecky, L.J., West, S.E., and Iglewski, B.H.**, 1997. Vfr controls quorum sensing in *Pseudomonas aeruginosa*. **179**, 3928-35.

2. **Anderson, P.M.**, 1983. CTP synthetase from *Escherichia coli*: an improved purification procedure and characterization of hysteretic and enzyme concentration effects on kinetic properties. **22**, 3285-92.

3. **Anderson, P.M. and Meister, A.**, 1965. Evidence for an activated form of carbon dioxide in the reaction catalyzed by *Escherichia coli* carbamyl phosphate synthetase. **4**, 2803-9.

4. **Ankenbauer, R., Hanne, L.F., and Cox, C.D.**, 1986. Mapping of mutations in *Pseudomonas aeruginosa* defective in pyoverdin production. **167** , 7-11.

5. **Baker, K.E., Ditullio, K.P., Neuhard, J., and Kelln, R.A.**, 1996. Utilization of orotate as a pyrimidine source by Salmonella typhimurium and *Escherichia coli* requires the dicarboxylate transport protein encoded by dctA. **178**, 7099-105.

6. **Beatson, S.A., Whitchurch, C.B., Sargent, J.L., Levesque, R.C., and Mattick, J.S.**, 2002. Differential regulation of twitching motility and elastase production by Vfr in *Pseudomonas aeruginosa*. **184**, 3605-13.

7. **Beck, D., Kedzie, K.M., and Wild, J.R.**, 1989. Comparison of the aspartate transcarbamoylases from *Serratia marcescens* and *Escherichia coli*. **264**, 16629-37.

8. **Becker, J. and Brendel, M.**, 1996. Molecular cloning and characterization of the *pyrB* gene of *Lactobacillus leichmannii* encoding aspartate transcarbamylase. **78**, 3-13.

9. **Bergh, S.T. and Evans, D.R.**, 1993. Subunit structure of a class A aspartate transcarbamoylase from *Pseudomonas fluorescens*. **90**, 9818-22.

10. **Bethell, M.R. and Jones, M.E.**, 1969. Molecular size and feedback-regulation characteristics of bacterial asartate transcarbamulases. **134**, 352-65.

11. **Blumer, C., Heeb, S., Pessi, G., and Haas, D.**, 1999. Global GacA-steered control of cyanide and exoprotease production in *Pseudomonas fluorescens* involves specific ribosome binding sites. **96**, 14073-8.

12. **Bonting, C.F., Kortstee, G.J., and Zehnder, A.J.**, 1991. Properties of polyphosphate: AMP phosphotransferase of *Acinetobacter* strain 210A. **173**, 6484-8.

13. **Brabson, J.S. and Switzer, R.L.**, 1975. Purification and properties of *Bacillus subtilis* aspartate transcarbamylase. **250**, 8664-9.

14. **Brint, J.M. and Ohman, D.E.**, 1995. Synthesis of multiple exoproducts in *Pseudomonas aeruginosa* is under the control of RhlR-RhlI, another set of regulators in strain PAO1 with homology to the autoinducer-responsive LuxR-LuxI family. **177**, 7155-63.

15. **Briskot, G., Taraz, K., and Budzikiewicz, H.**, 1986. Pyoverdin-type siderophores from *Pseudomonas aeruginosa*. **41**, 497-506.

16. **Brown, D.C. and Collins, K.D.**, 1991. Dihydroorotase from *Escherichia coli*. Substitution of Co(II) for the active site Zn(II). **266**, 1597-604.

17. **Budzikiewicz, H.**, 1993. Secondary metabolites from fluorescent pseudomonads. **10**, 209-28.

18. **Byrd, J.J., Xu, H.S., and Colwell, R.R.**, 1991. Viable but nonculturable bacteria in drinking water. **57**, 875-8.

19. **Calfee, M.W., Coleman, J.P., and Pesci, E.C.**, 2001. Interference with *Pseudomonas* quinolone signal synthesis inhibits virulence factor expression by *Pseudomonas aeruginosa*. **98**, 11633-7.

20. **Castuma, C.E., Huang, R., Kornberg, A., and Reusch, R.N.**, 1995. Inorganic polyphosphates in the acquisition of competence in *Escherichia coli*. **270**, 12980-3.

21. **Christopherson, R.I. and Jones, M.E.**, 1980. The effects of pH and inhibitors upon the catalytic activity of the dihydroorotase of multienzymatic protein *pyr1-3* from mouse Ehrlich ascites carcinoma. **255**, 3358-70.

22. **Christopherson, R.I. and Jones, M.E.**, 1979. Interconversion of carbamayl-L-aspartate and L-dihydroorotate by dihydroorotase from mouse Ehrlich ascites carcinoma. **254**, 12506-12.

23. **Chu, C.P. and West, T.P.**, 1990. Pyrimidine biosynthetic pathway of *Pseudomonas fluorescens*. **136 (Pt 5)**, 875-80.

24. **Collier, D.N., Hager, P.W., and Phibbs, P.V.Jr.**, 1996. Catabolite repression control in the *Pseudomonads*, pp. 551-561. *In* Regulation of Carbon Metabolism in Bacteria. CRC Press, Washington, D.C.

25. **Comolli, J.C., Hauser, A.R., Waite, L., Whitchurch, C.B., Mattick, J.S., and Engel, J.N.**, 1999. *Pseudomonas aeruginosa* gene products PilT and PilU are required for cytotoxicity in vitro and virulence in a mouse model of acute pneumonia. **67**, 3625-30.

26. **Costerton, J.W., Lewandowski, Z., Caldwell, D.E., Korber, D.R., and Lappin-Scott, H.M.**, 1995. Microbial biofilms. **49**, 711-45.

27. **Cox, C.D.**, 1986. Role of pyocyanin in the acquisition of iron from transferrin. **52**, 263-70.

28. **Cox, C.D. and Adams, P.**, 1985. Siderophore activity of pyoverdin for *Pseudomonas aeruginosa*. **48**, 130-8.

29. **Cox, C.D. and Graham, R.**, 1979. Isolation of an iron-binding compound from *Pseudomonas aeruginosa*. **137**, 357-64.

30. **D'Argenio, D.A., Calfee, M.W., Rainey, P.B., and Pesci, E.C.**, 2002. Autolysis and Autoaggregation in *Pseudomonas aeruginosa* Colony Morphology Mutants. **184**, 6481-6489.

31. **Dagert, M. and Ehrlich, S.D.**, 1979. Prolonged incubation in calcium chloride improves the competence of *Escherichia coli* cells. **6**, 23-8.

32. **Daniel, R., Kokel, B., Caminade, E., Martel, A., and Le Goffic, F.**, 1996. Assay of *Escherichia coli* dihydroorotase with enantiomeric substrate: practical preparation of carbamyl L-aspartate and high-performance liquid chromatography analysis of catalysis product. **239**, 130-5.

33. **de Kievit, T., Seed, P.C., Nezezon, J., Passador, L., and Iglewski, B.H.**, 1999. RsaL, a novel repressor of virulence gene expression in *Pseudomonas aeruginosa*. **181**, 2175-84.

34. **de Kievit, T.R., Kakai, Y., Register, J.K., Pesci, E.C., and Iglewski, B.H.**, 2002. Role of the *Pseudomonas aeruginosa las* and *rhl* quorum-sensing systems in *rhlI* regulation. **212**, 101-6.

35. **Denis-Duphil, M.**, 1989. Pyrimidine biosynthesis in *Saccharomyces cerevisiae*: the *ura2* cluster gene, its multifunctional enzyme product, and other structural or regulatory genes involved in *de novo* UMP synthesis. **67**, 612-31.

36. **Denning, G.M., Railsback, M.A., Rasmussen, G.T., Cox, C.D., and Britigan, B.E.**, 1998. *Pseudomonas* pyocyanine alters calcium signaling in human airway epithelial cells. **274**, L893-900.

37. **Deretic, V., Konyecsni, W.M., Mohr, C.D., Martin, D.W., and Hibler, N.S.**, 1989. Common Denominators of Promoter Control in *Pseudomonas* and Other Bacteria. **7**, 1249-1254.

38. **Deziel, E., Comeau, Y., and Villemur, R.**, 2001. Initiation of biofilm formation by *Pseudomonas aeruginosa* 57RP correlates with emergence of hyperpiliated and highly adherent phenotypic variants deficient in swimming, swarming, and twitching motilities. **183**, 1195-204.

39. **Diener, B., Carrick, L. Jr, and Berk, R.S.**, 1973. *In vivo* studies with collagenase from *Pseudomonas aeruginosa*. **7**, 212-7.

40. **Doremus, H.D.**, 1986. Organization of the pathway of *de novo* pyrimidine nucleotide biosynthesis in pea (Pisum sativum L. cv Progress No. 9) leaves. **250**, 112-9.

41. **Ellis, K.J. and Morrison, J.F.**, 1982. Buffers of constant ionic strength for studying pH-dependent processes. **87**, 405-26.

42. **Enderle, P.J. and Farwell, M.A.**, 1998. Electroporation of freshly plated *Escherichia coli* and *Pseudomonas aeruginosa* cells. **25**, 954-6, 958.

43. **Essar, D.W., Eberly, L., Hadero, A., and Crawford, I.P.**, 1990. Identification and characterization of genes for a second anthranilate synthase in *Pseudomonas aeruginosa*: interchangeability of the two anthranilate synthases and evolutionary implications. **172**, 884-900.

44. **Farinha, M.A. and Kropinski, A.M.**, 1990. Construction of broad-host-range plasmid vectors for easy visible selection and analysis of promoters. **172**, 3496-9.

45. **Fields, C., Brichta, D., Shepherdson, M., Farinha, M., and O'Donovan, G.**, 1999. Phylogenetic Analysis and Classification of Dihydroorotases: A Complex History for a Complex Enzyme. **7**, 49-63.

46. **Gallagher, L.A., McKnight, S.L., Kuznetsova, M.S., Pesci, E.C., and Manoil, C.**, 2002. Functions Required for Extracellular Quinolone Signaling by *Pseudomonas aeruginosa*. **184**, 6472-80.

47. **Gambello, M.J. and Iglewski, B.H.**, 1991. Cloning and characterization of the *Pseudomonas aeruginosa lasR* gene, a transcriptional activator of elastase expression. **173**, 3000-9.

48. **Gerhart, J.C. and Holoubek, H.**, 1967. The purification of aspartate transcarbamylase of *Escherichia coli* and separation of its protein subunits. **242**, 2886-92.

49. **Ginther, C.L. and Ingraham, J.L.**, 1974. Nucleoside diphosphokinase of *Salmonella typhimurium*. **249**, 3406-11.

50. **Godson, G.N. and Vapnek, D.**, 1973. A simple method of preparing large amounts of phiX174 RF 1 supercoiled DNA. **299**, 516-20.

51. **Grogan, D.W. and Gunsalus, R.P.**, 1993. *Sulfolobus acidocaldarius* synthesizes UMP via a standard *de novo* pathway: results of biochemical-genetic study. **175**, 1500-7.

52. **Gupta, S.K., Berk, R.S., Masinick, S., and Hazlett, L.D.**, 1994. Pili and lipopolysaccharide of *Pseudomonas aeruginosa* bind to the glycolipid asialo GM1. **62**, 4572-9.

53. **Hahn, H.P.**, 1997. The type-4 pilus is the major virulence-associated adhesin of *Pseudomonas aeruginosa*--a review. **192**, 99-108.

54. **Hassett, D.J.**, 1996. Anaerobic production of alginate by *Pseudomonas aeruginosa*: alginate restricts diffusion of oxygen. **178**, 7322-5.

55. **Hassett, D.J., Charniga, L., Bean, K., Ohman, D.E., and Cohen, M.S.**, 1992. Response of *Pseudomonas aeruginosa* to pyocyanin: mechanisms of resistance, antioxidant defenses, and demonstration of a manganese- co-factored superoxide dismutase. **60**, 328-36.

56. **Hassett, D.J., Cuppoletti, J., Trapnell, B., Lymar, S.V., Rowe, J.J., Sun Yoon, S., Hilliard, G.M., Parvatiyar, K., Kamani, M.C., Wozniak, D.J., Hwang, S.H., McDermott, T.R., and Ochsner, U.A.**, 2002. Anaerobic metabolism and quorum sensing by *Pseudomonas aeruginosa* biofilms in chronically infected cystic fibrosis airways: rethinking antibiotic treatment strategies and drug targets. **54**, 1425-43.

57. **Hazlett, L.D., Masinick-McClellan, S.A., and Barrett, R.P.**, 1999. Complement defects in aged mice compromise phagocytosis of *Pseudomonas aeruginosa*. **19**, 26-32.

58. **Heinrichs, D.E. and Poole, K.**, 1993. Cloning and sequence analysis of a gene (*pchR*) encoding an AraC family activator of pyochelin and ferripyochelin receptor synthesis in *Pseudomonas aeruginosa*. **175**, 5882-9.

59. **Hemmens, B. and Carrey, E.A.**, 1994. Proteolytic cleavage of the multienzyme polypeptide CAD to release the mammalian aspartate transcarbamoylase. Biochemical comparison with the homologous *Escherichia coli* catalytic subunit. **225**, 845-53.

60. **Holm, L. and Sander, C.**, 1997. An evolutionary treasure: unification of a broad set of amidohydrolases related to urease. **28**, 72-82.

61. **Hsieh, P.C., Shenoy, B.C., Jentoft, J.E., and Phillips, N.F.**, 1993. Purification of polyphosphate and ATP glucose phosphotransferase from Mycobacterium tuberculosis H37Ra: evidence that poly(P) and ATP glucokinase activities are catalyzed by the same enzyme. **4**, 76-84.

62. **Isaac, J.H. and Holloway, B.W.**, 1968. Control of pyrimidine biosynthesis in *Pseudomonas aeruginosa*. **96**, 1732-41.

63. **Jensen, K.F., Larsen, J.N., Schack, L., and Sivertsen, A.**, 1984. Studies on the structure and expression of *Escherichia coli pyrC*, *pyrD*, and *pyrF* using the cloned genes. **140**, 343-52.

64. **Jones, K.L., Hegab, A.H., Hillman, B.C., Simpson, K.L., Jinkins, P.A., Grisham, M.B., Owens, M.W., Sato, E., and Robbins, R.A.**, 2000. Elevation of nitrotyrosine and nitrate concentrations in cystic fibrosis sputum. **30**, 79-85.

65. **Jones, M.E.**, 1980. The genes for and regulation of the enzyme activities of two multifunctional proteins required for the *de novo* pathway for UMP biosynthesis in mammals. **32**, 165-82.

66. **Jones, M.E.**, 1980. Pyrimidine nucleotide biosynthesis in animals: genes, enzymes, and regulation of UMP biosynthesis. **49**, 253-79.

67. **Kamath, S., Kapatral, V., and Chakrabarty, A.M.**, 1998. Cellular function of elastase in *Pseudomonas aeruginosa*: role in the cleavage of nucleoside diphosphate kinase and in alginate synthesis. **30**, 933-41.

68. **Kantrowitz, E.R. and Lipscomb, W.N.**, 1988. *Escherichia coli* aspartate transcarbamylase: the relation between structure and function. **241**, 669-74.

69. **Karibian, D. and Couchoud, P.**, 1974. Dihydro-orotate oxidase of *Escherichia coli* K12: purification, properties, and relation to the cytoplasmic membrane. **364**, 218-32.

70. **Ke, H.M., Honzatko, R.B., and Lipscomb, W.N.**, 1984. Structure of unligated aspartate carbamoyltransferase of *Escherichia coli* at 2.6-A resolution. **81**, 4037-40.

71. **Kelln, R.A., Kinahan, J.J., Foltermann, K.F., and O'Donovan, G.A.**, 1975. Pyrimidine biosynthetic enzymes of *Salmonella typhimurium*, repressed specifically by growth in the presence of cytidine. **124**, 764-74.

72. **Kelly, K.O. and Deutscher, M.P.**, 1992. The presence of only one of five exoribonucleases is sufficient to support the growth of *Escherichia coli*. **174**, 6682-4.

73. **Kenny, M.J., McPhail, D., and Shepherdson, M.**, 1996. A reappraisal of the diversity and class distribution of aspartate transcarbamoylases in gram-negative bacteria. **142 (Pt 7)**, 1873-9.

74. **Kessler, E., Safrin, M., Olson, J.C., and Ohman, D.E.**, 1993. Secreted LasA of *Pseudomonas aeruginosa* is a staphylolytic protease. **268**, 7503-8.

75. **Kim, H.Y., Schlictman, D., Shankar, S., Xie, Z., Chakrabarty, A.M., and Kornberg, A.**, 1998. Alginate, inorganic polyphosphate, GTP and ppGpp synthesis co-regulated in *Pseudomonas aeruginosa*: implications for stationary phase survival and synthesis of RNA/DNA precursors. **27**, 717-25.

76. **King, E.O., Ward, M.K., and Raney, D.E.**, 1954. Two Simple Media for the Demonstration of Pyocanin and Fluorescin. **44**, 301-307.

77. **Kohler, T., Curty, L.K., Barja, F., van Delden, C., and Pechere, J.C.**, 2000. Swarming of *Pseudomonas aeruginosa* is dependent on cell-to-cell signaling and requires flagella and pili. **182**, 5990-6.

78. **Kohler, T., Kok, M., Michea-Hamzehpour, M., Plesiat, P., Gotoh, N., Nishino, T., Curty, L.K., and Pechere, J.C.**, 1996. Multidrug efflux in intrinsic resistance to trimethoprim and sulfamethoxazole in *Pseudomonas aeruginosa*. **40**, 2288-90.

79. **Kohler, T., van Delden, C., Curty, L.K., Hamzehpour, M.M., and Pechere, J.C.**, 2001. Overexpression of the MexEF-OprN multidrug efflux system affects cell- to-cell signaling in *Pseudomonas aeruginosa*. **183**, 5213-22.

80. **Kurachi, M.**, 1958. Studies on the Biosynthesis of Pyocyanine. (II). **36**, 174-187.

81. **Lache, M., Hearn, W.R., Zyskind, J.W., Tipper, D.J., and Strominger, J.L.**, 1969. Specificity of a bacteriolytic enzyme from *Pseudomonas aeruginosa*. **100**, 254-9.

82. **Larsen, J.N. and Jensen, K.F.**, 1985. Nucleotide sequence of the *pyrD* gene of *Escherichia coli* and characterization of the flavoprotein dihydroorotate dehydrogenase. **151**, 59-65.

83. **Latifi, A., Winson, M.K., Foglino, M., Bycroft, B.W., Stewart, G.S., Lazdunski, A., and Williams, P.**, 1995. Multiple homologues of LuxR and LuxI control expression of virulence determinants and secondary metabolites through quorum sensing in *Pseudomonas aeruginosa* PAO1. **17**, 333-43.

84. **Leoni, L., Orsi, N., de Lorenzo, V., and Visca, P.**, 2000. Functional analysis of PvdS, an iron starvation sigma factor of *Pseudomonas aeruginosa*. **182**, 1481-91.

85. **Loewen, P.C. and Hengge-Aronis, R.**, 1994. The role of the sigma factor sigma S (KatF) in bacterial global regulation. **48**, 53-80.

86. **Lomholt, J.A., Poulsen, K., and Kilian, M.**, 2001. Epidemic population structure of *Pseudomonas aeruginosa*: evidence for a clone that is pathogenic to the eye and that has a distinct combination of virulence factors. **69**, 6284-95.

87. **Long, C. and Koshland, D.E. Jr**, 1978. Cytidine triphosphate synthetase. **51**, 79-83.

88. **Lory, S.**, 1986. Effect of iron on accumulation of exotoxin A-specific mRNA in *Pseudomonas aeruginosa*. **168**, 1451-6.

89. **Maksimova, N.P., Blazhevich, O.V., and Fomichev, I.u.K.**, 1993. The role of pyrimidines in the biosynthesis of the fluorescing pigment pyoverdin Pm in *Pseudomonas putida* M. 22-6.

90. **Mandel, M. and Higa, A.**, 1970. Calcium-dependent bacteriophage DNA infection. **53**, 159-62.

91. **Matin, A.**, 1996. Role of alternate sigma factors in starvation protein synthesis--novel mechanisms of catabolite repression. **147**, 494-505.

92. **McKnight, S.L., Iglewski, B.H., and Pesci, E.C.**, 2000. The *Pseudomonas* quinolone signal regulates *rhl* quorum sensing in *Pseudomonas aeruginosa*. **182**, 2702-8.

93. **Meyer, J.M.**, 2000. Pyoverdines: pigments, siderophores and potential taxonomic markers of fluorescent *Pseudomonas* species. **174**, 135-42.

94. **Meyer, J.M., Neely, A., Stintzi, A., Georges, C., and Holder, I.A.**, 1996. Pyoverdin is essential for virulence of *Pseudomonas aeruginosa*. **64**, 518-23.

95. **Neuhard, J., Kelln, R.A., and Stauning, E.**, 1986. Cloning and structural characterization of the *Salmonella typhimurium pyrC* gene encoding dihydroorotase. **157**, 335-42.

96. **O'Donovan, G.A. and Gerhart, J.C.**, 1972. Isolation and partial characterization of regulatory mutants of the pyrimidine pathway in *Salmonella typhimurium*. **109**, 1085-96.

97. **O'Donovan, G.A. and Neuhard, J.**, 1970. Pyrimidine metabolism in microorganisms. **34**, 278-343.

98. **O'Toole, G.A., Gibbs, K.A., Hager, P.W., Phibbs, P.V. Jr, and Kolter, R.**, 2000. The global carbon metabolism regulator Crc is a component of a signal transduction pathway required for biofilm development by *Pseudomonas aeruginosa*. **182**, 425-31.

99. **O'Toole, G.A. and Kolter, R.**, 1998. Flagellar and twitching motility are necessary for *Pseudomonas aeruginosa* biofilm development. **30**, 295-304.

100. **Ocaktan, A., Yoneyama, H., and Nakae, T.**, 1997. Use of fluorescence probes to monitor function of the subunit proteins of the MexA-MexB-oprM drug extrusion machinery in *Pseudomonas aeruginosa*. **272**, 21964-9.

101. **Ochsner, U.A., Snyder, A., Vasil, A.I., and Vasil, M.L.**, 2002. Effects of the twin-arginine translocase on secretion of virulence factors, stress response, and pathogenesis. **99**, 8312-7.

102. **Ogawa, J. and Shimizu, S.**, 1995. Purification and characterization of dihydroorotase from *Pseudomonas putida*. **164**, 353-7.

103. **Ornston, L.N. and Stanier, R.Y.**, 1966. The conversion of catechol and protocatechuate to beta-ketoadipate by *Pseudomonas putida*. **241**, 3776-86.

104. **Paulsen, I.T., Brown, M.H., and Skurray, R.A.**, 1996. Proton-dependent multidrug efflux systems. **60**, 575-608.

105. **Pearson, J.P., Pesci, E.C., and Iglewski, B.H.**, 1997. Roles of *Pseudomonas aeruginosa las* and *rhl* quorum-sensing systems in control of elastase and rhamnolipid biosynthesis genes. **179**, 5756-67.

106. **Pesci, E.C.** , 2000. New signal molecules on the quorum-sensing block: response. **8**, 103-4.

107. **Pesci, E.C., Milbank, J.B., Pearson, J.P., McKnight, S., Kende, A.S., Greenberg, E.P., and Iglewski, B.H.**, 1999. Quinolone signaling in the cell-to-cell communication system of *Pseudomonas aeruginosa*. **96**, 11229-34.

108. **Pesci, E.C., Pearson, J.P., Seed, P.C., and Iglewski, B.H.**, 1997. Regulation of *las* and *rhl* quorum sensing in *Pseudomonas aeruginosa*. **179**, 3127-32.

109. **Pessi, G., Williams, F., Hindle, Z., Heurlier, K., Holden, M.T., Camara, M., Haas, D., and Williams, P.**, 2001. The global posttranscriptional regulator RsmA modulates production of virulence determinants and N-acylhomoserine lactones in *Pseudomonas aeruginosa*. **183**, 6676-83.

110. **Pessi, G., Blumer, C., and Haas, D.**, 2001. *LacZ* fusions report gene expression, don't they? **147** , 193-195.

111. **Phillips, A.T. and Mulfinger, L.M.**, 1981. Cyclic adenosine 3',5'-monophosphate levels in *Pseudomonas putida* and *Pseudomonas aeruginosa* during induction and carbon catabolite repression of histidase synthesis. **145**, 1286-92.

112. **Phillips, N.F., Horn, P.J., and Wood, H.G.**, 1993. The polyphosphate- and ATP-dependent glucokinase from *Propionibacterium shermanii*: both activities are catalyzed by the same protein. **300**, 309-19.

113. **Pick, U., Bental, M., Chitlaru, E., and Weiss, M.**, 1990. Polyphosphate-hydrolysis--a protective mechanism against alkaline stress? **274**, 15-8.

114. **Prescott, L.M. and Jones, M.E.**, 1969. Modified methods for the determination of carbamyl aspartate. **32**, 408-19.

115. **Preston, M.J., Seed, P.C., Toder, D.S., Iglewski, B.H., Ohman, D.E., Gustin, J.K., Goldberg, J.B., and Pier, G.B.**, 1997. Contribution of proteases and LasR to the virulence of *Pseudomonas aeruginosa* during corneal infections. **65**, 3086-90.

116. **Rahme, L.G., Stevens, E.J., Wolfort, S.F., Shao, J., Tompkins, R.G., and Ausubel, F.M.**, 1995. Common virulence factors for bacterial pathogenicity in plants and animals. **268**, 1899-902.

117. **Rahme, L.G., Tan, M.W., Le, L., Wong, S.M., Tompkins, R.G., Calderwood, S.B., and Ausubel, F.M.**, 1997. Use of model plant hosts to identify *Pseudomonas aeruginosa* virulence factors. **94**, 13245-50.

118. **Rao, N.N. and Kornberg, A.**, 1999. Inorganic polyphosphate regulates responses of *Escherichia coli* to nutritional stringencies, environmental stresses and survival in the stationary phase. **23**, 183-95.

119. **Rashid, M.H. and Kornberg, A.**, 2000. Inorganic polyphosphate is needed for swimming, swarming, and twitching motilities of *Pseudomonas aeruginosa*. **97**, 4885-90.

120. **Rashid, M.H., Rao, N.N., and Kornberg, A.**, 2000. Inorganic polyphosphate is required for motility of bacterial pathogens. **182**, 225-7.

121. **Rashid, M.H., Rumbaugh, K., Passador, L., Davies, D.G., Hamood, A.N., Iglewski, B.H., and Kornberg, A.**, 2000. Polyphosphate kinase is essential for biofilm development, quorum sensing, and virulence of *Pseudomonas aeruginosa*. **97**, 9636-41.

122. **Ratledge, C. and Dover, L.G.**, 2000. Iron metabolism in pathogenic bacteria. **54**, 881-941.

123. **Reimmann, C., Beyeler, M., Latifi, A., Winteler, H., Foglino, M., Lazdunski, A., and Haas, D.**, 1997. The global activator GacA of *Pseudomonas aeruginosa* PAO positively controls the production of the autoinducer N-butyryl-homoserine lactone and the formation of the virulence factors pyocyanin, cyanide, and lipase. **24**, 309-19.

124. **Reusch, R.N. and Sadoff, H.L.**, 1988. Putative structure and functions of a poly-beta-hydroxybutyrate/calcium polyphosphate channel in bacterial plasma membranes. **85**, 4176-80.

125. **Rumbaugh, K.P., Griswold, J.A., and Hamood, A.N.**, 2000. The role of quorum sensing in the in vivo virulence of *Pseudomonas aeruginosa*. **2**, 1721-31.

126. **Sander, E.G. and Heeb, M.J.**, 1971. Purification and properties of dihydroorotase from *Escherichia coli* B. **227**, 442-52.

127. **Sander, E.G., Wright, L.D., and McCormick, D.B.**, 1965. Evidence for function of a metal ion in the activity of dihydroorotase from *Zymobacterium oroticum*. **240**, 3628-30.

128. **Scapin, G., Sacchettini, J.C., Dessen, A., Bhatia, M., and Grubmeyer, C.**, 1993. Primary structure and crystallization of orotate phosphoribosyltransferase from *Salmonella typhimurium*. **230**, 1304-8.

129. **Schurr, M.J., Vickrey, J.F., Kumar, A.P., Campbell, A.L., Cunin, R., Benjamin, R.C., Shanley, M.S., and O'Donovan, G.A.**, 1995. Aspartate transcarbamoylase genes of *Pseudomonas putida*: requirement for an inactive dihydroorotase for assembly into the dodecameric holoenzyme. **177**, 1751-9.

130. **Schwartz, M. and Neuhard, J.**, 1975. Control of expression of the *pyr* genes in *Salmonella typhimurium*: effects of variations in uridine and cytidine nucleotide pools. **121**, 814-22.

131. **Schweizer, H.D.**, 1993. Small broad-host-range gentamycin resistance gene cassettes for site- specific insertion and deletion mutagenesis. **15**, 831-4.

132. **Schwyn, B. and Neilands, J.B.**, 1987. Universal chemical assay for the detection and determination of siderophores. **160**, 47-56.

133. **Semple, K.S. and Silbert, D.F.**, 1975. Mapping of the *fabD* locus for fatty acid biosynthesis in *Escherichia coli*. **121**, 1036-46.

134. **Serino, L., Reimmann, C., Baur, H., Beyeler, M., Visca, P., and Haas, D.**, 1995. Structural genes for salicylate biosynthesis from chorismate in *Pseudomonas aeruginosa*. **249**, 217-28.

135. **Shanley, M.S., Foltermann, K.F., O'Donovan, G.A., and Wild, J.R.**, 1984. Properties of hybrid aspartate transcarbamoylase formed with native subunits from divergent bacteria. **259**, 12672-7.

136. **Shepherdson, M. and McPhail, D.**, 1993. Purification of aspartate transcarbamoylase from *Pseudomonas syringae*. **114**, 201-5.

137. **Shiba, T., Tsutsumi, K., Yano, H., Ihara, Y., Kameda, A., Tanaka, K., Takahashi, H., Munekata, M., Rao, N.N., and Kornberg, A.**, 1997. Inorganic polyphosphate and the induction of *rpoS* expression. **94**, 11210-5.

138. **Stibitz, S., Black, W., and Falkow, S.**, 1986. The construction of a cloning vector designed for gene replacement in *Bordetella pertussis*. **50**, 133-40.

139. **Stintzi, A., Barnes, C., Xu, J., and Raymond, K.N.**, 2000. Microbial iron transport via a siderophore shuttle: a membrane ion transport paradigm. **97**, 10691-6.

140. **Stintzi, A., Evans, K., Meyer, J.M., and Poole, K.**, 1998. Quorum-sensing and siderophore biosynthesis in *Pseudomonas aeruginosa*: *lasR/lasI* mutants exhibit reduced pyoverdine biosynthesis. **166**, 341-5.

141. **Stover, C.K., Pham, X.Q., Erwin, A.L., Mizoguchi, S.D., Warrener, P., Hickey, M.J., Brinkman, F.S., Hufnagle, W.O., Kowalik, D.J., Lagrou, M., Garber, R.L., Goltry, L., Tolentino, E., Westbrock-Wadman, S., Yuan, Y., Brody, L.L., Coulter, S.N., Folger, K.R., Kas, A., Larbig, K., Lim, R., Smith, K., Spencer, D., Wong, G.K., Wu, Z., Paulsen, I.T., Reizer, J., Saier, M.H., Hancock, R.E., Lory, S., and Olson, M.V.**, 2000. Complete genome sequence of *Pseudomonas aeruginosa* PA01, an opportunistic pathogen. **406**, 959-64.

142. **Strych, U., Wohlfarth, S., and Winkler, U.K.**, 1994. Orotidine-5'-monophosphate decarboxylase from *Pseudomonas aeruginosa* PAO1: cloning, overexpression, and enzyme characterization. **29**, 353-9.

143. **Suh, S.J., Runyen-Janecky, L.J., Maleniak, T.C., Hager, P., MacGregor, C.H., Zielinski-Mozny, N.A., Phibbs, P.V. Jr, and West, S.E.**, 2002. Effect of *vfr* mutation on global gene expression and catabolite repression control of *Pseudomonas aeruginosa*. **148**, 1561-9.

144. **Syldatk, C., May, O., Altenbuchner, J., Mattes, R., and Siemann, M.**, 1999. Microbial hydantoinases--industrial enzymes from the origin of life? **51**, 293-309.

145. **Tang, H., Kays, M., and Prince, A.**, 1995. Role of *Pseudomonas aeruginosa* pili in acute pulmonary infection. **63**, 1278-85.

146. **Tang, H.B., DiMango, E., Bryan, R., Gambello, M., Iglewski, B.H., Goldberg, J.B., and Prince, A.**, 1996. Contribution of specific *Pseudomonas aeruginosa* virulence factors to pathogenesis of pneumonia in a neonatal mouse model of infection. **64**, 37-43.

147. **Taylor, W.H., Taylor, M.L., Balch, W.E., and Gilchrist, P.S.**, 1976. Purification of properties of dihydroorotase, a zinc-containing metalloenzyme in *Clostridium oroticum*. **127**, 863-73.

148. **Thoden, J.B., Phillips, G.N. Jr, Neal, T.M., Raushel, F.M., and Holden, H.M.**, 2001. Molecular structure of dihydroorotase: a paradigm for catalysis through the use of a binuclear metal center. **40**, 6989-97.

149. **Turnbough, C.L. Jr and Bochner, B.R.**, 1985. Toxicity of the pyrimidine biosynthetic pathway intermediate carbamyl aspartate in *Salmonella typhimurium*. **163**, 500-5.

150. **Usher, L.R., Lawson, R.A., Geary, I., Taylor, C.J., Bingle, C.D., Taylor, G.W., and Whyte, M.K.**, 2002. Induction of neutrophil apoptosis by the *Pseudomonas aeruginosa* exotoxin pyocyanin: a potential mechanism of persistent infection. **168**, 1861-8.

151. **Van de Casteele, M., Chen, P., Roovers, M., Legrain, C., and Glansdorff, N.**, 1997. Structure and expression of a pyrimidine gene cluster from the extreme thermophile *Thermus* strain ZO5. **179**, 3470-81.

152. **van Delden, C., Comte, R., and Bally, A.M.**, 2001. Stringent response activates quorum sensing and modulates cell density- dependent gene expression in *Pseudomonas aeruginosa*. **183**, 5376-84.

153. **Vasil, M.L. and Ochsner, U.A.**, 1999. The response of *Pseudomonas aeruginosa* to iron: genetics, biochemistry and virulence. **34**, 399-413.

154. **Vickrey, J.F., Herve, G., and Evans, D.R.**, 2002. *Pseudomonas aeruginosa* aspartate transcarbamoylase. Characterization of its catalytic and regulatory properties. **277**, 24490-8.

155. **Visca, P., Ciervo, A., and Orsi, N.**, 1994. Cloning and nucleotide sequence of the *pvdA* gene encoding the pyoverdin biosynthetic enzyme L-ornithine N5-oxygenase in *Pseudomonas aeruginosa*. **176**, 1128-40.

156. **Voulhoux, R., Ball, G., Ize, B., Vasil, M.L., Lazdunski, A., Wu, L.F., and Filloux, A.**, 2001. Involvement of the twin-arginine translocation system in protein secretion via the type II pathway. **20**, 6735-41.

157. **Wang, G.P., Lundegaard, C., Jensen, K.F., and Grubmeyer, C.**, 1999. Kinetic mechanism of OMP synthase: a slow physical step following group transfer limits catalytic rate. **38**, 275-83.

158. **Washabaugh, M.W. and Collins, K.D.**, 1984. Dihydroorotase from *Escherichia coli*. Purification and characterization. **259**, 3293-8.

159. **Washabaugh, M.W. and Collins, K.D.**, 1986. Dihydroorotase from *Escherichia coli*. Sulfhydryl group-metal ion interactions. **261**, 5920-9.

160. **West, S.E., Sample, A.K., and Runyen-Janecky, L.J.**, 1994. The *vfr* gene product, required for *Pseudomonas aeruginosa* exotoxin A and protease production, belongs to the cyclic AMP receptor protein family. **176**, 7532-42.

161. **Whiteley, M., Parsek, M.R., and Greenberg, E.P.**, 2000. Regulation of quorum sensing by RpoS in *Pseudomonas aeruginosa*. **182**, 4356-60.

162. **Wild, J.R., Belser, W.L., and O'Donovan, G.A.**, 1976. Unique aspects of the regulation of the aspartate transcarbamylase of *Serratia marcescens*. **128**, 766-75.

163. **Williams, J.C. and O'Donovan, G.A.**, 1973. Repression of enzyme synthesis of the pyrimidine pathway in *Salmonella typhimurium*. **115**, 1071-6.

164. **Williams, N.K., Manthey, M.K., Hambley, T.W., O'Donoghue, S.I., Keegan, M., Chapman, B.E., and Christopherson, R.I.**, 1995. Catalysis by hamster dihydroorotase: zinc binding, site-directed mutagenesis, and interaction with inhibitors. **34**, 11344-52.

165. **Wilson, R. and Dowling, R.B.**, 1998. Lung infections. 3. *Pseudomonas aeruginosa* and other related species. **53**, 213-9.

166. **Womack, J.E. and O'Donovan, G.A.**, 1978. Orotic acid excretion in some wild-type strains of *Escherichia coli* K- 12. **136**, 825-7.

167. **Yurgel, S., Mortimer, M.W., Rogers, K.N., and Kahn, M.L.**, 2000. New substrates for the dicarboxylate transport system of *Sinorhizobium meliloti*. **182**, 4216-21.

168. **Zimmermann, B.H. and Evans, D.R.**, 1993. Cloning, overexpression, and characterization of the functional dihydroorotase domain of the mammalian multifunctional protein CAD. **32**, 1519-27.

169. **Zimmermann, B.H., Kemling, N.M., and Evans, D.R.**, 1995. Function of conserved histidine residues in mammalian dihydroorotase. **34**, 7038-46.

170. **Zubay, G.**, 1973. *In vitro* synthesis of protein in microbial systems. **7**, 267-87.